Synthesis, Structure and Properties of a few Bis-Phenols and Diaryl Quinone Methides

A Dissertation submitted to the
Indian Institute of Technology Guwahati
as partial fulfillment for the Degree of
Doctor of Philosophy
in Chemistry

Submitted by

Rupam Jyoti Sarma

Department of Chemistry

Indian Institute of Technology, Guwahati

September 2005

Statement

I hereby declare that this thesis entitled "Synthesis, Structure and Properties of a few Bis-Phenols and Diaryl Quinone Methides" is the outcome of research work carried out by me under the supervision of Prof. Jubaraj B. Baruah, at the Department of Chemistry, Indian Institute of Technology Guwahati, India.

In keeping with the general practice of reporting scientific observations, due acknowledgement has been made whenever work described here has been based on the findings of other investigators.

Rupam Jyoti Sarma

Rupam Jyoti Sarma

September 27, 2005

IIT Guwahati

Certificate

It is certified that the work described in this thesis entitled "**Synthesis, Structure and Properties of a few Bis-Phenols and Diaryl Quinone Methides**" by Mr. Rupam Jyoti Sarma for the award of degree of Doctor of Philosophy is an authentic record of the results obtained from the research work carried out under my supervision in the Department of Chemistry, Indian Institute of Technology Guwahati, India and this work has not been submitted elsewhere for a degree.

Guwahati

Prof. Jubaraj B. Baruah

27th September 2005

INDIAN INSTITUTE OF TECHNOLOGY,GUWAHATI

Ph.D. GRADE CARD

ROLL NO : 016102202 **DEPT :** Chemistry

NAME : Rupam Jyoti Sarma

Semester I (July - November) 2001

Course	Course Name	Cr.	Gr.
CH 621	Newer Reagents for Organic Synthesis	6	AB
CE 610	Organometallics	6	AB

Semester Performance Index (S.P.I.) : 9.00
Cumulative Performance Index (C.P.I.) : 9.00

Semester II (January - May) 2002

Course	Course Name	Cr.	Gr.
CH 601	Physical Methods in Chemistry	6	AB
CH 630	A Fundamental Approach to Physical Chemistry	6	AA

Semester Performance Index (S.P.I.) : 9.50
Cumulative Performance Index (C.P.I.) : 9.25

Date : 29.06.2005 **Asst. Registrar (Academic)**

ASSISTANT REGISTRAR (ACADEMIC AFFAIRS)
Indian Institute of Technology Guwahati
Guwahati - 781 039, INDIA

CODE	GRADE POINTS
AA	10 Points
AB	9 "
BB	8 "
BC	7 "
CC	6 "
CD	5 "
DD	4 "
F	0 points and is a **FAILURE** grade
I	Incomplete
AU	Audit Course
NP	Failed in Audit Course
PP	Passed Audit Course

LEGENDS USED	
Cr.	Credit
Gr.	Grade

No Class or Division is awarded in this Institute.
The Cumulative Performance Index (C.P.I.) is

$$C.P.I. = \sum C_i P_i / \sum C_i$$ Where

C_i is the credit of the course

P_i is the grade point obtained by the student in the course

Acknowledgements

The enlightening experience of doing science under the guidance of Prof. Jubaraj B. Baruah can hardly be described in words. The numerous discussions and interactions I had with him expanded my horizons to hitherto unknown frontiers of science and knowledge. The pleasure of working with Prof.Baruah also reflects in his boundless enthusiasm and creativity. At times he seems more energetic amongst us, and most of the times it led to something worthwhile. I am indebt to this wonderful person for all that he has given me and above all for motivating me towards scientific research.

I am extremely grateful to Prof. Mihir K. Chaudhuri for being so considerate everytime I went to him, and for his constant encouragement. I am also grateful to the entire faculty and staff in the Department of Chemistry, Indian Institute of Technology Guwahati for providing a wonderful work atmosphere throughout this period.

At the same time I would like to convey my sincere gratitude to Dr. Ritu Kataky, in the Department of Chemistry, University of Durham for guiding and inspiring me throughout my stay in Durham. My special thanks to Prof. David Parker, the Head of the Department of Chemistry, University of Durham for his time and invaluable suggestions, and also for allowing me to use the facilities in the department. I am also thankful to the faculty and staff in this department for being so warm and supportive, even though the weather used to remain pretty cold outside.

My brief association with Dr. Andrei S. Batsanov and Dr. Andreas E. Goeta in Durham gave me gainful experience on the various aspects of single crystal X-ray crystallography. The content of this thesis would not have had the present form without their able guidance. I will be ever grateful to both of them for their time and advice.

I take this opportunity to thank Dr. Eric J.L. McInnes at the Department of Chemistry, University of Manchester for allowing me to avail the ESR facility there. I also thank him for his advice and valuable inputs during the ESR measurements.

The help and support of my lab mates, and my friends both in Durham and he have been fabulous. No words can express my thankfulness for giving me their time and companionship, which made the time spent in the laboratory pleasant and memorable.

I am grateful that Subrata Barooah inspired me into the realms of chemisty and motivated me to pursue it, and Diganta da for his encouragement. I would like to thank my mom, dad and my family whose love and support have meant so much to me and Mau for being such a true friend. Cheers!

I would like to thank Council of Scientific and Industrial Research, New Delhi (India) for Junior and Senior Research Fellowship. I also thank the British Council and the Commonwealth for sponsoring me as a Commonwealth Split-Site Fellow to visit University of Durham United Kingdom.

Preview

The chemistry of bis-phenols and its derivatives is one of the important aspects of synthetic organic chemistry. This subject has gained relevance because of the various applications of bis-phenols, which may involve some simple molecules or complex macromolecules containing the bis-phenol framework.

The work described in this thesis, "**Synthesis, Structure and Properties of a few *Bis*-phenols and Diaryl Quinone Methides**" details some of the important findings related to the synthesis of bis-phenols from phenol, 2.6-dimethylphenol and 2-naphthol. This thesis focuses on the structures and properties of the bis(4-hydroxy-3,5-dimethyl phenyl)(aryl) methanes, which hitherto has not been studied systematically. This study draws importance from another fact that these compounds can be precursors to diaryl quinone methides.

With a view to define such study we introduce a brief review of the state-of-art of *bis*-phenols and the different aspects related to the synthesis, structure, properties and applications and their analogs in the first chapter. The supramolecular assemblies from *bis*-phenols are also analyzed with suitable examples to illustrate the versatility of these molecules.

Some of the important aspects related to the synthesis of bis(4-hydroxy-3,5-dimethyl phenyl)(aryl) methanes are described in the second chapter. Several new bis-phenolic compounds are synthesized and characterized. In all these condensation reactions, we could obtain only the bis-phenols but no mono-condensation products were obtained. The reactions were carried out in one pot and under acidic conditions. We extended our study to synthesize molecules containing two units of bis-phenols connected by different spacers. A series of such molecules having an amide groups incorporated into the spacer are synthesized and characterized. Two methods are used for such synthesis. In the first method the amino group of bis(4-hydroxy-3,5-dimethylphenyl)(4-aminophenyl)-methane is functionalized with various acid dichlorides to obtain a series of amide bridged bis-phenolic compounds. In an alternative method, aromatic dialdehydes with different

spacers are reacted with 2,6-dimethylphenol to prepare bis-phenols with different space specially containing ether linkages.

Chapter 3 enumerates the X-ray crystallographic studies of the structure of bis-phenols. This study is done to unearth various weak interactions that lead to the observed solid-state structures of the bis-phenols. In this regard we have encountered various types of weak interactions, a few of which found to be crucial in the self-assembly of bis-phenols are also described. Different kind of inclusion compounds with benzene, toluene, acetonitrile, are discussed. The structures of self-assemblies by assistance of different halides, such as chloride, bromide, and fluoride with bis-phenols having nitrogen heterocycle as substituent is illustrated. The pyridyl bis-phenol may be protonated easily by addition of either hydrochloric acid or hydrobromic acid in the presence of catalytic amount of the corresponding copper (II) halide. Crystallization leads to the corresponding chloride and bromide pyridinium salts. The addition of hydrofluoric acid to bis(4-hydroxy-3,5-dimethylphenyl)(4-aminophenyl)methane gave the corresponding anilinium salt.

In chapter 4, a new method for the synthesis of 14-H-14-(aryl)dibenzoxanthenes is described. Some of 14-H-14-(aryl)dibenzoxanthenes are studied by X-ray crystallography. In the solid-state structure of 14-H-(2-nitrophenyl)dibenzoxanthene, intermolecular C–H···O interactions are observed among the molecules involving the aromatic C–H and the nitro groups.

Chapter 5 deals with the synthesis, characterization, and physical properties of a few diaryl quinone methides obtained from oxidation of the bis-phenols. These diaryl quinone methides form hydrogen-bonded structures and they are studied by crystallography. In some of these molecules intermolecular O–H···O=C and C–H···O interactions leads to the formation of tetrameric hydrogen-bonded rings, interlocked networks and hydrogen-bonded helices.

In Chapter 6, the solution properties of the quinone-methides are discussed. The ^{1}HNMR spectroscopy of the quinone methides in solution shows that they are tautomeric

at room temperature and that the phenolic-quinone tautomerism. These compounds are solvatochromic and shows distinct chromogenic properties in acid and basic medium. The spectrochemical properties of a compound depend on the polarity and the hydrogen-bonding ability of the solvents/medium. Depending on the solvent microenvironment, the compounds show distinct color changes.

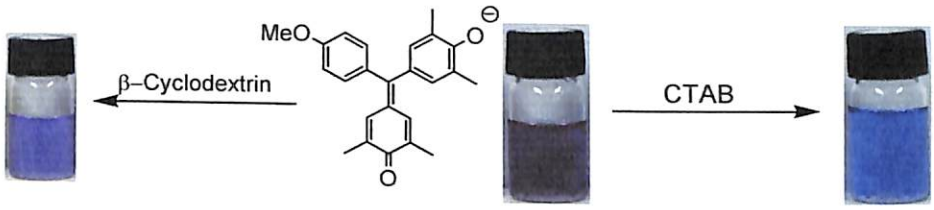

In this Chapter, the electrochemical aspects of the quinone methides are also discussed. From the cyclic voltammetry of selected quinone-methides, showed the formation of anion radicals which are further proved by in-situ electron spin resonance spectra..

The synthetic procedures and experimental details are given in the last chapter of the thesis. The cumulative references are listed towards the end of the thesis.

Contents

Statement

Certificate

Acknowledgements

Preview

Chapter 1:	Introduction	1
Chapter 2:	Synthesis and Characterisation of Bis-Phenols	25
Chapter 3:	Structures and Hydrogen-Bonding in Bis-Phenols	43
Chapter 4:	Synthesis and Structures of 14-Aryl-14-H-Dibenzo[*a,j*]-xanthenes	68
Chapter 5:	Synthesis and Structures of Diaryl Quinone Methides	73
Chapter 6:	Spectroscopic and Electrochemical Properties of Diaryl Quinone Methides	88
Chapter 7:	Experimental Section	113

References 165

List of Publications

Chapter 1

Introduction

1.1 Definition of Bis-Phenols

Bis-phenols, in a broad sense, can be defined as those organic compounds containing two phenol units that are connected by appropriately designed spacers. As the definition suggests, there are numerous ways of connecting two phenol units in order to construct a bis-phenol. However, this terminology has been restricted to those bis-phenols possessing methylene groups as the spacer, which are described by structure **1** (Fig.1). Within this structural framework, some examples are bis-phenol A (**2**), bis-phenol C (**3**) and bis-phenol F (**4**).

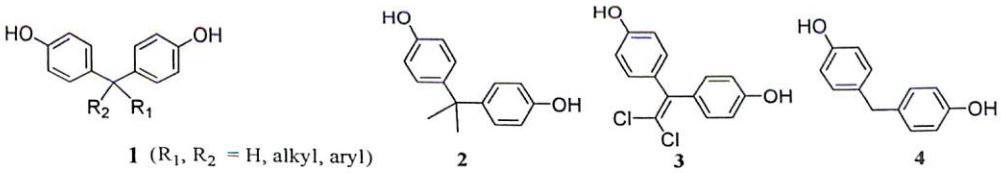

Fig.1

1.2 Genesis of the Chemistry of Bis-Phenols

Bis-phenols are important constituents of polymers and phenolic resins. Moreover, bis-phenols can be modified in order to generate different macromolecular architectures[1] and polymers[2]. For example, bis-phenol A, namely 2,2'-bis(4-hydroxyphenyl)propane (**2**) is used in the preparation of polycarbonates and polyethers. These polymers have important industrial applications[3,4]. This is exemplified by the preparation of cyclic oligomeric polycarbonates, **5** from bis-phenol A. In a simple synthetic route (equation 1), **5** can be converted into high molecular weight polycarbonates (**6**) using suitable catalysts[5].

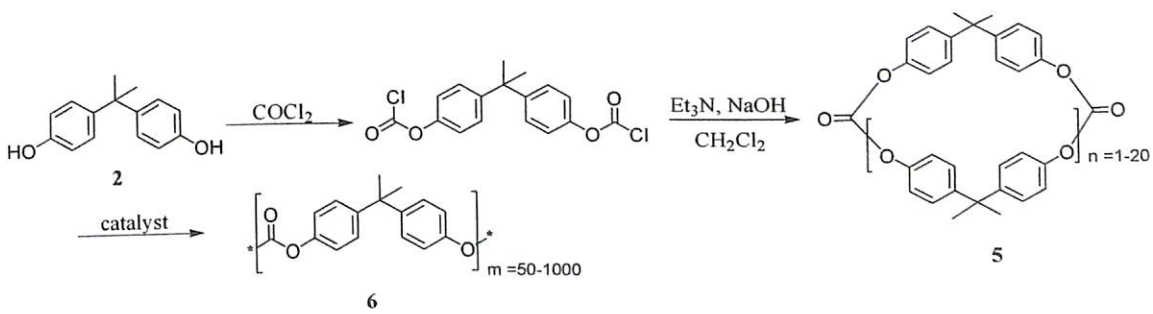

Equation 1 Synthesis of cyclic and linear polycarbonates from **2**

Among the different polymers that are built on the bis-phenol backbones, poly(ether-sulfones) have additional advantages of enhanced chemical and thermal stability. These polymers can be synthesized by different routes, and in most cases involve the polycondensation of the appropriate bis-phenol. For example, reaction of compound **2** with bis(4-halophenyl)sulfone in the presence of a base[3] (equation 2) results in the formation of polycondensation products (7). Thus, bis-phenols and the analogous compounds[6-8] can be used in the synthesis of industrially important cross-linked polymers.

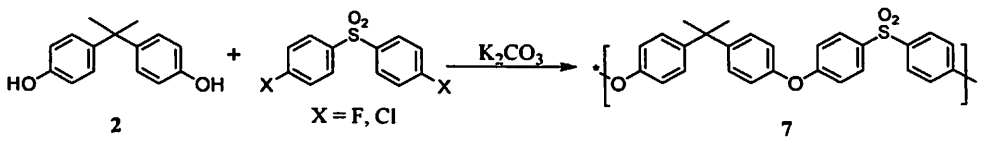

Equation 2 Synthesis of poly(ether)sulfone polymers from bis-phenol A

Polycondensation of the silylated tris(4-hydroxyphenyl)ethane with 4,4'-difluoro-benzenesulfone results in the formation of cyclic oligoethers, or bridged bicycles[9,10], which are double, triple or multiple branched. Similarly, when the silylated tris-phenol is polycondensed with equimolar amounts of 2,6-difluorobenzonitrile[11] polyethers are obtained.

Macrocyclic polymers, such as poly(ester)crowns[12] are synthesized from bis-phenols precursors. These polymers contain semi-rigid crown units incorporated into the polymer backbone as pendent units. These high molecular weight polymers have received attention for their cation binding abilities and host-guest properties. For instance, novel poly(ester) crowns containing crown macrocycles are synthesized by the condensation of bis-phenol A with bis(5-carboxy-1,3-phenylene)32-crown-10 and these polymers display ability to bind metal ions and organic cations.

The synthesis and structure of macrocycles (equation 3) and interlocked molecules such as [2]-catenanes[13] is an emerging field of research. It has been shown that such macrocyclic systems[14] can be constructed on bis-phenolic frameworks, and in this way synthesis of large molecular rings can be achieved.

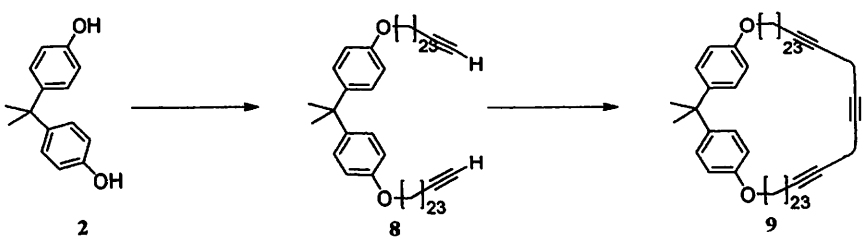

Equation 3 Formation of molecular rings, **9** from bis-phenol precursor

Applying the principles of carbonate template, large poly[2]catenanes have also been synthesized (Fig.2) by polymerizing suitably functionalised [2]catenanes[15]. These highly flexible catenanes display unusual liquid crystalline properties. The catenanes containing large rings are free to rotate about each other and exhibit fair degree of freedom for lateral displacement.

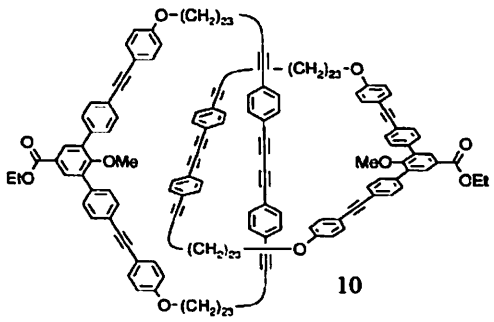

10

Fig.2

Novel molecular imprinted polymers[16, 17] containing amylose as the host matrix and **2** as the template are known. Such imprinted polymers can be used for synthesizing molecular recognition materials. Photochemical polymerization of modified acryloamylose in the presence of **2** as template gives a polymer that exhibits imprinting properties. These imprinted polymers are reported to exhibit reversible pH responsive binding with **2**.

Axially chiral bis-phenolic compounds such as 2,2'-bis-naphthol (**11**) have been used in stereoselective synthesis[18] and also as chiral host[72]. Ligands derived from chiral bis-phenol derivatives are known to catalyze asymmetric reductions, asymmetric aldol-type reactions[19], Diels-Alder reactions, ene reaction and polymerization reactions.

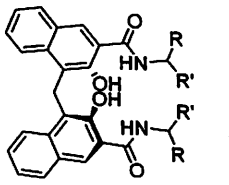

R, R' = alkyl, aryl, $SiMe_3$

11

Fig. 3

Bis-phenols and analogous compounds exhibit useful fungicidal[20,21] and bacteriostatic properties[22]. Of special interest are the antioxidant properties of bis-phenols[23] such as **12** that have found use in rubber chemicals. Phenolic hydroxy groups involved in hydrogen bonding are found to be less reactive towards peroxyl radicals than free hydroxy groups, which indicate that the reactivities will be less affected by hydrogen bond acceptor solvents. Different aspects related to the hydrogen-bonding and antioxidant activity of bis-phenols have

been studied using model compounds[24] such as 2,2'-methylene-bis(6-tert-butyl-4-methylphenol) (**12**), 4,4'-methylene-bis(2,6-di-tert-butyl-phenol) (**13**) and 2,2'-ethylidene-bis(4,6-di-tert-butylphenol) (**14**). From EPR studies the O–H bond dissociation enthalpies for the conversion of such compounds to the corresponding phenoxyl radicals can be determined.

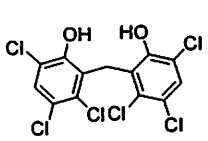

12

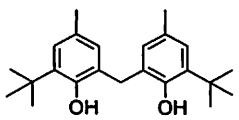

13

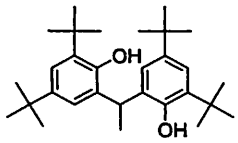

14

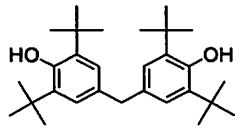

15

The antioxidant properties of bis-phenols such as **13** and **14** are quite remarkable[24] as compared to **15**. This is attributed to enhanced stability of the phenoxyl radical because of steric crowding around the phenolic hydroxy group. Moreover, the presence of intramolecular hydrogen bonding of the aryloxy radical with the other hydroxy group increases the stability of the intermediates. Concentration dependent FT-IR spectroscopy of the compounds in tetrachloromethane in the range 3800–3200cm^{-1} provides evidence for intramolecular hydrogen bonding in these compounds.

The presence of two hydroxyl groups in bis-phenols also make them attractive systems for the study of hydrogen bonded self-assembly from a supramolecular perspective. These aspects are discussed later in this Chapter.

1.3 Synthesis of bis-phenols

As already described, bis-phenols can have diverse structures and consequently different synthetic routes need to be employed. The synthetic routes devised for preparation of bis-phenols may involve a single step procedure or multiple numbers of steps. Among them, direct condensation of phenols with carbonyl compounds is one of the most general yet effective ways to prepare bis-phenols.

The condensation of phenols with carbonyl compounds can be performed in acidic medium with a number of variations in the reaction conditions[25]. Baeyer found that the reaction of phenols and aldehydes in the presence of acids[26] lead to the formation of arylmethanol (**16a**) intermediates, which react further to give diarylmethane derivatives, **16b** (equation 4).

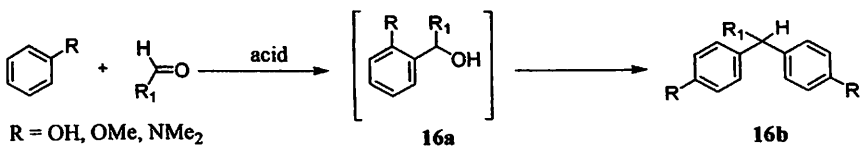

R = OH, OMe, NMe_2
R_1 = H, alkyl, Ph

16a **16b**

Equation 4

The condensation reactions involving unsubstituted phenols show para-selectivity. This arises because the electrophile generated by protonation of the aldehyde, preferentially attacks the para-position of the phenol to give the corresponding product. The reaction of phenol with a carbonyl compound, such as formaldehyde[27] can occur both at the ortho- and para-positions (equation 5). This reaction requires the presence of either an acid or a base, and results in the formation of phenol-formaldehyde resins, **17**.

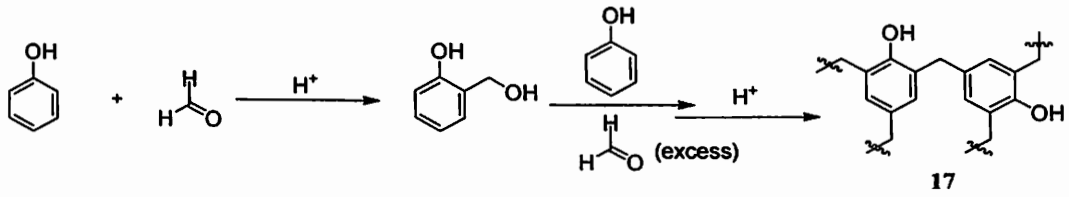

17

Equation 5

Beaver and Stoffel[28] extended the strategy used earlier by Baeyer[26], and synthesized a series of bis-phenols (**18**, **19**) from substituted phenols with a few aldehydes. The reaction occurs in a single step and requires the presence of acid.

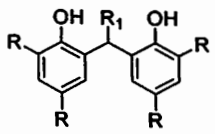

18

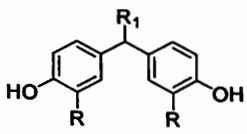

19

R = alkyl, aryl, chlorine
R_1= alkyl, aryl

It is observed that when the para-position of the phenol is free, only 4,4'-bis-phenols are obtained. Only in case of those phenols having substituents at the para-position, the ortho-coupled 2,2'-bis-phenols are obtained. Similarly the condensation of 2,3-disubstituted phenols with aliphatic aldehydes[29] results in the formation of 4,4'-diarylmethanes.

In case of the condensation reactions of phenols with cyclohexanones, a different procedure[30] is employed (equation 6). This procedure is useful in the synthesis of [bis(4-hydroxyphenyl)]-4-methyl-4-phenylcycloalkanes **20** and its derivatives. Typically, the reaction is performed by adding hydrochloric acid to mixture of phenol and the cyclohexanone derivative in the presence of α-mercaptopropionic acid.

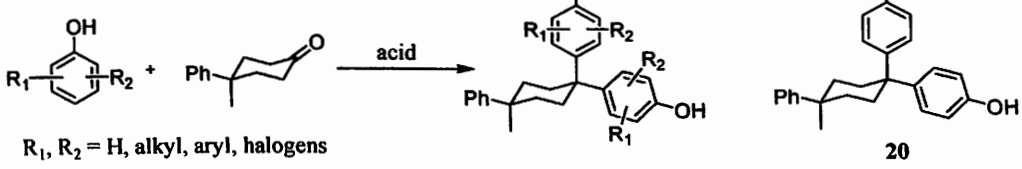

R_1, R_2 = H, alkyl, aryl, halogens

20

Equation 6

Bis-phenol A (**2**) can readily be synthesized by condensation of phenol with acetone in the presence of acid catalysts[31]. The condensation of phenol with aliphatic and aromatic aldehyde also occurs in the presence of heteropolyacids like phosphotungstic acid, $H_3PW_{12}O_{40}.25H_2O$ or its salts as catalysts[32]. In this process, the bis-phenol derivative is readily separated from the acid. Moreover, the acid is recovered from the aqueous phase can be recycled. This reaction is advantageous because heteropolyacids are non-corrosive and the reaction rates are not affected by the presence of water. This method can also be extended to the synthesis of bis-phenols from other substituted phenols. It is even more useful if the bis-phenol, which is prepared, can be separated by recrystallization. This in fact is made possible by use of a recyclable acidic cation exchange resin as catalyst, such as DOWEX 50WX4[33] for the condensation of phenol with the carbonyl compounds.

Similar to phenols, condensations of formaldehyde with suitably substituted naphthols can occur in the presence of acids (equation 7), resulting in the formation of the bis-naphthols[34] such as **21**.

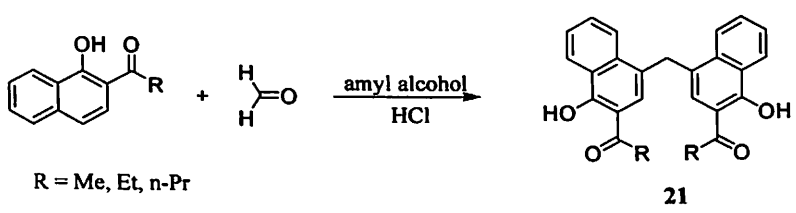

R = Me, Et, n-Pr

21

Equation 7

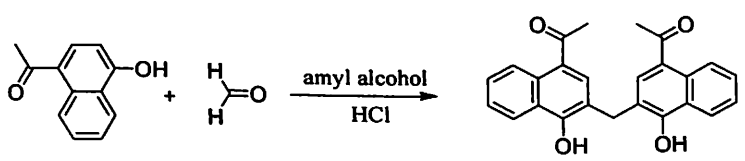

22a

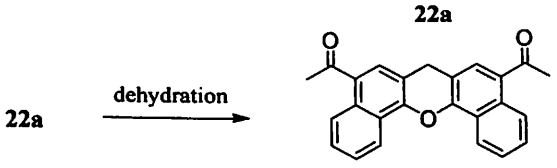

22b

Equation 8

The reactions of formaldehyde equivalents such as diethoxymethane with substituted naphthols work equally well, and give bis-naphthols as products. These naphthol-aldehyde condensations exhibit para-selectivity as in the case of phenols. Only when the para-position is occupied by substituents other than hydrogen, the incoming electrophile is directed towards the ortho-position (equation 8) so that bis-naphthols such as **22a** are obtained. These

compounds **22a** can readily undergo intra-molecular dehydration with $POCl_3$ leading to the formation of dibenzoxanthenes[35] (**22b**).

The Pechmann reaction[36] is a well-known method for the synthesis of coumarin derivatives. This reaction involves the condensation of phenolic compounds with ethyl acetoacetate in the presence of acid. However, the condensation of phenol and ethyl acetoacetate with hydrochloric acid as catalyst[37] can also lead to the formation of the bis-phenols such as 3,3-bis(4-hydroxyphenyl)butyrate. The analogous reaction of phenol with acetylacetone in the presence of hydrochloric acid gives two main products, 1,1,1-tris(4-hydroxyphenyl)ethane (**23**) and 2,2'-bis(4-hydroxy-phenyl)propane (**2**) as shown in equation 9.

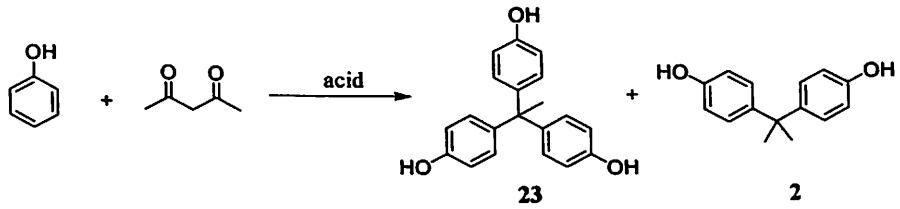

Equation 9

Thus the synthetic strategy for bis-phenols can readily be extended for the synthesis of C3-symmetric tris-phenols[38], by condensing suitably substituted phenols with hydroxy-substituted carbonyl compounds in the presence of acids.

A few bromo-substituted bis-phenols containing triphenylmethyl structures (**24**) were synthesized from simple and substituted phenols[39] (equation 10). These compounds are isolated as solvated adducts or inclusion compounds when recrystallized from solvents like benzene and toluene. This protocol can be easily extended for the aldehydes with various substituents (equation 10) and generally crystalline compounds are obtained.

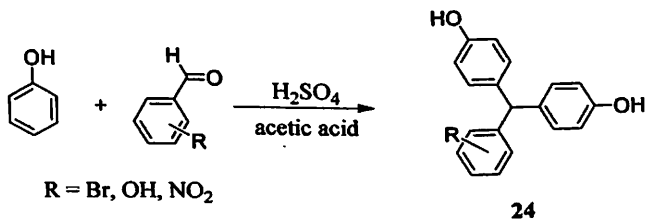

Equation 10

The synthesis of C_3-symmetric tris-phenol platforms[40], **25**, by reacting 2,4-di-tert-butyl phenol with 2,4-di-tert-butyl benzaldehyde in the presence of sulfuric acid is possible (equation 11). These tris-phenols (**25**) are structurally interesting molecules as they can adopt either cone conformations or partial cone conformations. The hydroxy groups of the phenol units on the

outer rim of the tris-phenols can be functionalized, which impart metal-binding properties to the frameworks.

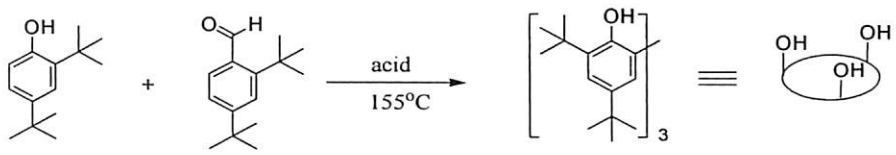

25

Equation 11

Bis-phenol sulfoxides such as **26** have been synthesized via a novel one-step synthetic route (equation 12). This is exemplified by the reaction of 4-methylphenol with thionyl chloride which occurs in the presence of aluminium chloride in dichloromethane[41,42].

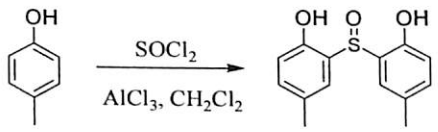

26

Equation 12

Synthesis of organometallic bis-phenols having ferrocene substituents, 1,1-bis(4'-hydroxy-phenyl)-2-ferrocenyl-but-1ene (**27**) have also been reported[43]. This reaction involves a McMurry Cross-Coupling (equation 13) between 4,4'-dihydroxy-benzophenone and the appropriate ketone.

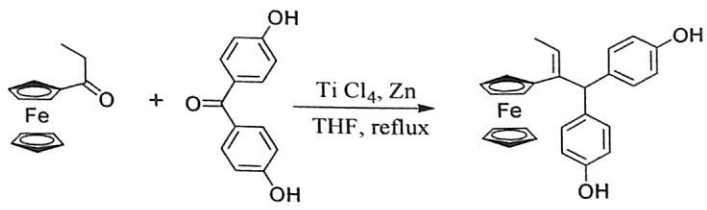

27

Equation 13

As mentioned earlier, condensation of phenol and formaldehyde can also occur under alkaline conditions. In the presence of a weak alkaline catalyst such as triethanolamine, the reaction rates are moderate. It has been found that the kinetics of the reaction involving both simple or alkylated phenols and paraformaldehyde follow first order rate law[44].

It is to be noted that the condensation reactions of phenols and aldehydes enable synthesis of symmetrical bis-phenols. However, the preparation of unsymmetrical bis-phenols, where the two phenolic components are different can also be achieved.

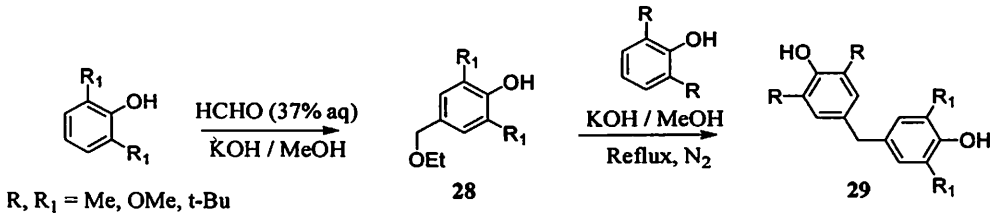

Equation 14

This synthesis is accomplished in two-steps[45]; in the first step 2,6-disubstituted phenols react with formaldehyde (equation 14) under alkaline conditions to give the alcohol or ether (**28**). The compounds **28** are then condensed with either symmetrical or unsymmetrical 2,6-disubstituted phenols in the presence of alkali to yield the corresponding bis(4-hydroxyaryl)-methanes, **29**.

Radical coupling reactions such as the dimerisation[46] of 2,6-di-tert-butyl-quinone methides (**30**) can also lead to bis-phenols derivatives. Thus, the bis-phenol **32** is obtained from the corresponding biradical intermediate, **31** (equation 15).

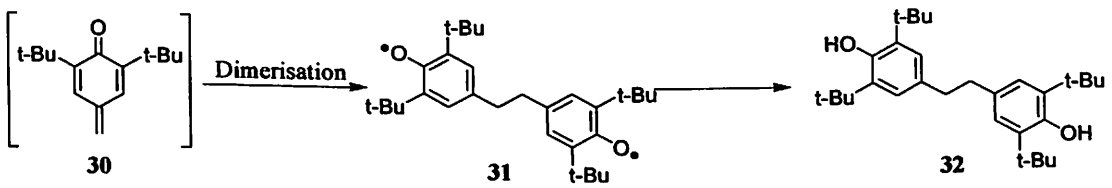

Equation 15

Bis-phenols having tetraphenylmethyl structures can be prepared from diaryl quinone methides such as **33** (equation 16).

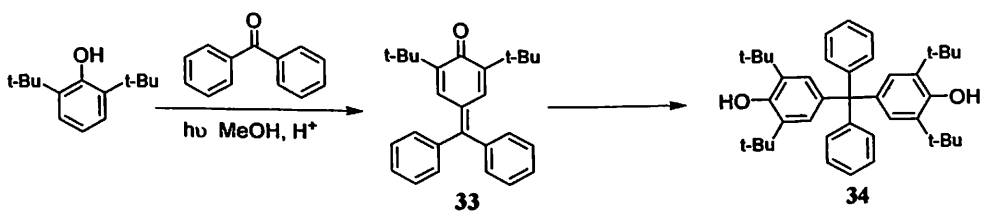

Equation 16

The compound **33** is obtained upon acid-catalyzed photo-addition of 2,6-di-t-butylphenol and benzophenone[47] in alcoholic solution. Further reaction of **33** in the presence of excess of 2,6-di-t-butylphenol to give the bis-phenol, 4,4'-dihydroxy-3,3',5,5'-tetra-t-butyl-tetra-phenylmethane, **34**.

Thus, the foregoing discussion highlights some of the synthetic methodologies used for the synthesis of bis-phenols and their analogs. Depending on the structure and the orientation of

the functional groups in the target bis-phenol, different synthetic routes need to be adopted. However, there is still scope for developing new environment friendly protocols for the synthesis of structurally diverse bis-phenols including asymmetric bis-phenols.

1.4 Hydrogen Bonding in Bis-Phenols and Analogs

The ability to predict and control intermolecular interactions in the solid state may have ramifications in the design and synthesis of solids and crystalline materials that have desired composition, topology, and reactivity[48]. In this regard, the hydrogen-bonded assemblies of bis-phenols that have trigonal or tripodal geometries are interesting because they lead to the formation of network structures.

Generally, O–H···O hydrogen bonding interactions between hydroxy groups are strong and highly directional. The hydroxy groups of phenolic derivatives are more acidic than that of alcohols, and hence they can form stronger hydrogen bonds as donors with suitable hydrogen-bonding acceptors. In certain cases the oxygen atom of the hydroxy group of the phenol can also behave as an efficient hydrogen bond acceptor. Thus it is reasonable to expect that the presence of two such O–H groups in a bis-phenol would impart intrinsic molecular and supramolecular dimensions to a bis-phenol.

Apart from O–H···O interactions, a few other intermolecular interactions[49] such as C–H···O, O–H···π, O–H···N (Fig.4) are also important in determining the solid-state structures of substituted bis-phenols. However, these C–H···O and O–H···π interactions are weak in nature compared to conventional hydrogen bonds. A detailed understanding of the energetic and geometrical aspects of these interactions is essential in the construction of porous frameworks, nano-structured materials and in catalysis.

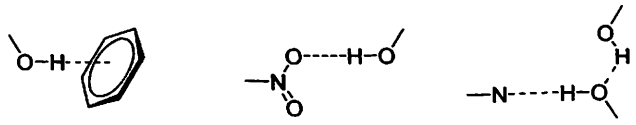

Fig.4 Examples of weak supramolecular interactions in bis-phenols

As far as the synthesis of porous materials is concerned, it is desirable to identify molecules that can generate open framework structures by self-assembly. In this regard, the presence of strongly hydrogen-bonding groups and structural rigidity is underlined. With this objective the hydrogen-bonded assembly of the bis-phenols such as 4,4'-bis(4-hydroxyphenyl) cyclohexanone and 4,4'-bis(3-methyl-4-hydroxyphenyl)cyclohexanone **(35a,b)** have been studied. It has been reported that the former gives rise to self inclusion host-guest structures, the latter exhibits interpenetration of non-identical networks[50].

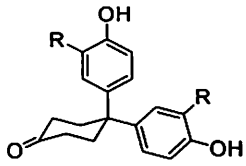

R = H, Me

35 (a, b)

The bis-phenol, 4,4-bis(4'-hydroxyphenyl)-1-cyclohexanol (**36**), has a T-structure[51], in which the cyclohexane ring adopts a chair conformation where the alcoholic hydroxy group is equatorial.

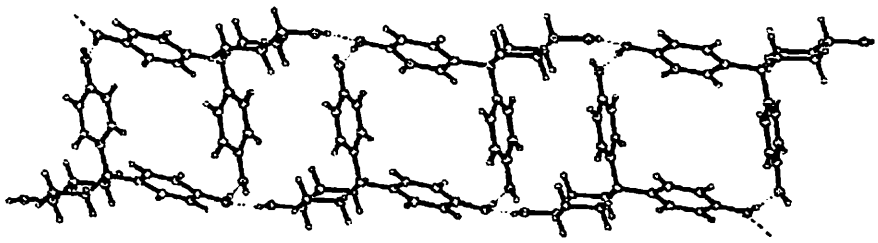

Fig.5 Structure of the supramolecular ladder formed by 4,4'-bis(4'-hydroxyphenyl)-1-cyclohexanol (**36**) along [010]

It has been reported that this molecule forms two-dimensional supramolecular ladders by self-assembly. The ladder structures are generated by O–H···O hydrogen bonded helices that run down [100]. The molecular and supramolecular synthons in this molecule are easily identified; three distinct O–H···O hydrogen bonds are formed, such that the donor-acceptor abilities of each of the three O–H groups are satisfied. The topology of the network finds parallel in three-connected coordination polymers. Interestingly, the spacers between the rungs of the ladder are determined by the sizes of the phenyl and cyclohexyl rings along [010], and that the individual ladders are hydrogen bonded into an infinite homodromic chain which gives rise to a helical structure running down [100] plane. Thus, the compound **36** generates open frameworks by self-assembly.

However, the tris-phenol analog, 1,3,5-tris(4-hydroxyphenyl)benzene, **37** which crystallizes in C2/c space group[52], does not have the open framework structures. The crystal structure shows that the hydroxy groups of the phenol residues are oriented such that they form a cooperative chain of five O–H···O hydrogen bonds (b, c, d, e, f) as shown in Fig.6. The formation of O–H···O hydrogen bonded chain is supplemented by C–H···O and O–H···π hydrogen bonds; the former precedes the chain of hydrogen bonds, while the latter terminates it. Similar observations involving finite hydrogen bonding chains have also been reported in certain carbohydrates[53].

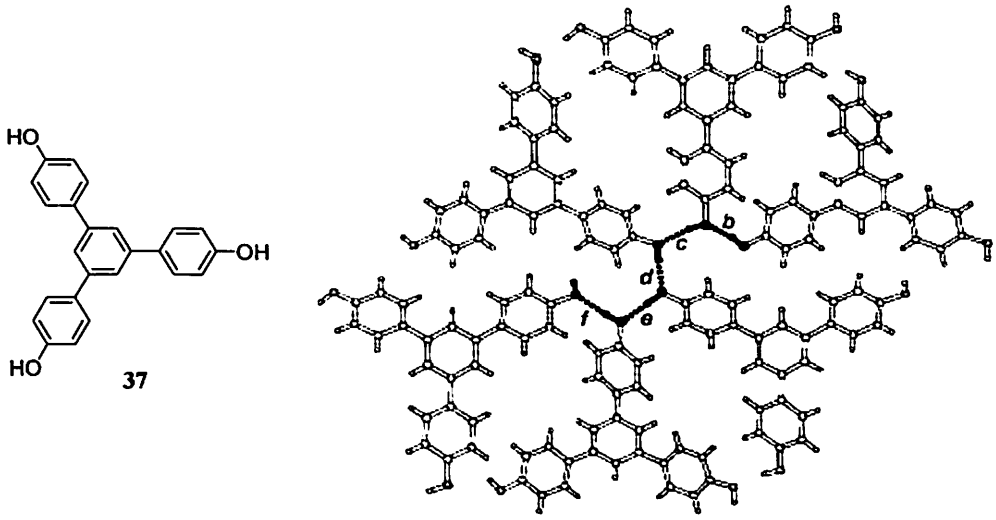

Fig.6 Structure of 1,3,5-tris(4-hydroxyphenyl)benzene, **37** and the cooperative chain of five O–H···O hydrogen bonds involving six molecules in the crystal.

It has been found that in linear hydrogen-bonded arrays, σ-cooperativity enhances the strength of individual hydrogen bonds as reflected in this system. This occurs through mutual polarization of the donors and acceptors along the chain of $O^{\delta-}–H^{\delta+}\cdots O^{\delta-}–H^{\delta+}\cdots O^{\delta-}–H^{\delta+}$ hydrogen bonds in such a way that for every additional hydrogen bond in the array, the average bond strength is increased.

Bis-phenols having triphenylmethyl frameworks can form interesting hydrogen-bonded assemblies[54,55] and give inclusion complexes[56] with solvents as guest molecules.

Self-assembly and inclusion properties of tris-phenols such as **38-40** show that molecular geometry and intermolecular hydrogen bonding interactions involving the O–H groups of phenols can result in interesting three-dimensional structures.

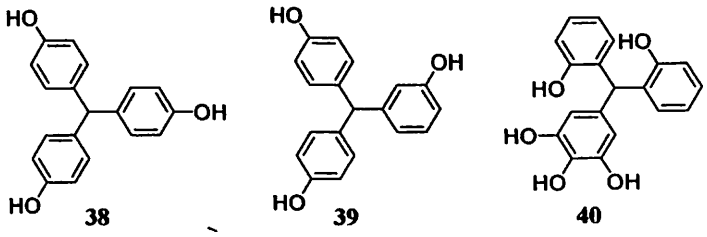

Tris(4-hydroxyphenyl)methane, **38** have been synthesized and its structure is determined by X-ray crystallography[51]. The hydroxy groups of tris-phenol molecules act as donors and acceptors of hydrogen bonds so that each molecule is bonded to six other molecules. In this structure, the O1–H groups act as donors to O2 at (x-½, y-½, z), which generate O–H···O hydrogen bonded chains parallel to [110].

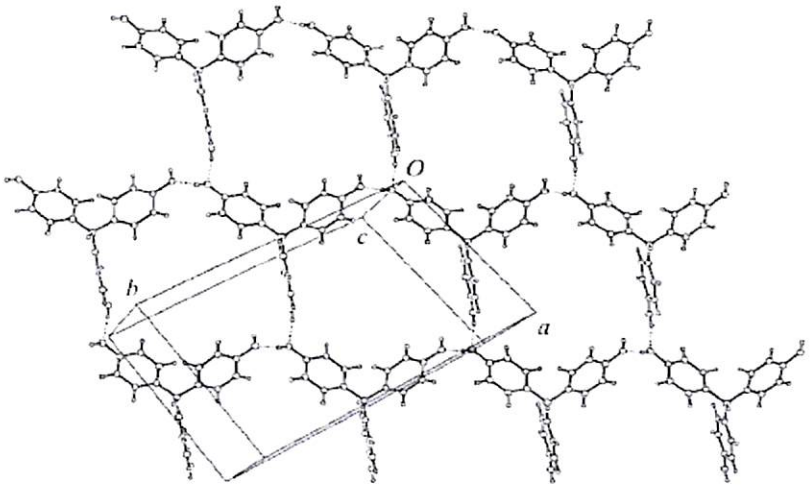

Fig.7 Structure of tris(4-hydroxyphenyl)methane **38** and a view of the two-dimensional square network parallel to [-111] plane

Hydrogen bonding between O3 (donor) and O1 (acceptor) at (1+x, y, 1+z) leads to a chain of molecules parallel to [101]. These two motifs are involved in the formation two-dimensional square networks (Fig.7) parallel to [-111] plane.

It has also been shown that each molecule of the tris-phenol **38** is linked to six adjacent molecules through O–H···O hydrogen bonds (O3–H···O1, 2.670Å, 161.9°; O2–H···O3, 2.679Å, 164.5°) such that each hydroxy group of the phenol participates in the formation of monohelical chains (Fig.8) running along the *a*-axis[52].

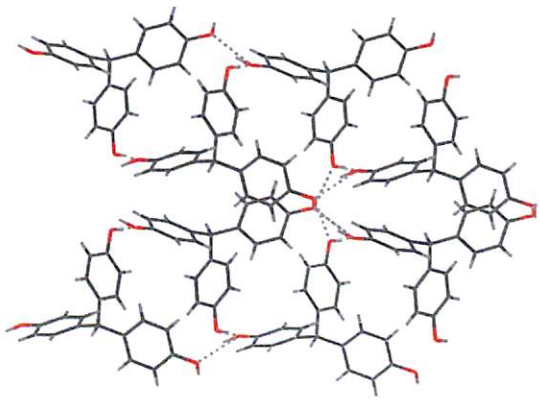

Fig.8 Intermolecular hydrogen bonding in **38** results in monohelical assembly of the tris-phenol molecules

The crystal structure of the tris-phenol **39**, shows that each molecule is linked to six symmetrically oriented tris-phenol neighbours through six hydrogen bonds (O2–H···O1 2.745 Å, 152.9°; O3–H···O2 2.786 Å, 147.9°; O1–H···O3 2.814 Å, 172.0°). This results in the formation of distorted ladder type hydrogen bonded chains (Fig.9).

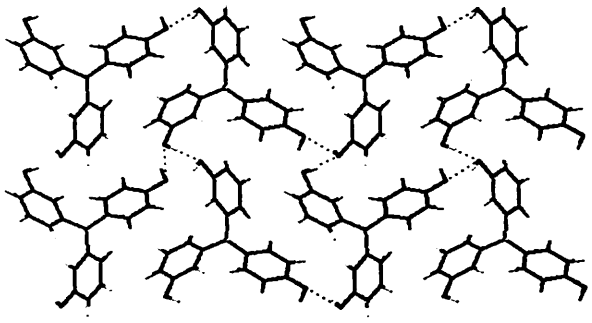

Fig.9 Hydrogen-bonded assembly of **39** leads to the formation of distorted ladders

The pentakis-phenol **40** crystallizes as a tetrahydrate in P-1 space group. In this case, the water molecules are anchored into the lattice through a network of intermolecular hydrogen bonds (O4–H···O4 2.762 Å, 160.2°; O2–H···O3 2.806 Å, 147.0°; O3s–H···O1s 2.778 Å, 162.7°; O1s–H···O4s 2.742 Å, 168.6°; O4s–H···O3s 2.765 Å, 175.7°), such that the cyclic hexamers (Fig.10) are formed. These cyclic hexamers formed by the water molecules adopt chair conformations of cyclohexane.

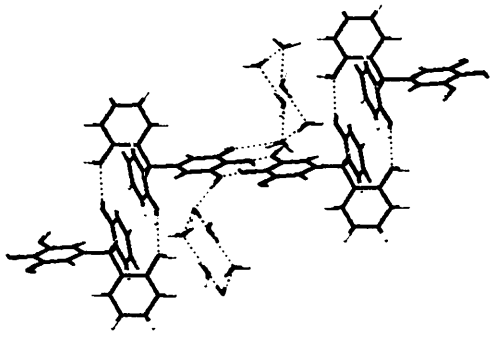

Fig.10 Intermolecular hydrogen bonding in the tetrahydrate of **40**

Similarly, the tetrakis-phenols **41–44** are important molecular tectons for crystal engineering. These compounds can form variety of hydrogen-bonded structures from which it is apparent that the hydroxy group of the phenol can direct the formation of highly porous hydrogen-bonded networks.

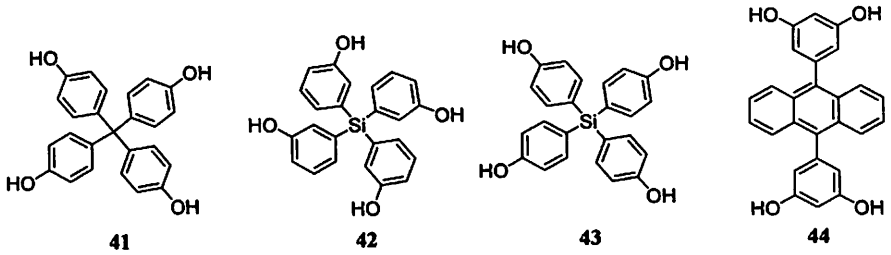

The crystal structure of the tetrakis-phenol **41** shows that each molecule is hydrogen-bonded to six neighboring tetrakis-phenols producing zig-zag chains running along the *c*-axis, and

measuring about 3.3 × 4.4 Å at the narrowest point. Approximately 28% of the volume of the crystals of tetrakis-phenol **41** is thus available for inclusion (Fig.11a,b), and ethyl acetate is found as guest[57].

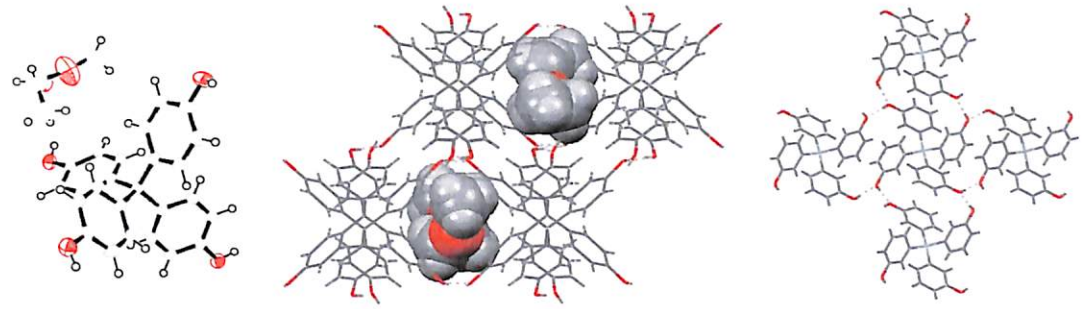

(a) (b) (c)

Fig.11 (a) Structure of the ethyl acetate adduct of tetrakis-phenol **41**, and (b) the inclusion compound in the crystal lattice (viewed normal to [001] plane); (c) Hydrogen-bonded assembly of tetrakis-phenol **42**.

The silane analogs of the tetrakis-phenols, **42** and **43** were also reported to produce a series of hydrogen bonded network structures when crystallized from ethyl acetate. The structure of the tetrakis-phenol **42** shows that each molecule is linked to four symmetrically oriented tetrakis-phenol neighbours (Fig.11c) through O–H···O hydrogen bonds. Similarly, each of the hydroxy groups of the tetrakis-phenol **43** participates in the formation of two intermolecular hydrogen bonds, both as donor and acceptor, producing helical chains that run parallel to the *c*-axis[57]. In this case, each molecule of **43** is linked to four symmetrically oriented neighbours through eight O–H···O hydrogen bonds, which creates a diamondoid network without interpenetration. The tetrakis-phenol **43** crystallizes as a monohydrate, with the water molecules being present in the lattice as structural elements. Each molecule of **43** forms hydrogen bonds with two molecules of water and four unsymmetrically oriented neighbouring molecules producing a close-packed structure. The tetrakis-phenol **44** in comparison has extended hydrogen-bonded networks and open frameworks with 62% porosity[58]. It is reported that the tetrakis-phenol **44** forms inclusion compounds with polar guests such as alcohols, esters, and ketones.

Branched phenols such as 1,1,2,2-tetrakis(4-hydroxyphenyl)ethane (**45**) is known to form crystalline inclusion complexes/compounds with N-donor compounds. Using this compound as complexing agent certain guest molecules have been isolated from mixtures[59,60]. It was also been reported[61] that the tetrakis-phenol **45** forms inclusion complexes with guest molecules such as 5-chloro-2-methyl-4-isothiazolin-3-one, **46** in 1:2 stoichiometry.

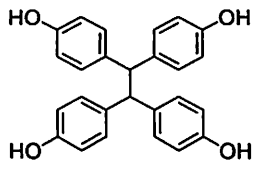

45

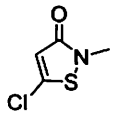

46

The crystal structure of this inclusion complex shows that each of the hydroxy groups of the phenol are hydrogen bonded to the hydroxy groups of four other molecules resulting in the formation of molecular sheets; thus the compound has a layered structure. Surprisingly the complex undergoes guest exchange in aromatic solvents such as p-xylene to give the 1:1:1 complex of phenol: **46**: p-xylene.

Bis-phenolic molecules bridged with groups such as biphenyl (**47**) or terphenyl[62] are potential tectons for crystal engineering.

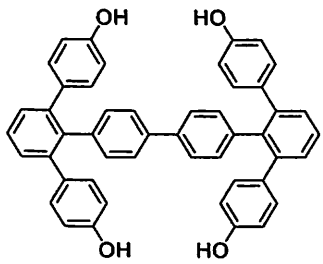

47

Because the phenolic groups are mounted on a rigid molecular scaffold and the torsion about the biphenyl bridge, the hydroxy groups of the phenol will be pointing in opposite directions. The report suggests that the biphenyl spacer control the angles between the hydroxy groups which facilitate the formation of directional O–H···O hydrogen bonds over close packing.

It has been reported[63,64] that the host molecule, hexakis(4-hydroxyphenyl)benzene, **48** gives rise to flexible yet non-penetrating hydrogen bonding networks. The report also shows that intermolecular O–H···O hydrogen bonding interactions between the radial hydroxy groups of **48**, lead to the formation of highly porous structures in the solid-state. The flexibility of these networks has been demonstrated by X-ray crystallography of the host-guest structures[65] formed with guest molecules such as methyl benzoate, ethyl acetate, diethyl ether, and dimethylformamide.

In the inclusion compound with diethyl ether (Fig.12), the hydroxy groups of the **48** take part in the formation of two-dimensional hydrogen bonded networks or sheets in which O2–H···O3 and O3–H···O1 distances are 2.81 and 2.74Å respectively. Each of these networks is infact an anti-parallel assembly of hydrogen-bonded ladders that leads to the formation of molecular tapes along the *b*-direction.

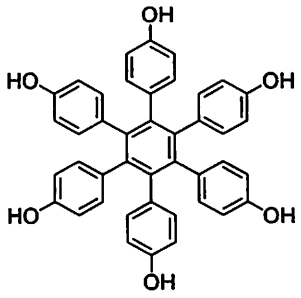

48

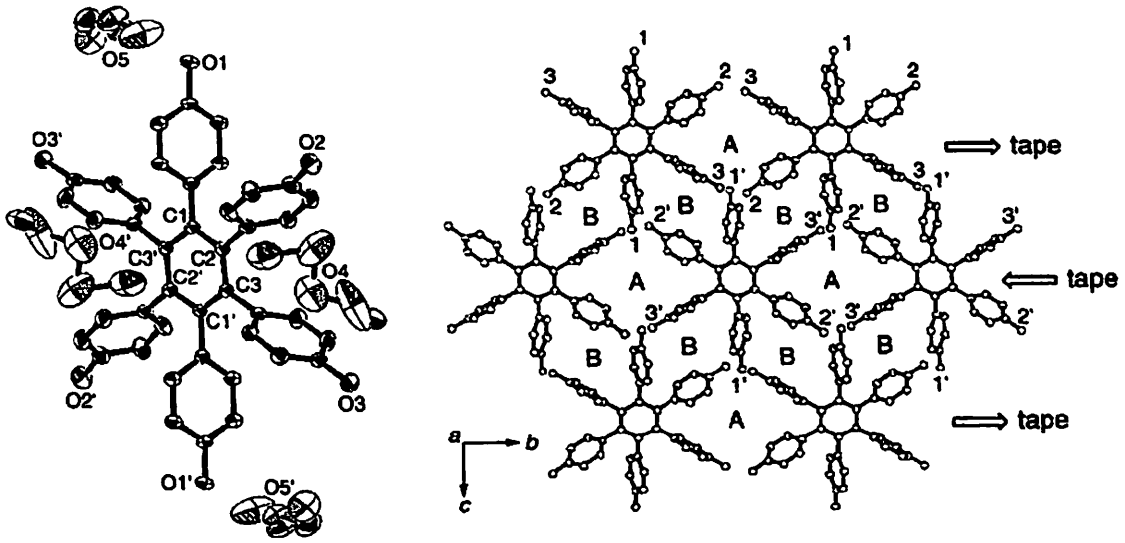

(a) (b)

Fig.12 (a) Structure of the inclusion co-crystal of hexakis(4-hydroxyphenyl)benzene (**48**) with diethyl ether; and (b) two-dimensional hydrogen bonded network (molecular sheet) parallel to the *a*-axis and the types of channels, **A** and **B** (the solvent molecules are omitted for clarity).

The molecular sheets linked by O3–H···O1 interactions are layered without translation such that two types of extended channels, **A** and **B** are formed along the *a*-axis. The structure shows that two of the four ether molecules present in adduct are hydrogen bonded to the O1–H of the phenol. The other two molecules are close to the aromatic core, such that the methyl groups are within 3.6Å from the face of the core.

In one of the early studies, the crystal structure of hydroquinone, i.e. 1,4-dihydroxybenzene and its polymorphs including the β–hydroquinone lattice is established[66-68]. The β–hydroquinone lattice belongs to the space group R–3 and has ability to form inclusion compounds with different guest molecules[69,70], including Ne, HF, H_2S, MeOH and even C_{60}. This structure of hydroquinone is also important because of its close resemblance to the rhombohedral lattice of β-polonium, which is also known to form inclusion compounds. The

crystal structure of the analogous bis-phenol, 4,4'-terphenyldiol (**49**) as a 1:1 adduct with dimethylsulfoxide (Fig.13) is known[71] and this compound does not have any polymorph.

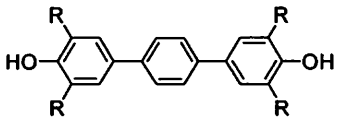

49: R = H
50: R = Me

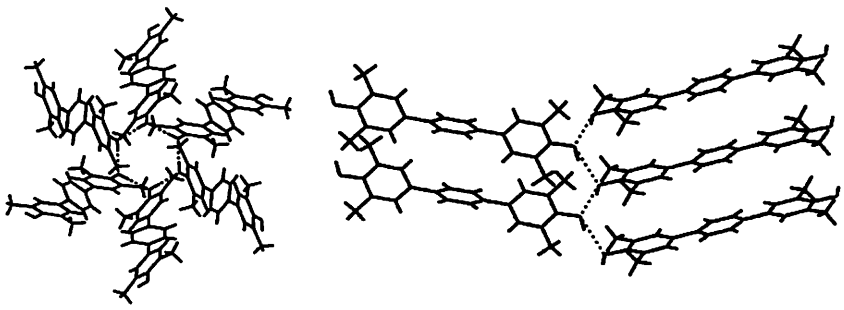

(a) (b)

Fig.13 Structures of 4,4'-terphenyldiol, **49** and 2,2',6,6'-tetramethyl-4,4'-terphenyldiol, **50**; (a) Polymorph of **50** that contains O–H···O hexamers, in R–3 space group and (b) the other polymorph of containing infinite O–H···O bonded chains in $P2_1/c$ space group

However, the homologous bis-phenol, 2,2',6,6'-tetramethyl-4,4'-terphenyldiol (**45**) does exhibit polymorphism (Fig.13), and two polymorphs are reported[71]. This compound **45** can crystallize in rhombohedral R-3 space group, and as a polymorph in $P2_1/c$ space group, thereby revealing striking similarity with β- and γ-hydroquinone lattices.

Compounds such as 2,5-diphenylhydroquinones, **11** and 1,1-bis(4-hydroxyphenyl)-cyclohexane **51** are also known to form inclusion compounds with suitable guests molecules. Thus, compound **11**, which is axially chiral have been used for studying molecular inclusion where it behaves as chiral host. It is found that N-alkylchinchonidinium halides[72] are effective substrates for the resolution of these chiral bis-phenols. Similarly, the inclusion complex of **51**, water and acetylacetone (1:1:1) is also characterized[73] that reveals selective inclusion of the enol form of acetylacetone (Fig.14).

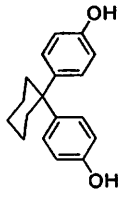

51

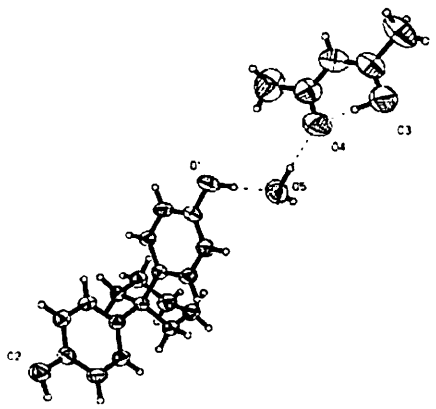

Fig.14 Crystal structure of the adduct of **51** with the enol form of acetylacetone

The inclusion of three picoline isomers with 2,2'-binaphthol occurs due to the formation of strong intermolecular O–H···N hydrogen bonding interactions[74]. It is observed that 2- and 4-picoline can selectively be enclathrated, which has been confirmed by thermal stability measurements and competition experiments. The structure of the 2-picoline inclusion compound is stabilized by strong intermolecular host···guest interactions that involve O_{host}–H···N_{guest} interactions, with a hydrogen bonding distance of 2.697(2) Å. Adducts of bis-phenols with amines have been studied[75] from the viewpoint of supramolecular chemistry and it is observed that like neutral phenols, phenolates are also important supramolecular motifs.

It is also reported that 2,2'-bis(4-hydroxyphenyl)propane (**2**) forms 1:1 complexes between and several alcohols, amines, hydrazine[76]. In case of the complex of **2** with methyl hydrazine (**52**), (equation 17) it is observed that the two components are connected by O–H···N hydrogen bonds[77]; one of the hydroxy groups of the phenol is linked to the amino group while the other to the methylamine nitrogen resulting in a centrosymmetric dimeric structure.

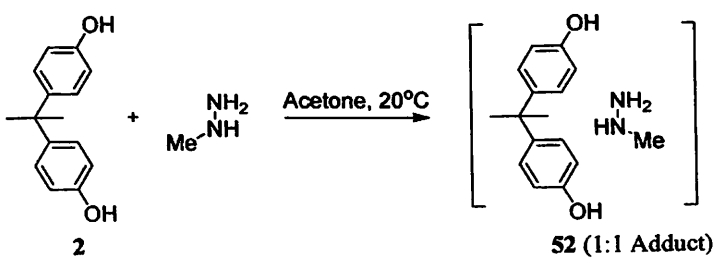

2 **52** (1:1 Adduct)

Equation 17

Tris(4-hydroxyphenyl)ethane (**23**) forms an adduct with 1,2-bis(4-pyridyl)ethane (**53**) which has 1:2 stoichiometry[53]. In this adduct, intermolecular O–H···O hydrogen bonding between the hydroxy groups of **23** lead to the formation of molecular sheets (Fig.15) that run parallel to [100]. These symmetry-related sheets are interlinked by O–H···N hydrogen bonds

involving the nitrogen atoms of **53**, which serve as hydrogen bond acceptors, thereby resulting in the formation open bilayers.

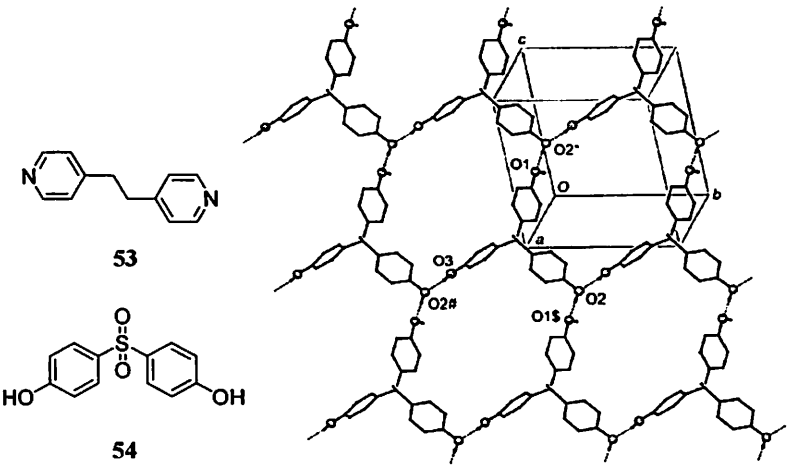

Fig. 15 Molecular sheets formed by **23** in the 1:1 adduct with 1,2-bis(4-pyridyl)ethane (**53**)

The structure of the 1:1 adduct of this tris(4-hydroxyphenyl)methane with 4,4'-bipyridine shows that one of the hydroxy groups of the phenol acts as hydrogen-bond donor to another oxygen atom of a phenol related by a *d*-glide, while the other two hydroxy groups are hydrogen bond donors to the bipyridyl groups. Thus, each tris-phenol molecule is connected to two other phenolic units through zigzag chains O–H···O hydrogen bonds. These hydrogen bonded chains which are parallel to [-101], are connected by weak C–H···O interactions and this leads to the formation of rectangular grids parallel to *ab*–plane, with voids of dimensions 9.6 × 12.5 Å. The nitrogen atoms of bipyridine serve as acceptors to the hydrogen bonds formed by the two of the hydroxy groups of the tris-phenol so that each rectangular network is connected to two others by bipyridine molecule.

Hydrogen bonding interactions between the bis-phenol **54** and bis(2-aminoethyl)-amine in the 1:3 adduct leads to the formation of novel three-dimensional frameworks[78]. The molecular structure shows that in this adduct, one of the bis-phenol molecules occupies a general position while the other across a twofold axis, together with the amine molecule, each with occupancy 0.5. The bis-phenol molecule that occurs in the general position is neutral while the one lying on the two-fold axis is anionic, because both of the protons are transferred to the amine (Fig.16). Thus, the three-dimensional supramolecular structure consists of only intermolecular O–H···O and N–H···O hydrogen bonds, except for the sulfone O-atom that is bonded to the neutral bis-phenol. In the 2:1 adduct of **23** with ethylene diamine, it is seen that the amine is the acceptor of O–H···N hydrogen bonds[79,80]. In contrast, the 2:1 adducts of phenol and ethylene diamine show that each nitrogen atom exhibits both donor and acceptor properties.

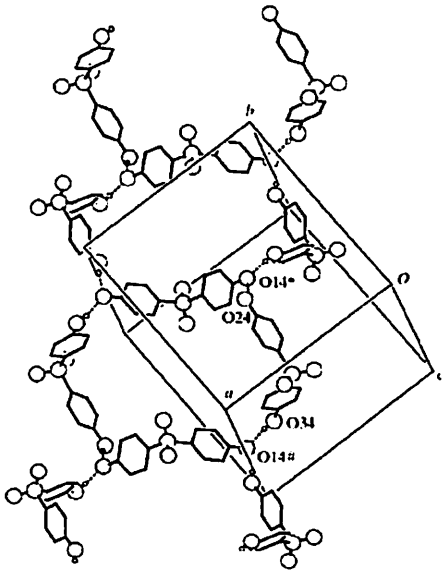

Fig. 16 View of the molecular ladders formed due to strong O–H···O hydrogen bonding interaction between the neutral and anionic units of bis-phenol **54** in the adduct.

Similarly, in the methanol-solvated adduct of 4,4'-biphenol and ethylene diamine, the nitrogen atoms acts both as donor and acceptor of hydrogen bonds in a continuous three-dimensional diamondoid network.

1.5 Scope of the Present Work

The study of hydrogen-bonded self-assembly in bis-phenols can have important applications in crystal engineering and solid-state chemistry. The understanding of the different types of intermolecular interactions that operate in bis-phenols will also elucidate the processes leading to self-assembled structures[81-85]. It is important to realize that the analysis of such systems will further strengthen our ability to predict and hence control intermolecular interactions in similar compounds. This will also enable us to design and construct more complex macromolecular and supramolecular systems.

Recently, the synthesis and properties of a series of phenol-based molecules, including molecules such as **55**, **56** and **57**, which are also referred to as dendron rod-coils[86] have been reported. These rod-coils can self-organize into discrete nanostructures through non-covalent interactions[87-89]. While the rod-coils (**55**) consisting of biphenyl esters and bulky amorphous coils assemble into discrete mushroom shaped nanostructures[90,91], the triblock rod-coils, **56** are found to be thermotropic liquid crystalline materials with birefringence from room temperature to 300°C when it becomes isotropic.

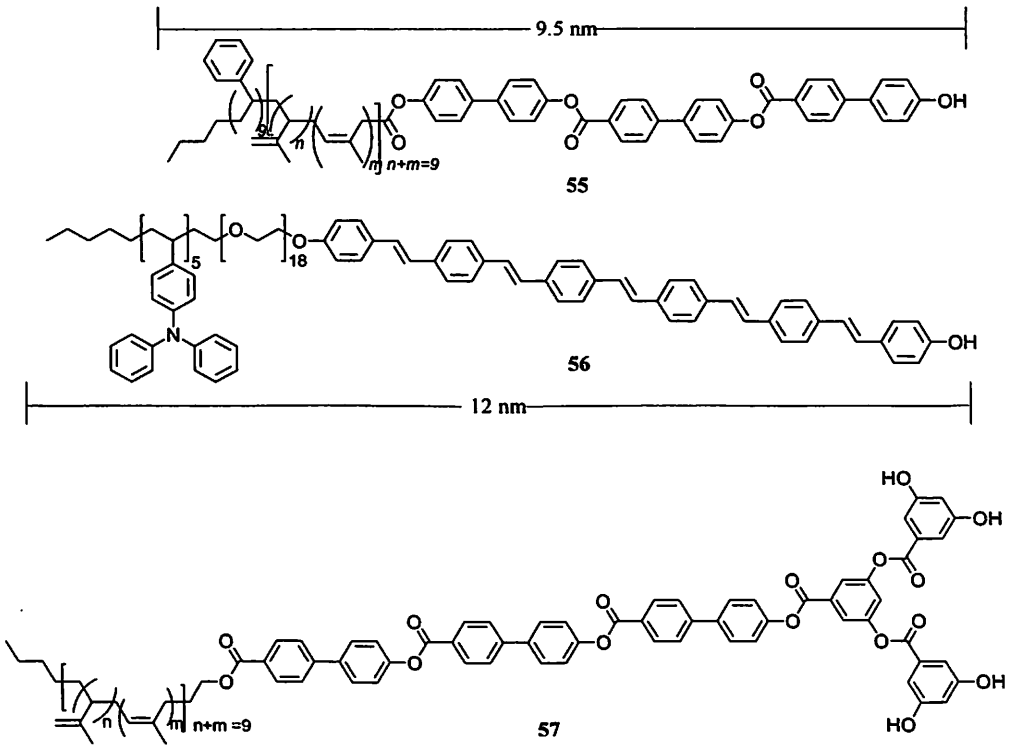

Electron diffraction studies on thin-films of **56** show that the rod segments are oriented perpendicular to the plane, so as to form crystalline domains that are interrupted by amorphous regions.

Similarly, it has been shown that the self-assembled nanostructures are obtained from bis-phenol based molecules such as **57**, which are also referred to as dendron rod-coils. The formation of such self-assembled structures is attributed to intermolecular hydrogen bonding between the hydroxy groups at the periphery of the dendron and aromatic π-π interactions between the biphenyl systems. Studies using transmission electron microscopy (TEM) and atomic force microscopy (AFM) show that these dendron rodcoils self-assemble to form network-like structures, which consist of nanoribbons that are 10nm in thickness and are microns in length.

The synthesis of flexible organometallic dialkynyldigold(I) **60**, from bis-phenol precursors such as **58** have shown that metal ion templating (equation 18) leads to topologically intricate molecules[93].

These molecules are attractive systems for the development of nanoscale devices. It is observed that in a bis-phenol having two aromatic rings that are bridged by methylene spacer, there are three possible arrangements of the molecular rings[93]. This result in the formation of different topological isomers such as self-assembled molecular rings (**61a**), [2]catenanes (**61b**, equation 19) and double-braided catenanes.

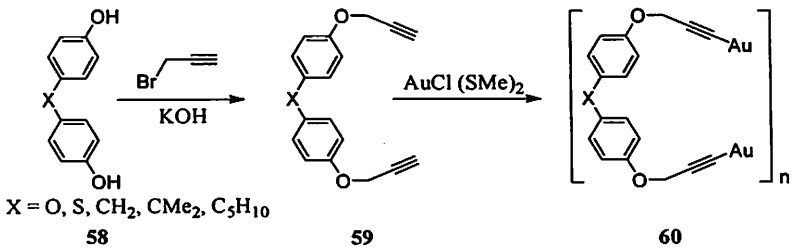

Equation 18

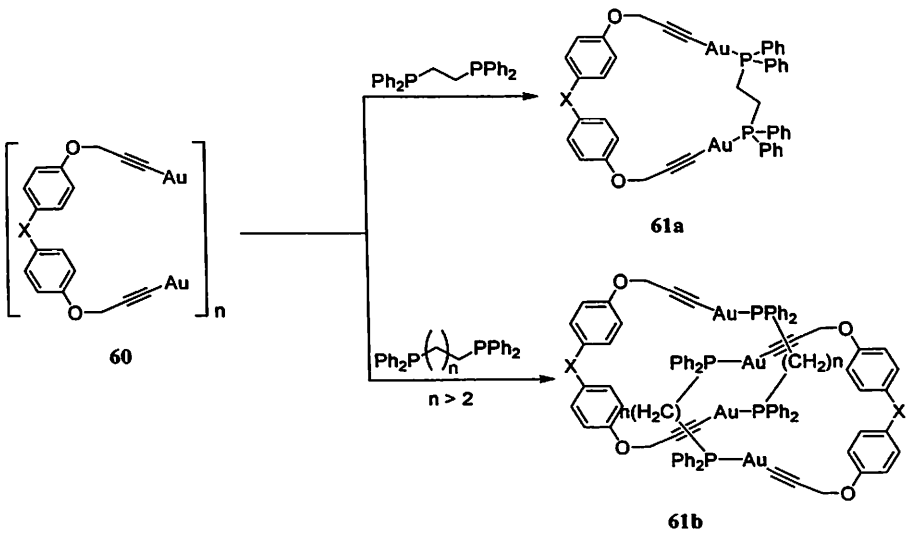

Equation 19

As already mentioned, the study of bis-phenol molecules assumes significance because of the potential applications of crystalline solids and microporous materials in separation technology, in gas adsorption, in catalysis and in performing solid-state reactions. Even though there are a number of reports regarding the synthesis of bis-phenols, the structural aspects need to be elucidated for better understanding. In this regard, bis-phenols having triphenylmethyl framework are attractive compounds as they possess the prerequisites that can lead to the formation of interesting hydrogen bonded assemblies and inclusions structures.

With this objective a series of bis-phenols, bis(4-hydroxy-3,5-dimethylphenyl)aryl methanes (**62**) are prepared and characterized. The crystal structures of these compounds have been studied in order to delineate the effects of different hydrogen-bond donor and acceptor groups in the formation of self-assembled structures. The presence of methyl groups in the near vicinity of the hydroxy groups of the bis-phenols leads to steric effects, which is reflected in the geometry of the hydrogen bonds.

It has been pointed out that the host-guest chemistry of the bis-phenol analogs is an important emerging area of research in supramolecular chemistry. Thus, in this study we also present a crystallographic study of the structures of the inclusion compounds obtained from a few bis-phenols to illustrate the guest binding properties of these compounds.

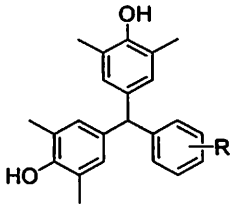

62

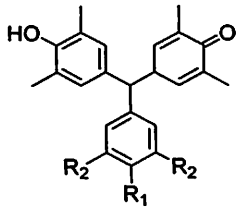

63

It is interesting to note that the bis-phenols readily undergo oxidation to give the corresponding quinone methide derivatives (**63**). We have prepared a few of the quinone methide derivatives. The quinone methides thus obtained have intramolecular donor–acceptor structures and hence have chromophoric properties. The chromophoric properties of these quinone methides are dependent on the electron delocalisation over the donor-acceptor framework. Besides this, understanding the solid-state structures of these compounds is an important issue in in crystal design. Accordingly, some of the compounds have been studied by crystallography.

Chapter 2

Synthesis and Characterisation of Bis-Phenols

As already described in Chapter 1, bis-phenols can be synthesized from both substituted and unsubstituted phenols by various methods. We have also mentioned that bis-phenols can be synthesized by direct condensation of phenols with carbonyl compounds, and that the reaction of unsubstituted phenol with carbonyl compounds in acid medium gives polymeric compounds. The synthesis and characterization of bis-phenols that contain triphenylmethyl framework is one of the objectives of this work. Among the different types of bis-phenols that have this structure, the focus is mainly on those compounds containing the 2,6-dimethylphenol units for the following reasons:

1. Selectivity in the formation of the desired product
2. Facile transformation of the functional groups without affecting the triphenyl methane framework of the molecules
3. Geometrical effects of the methyl groups on the structure and hydrogen-bonding properties of the bis-phenol molecules

2.1 Synthesis and Characterization of Bis-Phenols

In the present study we have extended the scope of the condensation reaction involving phenols with different carbonyl compounds to synthesize the series of bis-phenols, **2.1** and **2.2**. As pointed out it is essential that the synthetic routes which are employed results in the formation of the bis-phenol molecules having triphenyl methane structure and not polymeric compounds.

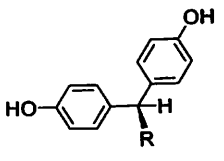

2.1

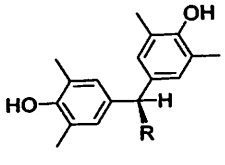

2.2

Moreover, we have prepared bis-phenols **2.1** by condensing phenol with a few aromatic aldehydes in 2:1 stoichiometry to illustrate the effectiveness of the synthetic routes. Depending on the reactivity of the phenol and the aldehyde, the reaction conditions need to be varied. Thus, we have performed the condensation reactions of both phenol and 2,6-

dimethylphenol with a few aromatic aldehydes in acidic medium and optimized them so as to obtain best synthetic results. In this regard three different procedures (Procedure **I**, **II** and **III**) have been adopted to prepare the bis-phenols, **2.1** and **2.2**.

In Procedure **I**, the bis-phenols are prepared by refluxing the phenol and the aldehydes in methanol in the presence of hydrochloric acid (equation **20**). These reactions are involving 2,6-dimethylphenol and most of the aromatic aldehydes are found to proceed efficiently resulting in the formation of the corresponding bis-phenols.

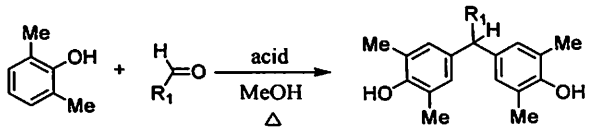

R_1= Phenyl (a)
4-Methylphenyl (b)
4-Methoxyphenyl (c)
4-Hydroxyphenyl (d)
4-Bromophenyl (e)
4-Nitrophenyl (f)
4-N,N-Dimethylaminophenyl (g)
4-Formylphenyl (h)
3-Formylphenyl (i)
4-Hydroxy-3-methoxyphenyl (j)
3,4-Dimethoxyphenyl (k)
3,4,5-Trimethoxyphenyl (l)
1-Naphthyl (m)
2-Naphthyl (n)
4-Pyridyl (o)
2-Pyridyl (p)

2.2

Equation 20

In contrast, the reaction between simple phenol and aldehydes mostly gave polymeric materials from which the desired bis-phenol, **2.1** could not be isolated. This route can be used for the synthesis of a variety of substituted bis-phenols, using 2,6-dimethyl phenol and different aromatic aldehydes (please refer to Table **7.1-7.4** in the experimental section, Chapter 7). Moreover, the reactions of 2,6-dimethylphenol under the above reaction conditions with aromatic aldehydes give good yields except for those containing electron-withdrawing groups. For instance, in the case of nitrobenzaldehydes, this procedure leads to the formation of resins. On the other hand, 2- and 3-hydroxybenzaldehydes give complex mixtures of products, which could not be separated.

Because the carboxonium ions /carbocations obtained upon protonation of benzaldehydes are weak electrophiles, their condensation is most effective with electron rich aromatic compounds such as phenols. However, depending on the substituents attached to the benzaldehydes the reactivity of the carboxonium intermediates will be different.

Procedure **II** is a variation of Procedure **I** in that the acid used consists of a mixture of sulphuric acid and acetic acid rather than the hydrochloric acid. Accordingly, in this protocol

the reactants are dissolved in acetic acid and the reaction mixture is cooled in ice. Then a mixture of acetic acid and concentrated sulfuric acid (4:1 v/v) is added to the reactants slowly with constant stirring. As the mixture tends to solidify upon standing, vigorous stirring is sometimes required to maintain homogeneity. This reaction mixture is then kept at ice-cold temperatures (-5 to 0°C) for 2-3 days after which the products are precipitated and recrystallized. In certain cases the desired compounds are obtained after purification by column chromatography.

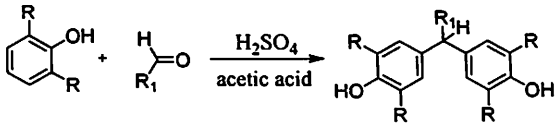

2.1: R = H
2.2: R = Me

Equation 21

Most of the bis-phenols **2.2** are prepared via Procedure **II**, and the products are obtained in good yields. Bis-phenol **2.2a** is obtained as colorless prismatic crystals while the tris-phenol **2.2d** is obtained as white needles. However, some of the bis-phenols including **2.2f**, **2.2g**, and **2.2l** are obtained as pale yellow or pink colored solids. It is to be noted that the reactions of 2,6-dimethylphenol with 4-nitrobenzaldehyde and 4-hydroxybenzaldehyde are quite efficient and the corresponding bis-phenols are obtained in good yields. The condensation reactions of 2,6-dimethylphenol with polyhydroxy-benzalaldehydes are not clean and give multiple products. In contrast, the reactions with 2- or 3-nitrobenzaldehydes give resinous products rather than the bis-phenols.

Procedure **II** has also been applied to the synthesis of the bis-phenols, **2.1** from unsubstituted phenols (p.s. Table **7.1**). The condensation of phenols with a few aromatic aldehydes (equation 22) has been optimized[96]. This procedure has been applied in the synthesis of the bis-phenols (**2.1**) discussed in this study.

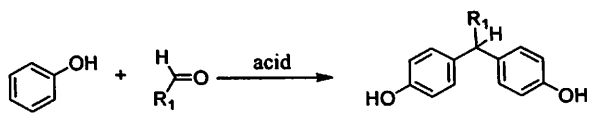

R_1= Phenyl (a)
2-Naphthyl (b)
2-Chlorophenyl (c)
4-Hydroxyphenyl (d)
3,4,5-Trimethoxyphenyl (e)

2.1

Equation 22

In most cases, condensation reactions involving phenol with aromatic aldehydes give resinous products along with the bis-phenols, which often lead to low yields of the desired products.

It is observed that the condensation reaction of 2,6-dimethylphenol and pyridine-4-carboxaldehyde did not occur with either of the procedures described above. This is probably because under these conditions only protonation of the pyridyl nitrogen is achieved rather than the carbonyl group. Thus we performed the condensation reaction with trifluoroacetic acid, which is a stronger Bronsted acid. This method, Procedure **III** requires the phenol and the aldehyde to be dissolved in dichloromethane in appropriate stoichiometry, to which trifluoroacetic acid is added. This reaction occurs quite smoothly at room temperature and with deactivated aldehydes such as pyridine-4-carboxaldehyde (equation 23) to give the corresponding bis-phenols in good yields.

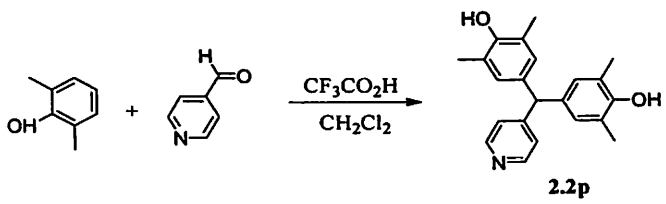

2.2p

Equation 23

Using this procedure, the condensation reaction of pyridine-2-carboxaldehyde with 2,6-dimethylphenol is also performed and the corresponding bis-phenol obtained in moderate yields. This reaction is carried out in controlled manner in order to achieve monocondensations of 2,6-dimethylphenol with both terephthaldehyde and isophthaldehyde, which give **2.2h** and **2.2i** as the major products. The bis-phenols prepared by this route are purified by crystallization.

As already mentioned, the bis-phenol **2.2f**, i.e. bis-(3,5-dimethyl-4-hydroxyphenyl)(4-nitrophenyl)methane is prepared by Procedure **II** only. However, the corresponding reduced compound, bis(3,5-dimethyl-4-hydroxyphenyl)(4-aminophenyl)-methane (**2.2q**) cannot be prepared by any of the procedures described above. In this case **2.2q** is obtained by catalytic reduction of **2.2f** using with Pd/C and hydrazine under refluxing methanol (equation 24). The reaction is efficient and the product **2.2q** is obtained in good yields, without side products. Moreover, the separation of the reduced product needed simple filtration to remove the catalyst and recrystallization.

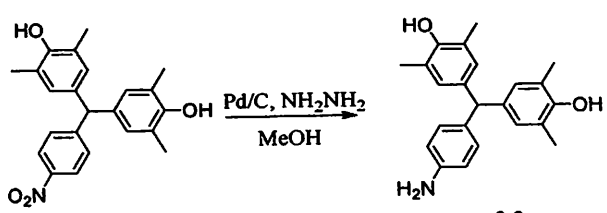

2.2f **2.2q**

Equation 24

In each case the bis-phenols have been characterized by FT-IR spectroscopy, NMR spectroscopy, and mass spectrometry. The structures of some of these compounds have been determined by X-ray crystallography. From the crystal structures of these compounds it is seen that the bis-phenol motif can take part in the formation of extensive hydrogen-bonding networks. These compounds can form molecular inclusion complexes with different solvent guests, such as acetonitrile, benzene, and toluene. These aspects are discussed in Chapter 3.

An important point which needs mention is that the bis-phenols **2.2** are sensitive to air and gradually become yellow in color because of oxidation that leads to the formation of trace amounts of diaryl quinone methides. Presence of electron-donating substituents makes the compounds more susceptible to oxidation. The synthetic and structural aspects of diaryl quinone methides are discussed in Chapter 5.

The bis-phenolic compounds are expected to self-assemble in solution through hydrogen bonding. Thus, the bis-phenols **2.2** have been studied in solution by FT-IR spectroscopy, UV-visible spectroscopy and NMR spectroscopy. The FT-IR spectrum of the compound **2.2a** in the solid state shows two O–H stretching bands (Fig.17) between 3600-3300cm^{-1}, corresponding to two types of hydroxy groups. The sharp band centered at 3589cm^{-1} indicates the presence of free hydroxy groups in **2.2a** that are not involved in hydrogen bonding. The broad absorption band at 3467cm^{-1} indicates that one of the hydroxy groups of **2.2a** takes part in the formation of intermolecular hydrogen bonds. Apart from these O–H stretching bands, the compound also shows multiple bands at 2918cm^{-1} arising from C–H stretching and ~1505cm^{-1} due to aromatic rings. Similar hydrogen bonding features are observed in the solid-state FT-IR spectrum of **2.2c**. In this case a sharp band is observed at 3574cm^{-1} corresponding to free hydroxy groups of the bis-phenol and a broad absorption around 3569cm^{-1} corresponding to hydrogen-bonded hydroxy groups.

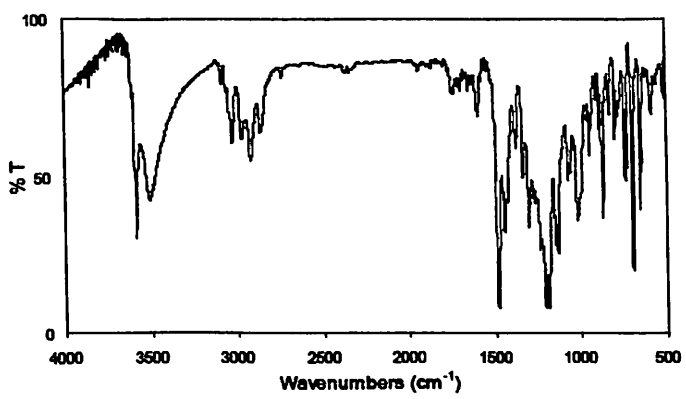

Fig.17 Solid-state FT-IR spectrum of **2.2a** shows absorptions due to free and hydrogen-bonded hydroxy groups at 3589cm^{-1} and 3467cm^{-1} respectively

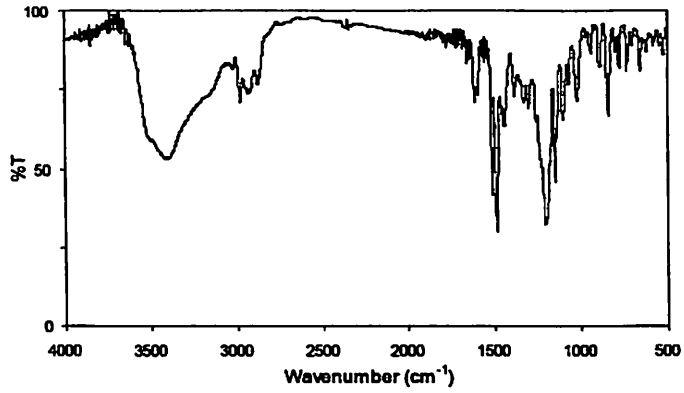

Fig.18 Solid-state FT-IR spectrum of **2.2d**

In contrast the FT-IR spectrum **2.2d** in the solid-state shows broad absorptions centered at 3493cm^{-1} indicating that the hydroxy groups of this bis-phenol are involved in extensive hydrogen bonding. Similar features are observed in the range 3500-3300cm^{-1} in the FT-IR spectra of **2.2f**, **2.2h**, **2.2j** and **2.2l** which indicates the presence of extensive intermolecular hydrogen bonding between the hydroxy groups of the bis-phenol molecules in the solid-state. The FT-IR spectra of the bis-phenols **2.2** containing both free and hydrogen bonded hydroxy groups show two absorption bands in the O–H stretching region, which are separated by $\Delta\nu$ = 42-138cm^{-1}.

The UV spectra of these bis-phenolic compounds are concentration dependent. For instance, the bis-phenol **2.2a** gives two absorption bands at 215nm and 277nm in methanol when the concentration < 0.13mM. The absorption band at 277nm is assigned to n-π^* transitions on the basis of the extinction coefficient of the band (ε_{max} = 4×10^{5}M^{-1}cm^{-1}). This band is more sensitive to concentration of the compound compared to the band at 215nm. This absorption could suggest aggregation of the bis-phenol molecules through intermolecular hydrogen bonding. Similar observations are made in most of the bis-phenols, although in case of **2.2d** this band is shifted to 287nm while for **2.2m** it is observed at 299nm. The effect of hydrogen bonding is also apparent in the UV spectrum of **2.2b** in hexane in which the two absorption bands occur at 246 and 285nm respectively, and the extinction coefficient of the latter, which is assigned to the intermolecularly hydrogen-bonded molecules, is higher.

The concentration dependent ^{1}H NMR spectra of the **2.2a** in $CDCl_3$ shows that the aromatic protons of the compound at δ_H 7.12 and δ_H 6.70 are not affected by increase in concentration. However the signal at δ_H 1.51 due to water suspended in $CDCl_3$ is shifted downfield to δ_H 1.60 (Fig.18) when concentration **2.2a** is ~1.0mM. Simultaneously, the signal due to the hydroxy groups of the bis-phenol (δ_H 4.50) become slightly broadened indicating the presence of solvent mediated proton exchange process.

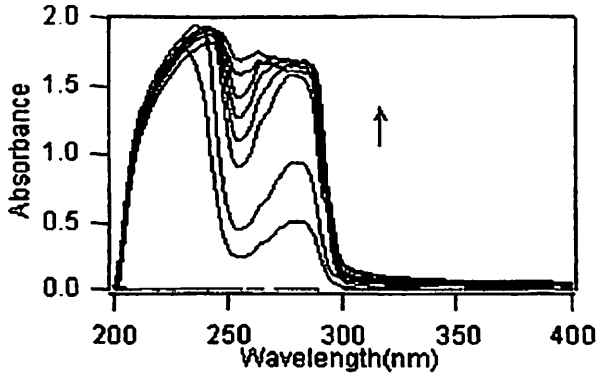

Fig.19 Concentration dependent UV spectrum of **2.2a** in methanol (concentrations 0.13mM, 0.27mM, 0.4mM, 0.53mM, 0.66mM, 0.8mM and 0.94mM)

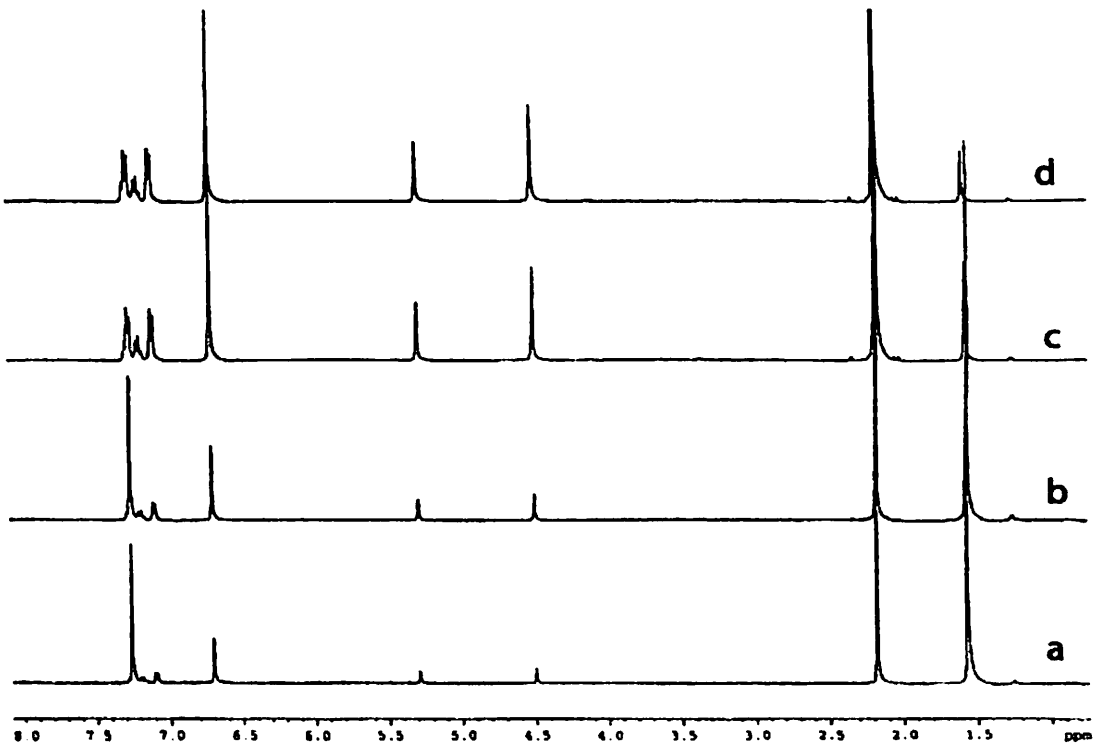

Fig.20 Concentration dependent ^{1}H NMR spectra of **2.2a** in $CDCl_3$ at room temperature (Concentration range: 0.13 to 1.0mM)

We have also observed that the NMR spectra of the bis-phenols exhibit solvent dependent behaviour. This is illustrated by the changes observed in positions of the aromatic protons in the ^{1}H NMR spectra of **2.2g** in methanol, acetonitrile and mixture of both the solvents (Fig.21). In methanol, the ^{1}H NMR spectrum of the compound shows two sets of doublets at δ_H 6.72 and 6.96 corresponding to the 1,4-dimethylaminophenyl units while the protons denoted H_α appear at δ_H 6.64. These signals for the same compound in acetonitrile appear at δ_H 6.70 and 6.89 (aromatic protons), and at δ_H 6.59 (H_α protons).

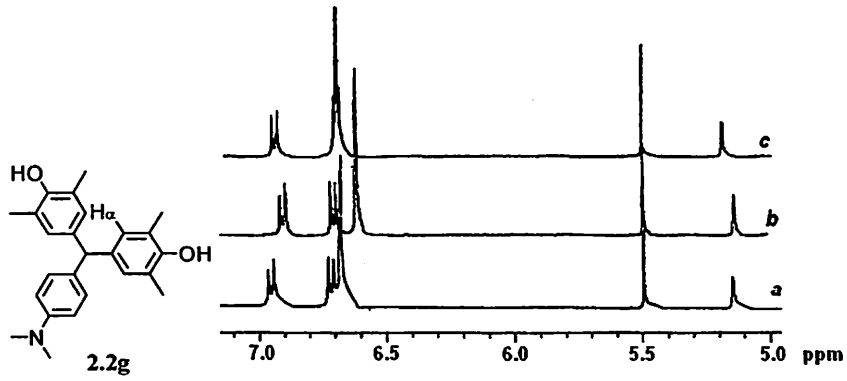

Fig.21 ^{1}H NMR of **2.2g** (a) in methanol (b) in acetonitrile (c) in 1:1 methanol-acetonitrile

On the other hand, the spectrum of the same compound in 1:1(v/v) composition of methanol and acetonitrile shows the signals due to aromatic protons at δ_H 6.71 and 6.91 and the H_α signal at δ_H 6.70. In $CDCl_3$, the aromatic signals of **2.2g** are observed at δ_H 6.69 and 6.98 while the H_α proton signal at δ_H 6.73.

2.2 Synthesis and Characterization of dimeric bis-phenols

The coupling of two bis-phenol units can be achieved by a number of routes to give dimeric compounds. In a simple strategy, two 4-hydroxybenzaldehyde molecules are coupled by using dibromoethane or ethylene glycol ditosylate to give dialdehydes, **2.4a**and **2.4b** which contain ether bridges (equation 26). The compounds **2.4** are then condensed with 2,6-dimethylphenol by Procedure **II** in order to obtain compounds **2.5** and **2.6** as the products.

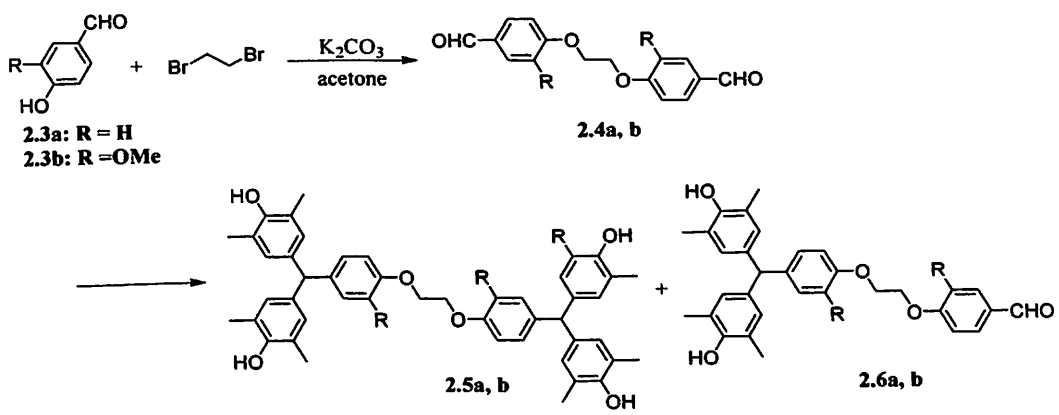

Equation 25

The formation of the mono-condensation product indicates that the reaction of the phenol with the dialdehyde (**2.4**) proceeds in steps, and the mono-condensation product initially formed reacts further to give the dimeric compound. In the case of **2.4a**, condensation reaction with 2,6-dimethylphenol gives multiple products from which only the bis-phenol

2.6a could be isolated as the main product. This happens because side reactions can occur on the phenyl ring that is linked to the ether bridge.

Alternatively, the dialdehyde **2.4b** prepared from 4-hydroxy-3-methoxy-benzaldehyde is relatively more hindered. Thus, the condensation reaction of 2,6-dimethylphenol with **2.4b** results in the formation of the bis-phenol dimer, **2.5b**, as the main product. Suffice to say that the procedure for coupling two bis-phenol units by ether bridges is applicable for the preparation of dimeric bis-phenols.

Similarly, another synthetic scheme has been designed with an objective to connect two such bis-phenol units through spacers having hydrogen bond donor and acceptor sites. As such the corresponding dimeric amide-bridged bis-phenol analogs have been prepared and characterized. It is known that primary and secondary amides, containing either aryl or alkyl spacers can self-assemble through hydrogen-bonding interactions between the amide groups on an up/down translational arrangement[11]; this results in the formation of β-sheet like structures in a highly symmetrical manner. Incorporation of two phenol end-groups in these molecules will lead to materials having useful optical and electrochemical properties. Importantly the fact that this phenolic unit can be oxidized photochemically could be crucial in its applicability as functional materials. However this aspect has not yet been studied except in certain phenoxyl based polymers and dimeric bis-galvinoyl[97].

Synthesis of the amide-bridged bis-phenols starts with the preparation of the amide derivative (**2.7**) from the corresponding diamine by reaction (equation 26) with bromoacetyl bromide.

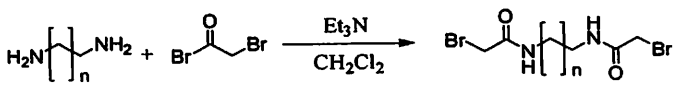

n = 1 (a), 2 (b), 3 (c), 8 (d) **2.7**

Equation 26

The diamine reacts with the acid bromide (1:2 stoichiometry) under ice-cold conditions and gives both the mono-bromoamide as well as the dibromo amide (**2.7**) as products. The desired dibromo amides **2.7** are separated from the mono-amide in moderate yields by precipitation.

Reactions between the dibromo amide derivatives **2.7** with 4-hydroxybenzaldehyde gives the corresponding amide ethers having aldehyde end-groups, **2.8** in moderate yields. Condensation of these dialdehydes, **2.8** with 2,6-dimethylphenol under acidic conditions result in the formation of the products **2.9** and **2.10** (equation 27), which are separated by chromatography.

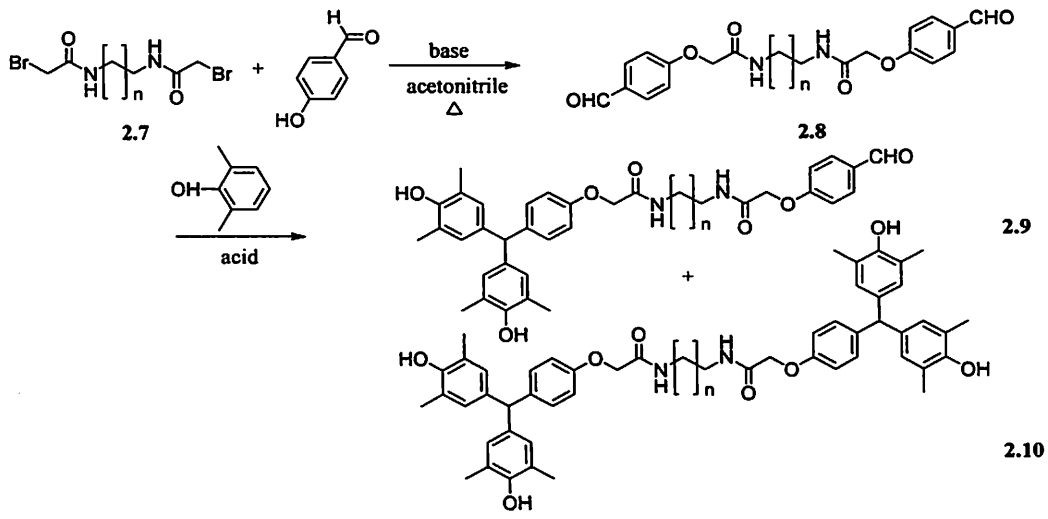

Equation 27

It may be mentioned here that in the compounds **2.9b** and **2.9c**, could not be obtained when the reaction of the corresponding dialdehydes were performed in the presence of excess 2,6-dimethylphenol. This strategy can be extended to the synthesis of dimeric amide-bridged bis-phenols, which have amide spacers of different chain lengths. In order to illustrate this, the synthesis of the dimeric bis-phenol **2.13** is described. In the first step, the dibromo amide **2.11** is prepared by reacting trans-1,2-cyclohexanediamine with bromoacetyl bromide. Subsequent reaction of the dibromo amide **2.11** with 4-hydroxybenzaldehyde gives the corresponding dialdehyde **2.12** (equation 29) as shown in the reaction scheme.

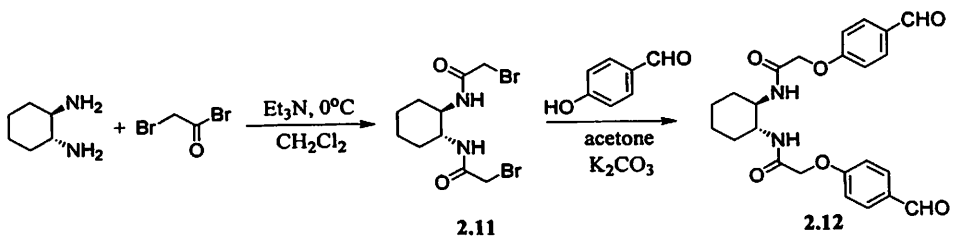

Equation 28

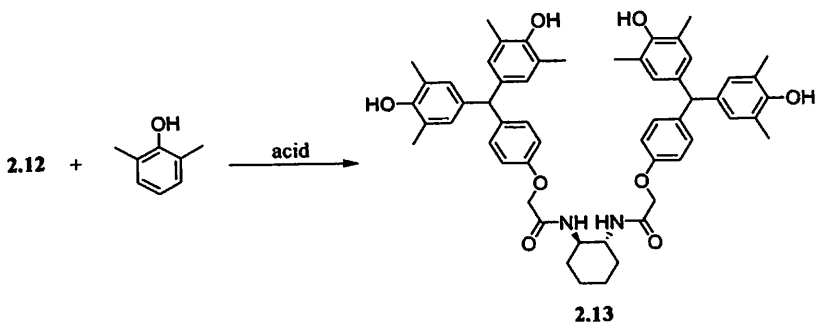

Equation 29

Subsequently, condensation of the dialdehyde (**2.12**) with 2,6-dimethylphenol according to Procedure **II** gives the corresponding dimeric bis-phenol **2.13**.

The bis-phenol **2.2q** reacts with benzoyl chloride in the presence of a tertiary amine to give the corresponding amide derivative **2.14a**. Similarly, the reaction with nicotinyl chloride results in the corresponding nicotinamide derivative, **2.14b** (equation 30).

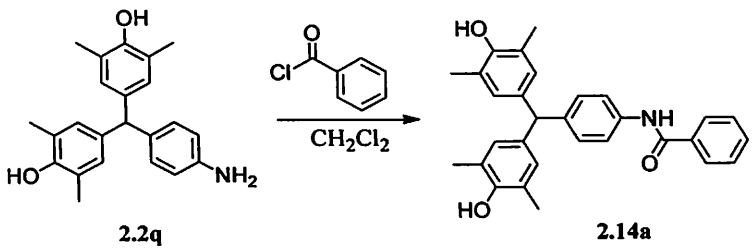

2.2q **2.14a**

Equation 30

In the same manner, the amide-bridged dimeric bis-phenols **2.15** can also be prepared from **2.2q** using dicarboxylic acid halides. Accordingly, this procedure can be described as a "convergent strategy". Thus isophthaloyl chloride reacts with **2.2q** (1:2 stoichiometry) and leads to the formation of the corresponding dimeric bis-phenol, **2.15a**. In the same way, terephthaloyl chloride reacts with **2.2q** and gives the amide-bridged dimeric bis-phenol **2.15b** (equation 31). The amide spacers in these compounds are rather rigid compared to those incorporated in **2.10** and hence the self-assembling properties of the two bis-phenol motifs are expected to be different.

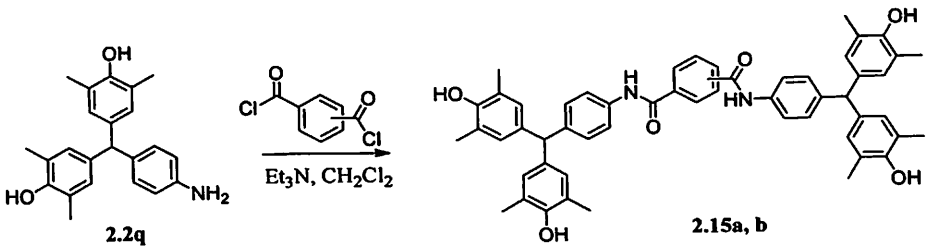

2.2q **2.15a, b**

Equation 31

The UV-visible spectroscopy and ^{1}H NMR spectroscopy of dimeric bis-phenols **2.10** reveal that these compounds have similar characteristics as the bis-phenols themselves. For example these compounds show distinct concentration dependent UV-visible features in the range 220-300nm. This is elucidated by the concentration dependent UV-spectra of **2.10a** in acetonitrile (Fig.22). At concentration < 0.46mM, the spectrum of **2.10a** in acetonitrile shows two absorption bands at 238nm and 277nm respectively. With increase in concentration, the intensity of the band at 277nm increases and reaches a maximum, and when the concentration of the compound is ~ 0.82mM, the two absorptions merge. Similar observations are made

with the bis-phenol **2.2a** in which intermolecular hydrogen bonding and proton exchange is suggested.

The amide-bridged bis-phenols can form different types of aggregates, based on whether the molecules adopt folded or stretched conformations. Electrospray mass spectrometric studies of the compounds **2.10** show that depending on the structures of the molecule, the nature of the self-assemblies they form in solution are different.

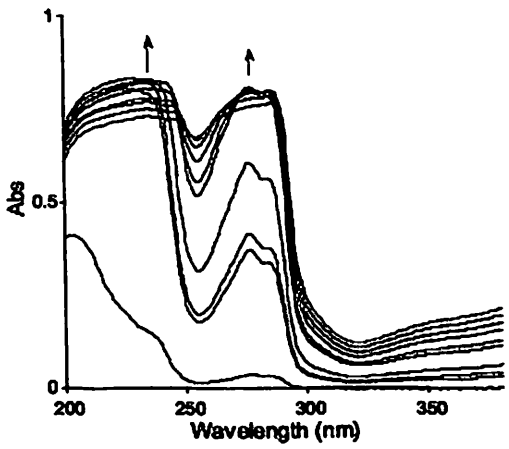

Fig.22 Concentration dependent spectrum of **2.10a** in acetonitrile (0.08 to 0.96mM)

For instance, the electrospray mass spectrum of **2.10a** in acetonitrile at concentration of 1.3mM shows the [M+ Na^+] molecular ion peak at m/z 859.4 (Fig.23). Presence of peaks at m/z 1695.9 corresponds to the [2M+ Na^+] ion, which indicate that in solution the bis-phenol molecules self-assemble (equation 32) to form dimeric structures. The signal at m/z 901.5 in the mass spectrum indicates the bis-phenol units are solvated with acetonitrile, which gives mass fragments such as [M+acetonitrile+Na^+]. This is quite reasonable because the acetonitrile molecules can coordinate to the hydroxy groups of the phenol through O–H···N hydrogen bonding interactions. Similarly, the electrospray mass spectrometry of other amide-bridged bis-phenols such as **2.10b** and **2.10c** show the formation of self-aggregated structures in solution. However, we found that neither electrospray mass nor MALDI-TOF spectrometry could give any indication of similar self-aggregation in the case of **2.10d**, at least up to concentrations of 1.5mM in acetonitrile.

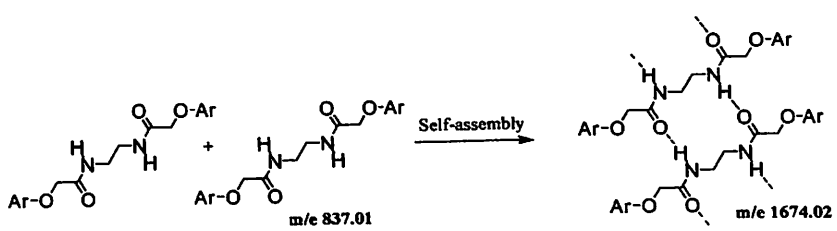

Equation 32

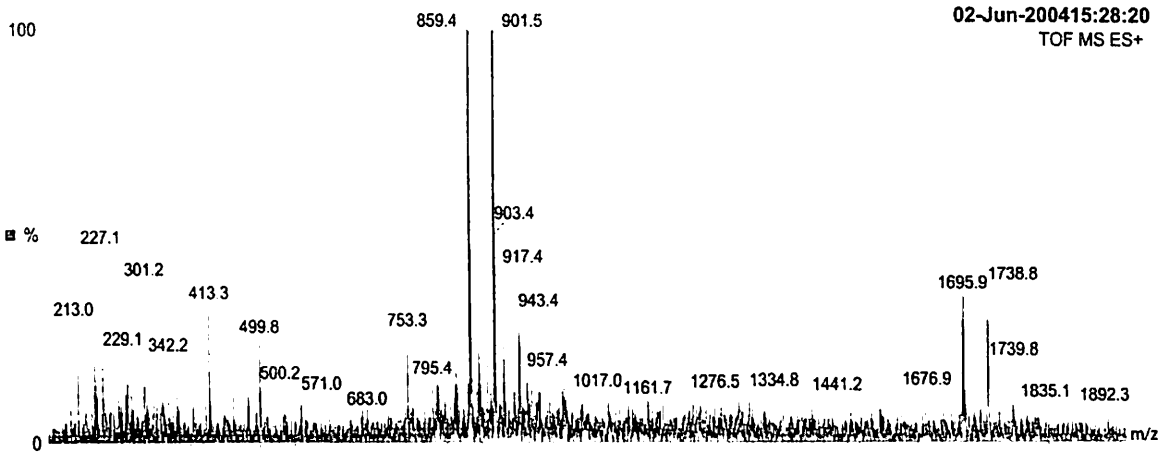

Fig. 23 Electrospray mass spectrum of **2.10a** that shows the presence of mass ions [M+Na$^+$] and dimers [2M+Na$^+$] having m/z 859.4 and m/z 1695.9 respectively. The signals at m/z 901.5 and 1738.8 indicate that acetonitrile molecules are associated with the molecular ions.

It may be mentioned that the dimeric bis-phenols **2.10** have relatively flexible amide bridges, so that they can either adopt stretched conformations or remain folded in solution. In the stretched conformations the molecules can form self-assembled structures, which are held together by intermolecular hydrogen bonding interactions. This is a property that depends on the polarity of the environment in which the molecule resides.

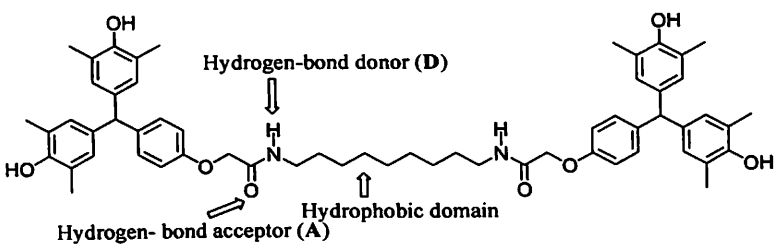

2.10d

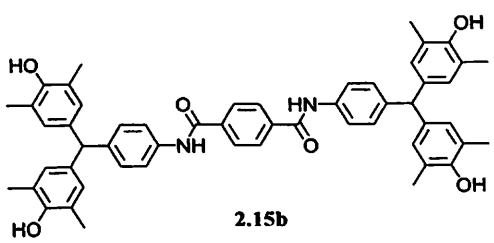

2.15b

Thus, it can be reasoned that the bis-phenol molecules self-assembly in solution through intermolecular hydrogen bonding networks involving the hydroxy groups of the phenol and the amide groups of the spacer. But as the length of the alkyl fragment of the spacer increases, the possibility of the molecules adopting folded conformations is substantially increased as in the case of **2.10d**. This perhaps explains the absence of higher aggregated structures in the case of **2.10d** except the molecular ion [M+Na$^+$] at m/z 957.18.

In this context it may be noted that the amide-bridged bis-phenols **2.15a** and **2.15b** have relatively rigid aromatic spacers. The presence of the aromatic spacer in these molecules is expected to introduce directionality to the donor...acceptor hydrogen bonding interactions. Thus, intermolecular hydrogen bonding interactions between the N-H and the C=O groups as well as the phenolic O-H groups should be crucial in determining the nature of the assembly. However, we could not observe the presence of self-assembled structures from electromass spectrometry.

From the results obtained from ^{1}H NMR studies of the compounds, it is obvious that the formation of such dimeric structures involves intermolecular hydrogen bonding between the amide groups (equation 32) of the bis-phenol molecules. The ^{1}H NMR spectrum of compound **2.10a** in $CDCl_3$ shows that the amide protons, **a** appear at δ_H 7.08, while the hydroxy protons, **b** appear at δ_H 4.64 as a broad singlet. The signals at δ_H 1.18 and 4.13 appear due to the presence of solvated ethanol, and so the corresponding correlation is marked in Fig.24 (a).

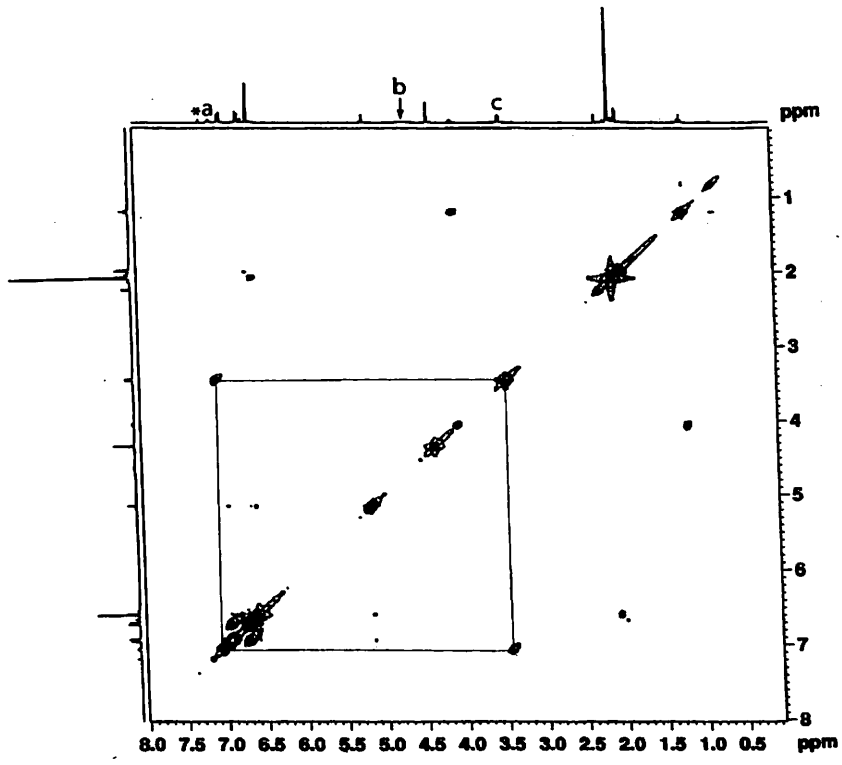

Fig.24(a) Proton HOMOCOSY of **2.10a** in $CDCl_3$ showing the correlations of the amide protons, **a** to the protons of the α-methylene groups, **c**. (* indicates solvent signal)

The characteristic signals due to the methyl protons appear at δ_H 2.12 while the aromatic protons are observed at δ_H 6.78 and 6.92 (A_2B_2 pattern). The proton HOMOCOSY of **2.10a** shows the amide correlations that involves the protons of the –COHN–CH_2– fragment which are designated as **a** and **c** respectively in Fig.24a.

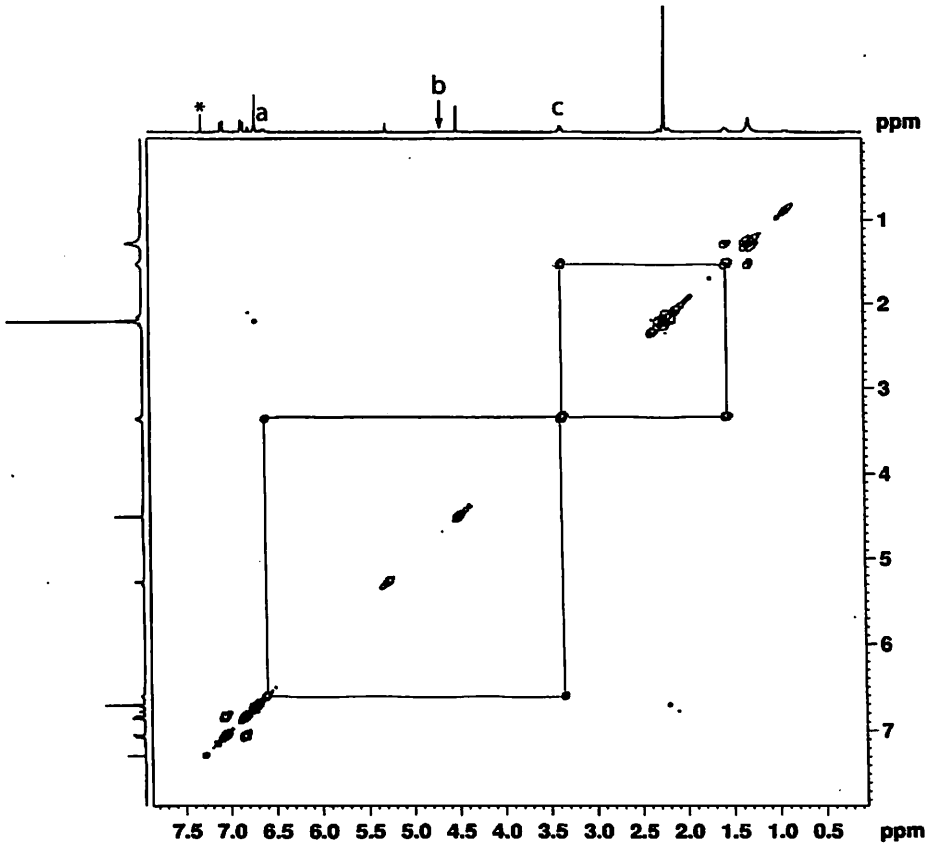

Fig.24 (b) Proton HOMOCOSY of **2.10d** in $CDCl_3$ showing the correlations of the amide protons (**a**) and the broad signal due to protons of the hydroxy group (**b**); aromatic correlations are obvious. (* indicates solvent signal)

The ^1H NMR spectra of the other dimeric bis-phenols **2.10** are similar. In case of **2.10d**, the ^1H NMR spectrum in $CDCl_3$ shows that the amide protons appear as triplet at δ_H 6.59. The broadening of the signal due to the hydroxy protons at δ_H 4.92 indicates that the bis-phenol molecules are associated through intermolecular hydrogen bonding. The proton signals due to the hydroxy groups of **2.10d** are not observed in the HOMOCOSY in $CDCl_3$. However, the protons correlations of **2.10d** involving the amide groups are distinctly identified from the HOMOCOSY in $CDCl_3$. The spectrum shows coupling between the amide N–H protons (**a**), and the α-methylene protons (**c**) of the alkyl fragment as defined in Fig.24b. The correlations between the signals due to the protons of the aromatic groups are obvious.

The ^1H NMR spectrum of **2.15a** in dimethylsulfoxide-d^6 shows that the hydroxy protons appear as a broad signal at δ_H 7.71, designated as **e**, while the two amide protons appear at δ_H 7.96 and 10.15 respectively. These signals are apparently broadened due to the presence of intermolecular hydrogen bonding between the hydroxy and the amide groups. The proton HOMOCOSY of this compound in dimethylsulfoxide-d^6 shows correlations between the proton signals of 1,3-disubstituted benzene ring of **2.15a** that appear at δ_H 7.56(t), 8.05(d) and

8.50(s) respectively (Fig.25). These are designated as **a** and **b** in the spectrum. From the correlation spectrum it is observed that the signals due to the A_2B_2.

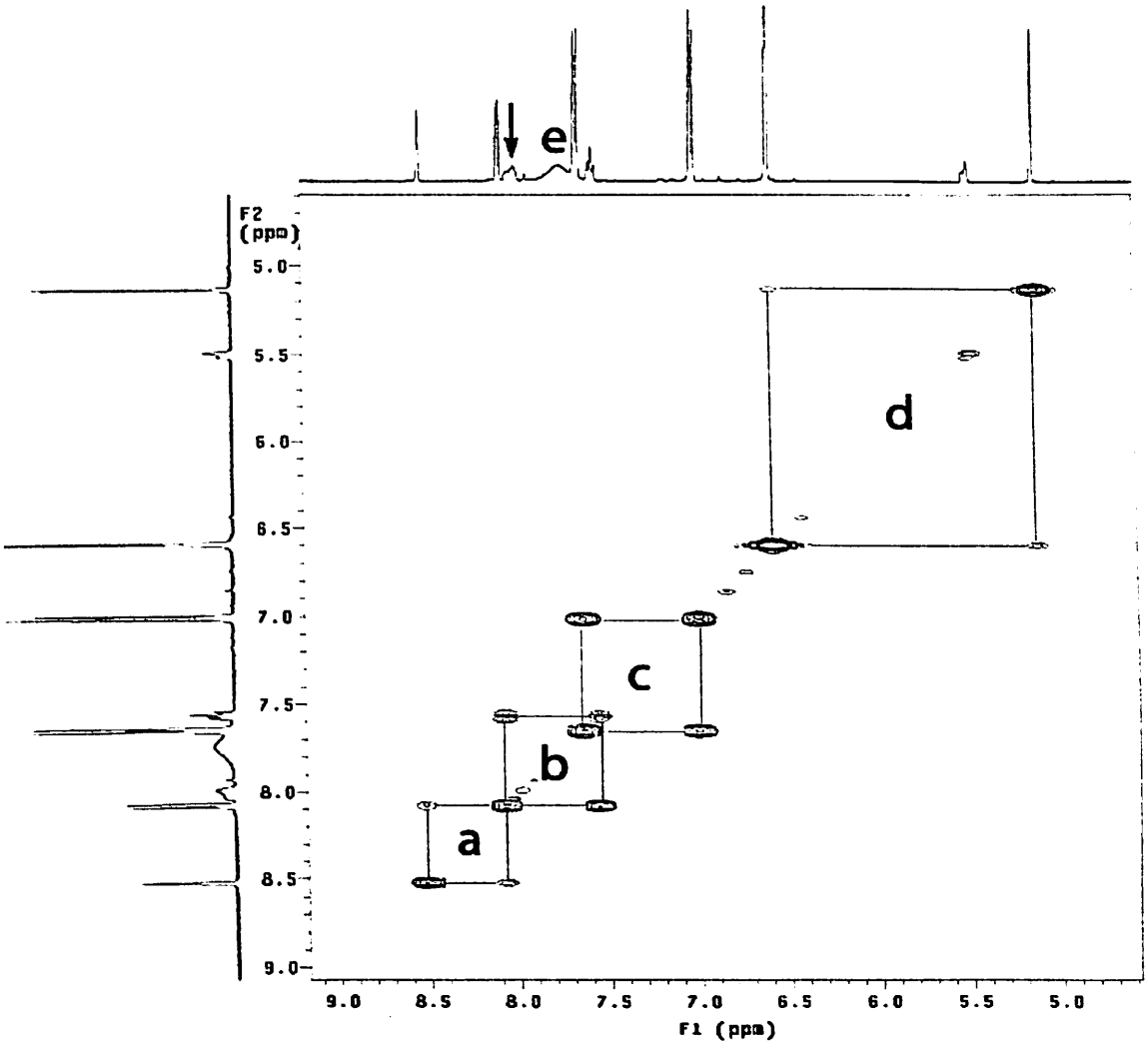

Fig. 25(a) Proton HOMOCOSY of **2.15a** in dimethylsulfoxide-d^6, where the amide and the hydroxy protons are observed as broad signals; the arrow-mark indicates one of the amide protons, and **e** indicates the signal due hydroxyl protons.

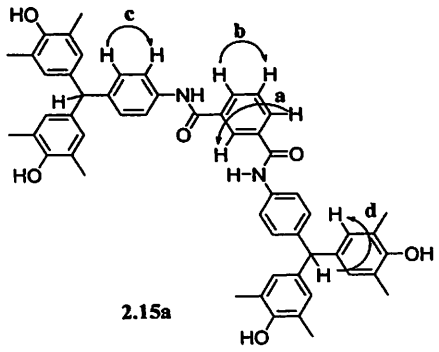

2.15a

Fig.25 (b) Correlations **a**, **b**, **c** and **d** in compound **2.15a** as indicated in the HOMOCOSY

We have studied the process of aggregation through self-assembly of these amide-bridged bis-phenols over highly ordered pyrolytic graphite (HOPG) using Atomic Force Microscopy (AFM). The samples concentrations used in this study were in the range of 0.1 to 3mM. For this purpose the samples were prepared by dissolving the compound in a suitable solvent such as chloroform or toluene. While preparing samples for the AFM experiment, aliquots of 10µl of these solutions were deposited onto freshly cleaved surfaces of graphite. The samples were kept in a closed and dust-free environment at room temperature for 6 hours while the solvent evaporates during this period. Then the samples deposited over the graphite surfaces are imaged using the atomic force microscope. The measurements are performed in the tapping mode using a cantilever having silicon tip. The imaging experiments were done in the tapping mode to minimise scratching and damage of the surface by the AFM tip.

We have observed that the structures obtained from **2.10d** when deposited from chloroform on HOPG show large globular microstructures (Fig.26a). These self-assembled structures obtained from **2.10d** have dimensions between 1.0 and 2.0µm. The structures observed over the graphite surfaces containing **2.15b** as the substrate shows the formation of long fibres having widths of 40 ± 10 nm, and having longitudinal dimensions of *ca.* 1µm as in Fig.27.

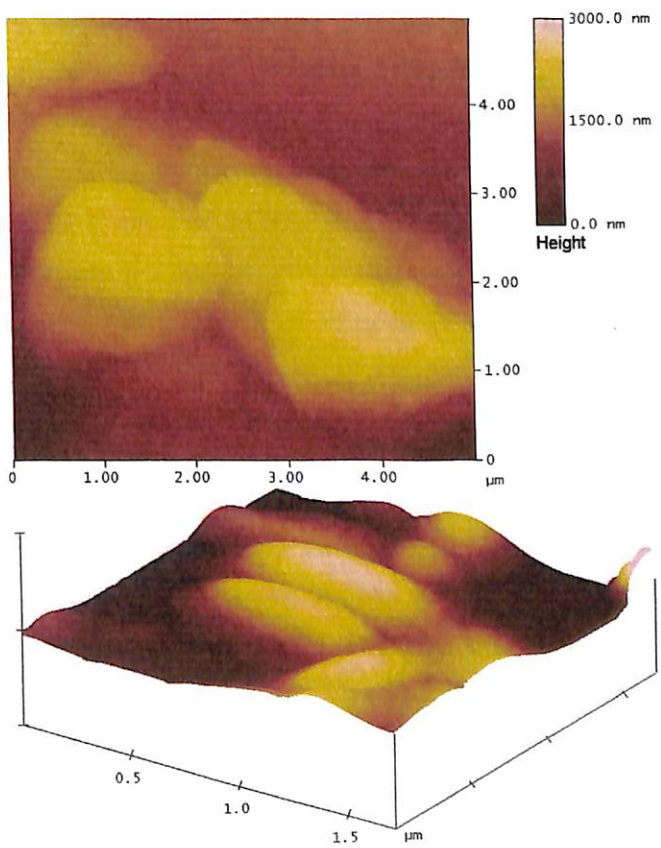

Fig.26 AFM image of **2.10d** over HOPG shows the formation of globular vesicle-like structures when deposited from chloroform

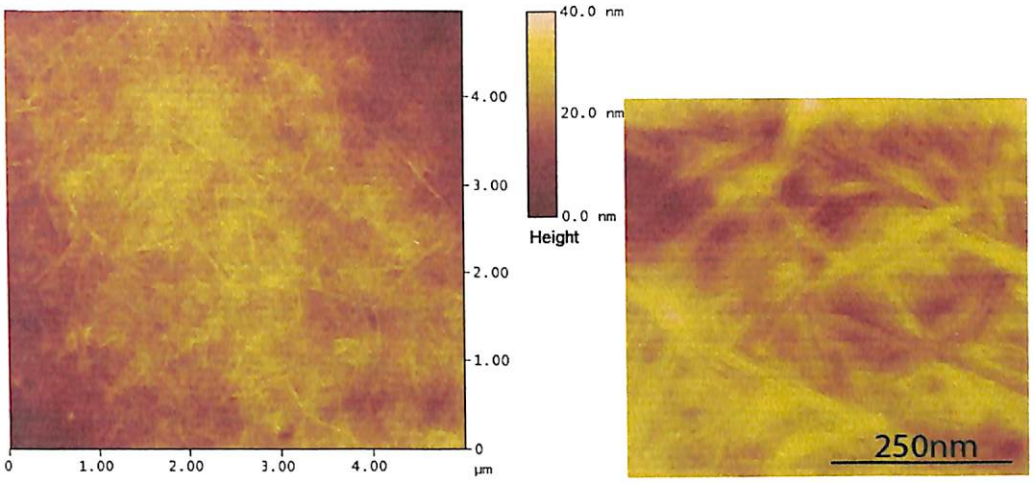

Fig.27 Self-assembled structures of **2.15b** on graphite surface; (right) the nanostructures of **2.15b** observed under higher resolution

At higher resolutions it is observed that the longitudinal dimensions of the structures formed by **2.15b** (Fig.27, right) are much larger than the lateral dimensions or thickness. The fibre-like structures presumably indicate that the molecules are not folded but aligned longitudinally. This suggests that the presence of the rigid spacer connected by the amide bridges prevent the molecules from folding and hence the molecules assume stretched conformations. From these observations we can infer that the compound **2.15b** spontaneously self-assembles through intermolecular N–H···O hydrogen bonds, and may also involve π-stacking interactions with the graphite surface. It is important to note that in the case of **2.10d**, the molecular structure itself allows it to fold such that it can self-aggregate to have multiple units which are hydrogen-bonded in three-dimensions. The presence of the self-complementary bis-phenol unit allows it to form large aggregates that appear as globular structures when studied by AFM.

In this Chapter, we have demonstrated the synthetic methods adopted for the bis-phenols **2.1** and **2.2** that are studied by us. The bis-phenols, **2.1** are prepared by condensing phenol with different aldehydes according to Procedures **II** or **III**. However, in case of the condensation of 2,6-dimethylphenol with different aldehydes Procedures **I**, **II** and/or **III** are followed so as to prepare the corresponding bis-phenols (**2.2**). The characterization of these bis-phenols in solution state is illustrated. We have also described a "divergent strategy" by which different amide-bridged bis-phenols **2.10** and **2.13** have been synthesized. An alternative "convergent strategy" has also been described which allows amide-bridged bis-phenols **2.15** to be synthesized from **2.2q**. We could also establish that the amide-bridged bis-phenols can form self-assembled structures, which is supported by mass spectrometry and complemented by AFM experiments.

Chapter 3

Structure and Hydrogen-Bonding in Bis-Phenols

As described in Chapter 1, bis-phenols and the derivatives self-assemble through intermolecular hydrogen bonding interactions leading to interesting supramolecular structures. There are many reports are devoted towards delineating these aspects in crystals and molecular solids. The solid-state structures of different bis-phenols that contain triphenylmethane frameworks are influenced mainly by strength of the hydrogen bonding interactions and the geometry of the molecules. The triphenylmethane derivatives adopt three-bladed propeller conformation in solution as well as in the solid state, and they are expected to behave as host lattices[98]. Even though bis-phenols are known to produce hydrogen-bonded network structures[50,51,57], the host-guest and inclusion properties of bis-phenols have very few reports. It is to be noted that host-guest and inclusion aspects of some of the phenol-based compounds[99,100] have been studied from the viewpoint of designing functional porous materials.

3.1 Structure of the Bis-Phenols and their Inclusion Compounds

We have studied the solid-state assembly of bis-phenols, in order to elucidate the effects of substituents on host-guest binding ability of these compounds. More specifically, we concentrated on the effects of the methyl substituents on the structures of the bis-phenols such as **2.2** and the possible manner in which these substituents can direct hydrogen-bonding interactions in the solid state. This is because the methyl groups in close proximity to the hydroxy groups can lead to weak C–H···O interactions apart from the conventional O–H···O and O–H···N hydrogen bonds.

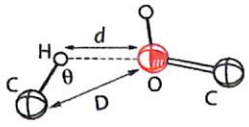

Although these C–H···O interactions are weak compared to O–H···O hydrogen bonds, their importance in determining the solid-state structures is substantial as evident from the ever-increasing amount of research being focused on this issue[94,95]. An understanding of these aspects will have important ramifications in the design and synthesis of porous frameworks, nanostructured materials and in catalysis.

Thus, we realized that a systematic study of the guest-host complexes of bis-phenols with π-aromatics could enable us to formulate a general concept on the inclusion chemistry of this class of compounds. Moreover, we have observed that several literature reports have highlighted bis-phenols with or without substituents for their geometrical and topological aspects[50-54,57]. We also realized that if two methyl groups are introduced ortho- to the hydroxy group in a bis-phenol, then these groups may introduce directionality to the O–H···O bonds. The participation of the methyl groups through weak C–H···O interactions can also affect the geometry of the bis-phenol containing the triphenylmethyl framework. With this background we have taken up structural aspect of various bis-phenolic compounds with or without guest molecules.

On this basis, the crystal structures of some bis-phenols, bis(4-hydroxy-3,5-dimethyl phenyl)(aryl)methanes (**2.2**, as in Chapter 2) are investigated with the aim to elucidate their solid-state structures and their inclusion properties as host materials. In this regard we describe the structures of **2.2** and identify the various hydrogen bonding motifs observed in their self-assemblies. The nature of hydrogen bonding in compounds **2.2** is compared with the structure of bis(4-hydroxyphenyl)(phenyl)methane, **2.1a** in order to elucidate the effect of methyl substituents flanking the hydroxy groups. This will also enable us to understand the effects of the methyl groups on the geometry of the bis-phenol molecules and the possible role of the substituents in the formation of hydrogen bonds.

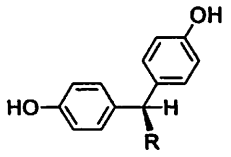

2.1

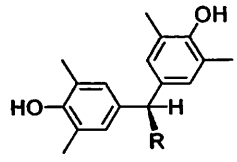

2.2

The bis-phenol, bis(4-hydroxyphenyl)(phenyl)-methane (**2.1a**) crystallizes in the rhomohedral R–3 space group. This lattice structure is observed in β–hydroquinone[66-68], Dianins' compound[102] and in some of the analogs, and more recently in 2,2,6,6-tetramethyl-4,4-terphenyldiol[71]. The solid-state FT-IR spectrum of the compound shows broad absorption at 3206cm^{-1} indicating the presence of strong hydrogen bonds.This molecule, **2.1a** has "T" geometry (Fig.27) and the crystal structure shows that one of the hydroxy groups (O2–H) of the bis-phenol is hydrogen bonded via a molecule of water to form a cyclic hexameric network, **A**. These hexameric networks lead to the formation of a water channel having diameter of 5.6Å along the *c*-direction. The hexameric units are stabilized through helical chains of hydrogen bonds **B**, involving the hydroxy groups, O1–H of **2.1a** as shown in Fig.28. These helical chains, **B** generated by O1–H···O1' ($d_{H\cdots O}$ 1.860Å; <O–H···O 171.9°) hydrogen bonding interactions between the hydroxy groups of the bis-phenol molecules run down the

crystallographic *c*-axis. This is an important feature of hydrogen-bonded self-assemblies of phenol and has been reported in certain cases[71].

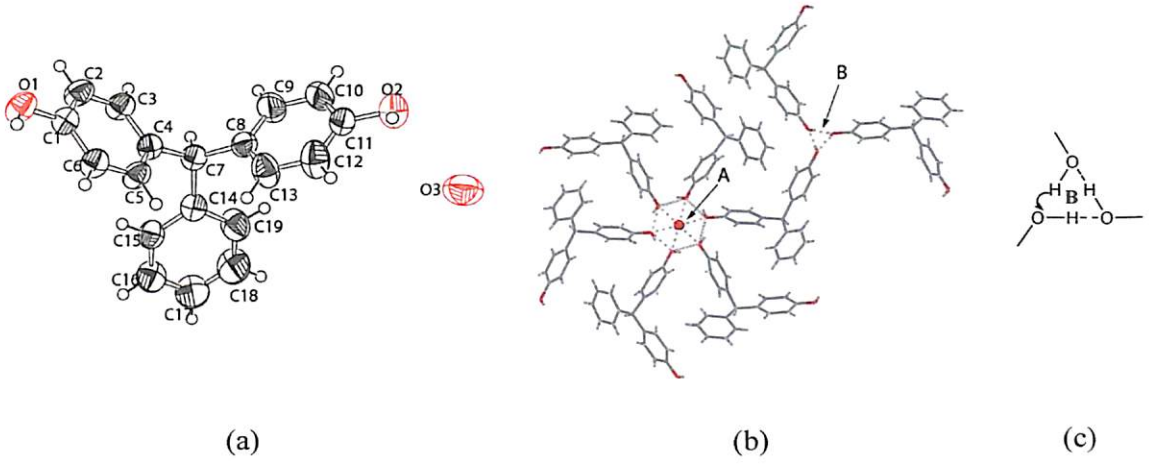

(a) (b) (c)

Fig.28 (a) Structure of **2.1a** (thermal ellipsoids drawn to 50% probability); (b) Formation of hexameric network (**A**) of hydrogen bonds involving the phenol (O2–H) and a molecule of water (O3) and the helical chains (**B**) involve hydrogen bonding between the O1–H groups

Presence of hexameric water channels is reported recently in calixarene derivatives[103], which are generated by hydrogen bonding interactions between a supramolecular unit consisting of six calix-arenes and two water molecules.

In order to rationalize the role of the methyl substituents in determining the orientation of the hydrogen bonds in such compounds, we studied the crystal structure of the bis-phenol, bis(4-hydroxy-3,5-dimethylphenyl)(phenyl)methane (**2.2a**). This compound crystallizes from ethyl acetate in the $P2_1/c$ space group. The asymmetric unit contains one molecule of the bis-phenol (Fig.29a) and Z = 4. The crystal structure of shows that the molecules related by screw axis are connected to each other through O2–H···O2' hydrogen bonds, which lead to the formation of infinite zigzag chains parallel to the *b*-axis (Fig.29b,c). Apart from this, weak C–H···O interactions involving C38–H as donor and O2–H as acceptor ($d_{H\cdots O2}$ 2.659 Å; <C–H···O 124.5°) also occur in the structure. The hydrogen bonding pattern described in **2.2a** is in sharp contrast to that observed in **2.1a**, indicating that the presence of methyl substituents ortho- to the hydroxy group restricts the orientation of the O–H···O bonds along with a concomitant reduction of the bond strengths.

In this regard it may be mentioned that the solid-state FT-IR spectrum of **2.2a** shows two distinct bands in the O–H stretching region (Fig.30); this includes a sharp band centered at 3589cm^{-1} that corresponds to the stretching of free hydroxy groups, which are not involved in hydrogen bonding. The broad absorption band at 3467cm^{-1} indicates the presence of hydroxy groups that are involved in hydrogen bonding. As expected from the FT-IR studies, the

crystal structure does show that one of the hydroxy groups (O1−H) of the bis-phenol does not take part in hydrogen bonding.

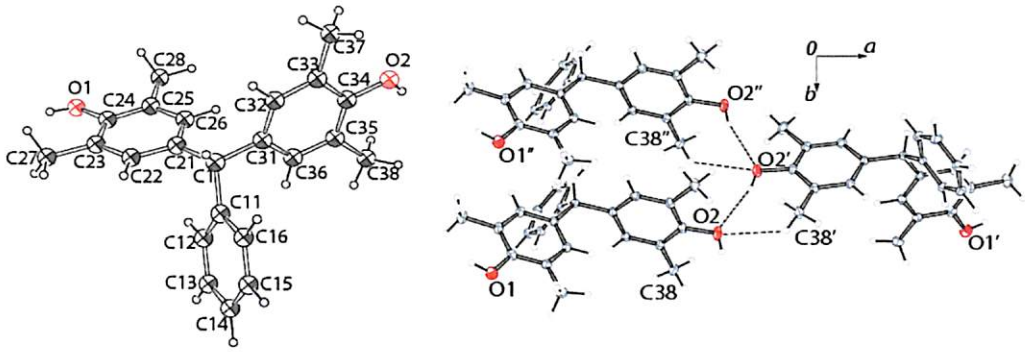

(a) (b)

Fig.29 (a) Crystal structure of **2.2a** (thermal ellipsoids drawn to 50% probability), and (b) Hydrogen-bonded chains between the hydroxy groups [$d_{H\cdots O2}$ 2.35(2) Å; 159.2(18)°] of **2.2a** along crystallographic *b*-axis

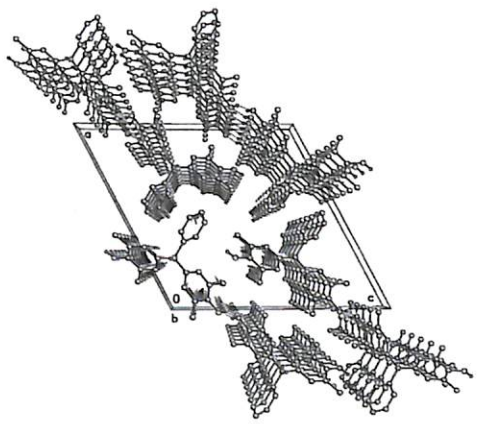

Fig.29 (c) Packing structure of **2.2a** viewed normal to *ac*-plane

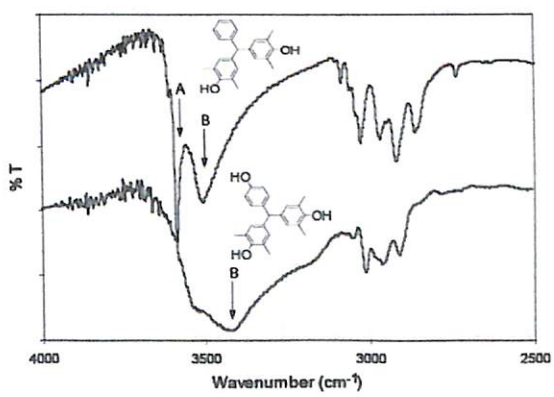

Fig.30 Solid-state FT-IR spectra of bis-phenols **2.2a** and **2.2d** to illustrate the difference in hydrogen bonding interactions for the two compounds

Bis(4-hydroxy-3,5-dimethylphenyl)(4-methoxyphenyl)methane (**2.2c**) crystallizes from ethyl acetate as colorless prisms in the triclinic P-1 space group . The solid-state FT-IR spectrum of the bis-phenol shows two absorptions in the O–H stretching region at 3580 (sharp) and 3519cm^{-1} (broad), reminiscent of the free hydroxy and hydrogen-bonded hydroxy groups. It may be mentioned here that the FT-IR spectrum of **2.2c** is similar to that of **2.2a** in the O–H stretching region. From the crystal structure it is seen that the presence of the methoxy group causes a dramatic change in the packing of the molecules.

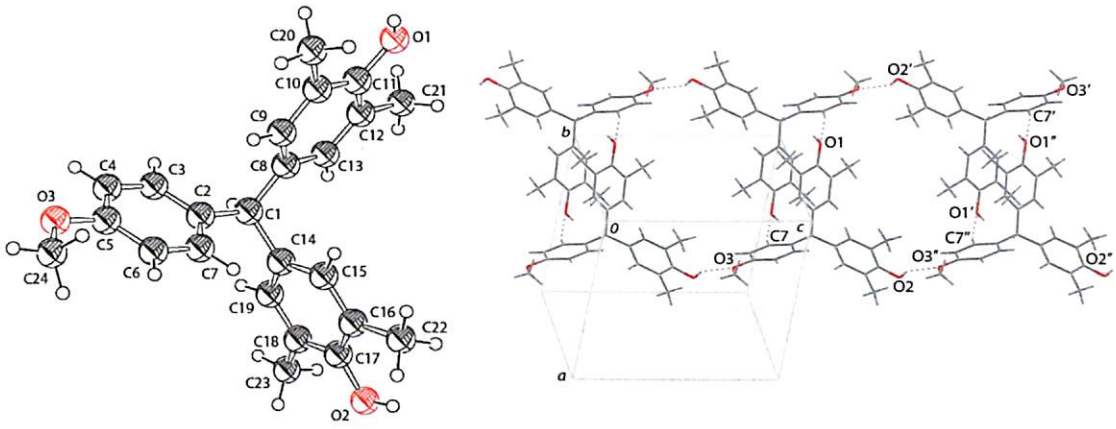

(a) (b)

Fig.31(a) Crystal structure of **2.2c** (thermal ellipsoids drawn to 50% probability), and (b) Molecular ladders formed by O2–H···O3 and C7–H···O1 interactions parallel to the *c*-crystallographic axes.

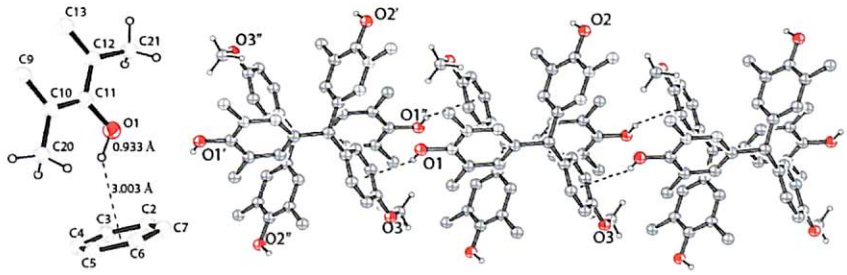

Fig.32 Intermolecular O1–H1o···π hydrogen bonding interaction between O1–H group and the aromatic ring of the **2.2c** that runs down *a*-axis

Table 3.1 Hydrogen bond geometry (Å, °) for the inclusion complex of **2.2c**

D–H···A	d (D–H)	d (H···A)	d (D···A)	<D–H···A
O2–H2o···O3 [x, y, z+1]	0.909	2.180	3.002	150.0
C7–H··· O1 [–x, –y+1, z–1]	0.975	2. 620	3.544	158.1

One of the hydroxy groups of the bis-phenol, O2–H of **2.2c** is the hydrogen bond donor while the methoxy group (O3) at (x, y, z +1) is the acceptor (Fig.31b). The other hydroxy group, O1–H resides in a position, which does not lead to the formation of O–H···O hydrogen bonds. However, this free hydroxy group, O1–H of **2.2c** acts as acceptor to C7–H thereby resulting in weak C–H···O interactions ($d_{H\cdots O1}$ 2.620Å; <C–H···O 158.1°) with the aromatic ring of another molecule having the methoxy substituent at (2–x, –y–1, –z). This weak interaction is supplemented by O(1)–H···π (aromatic) interactions (Fig.32) where the free hydroxy group is the donor and the aromatic ring containing the methoxy substituent ($d_{D\cdots A}$3.016Å, <D–H···A 136°) growing parallel to [010] is the acceptor. Thus, the molecules symmetrically related by translation along *c*-crystallographic axis are involved in the formation of intermolecular O–H···$\pi_{aromatic}$ interactions. The bonding distances observed in this structure reconciles quite well with the reported values[104]. The hydrogen-bond distances and geometries of the intermolecular interactions in **2.2c** are summarized in Table **3.1**.

Bis(4-hydroxy-3,5-dimethylphenyl)(4-hydroxyphenyl)methane **(2.2d)**, has three hydroxy groups, two of which are flanked by two methyl substituents at the ortho-positions while the other hydroxy group is not. Solid-state FT-IR spectrum of this compound (Fig.33) shows broad absorption band centered at 3493cm^{-1} indicating that the hydroxy groups are involved in intermolecular hydrogen bonding.

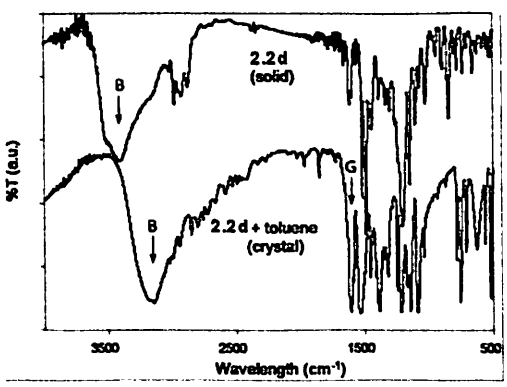

Fig.33 Solid-state FT-IR spectra of bis-phenol **2.2d** and the inclusion complex; '**B**' arises from the hydroxy groups of **2.2d** while the band '**G**' arises due to the presence of the toluene (guest) molecules in the lattice of **2.2d**.

The compound **2.2d** upon crystallization from toluene, gives prismatic yellow crystals and the structure corresponds to the 1:1 inclusion complex between the bis-phenol and the solvent. The FT-IR spectrum of the crystals of this inclusion complex (Fig.33) also shows that the hydroxy groups of the bis-phenol molecules are strongly hydrogen bonded. Thus, the broad signal (**B**) corresponding to hydrogen bonded O–H groups is shifted by 318cm^{-1} (= Δν) to 3175cm^{-1}. Apart from this, a strong absorption band centered at 1598cm^{-1} (**G**) is observed in

the FT-IR spectrum of the inclusion complex, which arises at due to the presence of the toluene molecules as guests in the lattice of the bis-phenol host.

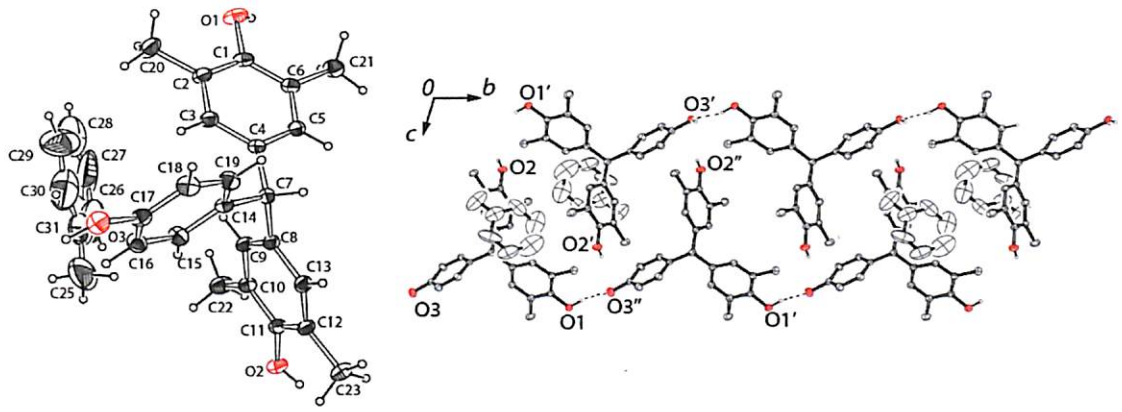

(a) (b)

Fig.34(a) Crystal structure of inclusion complex of toluene with **2.2d** (thermal ellipsoids drawn to 50% probability), and (b) Formation of hydrogen-bonded sheets along [100] plane from **2.2d** in the inclusion complex

Table 3.2 Hydrogen bond geometry (Å, °) for the inclusion complex of **2.2d**-toluene

D–H···A	d (D–H)	d (H···A)	d (D···A)	<D–H···A
O1–H1o···O3 [x, y+1, z]	0.814	1.990	2.726	150.0
O3–H2o···O2 [–x+1, –y+1, –z+2]	0.923	1.871	2.791	173.9
O2–H2o···O1 [x, y, z+1]	0.776	2.082	2.791	152.1

The crystal structure shows that the bis-phenol, **2.2d** adopts a layered structure in the solid-state. Thus O3 serves as the hydrogen-bond acceptor to O1–H ($d_{H\cdots O3}$ 1.990Å), and as donor to O2 (Fig.34b). In the same manner, O1 is the hydrogen-bond acceptor to O2'–H (Fig.35) and this process results in the formation of cyclic hexamers. These hydrogen bonded cyclic networks adopt the chair conformation of cyclohexane, and the hydrogen bond distances and geometries are summarized in Table **3.2**.

The toluene guest molecules are included between the molecules of **2.2d** (Fig.34b) and this lead to column–like structures parallel to the *a*-axis. Closer inspection of the structure shows that four molecules of **2.2d** that lie parallel to the [100] plane are hydrogen bonded through the hydroxy groups into a tetrameric unit, while another such molecule caps the tetramer in

such a way that the concave surface of the molecule faces inwards. Thus, each of the hydroxy groups of **2.2d** takes part in the formation of the tetramer, and the involvement of capping molecules results in the cyclic hexamer (Fig.35). The solvent molecules are encapsulated inside the resulting bowl-type cavity bounded by the hydrogen-bonding networks.

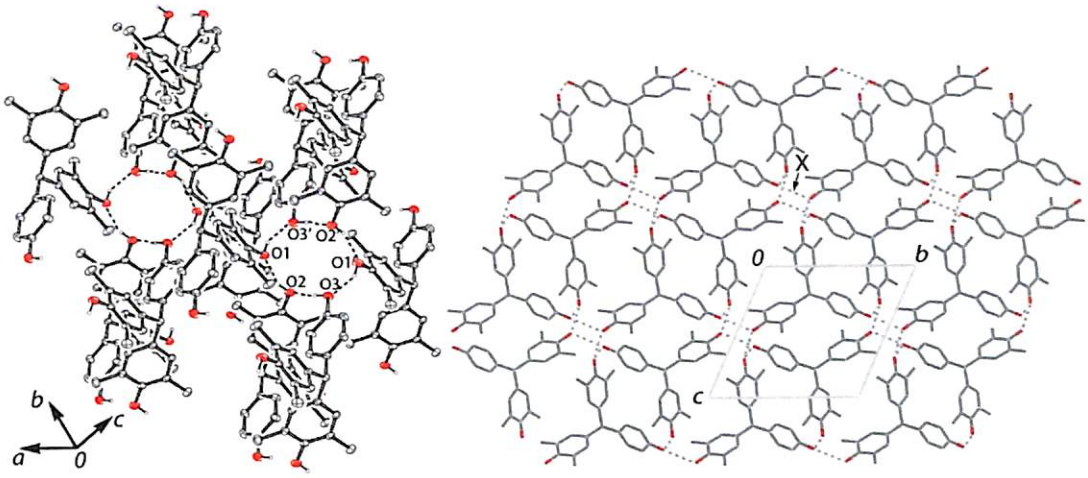

Fig.35 Cyclic hexamers ("**X**") generated by O−H···O hydrogen-bonding interactions in **2.2d**-toluene inclusion complex (toluene molecules omitted for clarity)

The 1:1 stoichiometry of the inclusion complex of **2.2d** with toluene is further confirmed by ^{1}H NMR experiments. Thermogravimetric analysis of the crystals shows that the loss of toluene molecules occurs between 130-133°C (p.s. the thermogram in Chapter 7, Fig.94).

The bis-phenol **2.2f** crystallizes from benzene-dichloromethane the 1:1 inclusion complex of benzene in $P2_1/n$ space group (Fig.36). The inclusion of molecules such as benzene in the lattice of bis(4-hydroxy-3,5-dimethylphenyl) (4-nitrophenyl)methane (**2.2f**), and the previous example gives an indication of the fact that the bis-phenols have tendency to form inclusion complexes with aromatic guests.

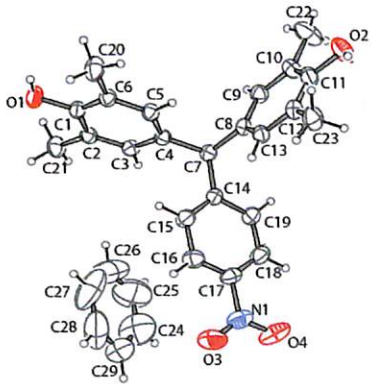

Fig.36 Crystal structure of the inclusion complex of **2.2f** with benzene (thermal ellipsoids drawn to 50% probability)

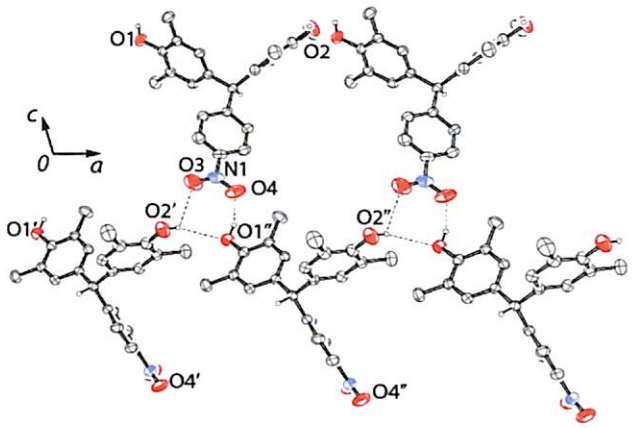

Fig.37 Two-dimensional hydrogen-bonded network involving the hydroxy groups and the nitro groups of **2.2f**

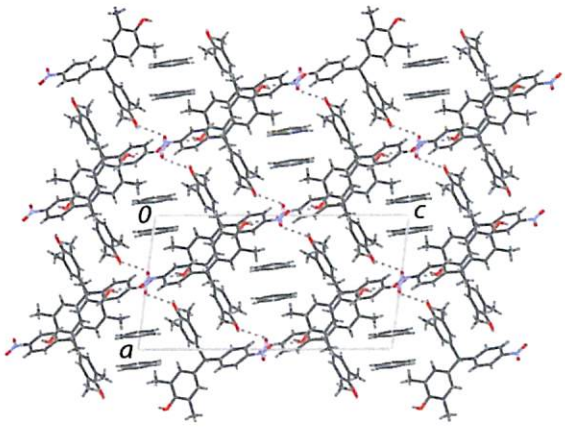

Fig.38 View of the packing of **2.2f** normal to the *ac*-plane and the benzene molecules included inside the cavities of the lattice

Table 3.3 Hydrogen bond geometry (Å, °) for the inclusion complex of **2.2f**-benzene

D–H···A	d (D–H)	d (H···A)	d (D···A)	<D–H···A
O1–H···O4 [x-1/2, –y+1/2, z+1/2]	0.888	2.031	2.867	156.3
O2–H···O3 [x+1/2, –y +1/2, z+1/2]	0.867	2.520	3.039	119.2
O2–H···O1 [x+1, y, z]	0.867	2.569	3.214	131.9

In this case, hydrogen-bonding interactions between the hydroxy groups of the bis-phenol leads to the formation of infinite O2–H···O1 ($d_{H\cdots O1}$ 2.569Å, <O2–H···O1 131.9°) chains parallel to the *a*-axis, and these chains are inter-woven through O1–H···O4 and O2–H···O3 hydrogen bonds involving the nitro group (Fig.37). The hydrogen bond distances and

geometries for this inclusion compound are summarized in Table **3.3**. Thus, the bis-phenol molecules self-assemble via intermolecular hydrogen bonds that involves the hydroxy groups of the phenol as donors and the nitro groups as acceptors, to result in two-dimensional network structures along the [010] plane. Each of the two-dimensional networks contains cavities, which are occupied by the benzene molecules. These cavities containing the solvent molecules extend along the *b*-axis (Fig.38) and this gives rise to a channel structure for the inclusion complex. The stoichiometry of the inclusion complex is found to be 1:1 from both ^{1}H NMR and thermogravimetric experiments.

Similarly, crystallization of bis(4-hydroxy-3,5-dimethylphenyl)(4-formylphenyl)-methane (**2.2h**) from benzene gives the corresponding 1:1 molecular complexes which crystallizes in $P2_1/n$ space group. Intermolecular hydrogen bonding between the hydroxy groups of the phenol and the carbonyl group generates two-dimensional network structures.

In this structure, the bis-phenol molecules are bound though an array of three hydrogen bonds involving O1−H, O2−H and the C=O groups, and the corresponding bond distances and angles are summarized in Table **3.4**. From the structure, it is evident that each bis-phenol molecule interacts with four neighbouring molecules by means of O−H···O hydrogen bonds. The hydrogen-bonded assembly of the bis-phenol molecules involving the hydroxy groups and the formyl group of **2.2h** leads to the formation of molecular ladders that extend parallel to the [010] plane. Each of these ladders assembles anti-parallel to each other along the *b*-axis. Thus the cavities are formed in between the rungs of the ladder that extend along the *b*-axis to lead to channels having dimensions ~7.0×8.2Å. These channels are large enough to accommodate the benzene molecules. The packing structure of this inclusion complex (Fig.40) shows striking similarity to that of **2.2f** both in terms of the dimensions of the cavity and guest (i.e. benzene) included.

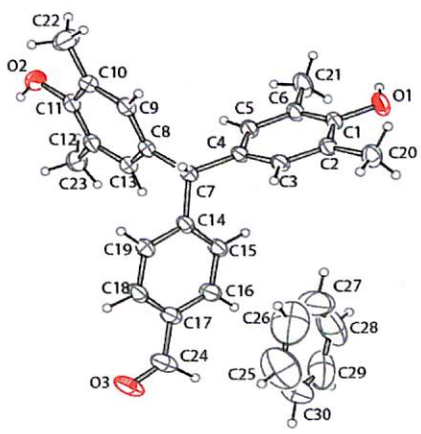

Fig.39 Crystal structure of inclusion complex of **2.2h** with benzene (thermal ellipsoids drawn to 50% probability)

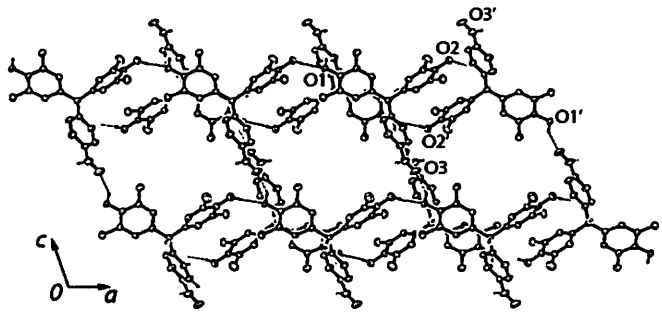

Fig.40 Formation of molecular ladders along [010] in **2.2h** along the [010] plane (benzene molecules are excluded for clarity)

Table 3.4 Hydrogen bond geometry (Å, °) for the inclusion complex of **2.2h**-benzene

D–H···A	d (D–H)	d (H···A)	d (D···A)	<D–H···A
O1–H1o···O3 [x–1/2, –y+3/2, z+1/2]	0.891	1.961	2.740	145.3
O2–H2o···O1 [x+1, y, z]	0.862	2.105	2.994	164.1

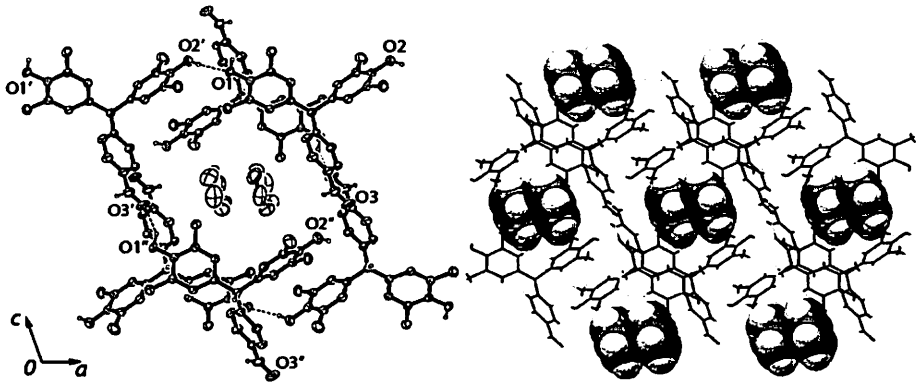

Fig.41 Packing of the benzene molecules in the lattice of **2.2h**; note the similarity to the inclusion complex with **2.2f**

Similarly, crystallization of bis(4-hydroxy-3,5-dimethylphenyl)(4-aminophenyl)methane (**2.2q**) from toluene results in the 1:1 inclusion complex of bis-phenol. The stoichiometry of the inclusion complex is determined from ^{1}H NMR and thermogravimetric measurements. Each of the bis-phenol molecules of **2.2q** in this inclusion complex is hydrogen bonded to six other molecules and a guest toluene molecule. The hydroxy groups and the amino group are involved in the formation of cooperative chain of hydrogen bonds (Fig.42b) with O2···O1 and O1···N1 distances being 2.725 and 2.824 Å respectively (the corresponding hydrogen bond distances and geometries are summarized in Table **3.5**). It is observed that formation of the cooperative hydrogen-bonding network also causes saturation of the donor and acceptor abilities of the hydroxy and the amino groups. In addition to the O–H···O and N–H···O

hydrogen bonds, weak N–H···π interactions ($d_{H\cdots\pi}$2.883 Å; 166.4°) are also present in the structure (Fig.43), which binds the toluene molecule to the amino group. Moreover the nitrogen atom of the bis-phenol in this structure is distinctly tetrahedral, such that the <C–N···H ranges between 104.5° to 107°.

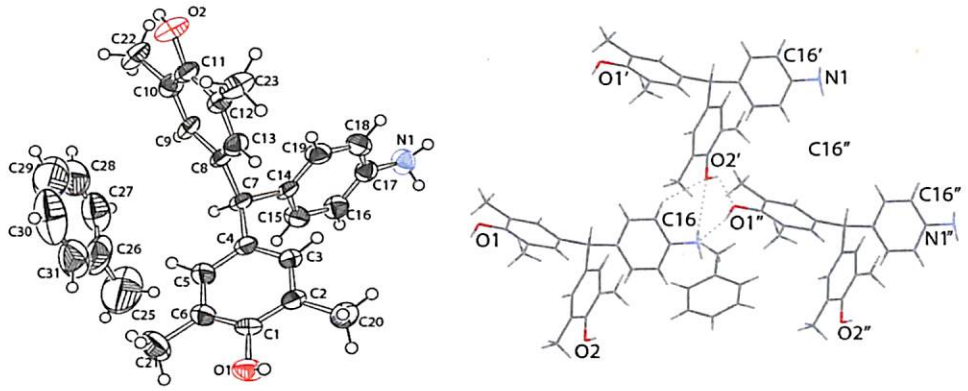

(a) (b)

Fig.42(a) Crystal structure of **2.2q**-toluene inclusion complex (thermal ellipsoids drawn to 50% probability), and (b) Intermolecular O–H···O, O–H···N and C–H···O hydrogen bonding interactions between the bis-phenol molecules in the inclusion complex

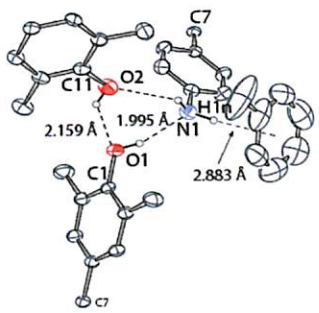

Fig.43 Cooperative chain of O–H···O–H···N–H···π hydrogen bonds in the **2.2q**-toluene inclusion complex

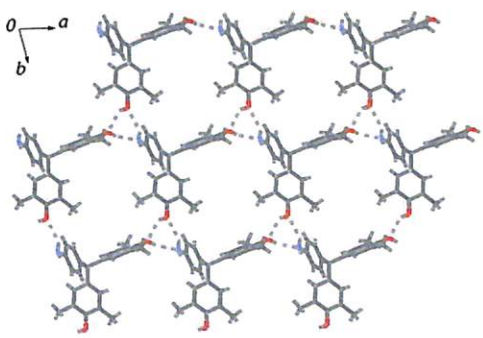

Fig.44 Two-dimensional hydrogen-bonded network of **2.2q**-toluene inclusion complex (as viewed normal to [001] plane; toluene molecules excluded for clarity)

Table 3.5 Hydrogen bond geometry (Å, °) for the inclusion complex of **2.2q**-toluene

D–H···A	d (D–H)	d (H···A)	d (D···A)	<D–H···A
N1–H2n···O2 [x, y–1, z]	0.913	2.424	3.078	128.6
O1–H1o···N1 [x+1, y, z]	0.855	1.995	2.824	163.1
O2–H2o···O1 [x–1, y+1, z]	0.769	2.159	2.725	130.9
N1–H1n···π	0.939	2.883	3.822	166.4

From the crystal structure of **2.2q**-toulene inclusion compound, it is observed that the hydrogen-bonding interactions between the bis-phenol molecules lead to the formation of two-dimensional networks that grow along the [001] plane. These are actually square nets (Fig.44) that give a layered structure, and the guest molecules occupy the cavities formed within these networks.

The inclusion ability of the bis-phenols is not restricted to aromatic guests only because polar guest molecules such as methanol and acetonitrile can also form inclusion complexes in certain cases. For instance, crystallization of bis(4-hydroxy-3,5-dimethylphenyl)(4-N,N-dimethylaminophenyl)methane, **2.2g** from acetonitrile results in the formation of its 1:1 inclusion complex which crystallizes in $P2_1/c$ space group. The crystal structure of the acetonitrile adduct of **2.2g** shows (Fig.45) that the bis-phenol molecules are linked by intermolecular O–H···O hydrogen bonding leading to the formation of one-dimensional chains.

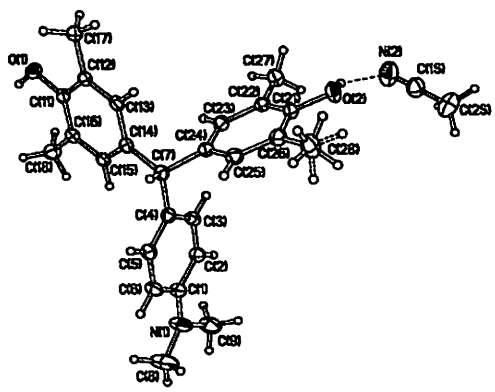

Fig.45 Crystal structure of the inclusion complex **2.2g** with acetonitrile (thermal ellipsoids drawn to 50% probability)

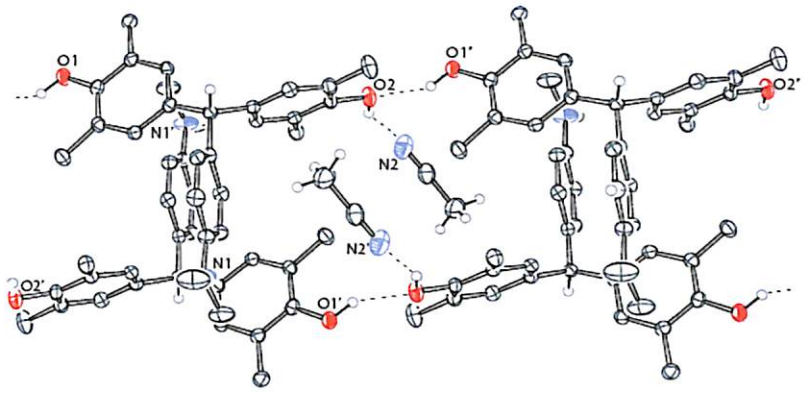

Fig.46 Intermolecular hydrogen bonding between the acetonitrile molecules and bis-phenol (**2.2g**) molecules in the inclusion complex showing O–H···O and O–H···N hydrogen bonds

Table 3.6 Hydrogen bond geometry (Å, °) for the inclusion complex of **2.2g**-benzene

D–H···A	d (D–H)	d (H···A)	d (D···A)	<D–H···A
O1–H···O2 [x+1, y, z]	0.893	1.943	2.751	150.2
O2–H···N2 [x, y, z]	0.923	2.033	2.845	147.2

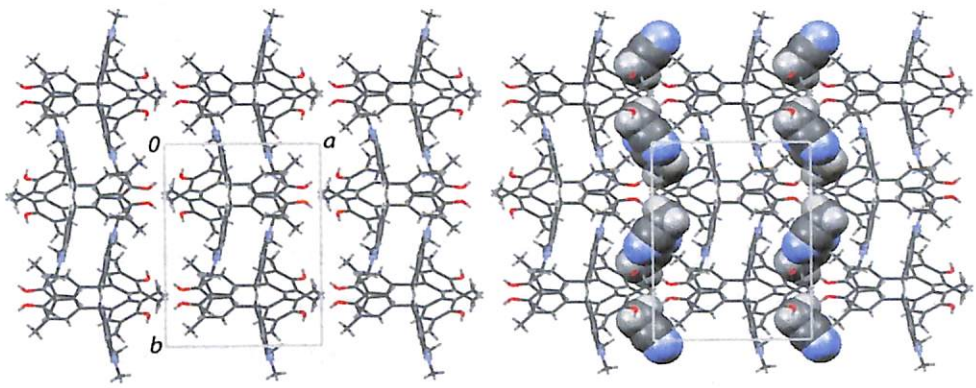

Fig.47 Packing structure of the host molecules of **2.2g** in the acetonitrile inclusion complex (left) without the solvent, and (right) with the solvent molecules in the lattice

The hydrogen-bonded chains run parallel to the *a*-crystallographic axis and the acetonitrile molecules are bonded to the hydroxy groups of the bis-phenol, O2–H that behave as the hydrogen bond donor (Fig.46). At the same time, O2–H forms hydrogen bonds with O1–H of another molecule, such that O2 behave as hydrogen bond acceptor ($d_{H\cdots O1}$ 1.943Å) thereby causing saturation of the hydrogen bonding potentials of both the hydroxy groups of **2.2g**. The hydrogen bond distances and angles corresponding to these intermolecular interactions are summarized in Table **3.6**.

In this adduct, the solvent molecules reside in the crystal lattice as pendants that are bound by O–H···N hydrogen bonds to the molecular chains of the bis-phenol molecules. In this case the $-NMe_2$ group of the bis-phenol are not involved in hydrogen bonding. From the packing structure of **2.2g**-acetonitrile adduct, it is observed that the solvent molecules occur in the lattice as hydrogen-bonded chains that run parallel to the *b*-axis. We have already described that the interaction of **2.2g** in acetonitrile can be monitored by ^{1}H NMR experiments (p.s. Chapter 2, Fig.21).

Subsequently the crystal structure of 2-[bis(4-hydroxy-3,5-dimethylphenyl)methyl]-pyridine (**2.2p**) has been studied in order to generalize the role of hydrogen bond donor…acceptor interactions in the formation of open framework structures. This compound crystallizes from ethyl acetate in the P-1 space group and shows extensive hydrogen bonded networks in the solid-state (Fig.48). The intermolecular hydrogen bonding interactions are listed in Table **3.7**.

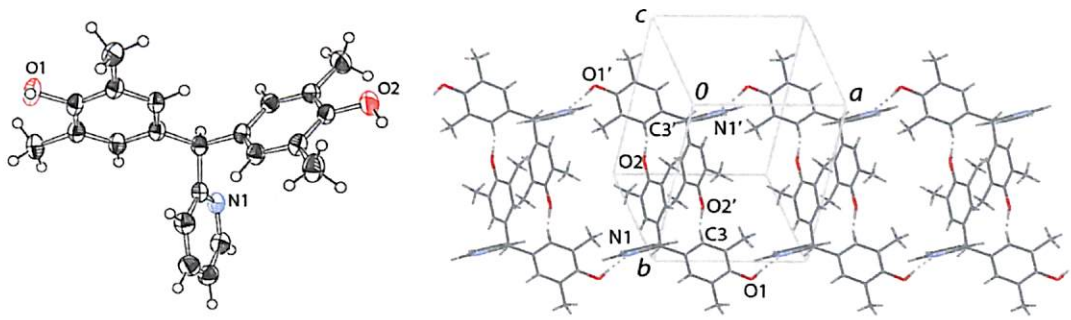

(a) (b)

Fig.48 (a) Crystal structure of 2-[bis(4-hydroxy-3,5-dimethylphenyl)methyl]pyridine (thermal ellipsoids drawn to 50% probability); (b) Intermolecular O–H···N and C–H···O hydrogen bonding leads to a layered structure.

Table 3.7 Hydrogen bond geometry (Å, °) for the inclusion complex of **2.2p**

D–H···A	d (D–H)	d (H···A)	d (D···A)	<D–H···A
O2–H···O1 [x+1, y, z]	0.857	1.989	2.802	157.8
O1–H···N1 [x, y, z]	0.903	1.895	2.734	153.6
C3–H···O2 [2-x, 1-y, -z]	0.980	2.558	3.426	147.5

While the hydroxy groups are capable of being both hydrogen bond donors and acceptors, the N atom of the pyridine ring only accepts hydrogen bonds. Of the two hydroxy groups of **2.2p**,

O1−H serves as hydrogen bond donor to N and the O atom behaves as acceptor to O2−H. Thus each bis-phenol molecule is connected to four neighbours through two O−H···O and two O−H···N hydrogen bonds, thereby forming two-dimensional networks (layers). The hydrogen-bonded layers are held together by intermolecular C−H···O interactions ($d_{H\cdots O2}$ 2.558Å; <C−H···O 147.5°) where oxygen atom of O2−H from one of the layer serves as acceptor to the C3−H donor from the adjacent layer.

Bis(4-hydroxy-3,5-dimethylphenyl)(4-pyridyl)methane (**2.2o**) crystallizes from ethyl acetate in $P2_1/n$ (Monoclinic) space group. This compound has two hydroxy groups and a pyridine unit, and the structure shows that one of the hydroxy groups (O2−H) serve as hydrogen bond donor to N atom of pyridine and acceptor to O1−H.

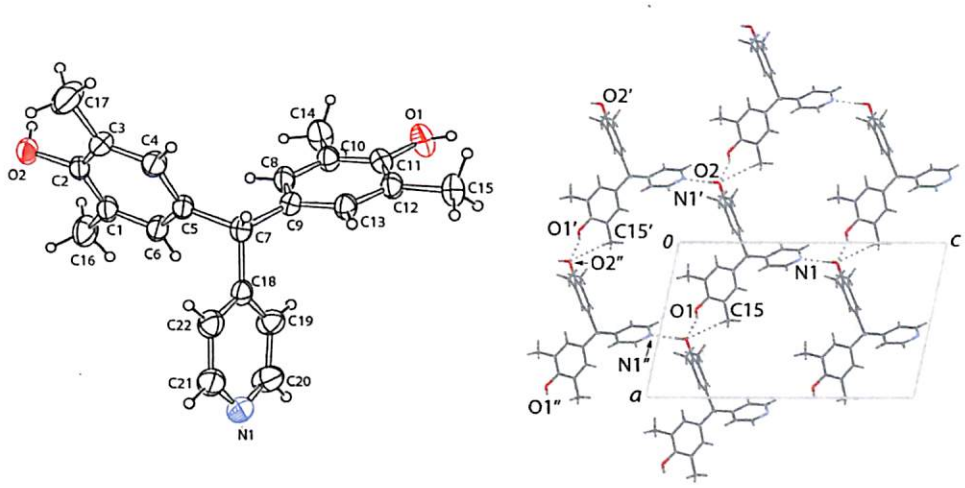

(a) (b)

Fig.49(a) Crystal structure of 4-[bis(4-hydroxy-3,5-dimethylphenyl)methyl]pyridine, **2.2p** (thermal ellipsoids drawn to 50% probability), and (b) Two-dimensional networks formed by intermolecular O−H···O, O−H···N and C−H···O hydrogen bonding interactions

Table 3.8 Hydrogen bond geometry (Å, °) for the inclusion complex of **2.2p**

D−H···A	d (D−H)	d (H···A)	d (D···A)	<D−H···A
O1−H···O2 [x+1, y, z]	0.820	1.963	2.729	159.2
O2−H···N1 [x−1/2, −y+1/2, z−1/2]	1.047	1.570	2.614	175.4

The packing structure shows weak C−H···O interactions ($d_{H\cdots O2}$ 2.704 Å, < C−H···O 120.2°) that involve the C15−H of the ortho-methyl group as donor and the oxygen atom of the hydroxy group, O2−H as acceptor (Fig.49b). The corresponding hydrogen bonding distances

and angles are given in Table **3.8**. Thus, a network of hydrogen bonds that includes O–H···O, O–H···N and C–H···O interactions link the bis-phenol molecules together resulting in the formation of two-dimensional sheets parallel to [010] plane. The packing structure of these molecular sheets in three dimensions also gives molecular ladders, which is not observed in case of **2.2p** even though it has a layered structure. This indicates the presence of open frameworks in the bis-phenol **2.2o** that can accommodate small guest molecules unlike **2.2p**, which has a close packed structure.

3.2 Halide mediated assembly of bis-phenols

The bis-phenol, 4-[bis(4-hydroxy-3,5-dimethylphenyl)methyl]pyridine (**2.2p**) contain a nitrogen atom that can be expected to coordinate to metal ions or Lewis acids. However, attempts to crystallize the corresponding halide salts from aqueous solutions containing equivalent amounts of HCl, **2.2p** and $CuCl_2 \cdot 2H_2O$ unexpectedly yielded **2.2p**·HCl (**2.2r**). This pyridinium salt and its analogue **2.2p**·HBr (**2.2s**) were also obtained from an acidic solution of **2.2p** and HCl (or HBr) in the presence of catalytic amounts of $CuCl_2 \cdot 2H_2O$, but in complete absence of the latter we could not obtain any hydrohalide salts crystals.

Crystal structures of 4-[bis(4-hydroxy-3,5-dimethylphenyl)-methyl]pyridinium chloride and bromide salts reveal that the compounds are isomorphous (Monoclinic, $P2_1/n$). The asymmetric unit in each of the salts contains three H atoms (two hydroxy and one pyridinium) capable of forming strong hydrogen bonds, and three potential acceptors, viz. two oxygen atoms and the halide anion.

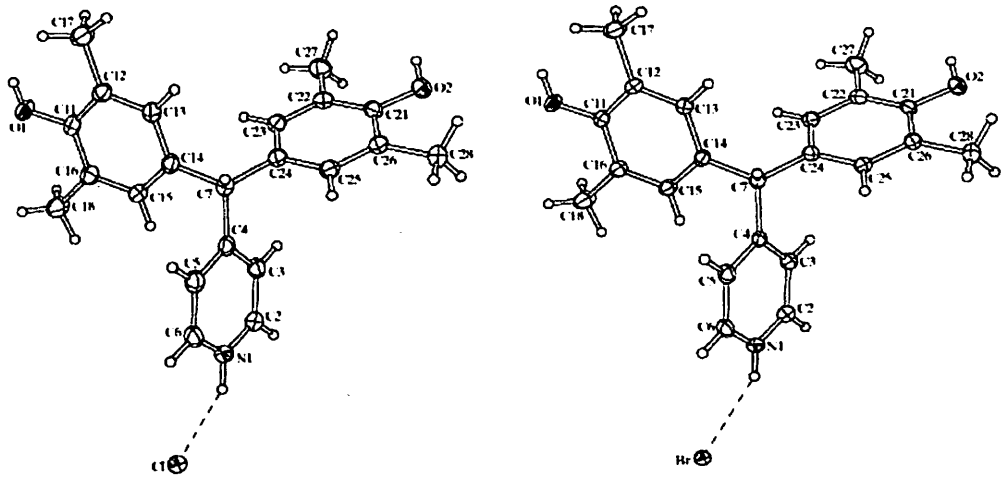

(a) (b)

Fig.50 Crystal structures of (a) 4-[bis(4-hydroxy-3,5-dimethylphenyl)methyl]-pyridinium chloride (**2.2r**) and (b) 4-[bis(4-hydroxy-3,5-dimethylphenyl)methyl]-pyridinium bromide (**2.2s**)

The anion and the three bonded hydrogen atoms are coplanar within 0.1 Å; the configuration can be described as T-shaped rather than trigonal (Fig.51) about the halide ions, which is relatively rare. Examples of T-shaped structural motifs involving halide ions are nonetheless reported in a few cases[105]. Infact, halide anions are known to behave as 'spherical' acceptors without any clearly favoured coordination geometry, although some preference towards quasi-tetrahedral and trigonal configurations can be discerned. These three strong hydrogen bonds link cations into infinite ribbons parallel to the crystallographic *b*-axis.

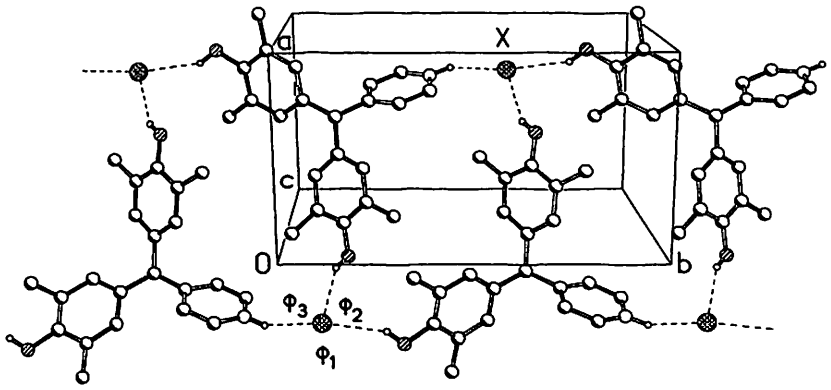

Fig.51 System of strong hydrogen bonds in structures **2.2r** (X=Cl) and **2.2s** (X= Br); H-X-H angles (°): ϕ1 171°, ϕ2 85°, ϕ3 103° in **2.2r**, ϕ1 173°, ϕ2 82°, ϕ3 105° in **2.2s**, e.s.d. ca. 1°.

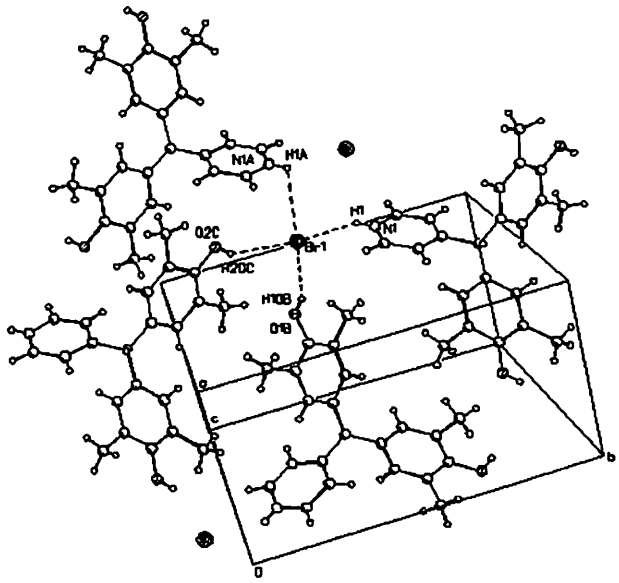

Fig.52 Crystal structure of **2.2s** and formation of N–H···Br^- and O–H···Br^- bridges

Besides, the anion participates in three weak interactions (Table **3.9**) with aromatic and methyl hydrogens, each of the six bonds being to a different cation. It is noteworthy that strong hydrogen bonds in **2.2s** are longer than in **2.2r**, roughly in line with the increase of the anionic radii (1.81 Å for Cl^- vs. 1.96 Å for Br^-)[106] but weaker hydrogen bonds lengthen much

less or even contract. The difference can be explained by higher polarisability of the bromide anion and hence higher (C)H···X dispersion interactions in **2.2s**, while this difference is less relevant for strong hydrogen bonds which have larger contribution of (time-independent) ion-dipole interaction. The weak hydrogen bonds are roughly normal to the T-plane of the strong ones, while the wide angle $\phi 1$ is occupied by the pyridine ring C(2) atom of another cation, generated by an inversion (1−x, 2−y, −z). The corresponding distances C(l)···C(2) 3.382(2) and Br···C(2) 3.458(1) Å are both shorter than the sums of van der Waals radii (3.53 and 3.65 Å, respectively)[107].

Table 3.9 Hydrogen bond geometry (Å, °) for **2.2r** (upper rows, X=Cl) and **2.2s** (lower rows, X=Br)

D−H···A	d (D···X)	d (H···X)	d (D-H-X)
N(1)−H···X	3.037(2)	2.13(3)	149(2)
	3.210(1)	2.33(3)	145(2)
O(1)−H···X (5/2−x,y−1/2,1/2−z)	3.073(2)	2.23(3)	144(2)
	3.199(1)	2.35(2)	146(2)
O(2)−H···X (x, y−1, z)	3.199(2)	2.35(3)	146(2)
	3.375(1)	2.61(3)	136(2)
C(7)−H···X (3/2−x, y−1/2, 1/2−z)	3.956(2)	2.90(2)	166(2)
	3.880(1)	2.84(2)	161(2)
C(17)−H···X (x+1/2, 3/2−y, z+1/2)	3.956(2)	2.91(2)	162(2)
	3.970(1)	2.97(2)	155(2)
C(18)−H···X (2−x, 2−y, −z)	3.803(2)	2.98(2)	134(2)
	3.826(1)	3.05(2)	130(2)

Slow evaporation of a methanol solution of bis(4-hydroxy-3,5-dimethylphenyl)(4-amino phenyl) methane containing aqueous HF gives the corresponding anilinium salt which crystallizes in P-1 (Triclinic) space group. The asymmetric unit of this salt contains one molecule of the protonated bis-phenol and an HF_2^- anion (Fig.53).

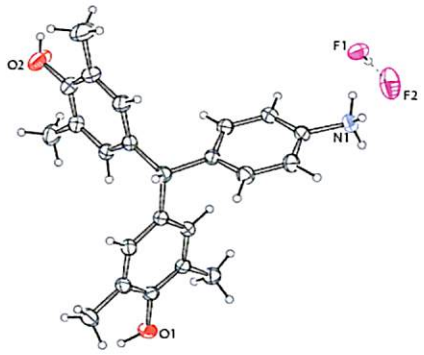

Fig.53 Crystal structure of **2.2q**-H_2F_2 (thermal ellipsoids drawn to 50% probability)

In this complex, protonation of the amino groups results in the formation of the corresponding anilinium salt with HF_2^- as the counter anions. The nitrogen atom of the protonated amino group of **2.2q** in this salt is found to adopt a tetrahedral geometry, with the average <C–N–H bond angle of 107.9°.

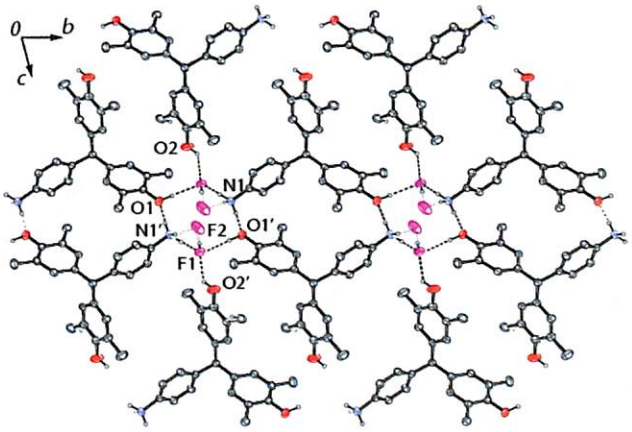

Fig.54 Packing structure of **2.2q**-H_2F_2 salt, viewed normal to *bc*-plane

Table 3.10 Hydrogen bond geometry (Å, °) for **2.2q**.H_2F_2

D–H···A	d (D–H)	d (H···A)	d (D···A)	<D–H···A
F1–H1···F2	0.939	1.310	2.207	157.6
O1–H1o···F1 [x, y–1, z]	0.917	2.150	2.946	144.6
N1–H16···F2 [x–1, y, z]	0.864	1.789	2.646	170.8
O2–H2o···F1 [–x+1, –y+1, –z]	0.939	2.883	3.822	166.4
N1–H15···O1 [–x+1, –y, –z+1]	0.911	2.195	3.062	158.9
N1–H13···F1	0.997	1.677	2.671	174.9

The structure of the salt also shows that the HF_2^- anions are hydrogen bonded to the hydroxy and the anilinium groups. The hydrogen bond geometry for this salt is given in Table **3.10**. While O(1)–H behaves as donor to F1, the hydroxy group, O(2)–H serves as both as donor (to F1) and acceptor (N1–H). As in the case of the halide salts of 4-[bis(4-hydroxy-3,5-dimethylphenyl)methyl]pyridine, the fluoride F2 ion is hydrogen bonded to O(1)–H, O(2)–H and N(1)–H, though the configuration of the three hydrogen bonds is trigonal. These hydrogen bridges involving F2 and the formation of O–H···O and N–H···O hydrogen-bonding interactions (Fig.54) results in the formation of cyclic networks that adopts chair conformation of cyclohexane. In the crystal structure of this adduct the protonated bis-phenol molecules form hydrogen-bonded dimers, which are held by N1–H···O1 ($d_{H\cdots O1}$ 2.195 Å, 158.9°) interactions.

From the analysis of the crystal structures of the bis-phenols and the inclusion complexes, some motifs have been identified that are useful supramolecular synthons for host design and crystal engineering. We have observed that the hydroxy groups of bis-phenols can give rise to linear infinite O–H···O hydrogen bonded chains (Synthon **I**) in certain cases. This is an important supramolecular synthon through which phenols are known to self-associate to give hydrogen-bonded structures. It has been pointed out that the hydroxy groups can serve both as donor and acceptor of hydrogen bonds. The flexibility of this synthon is reflected from the fact that in certain cases the chains have finite length, and can assume cyclic structures incorporating 4 to 6 phenol units. Among these structures, the cyclic hydrogen bonded network involving six phenol units (hexamers, Synthon **II**) is more stable and adopts the chair conformation of cyclohexane. Formation of cyclic hydrogen bonded network from bis-phenols have not been described elsewhere except for a few compounds including 2,2',6,6'-tetramethyl-4,4'-terphenyldiol. We have observed that such cyclic hexamers are obtained from bis-phenols such as **2.1a** or **2.2c** under conditions that lead to saturation of the hydrogen bonding donor and acceptor abilities of the hydroxy groups of the phenol unit.

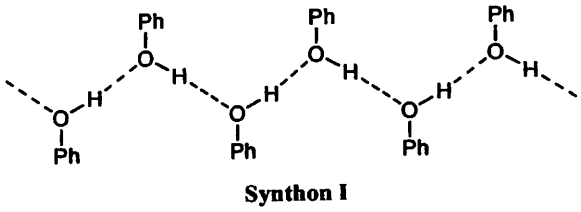

Synthon I

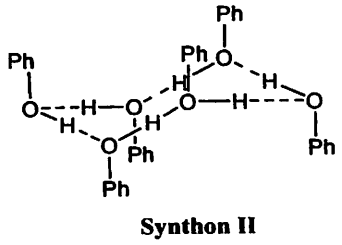

Synthon II

The bis-phenols **2.2** can self-assemble through intermolecular hydrogen bonding interactions, and such interactions also include C–H···O, O–H···π, and N–H···π hydrogen bonds. From the

examples described in this study it has been found that these weak interactions are important factors in determining the packing structure of the bis-phenol molecules.

The presence of two hydroxy groups in **2.2a** for instance leads to infinite hydrogen bonded chains, and these are supplemented by weak C–H···O interactions. As already explained intermolecular hydrogen bonding interactions in the corresponding phenol analog **2.1a** (which does not have the methyl groups) gives rise to cyclic hexamers such that water molecules are held inside the cavity of the hexamer. This is an illustration of the fact that even weakly interacting substituents such as the methyl group can affect substantial changes in the hydrogen bonded assembly of such bis-phenols. In this regard it needs to be pointed out that the C–H···O interactions are considered to be far weaker compared to the conventional O–H···O hydrogen bonds. However, by no means the weak interactions are less important as far as hydrogen bonded assembly of such compounds are concerned. Introduction of another hydroxy group into the 4-position of the phenyl ring of **2.2a** gives the tris-phenol, **2.2d**.

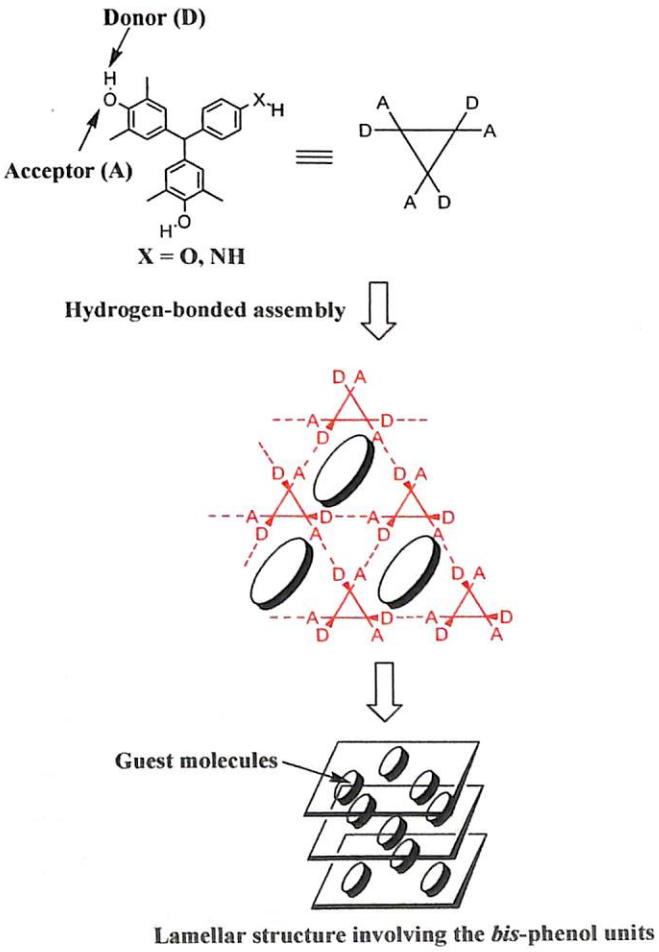

Scheme 1

As already described the tris-phenol, **2.2d** could only be crystallized as the toluene inclusion complex. The packing structure of **2.2d** in the inclusion complex shows the formation of hydrogen bonded cyclic hexamers, which involve each of the three hydroxy groups of the compound. It indicates that the presence of the hydroxy groups facilitates the formation of strong O–H···O hydrogen bonds by cooperative effect, but the orientation of the hydrogen bonds are determined by geometry of the functional groups in the molecule. Thus in this case, the geometry favors the formation of hydrogen bonded hexameric structures. In contrast, the packing structures of tris(4-hydroxyphenyl)methane shows that interactions between the hydroxy groups generate O–H···O hydrogen bonded chains parallel to [110]. These chains extend in two dimensions to form two-dimensional square networks parallel to $[\bar{1}\,11]$ plane. In the packing structure of this molecule the effect of C–H···O interactions are not apparent. The cooperative network of hydrogen bonds formed by the hydroxy groups of the tris-phenol extends in two dimensions to give molecular sheets. This sheet-like structure contains cavities, which are occupied by toluene (guest) molecules, is instrumental in the formation of crystalline inclusion complex of **2.2d** with toluene. Attempts to crystallize this compound from other solvents result in the formation of amorphous or sticky solids. This led us to reason the role of toluene in the crystallization and it appears that maximizing the hydrogen bonding potentials of the hydroxy groups stabilizes the structure. In this regard the triphenyl methane framework provides a rigid platform to the hydrogen-bonded structure.

Since the hydrogen bonding characteristics of the amino group resembles that of the hydroxy groups (both behave as donors and acceptors), we attempted crystallization of **2.2q** with benzene and toluene. However crystals could be obtained from toluene only and the structure did show the presence of toluene as guest. The packing structure of this inclusion complex also shows the formation of finite chains of hydrogen bonds involving the hydroxy and the amino groups and terminating with N–H···π interaction. Closer inspection of this hydrogen-bonding network shows that except for the N–H···π interaction, the packing structure of the bis-phenol molecules in the inclusion complex of **2.2q** is similar to that of **2.2d**, which also forms inclusion complexes with toluene. The formation of such layered structures from the bis-phenol molecules can be explained on the basis of Scheme 1. The hydroxy group or the amino groups can serve as donor as well as acceptor to hydrogen bonds, and under conditions that lead to saturation of hydrogen bonding potentials it is possible to obtain extended networks. Each of the hydroxy group of the bis-phenol molecule is hydrogen bonded to two molecules, so that **2.2d** is connected to six neighbors. The hydrogen bonding network extends in two-dimensions and evolves into a bilayer structure that has lateral dimensions of ~9.692Å in the case of **2.2d**. The hydrogen-bonded networks formed by the **2.2q** molecules also give two-dimensional layers as illustrates in Scheme 1. In this case also each bis-phenol molecule

interacts with six neighbors, including the toluene molecule. Thus, the guest molecules are held inside the cavities of the layers.

The structures of the 1:1 inclusion complex of the bis-phenols **2.2f** and **2.2h** with benzene also show that the host molecules form two-dimensional hydrogen bonded layers. However, the layered structure observed in this case has an important distinction from those with either **2.2d** or **2.2q** with toluene. An important distinction arises due to the structure of the bis-phenols; in the case of **2.2f** and **2.2h** the hydroxy groups behave both as donors and acceptors, while the –nitro and –formyl groups behave only as hydrogen bond acceptors (Scheme 2).

Thus, the competition between the acceptor abilities of the hydroxyl group and the nitro (**2.2f**) and formyl (**2.2h**) groups leads to selection of the stronger donor…acceptor interactions. In case of **2.2f** the O–H···O interactions involving only the hydroxy groups are weaker ($d_{D\cdots A}$ 3.215 Å) compared to O–H···O interactions involving the hydroxy and the nitro group, which is a strong hydrogen bond acceptor ($d_{D\cdots A}$ 2.873 Å and 3.040 Å).

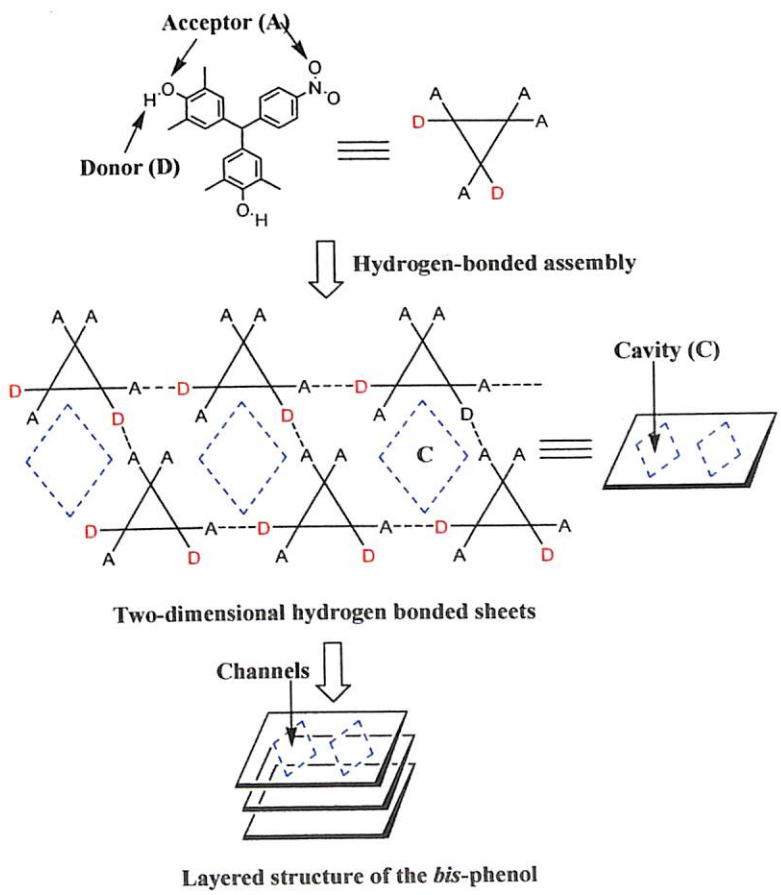

Scheme 2

In **2.2h**, the donor…acceptor (D···A) interactions between the hydroxy group and the formyl group are stronger, than hydrogen bonding O–H···O interactions involving only the hydroxy

groups. From the packing structures it is observed that hydrogen bonding between the bis-phenol molecules results in the formation of two-dimensional layers (sheets). These layers are formed by D···A interactions between hydroxy groups and the acceptor groups of the bis-phenol molecules (that extend along [010] plane) and in the process cavities are formed. Each of these supramolecular cavities bind two molecules of benzene and in three dimensions the packing of the layers give rise to channels. Consequently in both cases of bis-phenol molecules containing strong acceptors, channels are obtained (dimensions ca. 7.0 × 8.2Å) large enough to accommodate two benzene molecules.

We have also described that the chloride or bromide or fluoride ion can induce formation of anion template self-assemblies of bis-phenols containing protonable nitrogen atom.

Chapter 4

Synthesis and Structures of 14-Aryl-14*H*-Dibenzo[*a,j*]xanthenes

It has already been described in Chapter 1 that the condensation of phenols with carbonyl compounds gives bis-phenols. We have also shown that by adopting suitable procedures bis-phenols having diverse structures can be prepared. In this regard the syntheses of methyl-substituted phenols with different aromatic aldehydes are described in Chapter 2. These compounds are found to have immense potential from structural point of view as molecular synthons for crystal design. We realized that if such bis-phenol derivatives could be prepared from polyaromatic systems, it would widen the scope of our study. Subsequently, we have attempted preparation from 2-naphthol with different aldehydes. However the products obtained from these reactions turned out to be the dibenzoxanthene derivatives, **4.1** (as in equation 33). Thus, the results obtained from the study of the synthesis and structure of these dibenzoxanthenes derivatives are presented in this chapter.

We have prepared the dibenzoxanthenes (**4.1**) derivatives in a single step protocol[108] involving condensation of 2-naphthol with different aldehydes in the presence of acids (equation 33). The reaction medium used in this transformation contains mixture of acetic acid and sulfuric acid. From these reactions the dibenzoxanthene derivatives are obtained as crystalline products.

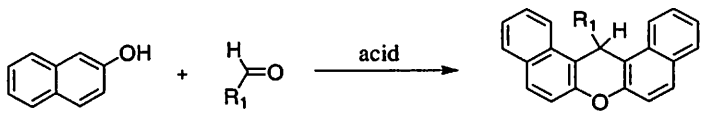

4.1 (a-f)

R_1: phenyl **(a)**
4-methylphenyl **(b)**
2-nitrophenyl **(c)**
4-bromophenyl **(d)**
4-nitrophenyl **(e)**
2-chlorophenyl **(f)**

Equation 33

The compounds **4.1a** and **4.1b** as well as **4.1f** are obtained as colorless crystalline solids while the compounds **4.1c** and **41.e** are obtained as pale yellow colored solids. In contrast the compound **4.1d** is obtained purple as colored solid. The dibenzoxanthene molecules have polyaromatic ring system and hence they are expected to have fluorescent properties.

Recently it has been reported that 14-alkyl-14-H-dibenzo[*a,j*]xanthenes can be synthesized by condensation of 2-naphthols with different aliphatic aldehydes[109,110]. However, the reactions of naphthols and aldehydes can also lead to calix[4]naphthalenes[111] or spirodienones[112]. These

results and from our observations we have clearly shown that by varying reaction condition one can obtain selective products from 2-naphthol condensation with aldehydes[34].

The dibenzoxanthene derivatives **4.1** have been characterized by IR spectroscopy, NMR spectroscopy, mass spectrometry, and elemental analysis. The crystal structures of a few such compounds have been determined by X-ray crystallography.

For example, the compound **4.1a** crystallizes as colorless plates from ethyl acetate in the monoclinic $P2_1/n$ space group (Fig.54). The asymmetric unit of this compound contains one molecule (Fig.55a), whereas the unit cell contents, Z=4. The molecules are held together by weak C(21)–H···O1 ($d_{H\cdots O1}$2.598Å, <C–H···O153.1°) interactions and this results in a close packed structure (Fig.55c). The phenyl ring at 14-position makes an angle of 114° with the plane of the xanthene ring and this gives a T-shape to the molecule. From the packing structure it is observed that intermolecular C–H···O interactions lead to the formation of hydrogen bonded pairs (Fig.55b).

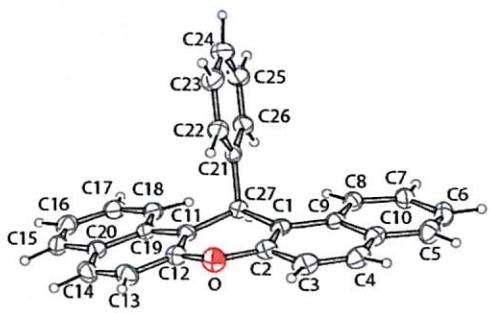

Fig.55 (a) Crystal structure of 14-(phenyl)-14-H-dibenzo[*a,j*]xanthene, **4.1a** (thermal ellipsoids drawn to 50% probability)

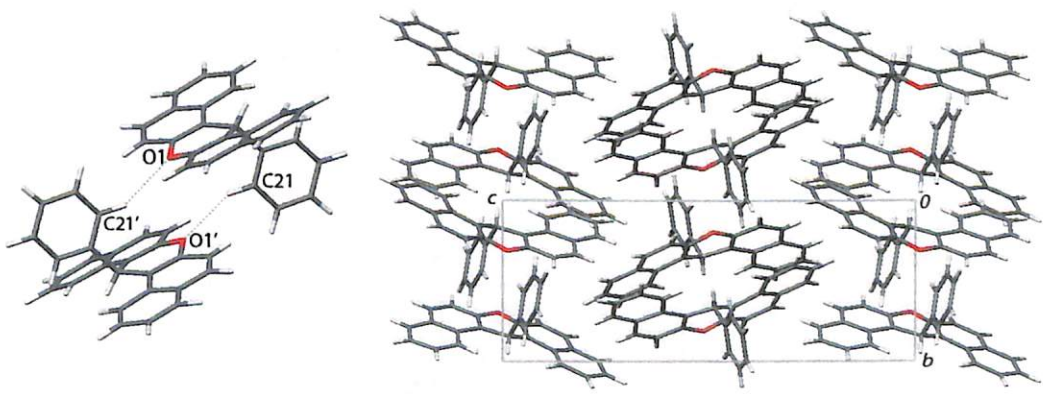

(b) (c)

Fig.55 (b) Weak C(21)–H···O interactions in **4.1a** and (c) the packing structure

The compound **4.1b** crystallizes as colorless rods from tetrahydrofuran which belongs to orthorhombic Pna2(1) space group (Z=6). In this molecule the 4-methylphenyl group at 14-position makes an angle of 111.6° to the plane of the xanthene rings, and the torsion angle (C10/12-C11-C22-C23) is close to 60°. This means that the plane defined by benzene ring of the 4-methylphenyl group (Fig.56a) is staggered relative to the conformation of C11. This obviously leads to minimization of steric repulsion between the pyran ring and the C–H bond. It is to be noted that in case of the substituent at 14-position of the dibenzoxanthene unit also adopts similar staggered conformations. The packing of the molecules (Fig.56b) give rise to layered structures with interlayer distance of 4.00(2) Å suggesting the absence of any π-π interaction between the molecules in the layers.

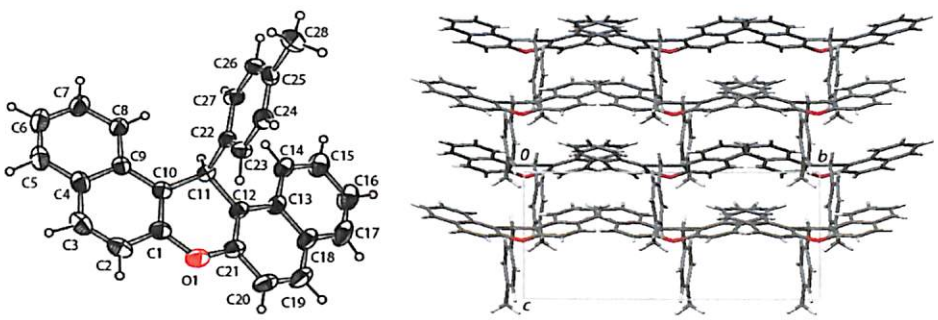

(a) (b)

Fig.56 (a) Crystal structure of 14-(4-methylphenyl)-14-H-dibenzo[*a,j*]xanthene **4.1b** (thermal ellipsoids drawn to 50% probability) and (b) the packing structure of the molecules

Crystallization of the compound **4.1c** from ethyl acetate gives hexagonal yellow needles, and these crystals belong to orthorhombic Cmc/2 space group. The yellow color of this compound obviously comes from the presence of the nitro group. The asymmetric unit contains one-half of the molecule (Fig.57), which results from the pseudo-symmetry involving a mirror plane passing through O1, C11, C12 and C15. Thus, the N atom and O2 of the nitro group is disorder with 50% occupancy about this mirror plane.

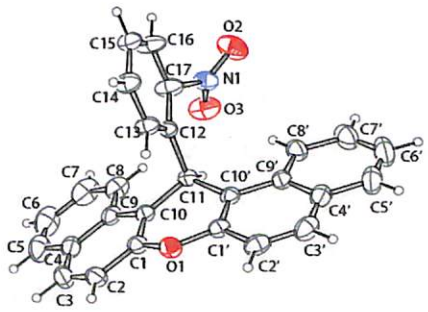

Fig.57 Crystal structure of 14-(2-nitrophenyl)-14-H-dibenzo[*a,j*]xanthene, **4.1c** (thermal ellipsoids drawn to 50% probability)

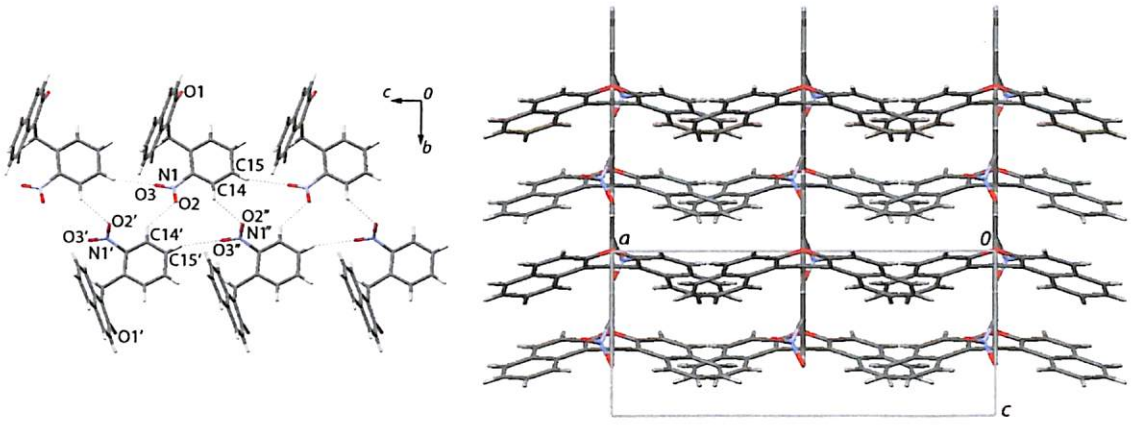

(a) (b)

Fig.58 (a) Hydrogen-bonded tapes along *c*-axis in **4.1c**, and (b) Packing structure viewed normal to the *ac*-plane

The presence of weak intermolecular C14'–H···O2 ($d_{H\cdots O2}$ 2.706Å, <C–H···O 127.6°) and C15'–H···O3" ($d_{H\cdots O2}$ 2.581Å, <C–H···O 160.2°) interactions lead to hydrogen-bonded tapes (Fig.58a) which grow along *c*-axis. The weak hydrogen bonds observed in this structure involve C14–H and C15–H as the donors and the oxygen atoms of the nitro groups as the acceptors. These hydrogen-bonded tapes run in the same direction in the packing structure (Fig.58b) which gives rise to a layered structure and the inter-layer separation in this compound is ca. 3.973 (3)Å.

These compounds absorb in the range of 340-400nm in the UV-visible spectra. Since the dibenzoxanthene derivatives (**4.1**) contain polyaromatic ring systems, they are expected to be fluorescent in solution. Moreover, the fluorescence properties of these compounds and the characteristic emissions wavelengths would be different depending on the nature of substitutents. Thus, we present the fluorescent properties of dibenzoxanthenes (**4.1**) from which it is evident that these properties are dependent on the nature of the substituents. This is illustrated by comparing the fluorescence spectra of **4.1b** and **4.1c** in tetrahydrofuran.

Excitation of **4.1b** in tetrahydrofuran at 340nm results in a strong fluorescence emission with λ_{max}359nm (Fig.59a). In contrast the excitation of **4.1c** at 390nm shows only a weak emission band centered at λ_{max}493nm. The red shifting of the excitation and the emission bands in the case of **4.1c** compared to **4.1b** is probably due to the presence of the electron-withdrawing nitro group. It may be noted that when the fluorescence spectra of the two compounds, keeping ceoncentration same in both cases. However, the presence of the nitro also quenches the fluorescence of these dibenzoxanthenes. In the same solvent and similar concentrations, the compounds **4.1a** shows emission at 346nm (excitation at 325nm) and **4.1f** shows only a

weak emission at 362nm (excitation at 340nm). However, the compounds **4.1e** and **4.1f** are fluorescent inactive, although they do show UV-visible absorptions at 384nm and 412nm respectively.

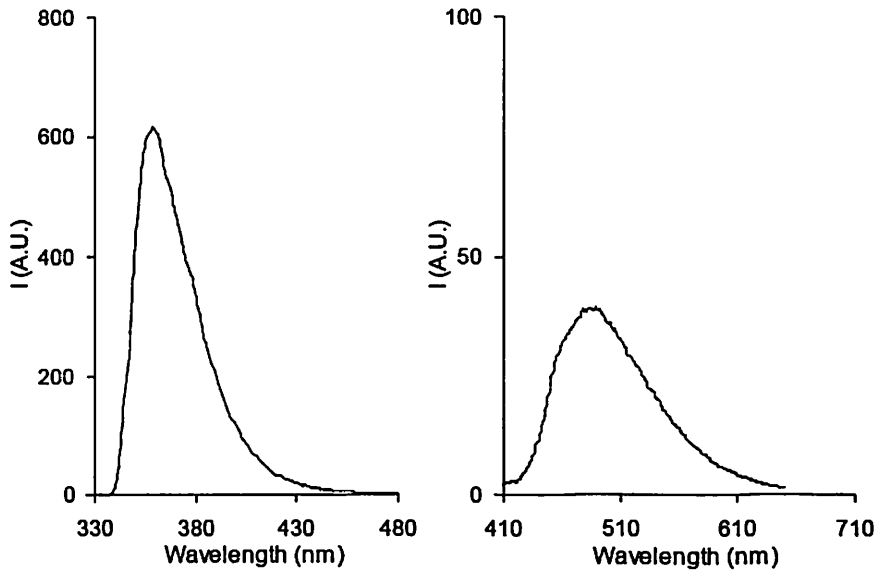

(a) (b)

Fig.59 Fluorescence emission spectra of (a) **4.1b**, (b) **4.1c** in tetrahydrofuran on excitation at 340 and 390nm respectively (concentration 10^{-5}M)

Thus, we have demonstrated the synthesis, characterization, and structures of a few dibenzoxanthene derivatives along with their fluorescence properties. These compounds have potential applications as laser materials and in chemotherapy as analogous compounds are known to possess such properties[113]. From our crystallographic studies we could establish that these molecules adopt close-packed structures, which are held by weak C–H···O interactions. The molecules having substituents at the bridging carbon of the pyran ring which links two naphthalene rings possess T-geometry and these compounds gives layered structures in the solid-state.

Chapter 5

Synthesis and Structures of Diaryl Quinone Methides

Quinone methides occur as key intermediates in some important chemical transformations[114-117] and are also found to as intermediates in certain biological reactions[2] involving vitamin K_1, K_2 and vitamin E[118,119]. Interaction between bio-molecules and the electrophilic oxidation products like quinone methides are often lead to cytotoxic effects and enzyme inhibition[120-123].

The quinone methides can be described by dipolar structures, which show that molecules have nucleophilic center at the oxygen atom and electrophilic center at the carbon-atom of the methylene group. This makes the simple quinone methides such as **62** extremely reactive and can be used both as electrophilic as well as nucleophilic synthons during synthesis.

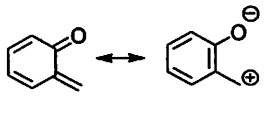

62a

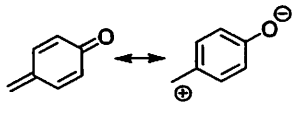

62b

5.1 Synthesis of Quinone Methides

Synthesis of some rather unstable quinone methides, **63** and **64** is achieved by oxidizing the corresponding phenols with silver oxide in carbon tetrachloride[124]. The compounds are characterized by insitu NMR spectroscopy, and for certain quinone methides with unsymmetrical substituents on the terminal methylene, the ring protons are non-equivalent on the NMR time-scale. This is attributed to van der Waals deshielding.

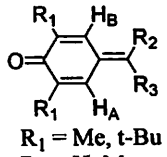

R_1 = Me, t-Bu
R_2 = H, Me
R_3 = H, Me, CH_2=CH_2

63a-c

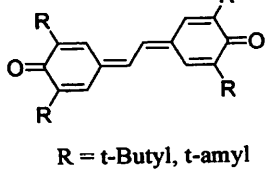

R = t-Butyl, t-amyl

64a,b

As already discussed in Chapter 1, bis-phenols such as **29** are oxidized by PbO_2 (equation 34) to the corresponding quinone methides (**65**), and to the phenoxyl radical derivatives (**66**), which are related to the free radical galvinoxyl[45]. These galvinoxyl radicals exhibit strong coupling with the compounds having methoxy groups.

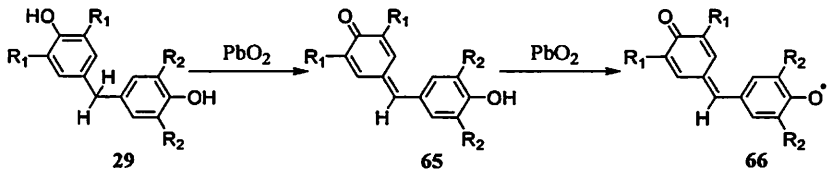

R_1 =Me, t-Bu, OMe
R_2 = Me, t-Bu, OMe

Equation 34

Similarly, oxidation of 2,6-dimethylphenols with metal oxides or by $K_3[Fe(CN)_6]$ in basic medium (equation 35) also produces quinone methide intermediates such as **67** which are however rather unstable.

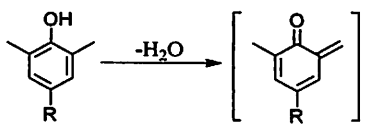

67

Equation 35

Quinone methides, which contain bulky substituents such as phenyl groups, are comparatively more stable. Thus, bis-phenols having ferrocene substituents are oxidized to the corresponding quinone methides, **68** (equation 36).

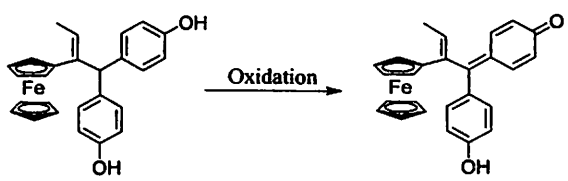

27 **68**

Equation 36

Moreover, substituted quinone methides such as **33** can be prepared by irradiating an alcoholic solution of 2,6-di-t-butylphenol and benzophenone (equation 37) in the presence of catalytic amount of mineral acid[47].

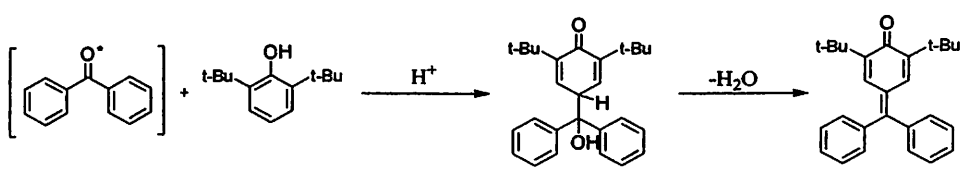

33

Equation 37

Quinone methides having tri-aryl structures such as **70**, which are also called galvinols can be synthesized following an organometallic pathway[125] by treating the respective carboxylic ester (equation 38) with (2,6-di-tert-butyl-4-lithium-phenoxy) trimethylsilane (**69**) and hydrolysis of the trimethyl silyl protecting group.

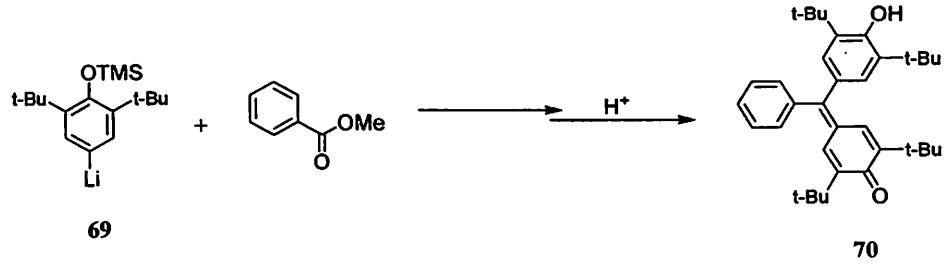

69 **70**

Equation 38

Quinone methides bridged by disulfide bridges, **72** are synthesized[126] by condensation of the lithiated phenol (**69**) with the appropriate ester (**71**). The intermediate **72** undergoes oxidation in air to give the corresponding disulfide bridged bis-galvinoxyl, **73** (equation 39).

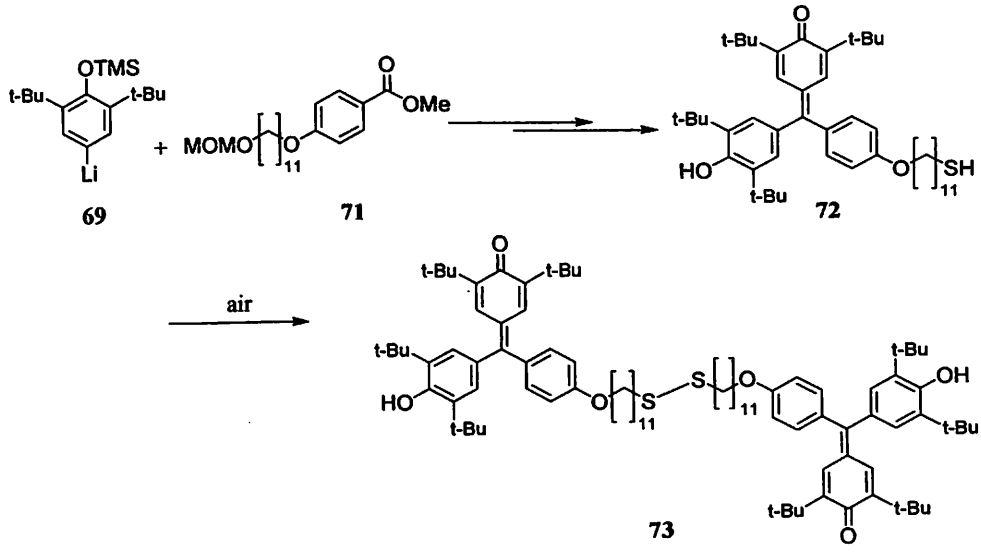

69 **71** **72**

73

Equation 39

As mentioned already, the bis-phenols, bis(4-hydroxy-3,5-dimethylphenyl)(aryl)methane (**2.2**) are obtained as colorless to pale yellow compounds, which undergo gradual change in color when exposed to air and finally become red or purple. This color change in **2.2** is attributed to oxidation that leads to the formation of the corresponding quinone methide derivatives, **5.1**. However similar phenomenon is not observed in case of the bis-phenols bis(4-hydroxy-phenyl)(aryl)methane (**2.1**) which are mostly colorless to pale yellow in color. It has been found that chemical oxidation of a bis-phenol can also results in the formation of the corresponding quinone methides derivative. The quinone methide derivatives contain

phenol and quinone groups that are separated by methine spacers. The phenol units exhibit electron donor properties while the quinone groups behave as acceptors. Thus these compounds have conjugated structures, which should be reflected in their solid-state and solution properties. The synthesis and structures of a few diaryl quinone methide derivatives are described in this chapter.

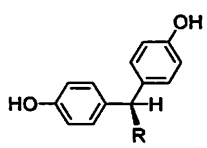

2.1

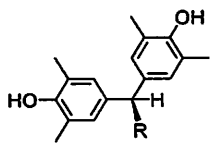

2.2

We have found that oxidation of bis-phenols (**2.2**) occur with oxidants like ammonium persulfate. This method involves oxidation of one of the phenol units of the bis-phenol and this results in the formation of the diaryl quinone methides, **5.1**. The oxidation of bis-phenols with ammonium persulfate[101] is performed in aqueous acetonitrile solution (equation 40).

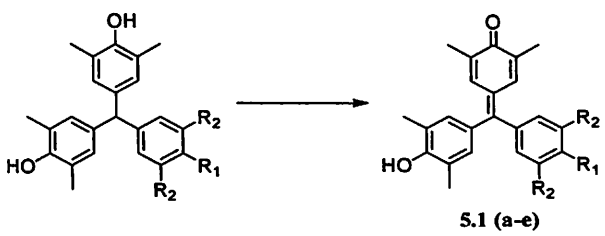

5.1 (a-e)

Equation 40

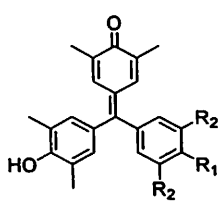

5.1 (a-e)

a: R_1 = H; R_2 = H
b: R_1 = H; R_2 = Me
c: R_1 = H; R_2 = OH
d: R_1 = H; R_2 = OMe
e: R_1 = OMe; R_2 = OMe

It is noteworthy that the compound **5.1c** could be selectively prepared by oxidation of the corresponding tris-phenol, **2.2d** (equation 41) using the conditions described above. In this case the presence of methyl substituents ortho- to the hydroxy group is expected to increase the stability of the quinonoid structures.

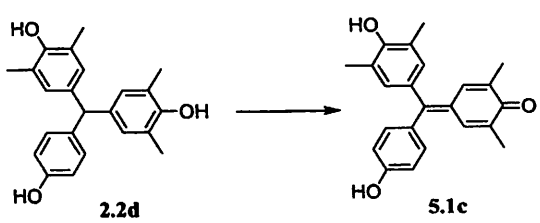

2.2d **5.1c**

Equation 41

It is observed that the oxidation occurs such that the quinone unit resides in the position of the more substituted phenol unit rather than the unsubstituted phenol ring. This oxidation reaction is effective in case of bis-phenols containing electron donating substituents. The presence of electron-withdrawing substituents makes the bis-phenols less susceptible to oxidation with ammonium persulfate. However, our attempts to oxidize these bis-phenols with other reagents such as pyridinium chlorochromate, silveroxide and potassium ferricyanide led to multiple products, which could not be separated.

The quinone methides (**5.1**) are obtained as highly coloured crystalline compounds that have poor solubilities in organic solvents, and almost insoluble in water. The quinone methides have been characterized by IR spectroscopy, NMR spectroscopy and mass spectrometric techniques. The quinone methides behave as chromophores and are sensitive to acids and bases. Spectroscopic and electrochemical properties of these compounds have been done with the objective that the molecules with hydroxy or methoxy groups in the periphery resembles the galvinol system, and is described to exhibit interesting electronic properties. These aspects for the diaryl quinone methides **5.1** are discussed in Chapter 6.

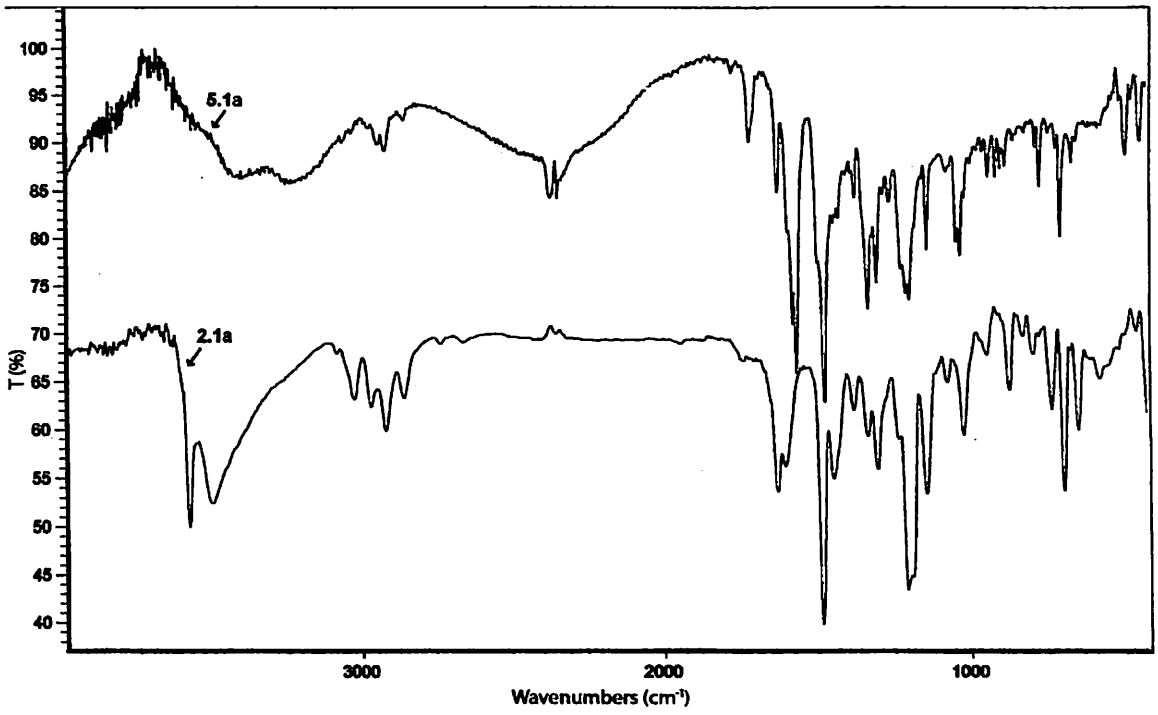

Fig.60 FT-IR spectrum of **5.1a** compared with the corresponding bis-phenol **(2.1a)**

The FT-IR spectra of the quinone methides **5.1** shows the presence of broad absorption bands in the region 3500-3000cm^{-1}, indicating that the hydroxy groups are extensively hydrogen bonded. This is illustrated by the solid-state FT-IR spectrum of **5.1a** (Fig.60), which has

broad absorption bands centered at 3164 and 3280cm^{-1}. Compared to the corresponding bis-phenol **2.2a**, the hydroxy stretching bands are shifted towards lower frequencies indicating efficient hydrogen bonding.

The structures of these compounds have also been studied by X-ray crystallography. From the analysis of the crystal structures we expect to identify the different hydrogen-bonding motifs in these quinone methides.

5.2 Structures of Diaryl Quinone Methides

The diaryl quinone methides described here have triphenylmethyl frameworks and crystal structures show that these compounds adopt propeller conformations both in solution as well as in the solid-state. These compounds contain both phenolic and quinone groups that are separated by methine groups. The structural aspects of the quinone methides are studied in order to understand the nature of intermolecular hydrogen bonding interactions in such molecules that have the phenol and quinone units in conjugation. It will be interesting to know whether the presence of donor-acceptor in conjugation can influence the solid-state structures of these compounds. Thus, such a study of the structures and properties of these compounds can be applicable in the design of novel materials[127] having useful electronic, host-guest and catalytic properties.

It is expected that introduction of substituents in the vicinity of the hydroxy groups would affect the geometry of the hydrogen bonding interactions between the hydroxy groups of the phenol (as donors) and the carbonyl groups of the quinone part (as acceptors). We have studied the effect of the methyl groups as substituent that are positioned ortho- to the hydroxy and the quinone unit.

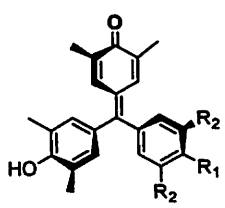

5.1 (a-e)

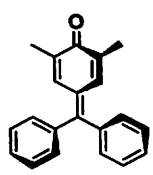

5.2

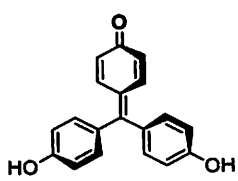

5.3

In this regard the crystal structures of the quinone analogs, 2,6-dimethyl-4-(α,α-diphenylmethylene)-1,4-benzoquinone, **5.2** (2,6-dimethylfuchsone), and 4-[bis(4-hydroxy-phenyl)-methylene] cyclohexa-2,5-dienone, **5.3** can be compared. It has been reported that **5.2** has two polymorphic forms[128], α and β; interestingly, the racemic crystals of the α-form undergoes thermal conversion to give chiral crystals in the β-form.

The compound, 4-[bis(4-hydroxyphenyl)methylene]-cyclohexa-2,5-dienone (rosolic acid, **5.3**) is similar to both **5.1** and **5.2** in terms of the triphenyl methyl structure. However, in case of **5.3**, the presence of oxygen atoms at the 4-positions in the form of two phenol moieties and a quinone unit is expected to result in the formation of intermolecularly hydrogen-bonded networks. Thus, the crystal structure of **5.3** has been studied because this molecule is structurally related to the diaryl quinone methides **5.1**, and hence important in elucidating the structural aspects of the quinone methides.

The compound **5.3** crystallizes from ethyl acetate as the 1:1 adduct, in the monoclinic $P2_1/n$ space group. The crystal structure shows this molecule to adopt a propeller conformation in the solid-state (Fig.61a), and the exocyclic double bond, C(7)=C(8) is twisted by ~27° relative to the plane of the quinone ring. Presumably this happens due to repulsion between the hydrogen atoms attached to C5/C13 and C9/C19 of the molecule.

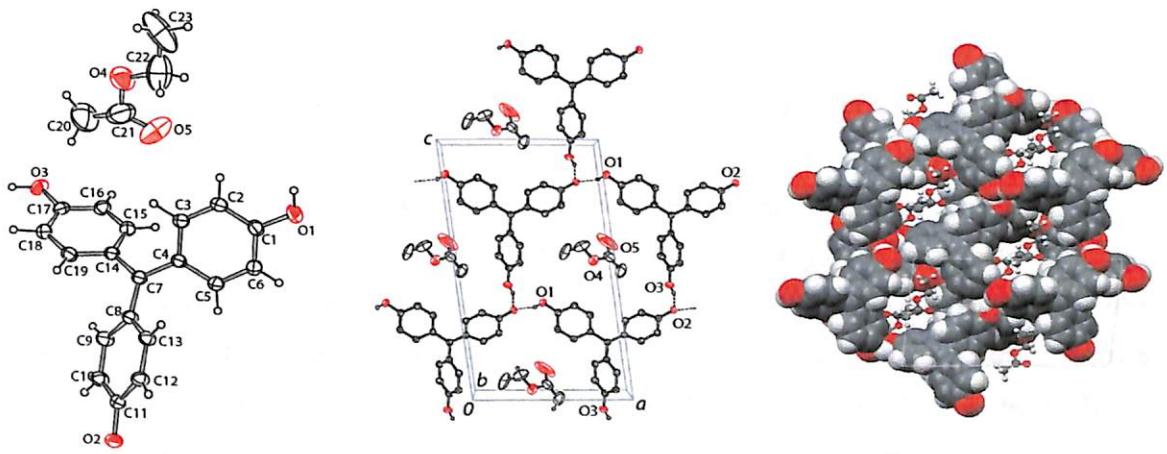

(a) (b) (c)

Fig.61 (a) Crystal structure of the 1:1 inclusion complex of **5.3**-ethyl acetate (b) Intermolecular hydrogen bonded layers contain ethyl acetate molecules in the cavities, and (c) Packing structure shows the orientation of the one dimensional channels

Table 5.1 Hydrogen bond geometry (Å, °) for the inclusion complex of **5.3**-ethyl acetate

D–H···A	d (D–H)	d (H···A)	d (D···A)	< D–H···A
O1–H1o···O2 [x–1, y, z]	0.894	1.756	2.636	167.7
O3–H2o···O2 [x–1, –y+1, z–1/2]	1.051	1.703	2.651	147.5

In the ethyl acetate inclusion complex of **5.3**, it is observed that the hydroxy groups of the molecules form strong hydrogen bonds to the quinone groups. The quinone oxygen O2 acts as two-point acceptor to the hydroxy groups, O(1)–H and O(3)–H, which serve only as hydrogen bond donors. The intermolecular hydrogen-bond distances and geometries of this inclusion compound are given in Table **5.1**. The interactions between these hydrogen bonded chains lead to the formation of two-dimensional networks (square nets, Fig.61b) that are parallel to that run parallel to the [010]. Moreover, the network structure shows the presence of intermolecular C–H···O ($d_{H\cdots O3}$ 2.492Å; < C–H···O 136.4°) interactions involving C12–H as the donor and the oxygen atom of O3–H as the acceptor. This C–H···O interaction is probably facilitated by the complementary O–H···O hydrogen bonds involving the carbonyl group of the quinone unit that is ortho- to C(12)–H as shown in Synthon **III**.

The geometrical aspects of such weak C–H···O interactions have also been described in 4,4-diphenyl-cyclohexa-2,5-dienone analogs[130]. The two-dimensional networks (that have also been called as square nets) formed by **5.3** molecules have cavities, which accommodate the ethyl acetate molecules. Weak C–H···O ($d_{H\cdots O5}$ 2.589Å; 118.4°) interactions are observed between the solvent molecules and the host molecules in lattice involving C(3)–H as the donor and oxygen O(5) of ethyl acetate as the acceptor. The symmetry related 2D networks pack along the *b*-direction so that the cavities are retained (Fig.61c) in the form of one-dimensional channels having dimensions ~7.0Å × 7.6Å, which are occupied by the ethyl acetate molecules. In the inclusion complex of **5.3** with ethyl acetate, the solvent molecules are disordered about a 2-fold axis passing through O(4), which relate C(21) and C(22) by symmetry. Thus, the molecule is refined so that O(5) has 75% occupancy at C(21), and the large ellipsoid of C(22) (refined 100% occupancy) indicative of the nature of the disorder at that position.

It may be mentioned that the quinone methide analog, 4,4-diphenyl-cyclohexa-2,5-dienone (**5.4a**), has four independent polymorphic forms[129]. In this case each of the four polymorphs was characterized by single crystal diffraction and nineteen unique hydrogen-bonding patterns could be identified. It may be noted that the synthons **III-V** have been described in analogous quinonoid systems, and such interactions have important structural implications [130]. In one of the polymorphic forms of **5.4a**, the screw-axis related molecules self-assemble (Fig.62a) through intermolecular C–H···O hydrogen bonding interactions leading to the formation of helices. In contrast, the self-assembly of **5.4b** (Fig.62b) gives rise to hydrogen bonded tapes which are mediated by intermolecular C–H···O interactions ($d_{H\cdots O}$ 2.66Å, <C–H···O 160.6°). Since the biphenyl groups do not take part in the usual herringbone T-motif or aromatic π-stacking interactions, self-inclusion is not observed. This leads to the

formation of host-matrices that have open frameworks and are assembled through weak interactions. These structures have versatile inclusion abilities and form host-guest structures.

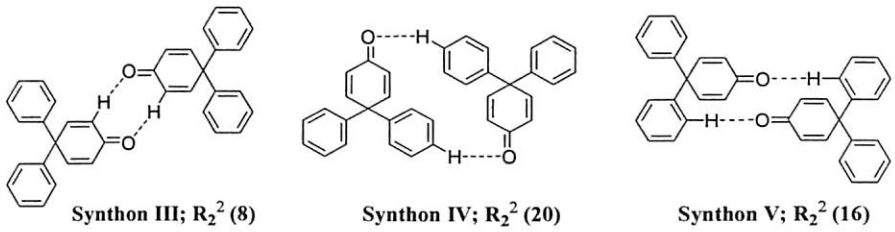

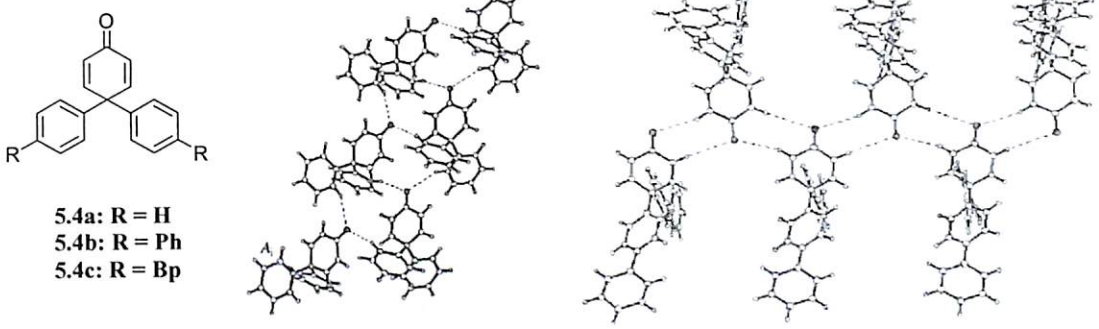

(a) (b)

Fig.62 (a) Structure of the C–H···O hydrogen-bonded helices, *C*(8), in 4,4-diphenyl-2,5-cyclohexadienone (**5.4a**) between 2_1-related molecules in one of the polymorph (b) Structure of the C–H···O hydrogen bonded tape in **5.4b** along *bc*-direction[130]

We have found that compound, 4-[(4-hydroxy-3,5-dimethylphenyl)(phenyl) methylene]-2,6-dimethylcyclohexa-2,5-dienone (**5.1a**) crystallizes as red plates from acetonitrile in P-1 space group.

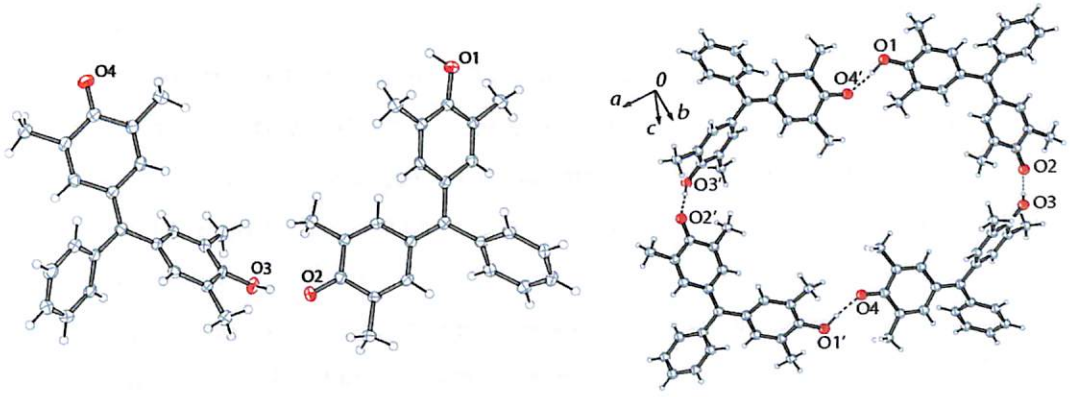

(a) (b)

Fig.63 (a) Structure of **5.1a** (thermal ellipsoids drawn to 50% probability), and the (b) hydrogen-bonded cyclic tetramer

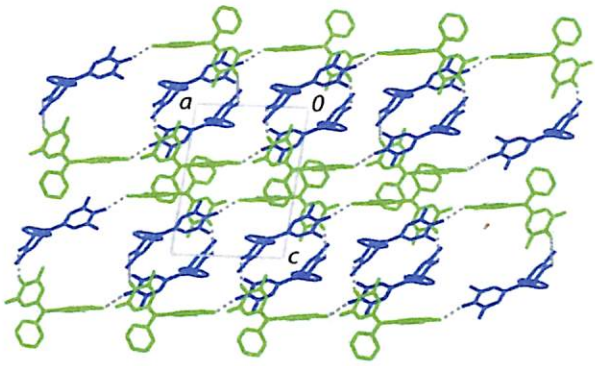

Fig.64 Packing of **5.1a** with symmetry independent molecules shown in green and blue

Table 5.2 Hydrogen bond geometry (Å, °) for the inclusion complex of **5.1a**

D–H···A	d (D–H)	d (H···A)	d (D···A)	<D–H···A
O1–H1···O4 [x–1, y, z]	0. 933	1.783	2.694	167.3
O3–H2o···O2 [x–1, –y+1, z–1/2]	0.963	1.773	2.724	172.3

The crystal structure shows that the asymmetric unit (Fig.63a, 64) contains two independent molecules. The crystal structure of **5.1a** it is observed that the molecules form hydrogen-bonded tetramers (Fig.63b). The carbonyl group of the quinone unit and the hydroxy group of the phenol unit are involved in the formation of the cyclic network of hydrogen bonds. From the structure of this molecule, the carbonyl bond lengths, C24–O2 and C54–O4, of the quinone units are found to be 1.253 and 1.256Å respectively, while the corresponding bond lengths of the double bonds C1–C21 and C2–C51 are 1.387 and 1.393Å. The two double bonds, C1–C21 and C2–C51 are also twisted by 18° and 24° respectively, due to the repulsion between the hydrogen atoms attached to C26 and C32, as well as C12 and C22 present in the two aryl rings. Moreover, the oxygen atom of the carbonyl group C54–O4 in the quinone part serves as hydrogen bond acceptor to O1–H (dH···O4 1.769Å, <O–H···O 172.2°) and C12–H (dH···O4 2.567Å, <C–H···O 139.0°). It is observed that the C–H···O interaction involving C12–H from one of the tetrameric unit and C54–O4 of another tetrameric unit related by [-x, 2-y, -z] causes stacking of the tetramers along the *b*-axis. The intermolecular hydrogen-bond distances and geometries for **5.1a** are listed in Table **5.2**.

The quinone methide, 4-[(4-hydroxy-3,5-dimethylphenyl)(4-hydroxyphenyl)-methylene]-2,6-dimethylcyclohexa-2,5-dienone (**5.1c**) crystallizes from acetonitrile as red crystals that belong to C2/c (Monoclinic) space group.

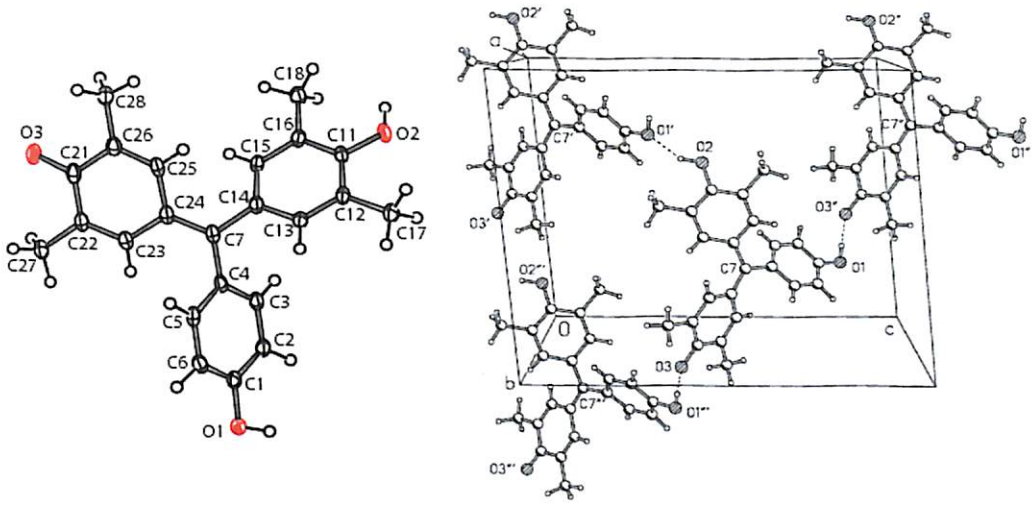

(a) (b)

Fig. 65 (a) Crystal structure of **5.1c** (thermal ellipsoids drawn to 50% probability), and (b) Hydrogen bonding interactions in **5.1c**

Table 5.3 Hydrogen bond geometry (Å, °) for the inclusion complex of **5.1c**

D–H···A	d (D–H)	d (H···A)	d (D···A)	<D–H···A
O1–H···O3 [x+1/2, –y +1/2, z +1/2]	0. 953	1.703	2.650	178.3
O2–H···O1 [x–1/2, –y+1/2, z +1/2]	0.993	1.943	2.867	154.2

This crystal structure of **5.1c** shows that the molecule has no crystallographic symmetry (Fig.65a) and that the molecules are assembled through an extensive network of O–H···O hydrogen bonds involving the hydroxy groups of the phenol units and the carbonyl group of the quinone. The hydroxy group, O2–H is the hydrogen bond donor to O1–H which is in turn bonded to the C=O group of the quinone, which serves as the acceptor. Weak intermolecular C–H···O interactions ($d_{H\cdots O3}$ 2.573Å, <O–H···O 126.8°) between the carbonyl group of the quinone units and C2–H are also observed in the structure. The hydrogen-bond distances and geometries of the intermolecular interactions in **5.1c** are summarized in Table **5.3.** These intermolecular hydrogen-bonding interactions cause the molecules to form square networks, which extend in step-like manner which extend in two-dimensions to produce sheet-structures (Fig.65b).

However, an important aspect of this structure is the interpenetration of two of the hydrogen-bonded sheets in such a way that it gives rise to self-inclusion structures (Fig.66). Thus, one

of the vertices of the square network occurs as the guest in the cavity generated by the other sheet.

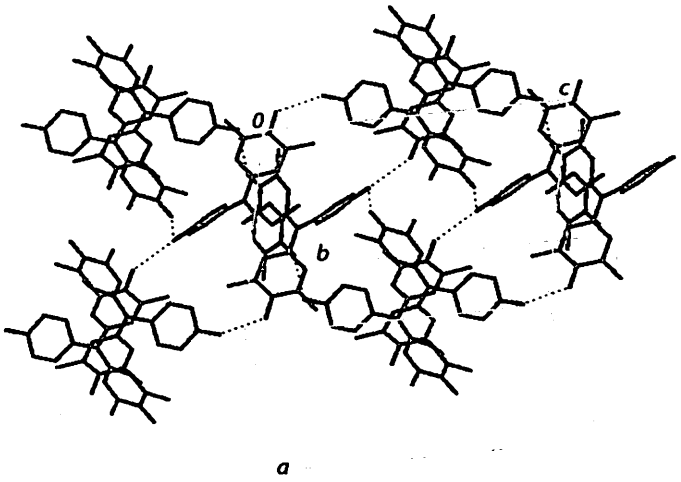

Fig.66 Packing diagram showing the formation of self-inclusion networks of **5.1c**

The concept of self host-guest structures is recently illustrated in 4,4-bis(3-methyl-4-hydroxyphenyl)-cyclohexanone[50]. The crystal structure of the keto bis-phenol described in this example contains two symmetry independent molecules in the asymmetric unit and each of the two molecules show different hydrogen-bonding properties at the supramolecular level.

The compound **5.1d** gives dark purple crystals and crystallizes from acetonitrile in $P2_1/c$ (Monoclinic) space group. The molecule **5.1d** has no crystallographic symmetry (Fig.67a) and is similar in conformational to 2,6-dimethyl-4-(diphenylmethylene)-cyclohexa-2,5-dienone (**5.4a**) in one of its three polymorphs[50]. The torsion angles about the C(7)–C(4) and C(7)–C(14) single bonds are 39.5° and 36.5° respectively, while the central carbon atom (C7) has trigonal planar geometry. It is important to note that the C(7)=C(24) is twisted by 18.0°, similar to the case of **5.1a** due to steric repulsion between peri-H atoms attached to C5/C23 and C15/C25 respectively. These interactions account for the lack of aromatic π-stacking interactions in the packing of these molecules.

The crystal structure of **5.1d** shows that the molecules self-assemble though intermolecular O–H···O hydrogen bonds between the carbonyl group of the quinone and the hydroxy groups of the phenol units. The hydrogen-bond distances and geometries for **5.1d** are given in Table **5.4**. It is observed that these interactions lead to the formation of infinite chains of hydrogen bonds (Fig.67b), so that the molecules pack helically along the *b*-crystallographic axis.

From the crystal structures of **5.1c** and **5.1d** it is observed that these molecules are iso-structural and their packing structures are determined predominantly by intermolecular hydrogen-bonding interactions.

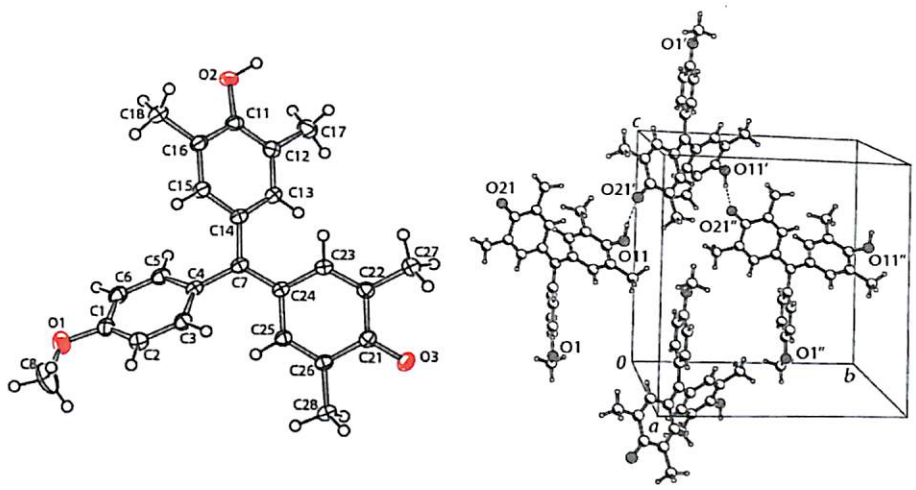

(a) (b)

Fig. 67(a) Crystal structure of **5.1d**, (thermal ellipsoids drawn to 50% probability) and (b) hydrogen-bonded helices parallel to the *b*-axis

Table 5.4 Hydrogen bond geometry (Å, °) for **5.1d**

D–H···A	d (D–H)	d (H···A)	d (D···A)	<D–H···A
O1–H···O3 [x+1/2, –y +1/2, z +1/2]	0. 953	1.703	2.650	178.3
O2–H···O1 [x–1/2, –y+1/2, z +1/2]	0.993	1.943	2.867	154.2

The central C(7) atom has planar-trigonal bond geometry, with the two planar benzene rings and one nearly-planar quinonic ring (Q) inclined to its plane in a propeller-like fashion.

A comparison of the bond distances for the quinone methides **5.1**, **5.2** with **5.3** indicates that quinone rings in the former (i.e. **5.1a**, **5.1c** and **5.1d**) have somewhat less quinonic character than in **5.2**, while the hydroxy-substituted phenyl rings acquiring quinone character (although not the methoxy-substituted ring in **5.1d**). In these quinone methides, **5.1** the reduction of the quinone character is obviously assisted by the existence of strong intermolecular hydrogen bonds of O–H···O=C type, viz. O(1)–H···O(4) and O(3)–H···O(2) in **5.1a**, O(1)–H···O(3") in **5.1c** and O(11)–H···O(21') in **5.1d**. Moreover, the O–H···O hydrogen bonding interactions assemble these molecules into infinite zig-zag chains except **5.1a**, the general directions of which are parallel to the crystal axes *c* (in **5.1c**) or *b* (in **5.1d**). The structure of **5.1c** contains also hydrogen bonds between two hydroxy groups, O(2)–H···O(1') and its equivalents, which join the chains into layers of molecules parallel to the [101] plane. However, these bonds are ca. 0.2 Å longer than the O–H···O=C hydrogen bonds.

The quinone methide **5.1e** crystallize from acetonitrile as red needles, in the C2/c space group. The crystal structure shows that the molecule (Fig.68) is located on a crystallographic twofold axis, that passing through the atoms C(1), C(4) and C(7). The methoxy group O(1)C(5)H3 is disordered between two positions related by this axis. The high displacement parameters of the O(3)C(6)H3 group also indicate a disorder, probably of a continuous character, which could not be represented satisfactorily by discrete atomic positions. Chemically, the twofold axis is a spurious one, relating a quinonic and a phenolic moiety. Intermolecular hydrogen bonding interactions lead to the formation of hydrogen bonded chains (Fig.69) that grow parallel to the *ab*-plane.

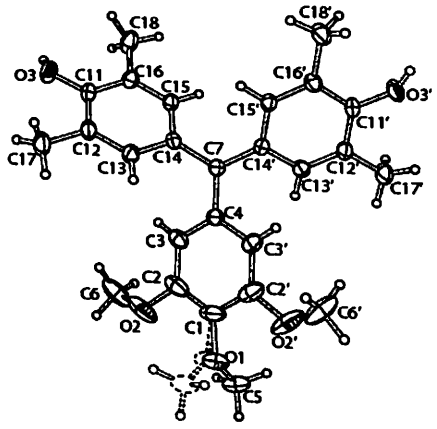

Fig.68 Crystal structure of **5.1e** (thermal ellipsoids drawn to 50% probability)

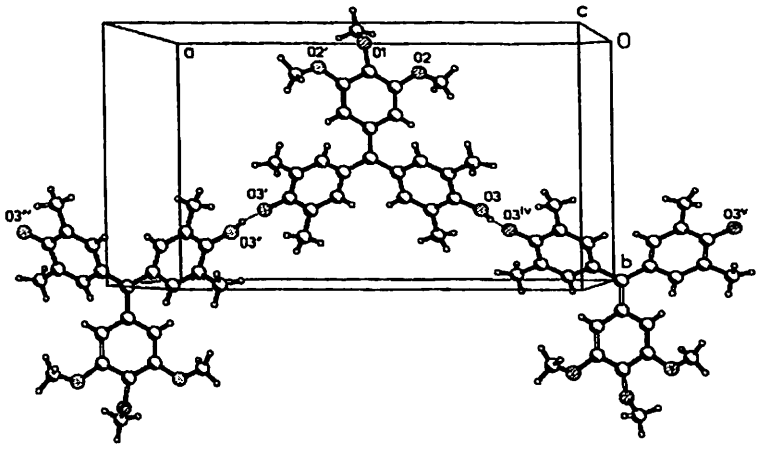

Fig.69 Structure of hydrogen bonded chains of **5.1e** parallel *ab*-plane

The observed geometry of the carbon-oxygen skeleton is the average of the two structures. The O(2) atom and its equivalent via an inversion centre form an intermolecular O(3)···O(3") contact of 2.682(3) Å, with a small but significant peak of electron density corresponding to a 50% occupied hydrogen position. Thus we observe a superposition of a –O(3)–H...O(3")=

and a =O(2)...H–O(2")– hydrogen bonds [O(2)–H 0.97 Å, H···O(2") 1.73 Å, <O–H···O 169°], linking the molecules into infinite chains parallel to the [101] crystallographic direction.

As in **5.1c** and **5.1d**, the C(7) atom in **5.1e** has a planar-trigonal geometry, with a propeller orientation of the three benzene/quinone rings around it. The torsion angles around the C(4)-C(7) and C(7)-C(14) bonds are 29.7° and 33.3°, respectively. In **5.1e** the torsion angles around the C(7)–C(4) and C(7)–C(14) single bonds are 42.4° and 34.4° respectively. More remarkable is the substantial twist around the double bond C(7)=C(24), amounting 20.1° in **5.1e** (cf. 18 to 20° in **5.2**), obviously due to steric repulsion between peri-H atoms. Such conformation of the molecules precludes any effective stacking of the rings. The O–H···O=C interactions in **5.1e** are quite strong as apparent from the O–H···O=C bond distances (dH···O31.73 Å, <O–H···O 168.7°). It also reveals that the carbon-oxygen, C(11)=O(3) (dC=O 1.307 Å) bond distance is intermediate between a single and a double bond.

In summary, we have described the synthetic and structural aspects of a few diaryl quinone methides. From the discussion, it is evident that intermolecular interactions between the hydroxy groups of the phenol and the carbonyl groups of the quinone in **5.1** give different structural motifs, including cyclic networks and two-dimensional hydrogen bonded sheets.

Chapter 6

Spectroscopic and Electrochemical Properties of Diaryl Quinone Methide

In Chapter 5, the structural study of the diaryl quinone-methides **5.1** has shown that the molecules are extensively hydrogen bonded in the solid-state. It has also been mentioned that these compounds have a quinone group and a phenol group separated by a methine carbon. So it is expected that these molecules should be delocalised over these two rings. Such delocalisation may be reflected in the solution properties. With this background we have studied the spectroscopic properties of the diaryl quinone methides in different solvents and microenvironment. It is important to note at this juncture that due to the presence of quinonic chromphore in all the compounds under investigation, they have well defined visible absorptions in solution. This provided a means to undertake visible spectroscopic study.

6.1 Proton NMR Studies and phenol-quinone ring exchange

When phenol and quinone units are part of a conjugated system, then these two groups can interconverts via proton shift from the phenol to the quinone group[131]. The solvent polarity will have a definite role in the degree of delocalisation or exchange of ring. The process may be illustrated by taking an example of quinone-methide **5.1a**. Since in quinone methide **5.1a** the phenol and the quinone group are in conjugation it may undergo phenol-quinone ring exchange as shown in fig 70. In this process the ring **P** and ring **Q** will interchange and it may be not be possible to distinguish the two rings at ambient condition. This is a general phenomenon and expected in all the quinone-methides **5.1** that are under consideration. In order to establish this phenomenon we performed NMR studies of the quinone methides in different solvents.

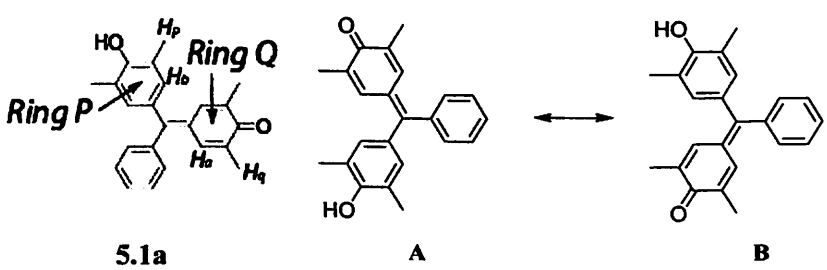

5.1a **A** **B**

Fig.70

The ^1H NMR spectrum of **5.1a** in $CDCl_3$ shows distinct singlet at δ_H 2.26 due to six protons and two singlets at 2.00 and 2.03 respectively for three protons each; these signals arise from

the methyl groups attached to the phenol (H_p) and the quinone (H_q) rings of the molecule. The protons H_a corresponding to the quinone ring appear as a singlet at δ_H 6.83 while those of the phenol ring (H_b) at δ_H 7.06. The protons signals due to the phenyl ring are observed at δ_H7.22 and 7.43 respectively, while the proton from the hydroxyl group appears at δ_H4.92. The NMR spectrum of this compound was also recorded in dimethylsulfoxide-d^6, which did not show difference from the one recorded in chloroform-d. This indicates that the molecule has less delocalisation over the quinone and phenol ring in solution. The ^{1}H NMR spectrum for **5.1a** is also found to be invariant of concentration of the compound. Thus, it may be concluded that the extent of delocalization over the two rings in the case of **5.1a** is not significant. However, the proton nmr spectrum of **5.1b** revealed an interesting feature that the two rings namely **P** and **Q** (analogous to Fig.70) are equivalent. The signals due to the methyl protons of the quinone and phenol units are not distinguishable but appear as broad singlet at δ_H 2.04 while the hydroxy proton appear at δ_H 8.87. The signal from the aromatic protons (H_a and H_b) of two rings **P** and **Q** appear as a singlet at δ_H 6.93. The signals corresponding to the A_2B_2 system from the other aromatic protons of **5.1b** are observed at δ_H 7.08 and 7.29 (doublets). The compound **5.1b** is less soluble in chloroform and so the NMR was recorded in dimethylsulfoxide -d^6 only.

However, a significant effect of solvent and concentration is observed in the ^{1}H NMR of **5.1c**. This compound is however insoluble in chloroform and so the studies were performed in dimethylsulfoxide and acetone. At concentrations of *ca.* 0.3mM, the ^{1}H NMR spectrum of **5.1c** in dimethylsulfoxide-d^6 shows a broad signal at δ_H 2.06 corresponding to the methyl groups of the rings **P** and **Q** (Fig.71).

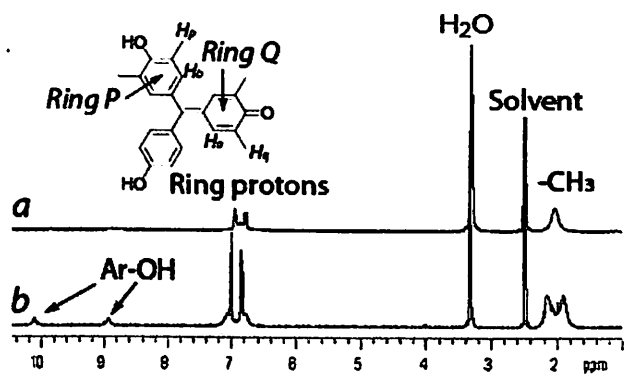

Fig.71 ^{1}H NMR spectrum of **5.1c** in dimethylsulfoxide-d^6 at different concentrations (*a*) 0.3mM and (*b*) 1.0mM

Similarly the aromatic protons of the phenol and the quinone units coalesce into a broad signal that appears at δ_H 6.94. The equivalence suggests the delocalised nature of the rings **P** and **Q** of the molecule in dimethylsulfoxide. When we studied the ^{1}H NMR spectrum of the

compound **5.1c** in acetone-d^6 (Fig.72) it is observed that the signals due to the methyl protons of the quinone unit appear as doublet at δ_H 1.96 and the protons of the methyl group of the phenol unit appear at δ_H 2.29. At the same time the signals from H_a (ring **Q**) are observed as doublets at δ_H 7.21 while those of the phenol unit (ring **P**) appear as singlet at δ_H 6.89.

We have observed that in **5.1d** and **5.1e** the **P** and **Q** rings in dimethylsulfoxide-d^6 are equivalent. For **5.1e** in acetone-d^6, the signals due to the methyl protons of quinone and phenolic units are observed at δ_H 1.95 and 2.27 respectively. However, in dimethylsulfoxide-d^6 the protons of the methyl groups from ring **P** and **Q** of **5.1e** merges into a broad signal at δ_H 2.06. This suggests extensive delocalisation that is induced by strong hydrogen-bonding interactions of the compound with the solvent. The effect is also translated to the proton signals of the aromatic rings, namely the protons on the quinone and phenyl rings could not be distinguished, and they appeared as a broad signal at δ_H 6.96.

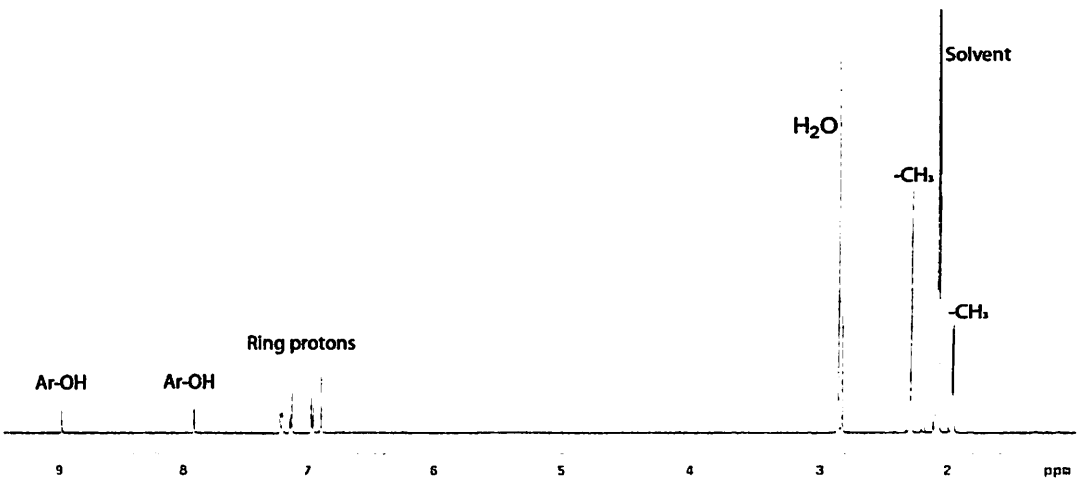

Fig. 72 ^{1}H NMR spectrum of **5.1c** in acetone-d^6 at room temperature

These differences in the NMR spectra of the quinone methides can be rationalized as follows: A polar solvent such as dimethylsulfoxide behaves as a stronger base than acetone and induces necessary polarisation of **5.1e**. The equivalence of the methyl groups of the rings **P** and **Q** indicate that the rings are free to rotate about the bond connecting the rings to the methine carbon.

An important temperature dependent phenomenon is observed in the ^{1}H NMR spectrum of **5.1e** in $CDCl_3$. The room temperature spectrum shows (Fig.73a) that the molecule methyl groups in the phenol and the quinone rings are equivalent on the NMR timescale. Thus only one proton signal is observed at δ_H 2.11 for the methyl groups on the phenol and the quinone rings. The protons H_a and H_b corresponding to the quinone and the phenol rings appear as a sharp single at δ_H 7.05. The position of these signals due to the methyl protons and the

aromatic protons remain unchanged at δ_H –30°C (Fig.73b). However, the proton signals that appear at δ_H 2.11 and at δ_H 7.05 shows distinct broadening on cooling. This indicates that with lowering of temperatures, the rotation of the rings become slower and subsequent retardation of ring-exchange causes the broadening of the signals. Due to poor solubility we could not measure ^{1}H NMR spectra of this compound below -30°C.

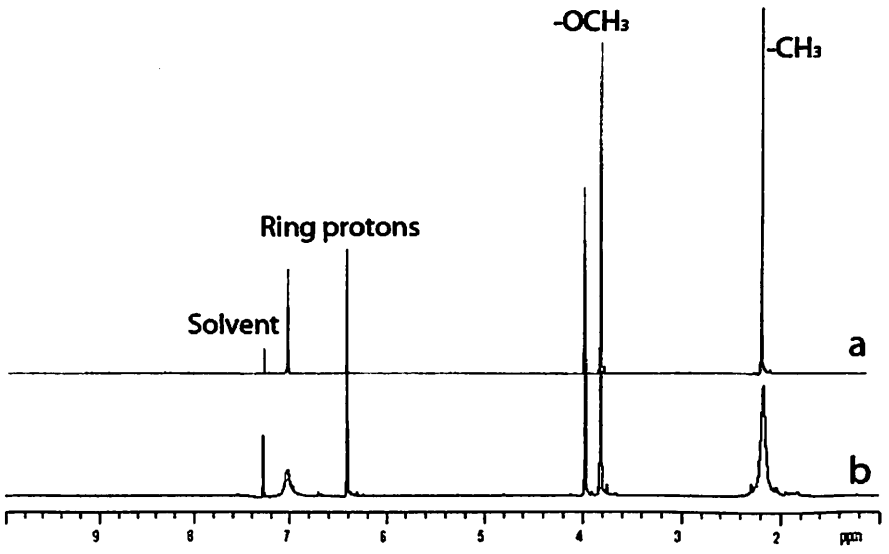

Fig.73 ^{1}H NMR spectra of **5.1e** in $CDCl_3$ (a) at room temperature (b) at -30°C

It is obvious that under conditions that favor strong hydrogen bonding the delocalisation/interaction between the phenyl and the quinone rings is more. Under such circumstances the two sets of methyl signals corresponding to the quinone and the phenol units are indistinguishable in the NMR spectra. It is to be noted that the differences in the NMR spectra can be interpreted in terms of a resonance effect that occurs due to delocalisation between the two different types of rings. The presence of strongly electron-donating substituents such as methoxy groups has a complementary effect in the delocalisation process.

6.2 UV-visible Studies and Solvatochromism

From the proton NMR study of the quinone methides **5.1** we could observe that the extent of delocalization between the phenol and the quinone rings is highly solvent dependent. UV-visible absorption spectroscopy is one of the most effective techniques of studying solute-solvent interactions[132]. Since the quinone methides have chromophoric quinone groups, we performed visible spectroscopic studies to explore whether such properties are reflected in different solvents. It is also expected that the properties of the compounds should also depend on factors such as pH and microenvironment.

From the UV-visible studies of the quinone methides, **5.1** we observed that the compounds do exhibit solvent-dependent changes in the absorption spectra. For example the neutral quinone methide, 4-[(4'-hydroxy-3',5'-dimethylphenyl)(phenyl)methylene]-2,6-di-methylcyclohexa-2,5-dien-1-one, **5.1a** in methanol has absorption with λ_{max}430nm whereas in acetonitrile it is observed at 399nm. Similarly, in methanol **5.1b** has absorption maximum at 436nm, while in case of **5.1c** and **5.1d** this absorption band in methanol is observed at λ_{max}456nm and 445nm respectively. A series of measurements have been done for the quinone methides **5.1** in different solvents by UV-visible spectroscopy and the results are summarized in Table **6.1**.

Since the phenolic (donor) and quinonic groups (acceptor) are in conjugation in these molecules, the ground states are polar and this results in the solvatochromic nature of **5.1**. We have looked at the different parameters that can contribute to solvatochromicity. For instance, solvation of the molecules and intermolecular solute-solvent interactions that leads to changes in the electron delocalisation. The UV-visible studies involving the quinone methides are performed in different solvents with added hydrochloric acid. It is observed that the addition of acid leads to characteristic changes in the visible spectrum of each compound along with the appearance of a new absorption band at longer wavelengths. The absorptions positions upon addition of acid for the corresponding to the quinone methides are listed in Table **6.1**. The results show that the absorption spectra of these compounds have distinct absorptions in the presence of acid; moreover the positions of absorption under acidic conditions are decided by the nature of the solvent.

We have also studied the pH dependent properties of the quinone methides. In this regard we performed a series of pH titrations using the compounds **5.1** in methanol/water or ethanol/water and monitored the absorption spectra for each of the compounds by visible spectroscopy. As an illustrative example, the compound **5.1a** in 1:4 methanol/water has absorption at λ_{max}430nm under neutral conditions, and the solution has yellow color. In the presence of hydrochloric acid, an additional absorption is observed at λ_{max}524nm. In this acidic pH, the color of the solution of **5.1a** becomes pink. The addition of base also causes a change in the color of the solution and at pH > 8, the solution of **5.1a** turns blue, and the corresponding visible spectrum shows a new absorption at λ_{max}592nm (Fig 74).

Similar pH titrations were performed for each of the quinone methides **5.1** and the color properties of the solution monitored by visible spectroscopy. Based on these pH dependent visible studies of the diaryl quinone methides **5.1**, we have been able to establish that the absorption spectra of each of these compounds are sensitive to the pH within the range 2 to 8. Such study has revealed that these compounds exist in distinct colored states corresponding to acidic, neutral, and basic pH.

Table 6.1 Solvent-dependent absorptions of **5.1** in neutral and cationic states

Sl. No.	Solvent					
		5.1a	**5.1b**	**5.1c**	**5.1d**	**5.1e**
1	Dichloromethane	416	413	*	418	416
2	Chloroform	412	415	*	418	417
3	Acetonitrile	399	408	417	416	411
4	Acetonitrile + HCl	519	511	492	496	515
5	Dimethylformamide	433	439	434	428	422
6	Dimethylsulfoxide	436	440	438	432	429
7	Tetrahydrofuran	416	416	417	416	416
8	Dioxane	413	412	412	410	411
9	Methanol	432	436	456	445	438
10	Methanol + HCl	524	520	496	504	524
11	Ethanol	436	438	453	447	440
12	Ethanol + HCl	526	521	498	508	525

* **5.1c** is insoluble both in dichloromethane and chloroform

Table 6.2 Solvent-dependent absorptions of **5.1** in the anionic states

	Solvents	λ_{max}(nm)				
Sl. no.		**5.1a**	**5.1b**	**5.1c**	**5.1d**	**5.1e**
1	Methanol	592	589	566	584	591
2	Ethanol	596	591	576	592	600
3	Acetonitrile	591	589	596	600	603
4	Dimethylformamide	596	592	600	608	610
5	Dimethylsulfoxide	596	592	606	610	613
6	Ethanol + Water (1:4,v/v)	590 *	584 *	572	578	581

* Absorptions correspond to methanol/water (1:4) solvent

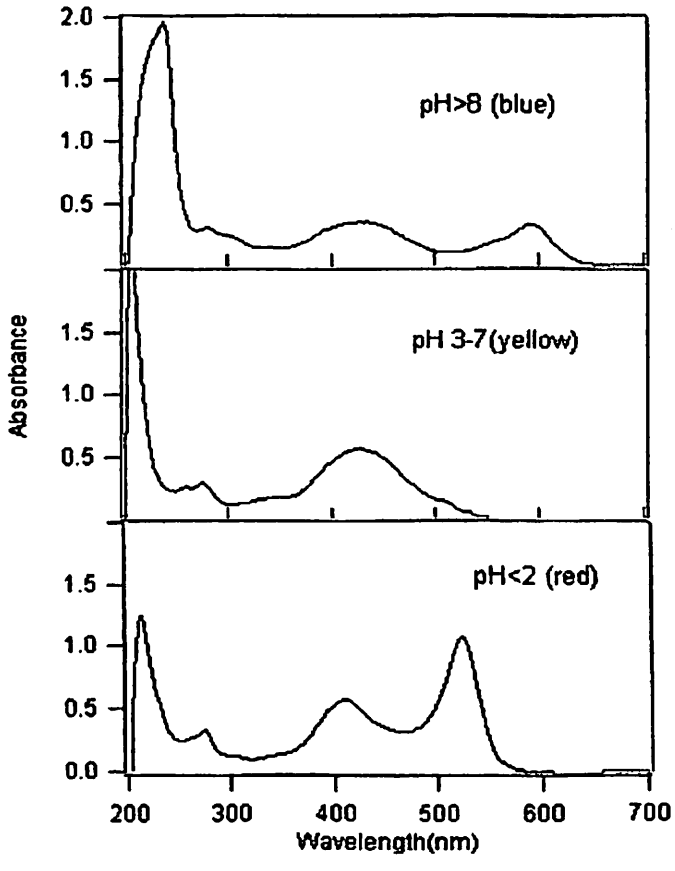

Fig.74 UV-visible spectra of **5.1a** at different pH in methanol/H_2O (1:4)

However, it is to be noted that the three-state phenomenon described for **5.1** is not observed in case of the aurine indicators such as rosolic acid (**5.3**). This compound has a structure similar to that of the diaryl quinone methide, but shows a color change from yellow to red in the pH range 5.0-6.8. The three-state phenomenon is observed due to the facile formation of the cations and anions species from the diaryl quinone methides (Scheme 3). A cationic state (**B**) is generated by protonation of the compounds using a mineral acid and anion formation (**C**) occurs in basic medium due to deprotonation of the hydroxy group of the phenol unit.

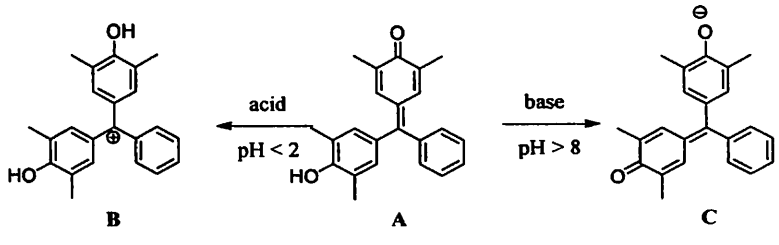

Scheme 3

Triarylmethyl cations are relatively easy to generate[133-136] and are amongst the best-known classes of stable carbocations[137, 138]. In this regard it can be noted that the quinone methide system is advantageous because simple mineral acids can lead to the generation of the cations.

These cations generated from the quinone methides exhibit chromophoric properties in solution. The chromophoric nature of the triphenylmethyl systems under acidic conditions are discussed elsewhere[139,140]. This property provides a convenient spectro-photometric method for the estimation of trityl groups[139], which are frequently used in the synthesis of glycosides, substituted nucleosides, and in peptide synthesis[141,142]. The trityl group is analysed by treating the substrate/analyte with acid and then the concentration is determined by colorimetry.

We have found that the absorption spectrum of the cations obtained from **5.1** are affected by the solvent (entry No.4,10,12 of Table **6.1**). The cation generated from **5.1a** absorbs at 526nm in ethanol, 524nm in methanol and at 519nm in acetonitrile. Likewise, protonation of **5.1c** or **5.1d** results in the formation of the corresponding cations that have distinct absorption spectra. The absorption spectrum shows that the intensity of absorption corresponding to the cationic state increases with the increase in concentration of the acid, and reaches a maximum (Fig.75a). However, in case of **5.1d** in methanol it is observed that the absorption band shows a maximum at 504nm with a shoulder at 466nm. Similar feature is also observed in case of **5.1e** in methanol but not in case of **5.1a-c**. This asymmetry in the absorption band probably arises from the presence of two non-equivalent forms contributing to the delocalised structures, which invokes the participation of both the methoxy and the hydroxyl groups.

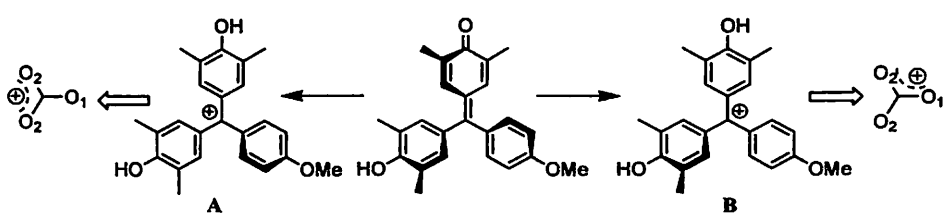

Scheme 4

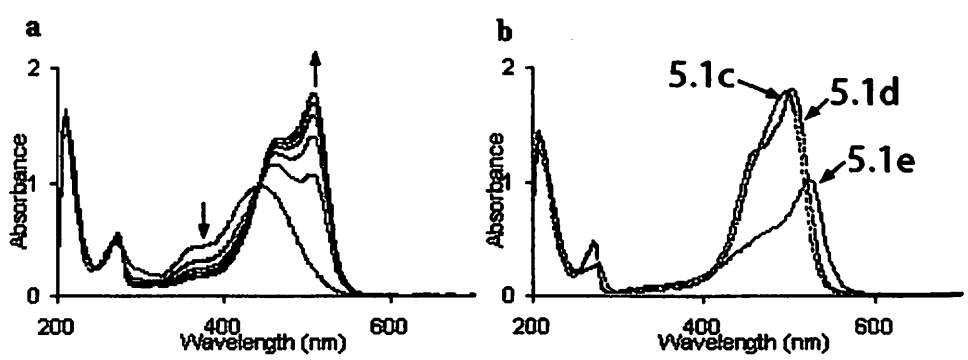

Fig.75(a) Titration of **5.1d** with hydrochloric acid in ethanol and the changes in the corresponding UV-vis spectra (b) UV-vis spectra upon addition of 0.1M hydrochloric acid in ethanol: **5.1c**, (498nm, ε $6.46\times10^{4}M^{-1}cm^{-1}$); **5.1d** (508nm, ε $5.44\times10^{4}M^{-1}cm^{-1}$) and **5.1e**, (525nm, ε $2.96\times10^{4}M^{-1}cm^{-1}$)

The positive charge of the cation can delocalise simultaneously over two of the rings in the system (cf. O1-O2 in the motif of Scheme 4), so that the O1...O2 delocalised state is different from O2...O2 state. Thus asymmetric effect arises which is reflected in the absorption spectrum of the molecules. As such the absorption band for the cation of **5.1e** in methanol shows a maximum at 524nm with a shoulder at 472nm. However such features are not observed in the case of the cationic species of **5.1a** in methanol (Fig.75) perhaps because the contribution of the phenyl group is not much compared to the O2...O2 delocalisation. The features observed in the absorption spectra of the quinone methides thus provide qualitative insights into the delocalised state of the molecule in the cationic state. The presence of delocalised states in isomeric forms of triphenylmethane derivatives were first demonstrated by Strohbusch[133] where the dissimilar rings gave interesting absorption characteristics. However in this study it is shown that even minor changes in the substitution involving hydroxy or methoxy can be used to identify the effect of delocalisation in isomeric cations.

In order to look at the possible isomeric cations that may arise from the presence of nitrogen-based functional groups, the cations obtained from 4-[(4'-hydroxy-3',5'-dimethylphenyl)(4-N,N'-dimethylaminophenyl)methylene]-2,6-dimethyl-cyclohexa-2,5-dienone, **5.1f** on addition of hydrochloric acid has been studied by UV-visible spectroscopy. The absorption spectrum of the compound in methanol in the absence of acid shows a broad band with maximum at 522nm (ε $2.04\times10^4 M^{-1}cm^{-1}$). Addition of hydrochloric acid to this solution gives two distinct absorptions at 453nm (ε 1.58×10^4 $M^{-1}cm^{-1}$) and 551nm (ε 2.46×10^4 $M^{-1}cm^{-1}$) respectively and the intensity ratio of the two absorptions bands is ca. 2:1. On the basis of our previous results, we have assigned the two absorption bands to the formation of the corresponding isomeric cations, **B** and **C** as described in Scheme 5.

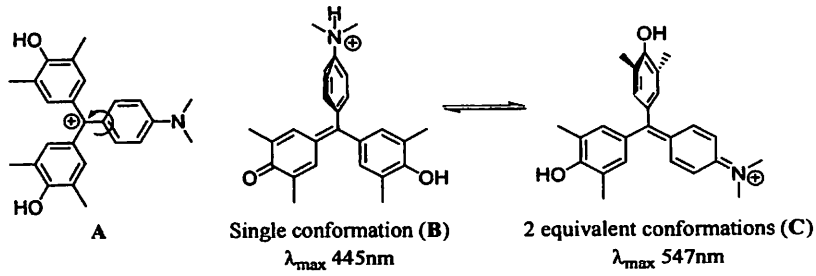

Scheme 5

We have already discussed in the context of the observation of isomeric cations of **5.1d** that the quinone methides adopt propeller-like conformations and this precludes the participation of both the oxygen atoms and the $-NMe_2$ group in the delocalisation of the cation. Because of this two possibilities arise, and these are illustrated in Scheme 5.

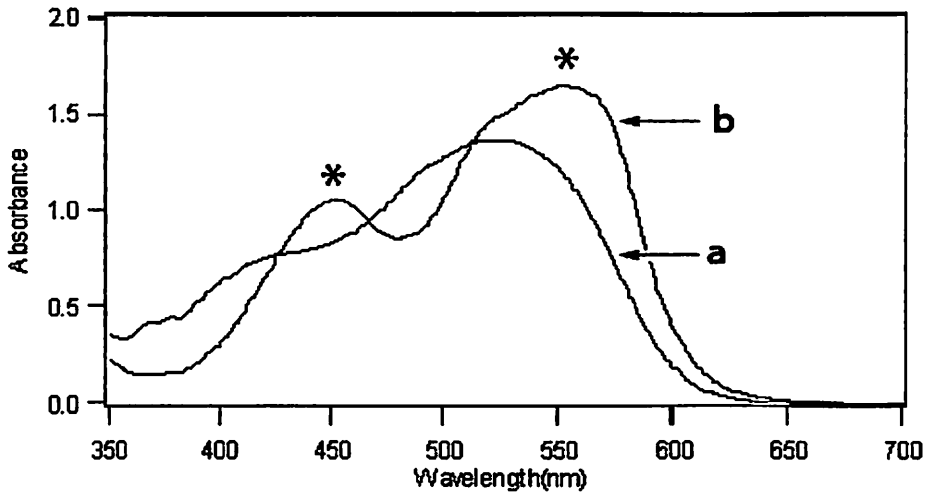

Fig.76 Change of absorbance of **5.1f** (a) in methanol (6.7×10^{-5}mM); (b) on addition of HCl (4µl of 0.1M). The absorptions denoted '*' corresponds to the isomeric cations

The presence of the -NMe_2 group in the compound (as shown in Scheme 5) thereby enables us to distinguish two distinct cationic states, **B** and **C** in the absorption spectrum. It is noteworthy that when the hydroxy group of the phenol ring participates in the delocalisation along with the quinone unit, the two rings are coplanar and this can be described by structure **B** in Scheme 5. When delocalisation involves the –NMe_2 group and the oxygen atoms, two degenerate delocalised states can be identified (**A**). Thus, we are able to ascribe the intensity ratio of the two peaks in the absorption spectra to the number of equivalent delocalised states in the cation.

In the presence of a base, in the form of amine, the solution absorption spectrum of the quinone methide such as **5.1a** changes and a new absorption band appears at longer wavelengths. The color change that occurs upon addition of the amine can also be detected visually. This is due to formation of anion from the quinone methide, which is in the form of a delocalised phenolate anion. The position of the absorption band for the anionic state of the quinone methide depends on the solvent as well as the substituents on the compound. Thus, we studied the solvent-dependence of the anionic state of these quinone methides by visible absorption spectroscopy. The results obtained from this study are listed in Table **6.2**.

These results clearly indicate that the solvent has a role in the delocalizing of the anionic form too. Our results also demonstrate that the cationic, anionic and neutral states of the quinone methides are reversibly generated upon addition of acids or bases, and yet the compounds retain their identity. The changes in the optical properties on addition of acids and bases could be monitored by absorption spectroscopy and reproducibility of the results has been tested for twenty-five cycles. Thus, these compounds are prospective candidates for pH indicator.

6.3 Encapsulation of quinone methides by cyclodextrins

As mentioned earlier, the quinone methides under consideration have low solubilities in organic solvents and almost insoluble in water. We have also discussed that the quinone methides exhibit color changes at different pH and both the acidic as well as alkaline states could be identified by the changes in the absorption spectra. However, neither the cationic state nor the anionic state could be stabilized in 1:4 methanol/water because of precipitation of the quinone methides.

With the objective of stabilizing the anionic species in solution we employed a pre-organized host to capture the anion in solution once it is formed. Thus, we performed pH titrations of the diaryl quinone methides **5.1** in the presence of α-, β-, and γ-cyclodextrins in ethanol/water solutions. In each case, triethylamine has been used as the base used for performing the titrations. From the titration curves we could identify the end-points that correspond to the neutralization of the phenol unit of the **5.1**. In each case we observed only one inflection in the pH titration curves, which indicates that the presence of cyclodextrins has no effect on the end-point. It has been found that the pH titration curve of **5.1d** with triethylamine in the presence of β–cyclodextrin has two inflection points. The pH titration of the same compound without cyclodextrins gives a plot that has only one inflection (Fig.77), just as expected. This is an indication that the compound **5.1d** does interact with β–cyclodextrin.

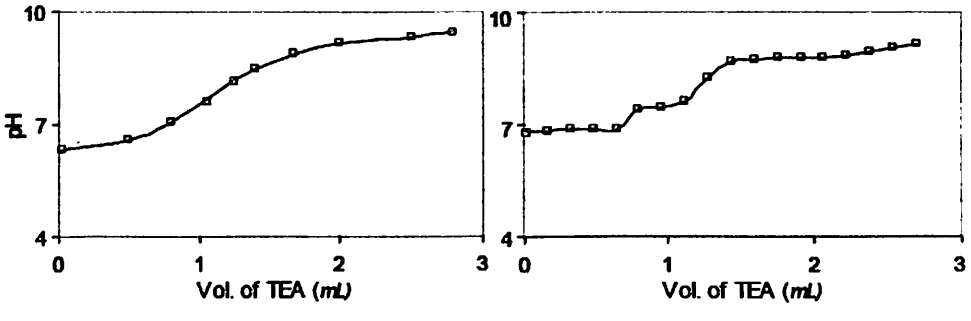

Fig.77 Titration of **5.1d** with triethylamine (left) in the absence of cyclodextrin and, (right) in the presence of 2mM cyclodextrin solution

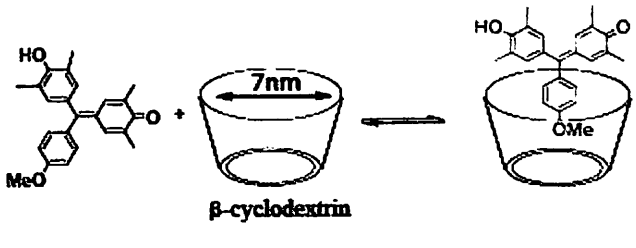

Equation 42

In order to understand this process we performed the same experiment with **5.1d** in the presence of different cyclodextrin and compared the changes in the absorption spectra at pH 4.0, 6.9 and 9.0. It is observed that at pH 4.0 and 6.9, the quinone methide **5.1d** has visible absorption at 447nm (ε $10^5 M^{-1}cm^{-1}$) in aqueous ethanol (1:4 v/v). The same compound under identical conditions but in the presence of β-cyclodextrin has absorption at 456nm. This suggests the presence of β-cyclodextrin in solution has an effect on the electronic spectra of **5.1d**. On the other hand at pH 9.0, the absorption spectrum of **5.1d** with β-cyclodextrin in aqueous ethanol has absorption at 595nm. The compound **5.1d** under identical conditions but without β-cyclodextrin has absorbance at 581nm, which is due to the anion of **5.1d**.

These results show that the compound in neutral form as well as its anion interacts weakly with β-cyclodextrin. Such interaction could arise from the encapsulation of **5.1d** into the cavity of β-cyclodextrin as shown in equation 42. It is found that the inclusion process is selective for β-cyclodextrin, because similar changes are not observed for α- and γ-cyclodextrins neither in the titration plots nor by visible spectroscopy. The shifts observed in the absorption positions of **5.1d** both in the neutral and as well as basic medium indicate that the interaction between quinone methide and the host is not effected by the pH of the medium.

Further studies using ^{1}H NMR spectroscopy was performed in order to identify the manner in which **5.1d** interacts with β-cyclodextrin. The NMR experiments were performed in dimethylsulfoxide-d^6 (since ethanol-d^6 was not available with us), which provided more evidence regarding the encapsulation in β-cyclodextrin. Thus, we recorded the ^{1}H NMR spectrum of both **5.1d** and β-cyclodextrin and then **5.1d** in the presence of β-cyclodextrin. In the absence of the cyclodextrin host, the spectrum of **5.1d** shows only a broad unresolved signal at δ_H 2.05 corresponding to the methyl protons of the phenol and the quinone units. We have already shown that this happens in dimethylsulfoxide because the phenol and the quinone rings are rendered equivalent on the NMR timescale by solvent-mediated proton shift. Thus, the aromatic protons from the phenol and the quinone rings appear at δ_H 6.96 while the protons of the methoxy group appear at δ_H 3.85 (Fig.78a). The proton signals of cyclodextrin molecules appear at the expected positions as shown in Fig.78b.

In the presence of β-cyclodextrin, the ^{1}H NMR spectrum of **5.1d** shows distinct changes in the proton signals arising from the methyl groups of the quinone and the phenol units (Fig.78c). Thus, three signals are observed that appear at δ_H 1.87, 2.04 and 2.14 (denoted * in Fig.78), the former two signals due to the quinone unit and the latter due to phenol units of the molecule. The proton signals of the methoxy group are also moves upfield to δ_H 3.78 due to on interaction with β-cyclodextrin.

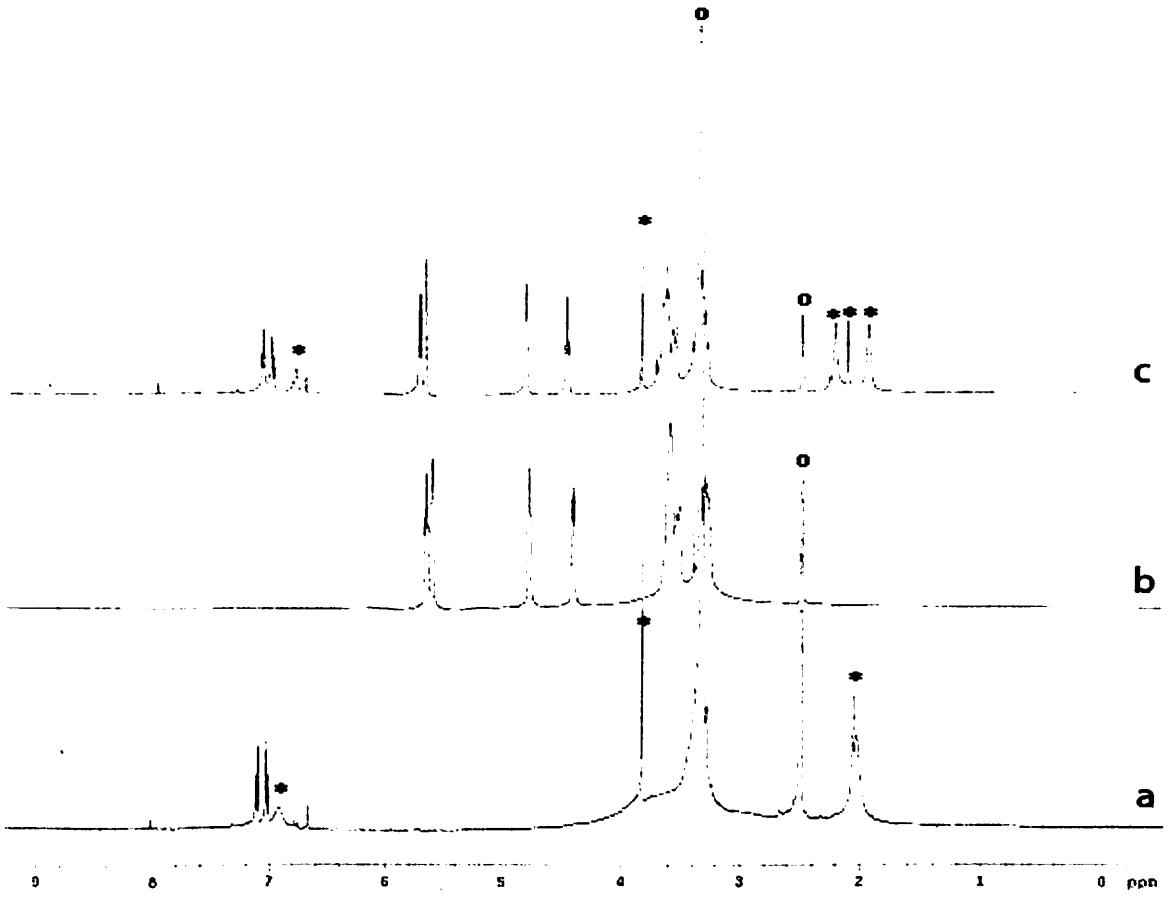

Fig.78 ^{1}H NMR spectra of (a) **5.1d** (signals denoted with *), (b) β-cyclodextrin, and (c) quinone methide **5.1d** in the presence of β-cyclodextrin in dimethylsulfoxide-d^{6} (**o** indicates solvent signals)

There is also a significant shift in the quinonic protons of this quinone methide; on interaction with β-cyclodextrin it shifts from δ_H 6.8 to 6.9. The observation of three signals due to methyl protons of **5.1d** in the presence of β-cyclodextrin suggests that because of inclusion inside the cyclodextrin cavity, rotation of the phenolic ring about the bond to the methine carbon is restricted. It is also interesting to note that the compound **5.1d** shows only a broad singlet for the aromatic methyl protons. This happens due to delocalisation of π–electrons over the two rings making them close to equivalent, thus, the encapsulation of the compound possibly decreases the delocalisation and allowing the two rings to be distinguishable. It is important to note that all the compounds **5.1** do not show any significant change in their visible absorption spectra in the presence of either of α- or γ-cyclodextrins at the pH 4.0, 7.2 and 9.0.

However, we could not ascertain the nature of association between of β-cyclodextrin with **5.1d**. The poor solubility of this quinone methide made NMR measurements at low temperatures difficult because of which the association constants could not be evaluated. We

also tried to determine the stoichiometry of the quinone methide **5.1d** and cyclodextrin adduct by preparing a Job plot, but the high extinction coefficients precluded concentration dependent study. However, from pH titration plot we could clearly distinguish the two neutralizations at pH 7.3 and 8.4 respectively. Although this experiment does not allow us to make conclusion on the nature of the adduct but it clearly depicts that at room temperature approximately 50% of the molecule **5.1d** gets encapsulated into the cyclodextrin.

We have analyzed the structural data for the quinone methides and made a comparison with the dimensions of the cyclodextrins in order to explain the observations. It is obvious from the crystal structures of the compounds **5.1d** that the diaryl quinone methides adopt propeller conformations in the solid state. Thus it is reasonable to expect that only one of the rings can be included inside the cavity of β-cyclodextrin. For this purpose we examined dimensions of different segments of the quinone methdies and made a comparison with reported data in the literature on the dimensions of cyclodextrin cavities. The distances of the segments that may get encapsulated to cyclodextrin are demarcated in Fig.79. The distances that would play the crucial role in the formation of inclusion compound are listed in Table 6.3.

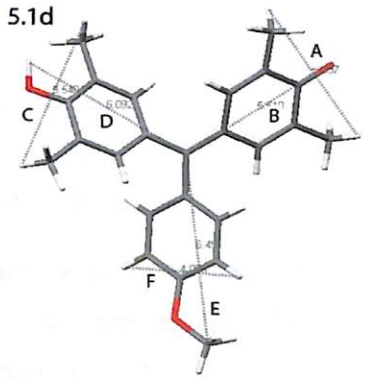

Fig 79 A representative example **5.1d** to define different segments A, B, C, D, E and F; the same representation applies to the segments for the **5.1a, 5.1c, 5.1e** (refer Table **6.3** for distances)

Table **6.3** suggests that each of the aromatic rings except one ring of **5.1d** has appropriate dimensions to be accommodated inside the cavity of β-cyclodextrin. The cavity size of α-cyclodextrin is too small to accommodate any of the segments of the quinone methides, **5.1** whereas the diameter of γ-cyclodextrin being 9.5Å would allow easy de-encapsulation due to weaker interactions relative to β-cyclodextrin.

The nature of the cyclodextrin cavity in each of the forms facilitates encapsulation of the hydrophobic part into their cavity[144], thus the aromatic ring containing hydroxy group is less

likely to be encapsulated into the cavity. Logically it can be predicted that the rings having correct sizes, and having more hydrophobicity will preferentially be encapsulated into the cavity of β-cyclodextrin. These molecules have conjugation between the two rings making them equivalent and they are unlikely to get encapsulated into the cavity of β-cyclodextrin due to their hydrophilic nature. The smaller dimension of the phenyl ring (**E, F**) of compound **5.1a** suggests that this molecule can only be loosely encapsulated inside cyclodextrin due to weaker interactions. On the other hand **5.1c** is substantially more hydrophilic due to the presence of two hydroxy groups and a quinone group, which are delocalized.

Table 6.3 Distances between different segments[#] in **5.1**

Distances (Å)	**5.1a**	**5.1c**	**5.1d**	**5.1e**
A	5.395	6.533	5.360	6.026
B	5.506	5.523	5.510	5.561
C	5.917	6.174	6.540	6.560
D	6.049	6.597	6.123	6.092
E	5.235	6.032	6.492	7.307
F	4.040	4.204	4.063	7.542

[#] As designated in Fig.79

Accordingly, it is reasonable that the molecule will not be encapsulated inside the cavity of cyclodextrins even if it satisfies the size criterion. In the case of **5.1e**, however the large dimensions of the trimethoxyphenyl ring (**E, F**) makes it obvious that encapsulation will not be favored. In fact, the structural analysis of the quinone methides justify the observed inclusion of **5.1d** inside β-cyclodextrin, which is reflected both in the neutral and anion state.

6.4 Inclusion of quinone methides into micelles of a cationic surfactant

We have discussed in the previous section that the encapsulation of the quinone methides in cyclodextrins is determined by the structure of the molecule. Since cyclodextrins are rigid molecules having well-defined cavity sizes, it is obvious that they should exhibit selective encapsulation of the guest molecules. We have demonstrated this by using compounds **5.1**, which have rings of different dimensions and also described the selective encapsulation of **5.1d** in the cavity of β-cyclodextrins.

In contrast, surfactants are self-assembled supramolecular systems and can form flexible aggregates depending on the solvent environment. Thus, micelles generated from cetyl

trimethyl ammonium bromide (CTAB) with different amounts of 1,3,5-trimethylbenzene can be used to modify silica to obtain materials having different pore sizes[145]. This observation suggests that an electron rich aromatic compound[146] can form a component of such micelle. Similarly, it is reported[147] that added counter anions do affect micelle formation in some surfactants and the variation in their aggregation numbers can be correlated to the electrolyte concentrations.

In this regard, an aromatic compound that contains a chromophore whose color property is sensitive to solvent or microenvironment would be of interest to study the nature of inclusion by micelles. With the background that the visible spectra of the quinone methides **5.1** are sensitive to the solvent, we studied the possible encapsulation of quinone methides in the micelles obtained from the surfactant, CTAB.

We found that the absorption maximum of the anion of **5.1c** at 572nm in aqueous ethanol (5% v/v) shifts to 562nm upon addition of excess amount of an aqueous CTAB solution. It is to be noted that this shift is dependent on the concentration of CTAB both in terms of intensity as well as position of absorption maximum. However, the changes observed in the absorption spectra of **5.1c** at pH 9.0 in the presence of increasing concentrations of CTAB are not regular. As a result we could not arrive at a definite conclusion about the encapsulation of **5.1c** in the micelles.

It has already been mentioned that at alkaline pH, the visible spectra of **5.1d** in aqueous ethanol has absorption at 578nm. To this solution that contains **5.1d** in the anionic form, we added the solution of the surfactant in small aliquots. At low concentrations of CTAB, the absorbance at 578nm shows a distinct decreasing trend as shown in Fig.80a and reaches a minimum. As the concentration of CTAB increased beyond 0.6mM, a new absorption is observed at 593nm. This shift in the absorption maxima by 15nm is attributed to the change in the microenvironment around the anion of **5.1d**. Moreover, there is a distinct change in the color of the solution, from purple before addition of CTAB to blue when concentration of CTAB is more than 0.6mM.

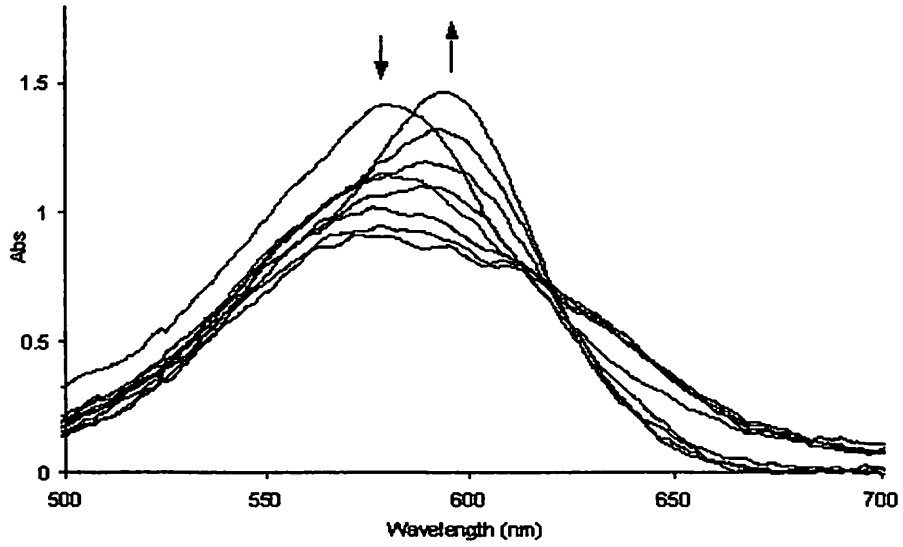

Fig.80(a) Change in absorbance of **5.1d** (10^{-5}mM) at pH 9.0 upon addition of CTAB; downward arrow indicates the changes at 578nm while upward arrow indicates the changes at 593nm.

In this case we are able to correlate these observations by plotting the changes in absorbance at 578nm and 593 nm versus concentration of CTAB (Fig.80). This plot shows that as the concentration of CTAB increases there is a decrease in the absorbance at 578nm, and leads to a minimum when the surfactant concentration is 0.62mM. Beyond this, the absorbance at 593nm increases with corresponding increase in the concentration of CTAB, while that at 578nm increases slightly. The variation in the absorbance is not explicit because the two absorptions are too closely spaced, and this has an overlapping effect. In a normal case when these two peaks are well separated, it would have been anticipated that the absorbance at 578nm should decrease while the absorbance at 593nm increase with increase in the CTAB concentration. In that case, the intersection of the plots of concentration versus the corresponding absorbances at 578nm and 593nm should give the critical micelle concentration (CMC) for the surfactant. This is however possible by separating the Gaussian components of the two absorption bands such that both the absorption peaks have normal Gaussian shapes. From this analysis the corrected values for the changes in absorbance can be obtained as shown in Fig.80b(right). Thus, the point at which the two plots intersect (i.e. minimum) gives the critical micelle concentration (CMC) of the surfactant and it is found to be 0.62mM. Similar values for the CMC of CTAB are obtained when either **5.1a** or **5.1b** are used as the chromophoric probes. However, the value for the CMC for CTAB obtained in this case is about 22% lower than the reported value of 0.8mM[148]. This deviation may be attributed to the difference in the solvent used during the experiment. Due to extremely poor solubility of these compounds in aqueous solutions, we had to perform the experiment using

aqueous ethanol (2%, v/v) solution of **5.1d**, which was added to the aqueous surfactant solution.

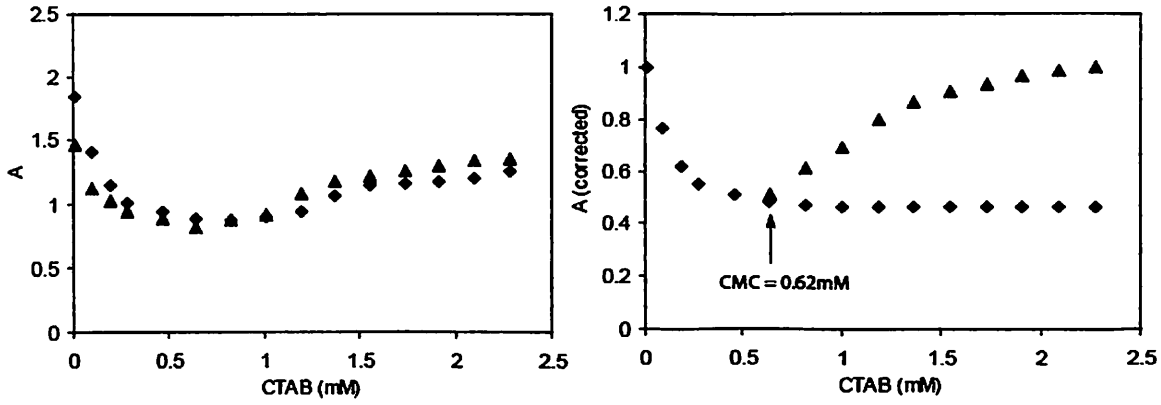

Fig.80b: (left) Apparent changes in the absorbance change for **5.1d** (10^{-5}mM) at pH 9 with change in concentration of CTAB, and (right) corrected plots of absorbance versus concentration of CTAB

In aqueous solutions the surfactant, CTAB, assemble in such a way that the hydrophobic alkyl groups avoid contact with water while the polar groups can interact with water. This drives the formation of micelles in aqueous solution provided the concentration exceeds the CMC for the surfactant. However, in the solvent system consisting of aqueous ethanol, the structure of the Stern layer of the micelle is modified in two ways (a) by decreasing water molecules in the Stern layer and (b) by increasing electrostatic repulsion between the ionic head-groups. Thus the methylene groups of the alkyl chain can avoid contact with water, which drives the free energy for the incorporation of a surfactant molecule more negative. Consequently a decrease in the CMC is observed. This also indicates that quinone methide is being held in the relatively non-polar interior of the micelle.

In order to prove this fact it was necessary to find out the CMC with an analogous compound in aqueous medium. The compound **5.1e** is more soluble in water compared to any of the other quinone methides (**5.1**). Thus, we performed the same set of experiments with CTAB as the surfactant, but **5.1e** as the chromophoric probe. It is found that at pH 9.0, the aqueous solution of the anion of **5.1e** has absorption at 581nm. With the addition of CTAB solution the absorbance at this position decreases and when the concentration of the surfactant exceeds ca. 0.70mM a new absorption is observed at 596nm. Subsequently, the absorbances at 581nm and 596nm are plotted versus the corresponding concentrations of CTAB, which gives a graph similar to that for **5.1d**. Apparently, the absorption spectrum of this compound also exhibits the same features as observed for **5.1d**, and the absorptions at the two positions are not independent of each other. Therefore, by considering that both the absorption peaks have

normal Gaussian shapes we obtained the normalized values of the absorbances, A(corrected) for both the peaks at 581nm and 596nm. The plot of A(corrected) for the two absorptions at 581nm and 596 nm versus concentration of CTAB (Fig.81) gives an intersection at 0.80mM. This value corresponds to the CMC of CTAB in aqueous solutions and to the reported value.

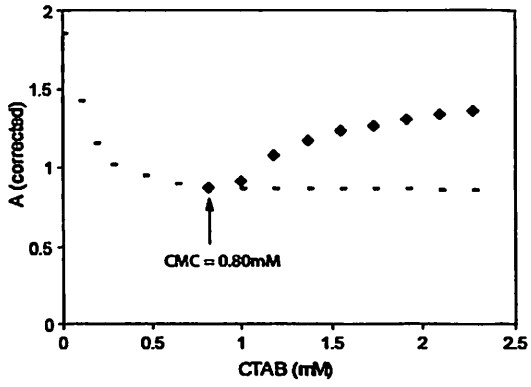

Fig.81 Plots of corrected absorbance for **5.1e** at 581nm (-) and 596nm (■) versus concentration of CTAB at pH 9.0

Thus, in this study we could develop a method to determine the CMC with a mixed solvent system, but in alkaline medium.

The experiments performed with different concentrations of the quinone methides **5.1** indicate that the CMC of the surfactant is independent of the concentration. It is obvious because the micelles formed by the surfactant molecules are dynamic systems and have lifetimes of the order of milliseconds. Thus, the micelles form and disintegrate continuously in solution so that the quinone methide anion is bound reversibly. The study also shows that the CMC of the surfactant is independent of the nature of chromophore but depends on the nature of the solvents. However, we could not apply this method to determine the CMC of CTAB at neutral pH. This again is a consequence of the fact that the quinone methides **5.1** tends to precipitate from the solution.

6.5 Electrochemistry of quinone methides

Polyradical systems containing pendant groups and linked though a π-conjugated backbone have been investigated extensively[149-151] for designing molecular magnetic materials. Phenoxyl radicals are known to be persistent enough under ambient conditions and also exhibit adequate magnetic interaction and stability. The presence of the conjugated backbone enables effective exchange coupling of the electrons, which is essential for magnetic ordering in the material[152-155]. Phenol centers that are separated by suitable spacers are known to oxidized to the corresponding phenoxyl radicals (**B**) and subsequently to the quinonoid (**C**) [156] singlet state as shown in equation 43. The generation of such radical systems constitutes one

of the important strategies in the design of organic molecular ferromagnets[155]. The quinone state **C** is ESR silent, the radical states are not. The extended linear π-system in these molecules favour the quinone states instead of the radical states, with the possibility of equilibrium between the two.

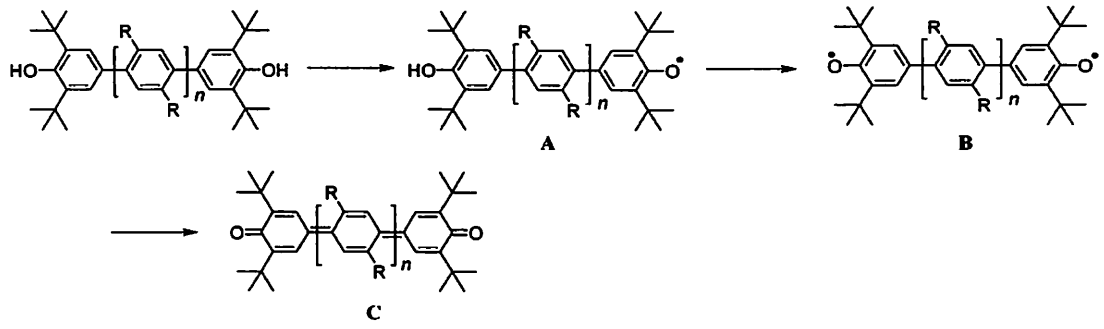

Equation 43

Since the ESR spectra show hyperfine splitting, it provides a convenient tool to study among other aspects, the effect of different substituents on the magnetic behavior of radical systems. The galvinol systems[158] have proved to be extremely useful in studying the dynamic effects in doublet spin states, including electron-electron exchange and dipolar interactions in galvinoxyl diradicals (equation 44).

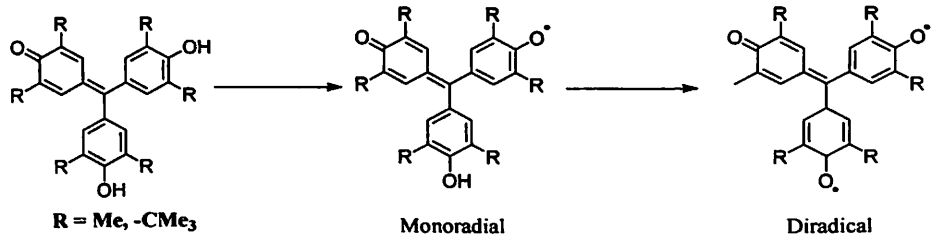

Equation 44

It has been discussed in Chapter 6 that the bis-phenols **2.2** undergo oxidation to yield the corresponding diaryl quinone methides. Given the close resemblance of these compounds to the galvinol system we decided to study the radicals generated from the diaryl quinone methides, **5.1**. For this purpose we generated the radical species in solution by electrochemical reduction and studied their formation using in-situ ESR spectroscopy.

Cyclic voltammograms of the quinone methides **5.1a** in acetonitrile show a quasi-reversible redox couple at-1.41V. This may be due to the reduction of the quinone unit (Fig.82).

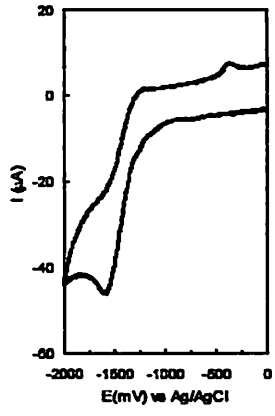

Fig.82 Cyclic voltammogram of **5.1a** in acetonitrile at scan rate100mV/s, with TBAP as supporting electrolyte

On the other hand, the cyclic voltammogram of quinone methide **5.1c** shows a quasi-reversible redox couple at $E_{1/2}$ –850mV at scan rate of 100mV/s (Fig.83). At slower scan rates the Ip_a/Ip_c ratio for this redox couple is found to be close to unity. We have also observed that the position and Ip_a/Ip_c ratio of the redox couple is dependent on the scan rate. As the scan rate increases, the cathodic peak shifts to more negative potentials while the anodic peak current decreases, as shown by the cyclic voltammogram of **5.1c** at scans rates of 300mV/s. Since we could not observe the second reduction cycle for **5.1c** at even higher reduction potentials, it became necessary to study the in-situ ESR of the reduced species. Therefore, the compound **5.1c** in dry acetonitrile was electrolyzed at E –1000mV in order to generate radical species. In-situ ESR spectroscopy however did not reveal any signal that could suggest the absence of radical species in the solution. These results gives an indication that the quinone methide undergoes reduction but the reduced species may be fast transformed to some species that can not be detected by ESR.

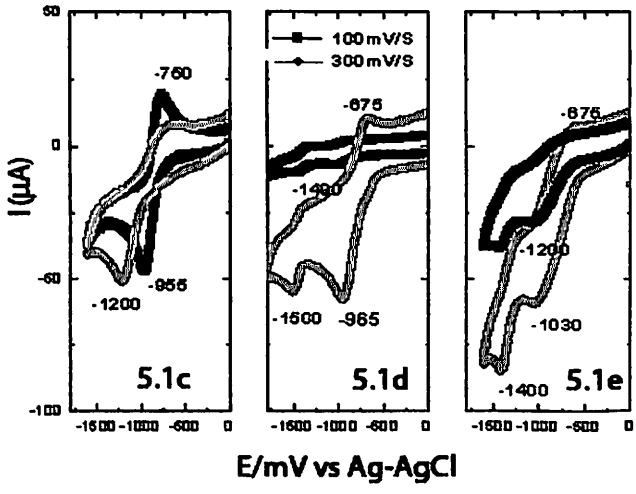

Fig.83 Cyclic voltammograms of **5.1c-e** in acetonitrile at scan rate100 and 300mv/s

Cyclic voltammograms of **5.1d** recorded in acetonitrile at different scan rates are shown in Fig.83. In this case, two quasi-reversible redox couples were obtained, viz. at E –965/-675mV and –1500/-1400mV respectively, which are assigned to **5.1d/5.1d**$^{\bullet-}$ and **5.1d**$^{\bullet-}$**/5.1d**$^{-}$. Similar quasi reversible redox couples are also observed in the case of **5.1e**. However, two quasi-reversible redox processes are observed at the potentials of E –1400/-1300mV, and –1030/-675mV, respectively. In this case the positions of the redox couples were found to be invariant irrespective of the scan rates. There is a marked decrease in Ip_c with respect to the corresponding Ip_a on increasing scan rates as shown in Fig.83. On increasing the scan rate the Ip_a/Ip_c also differs much from unity as in the case of the other couple.

These results can be explained with the help of a sequence of interconvertible species that are illustrated in Scheme 6. As shown in Scheme 6, the radical anions are obtained by one electron reduction of neutral **5.1c** by supply of electron from external source. In the case of **5.1c** the radical **A** (Scheme 7) would have only option to revert back to the parent compound. If this decay process is fast the system should not show any property of radical but should form the parent compound but still be electroactive with a reversible one-electron redox process, which is in fact seen, in the cyclic voltammogram of **5.1c**.

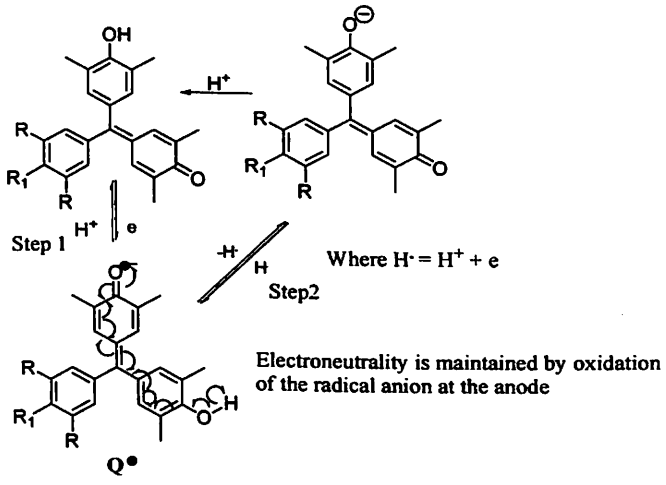

Scheme 6

But in the case of **5.1d** and **5.1e** the presence of methoxy group at the para position allows an additional delocalisation step that is represented in Scheme 7. The radical species **A** and **B** (Scheme 7) are energetically different thus if they are to be generated independently they would require different oxidation potentials. Accordingly two sets of redox couples are observed that corresponds to generation of each of these species, **A** and **B**.

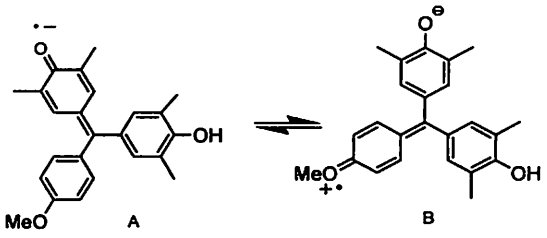

Scheme 7

In order to establish the Schemes 6 and 7 we performed controlled electrolysis coupled with electron spin resonance spectroscopy. It is found that during controlled electrolysis with –1200mV the acetonitrile solution **5.1c** does not show ESR signal. This can only happen due to a fast conversion of the radical anion to the parent compound, which means that the step 1 is the rate-determining step for the process. The in-situ ESR spectra of **5.1d** and **5.1e** provide evidence in support of the transformations described in Schemes 6 and 7.

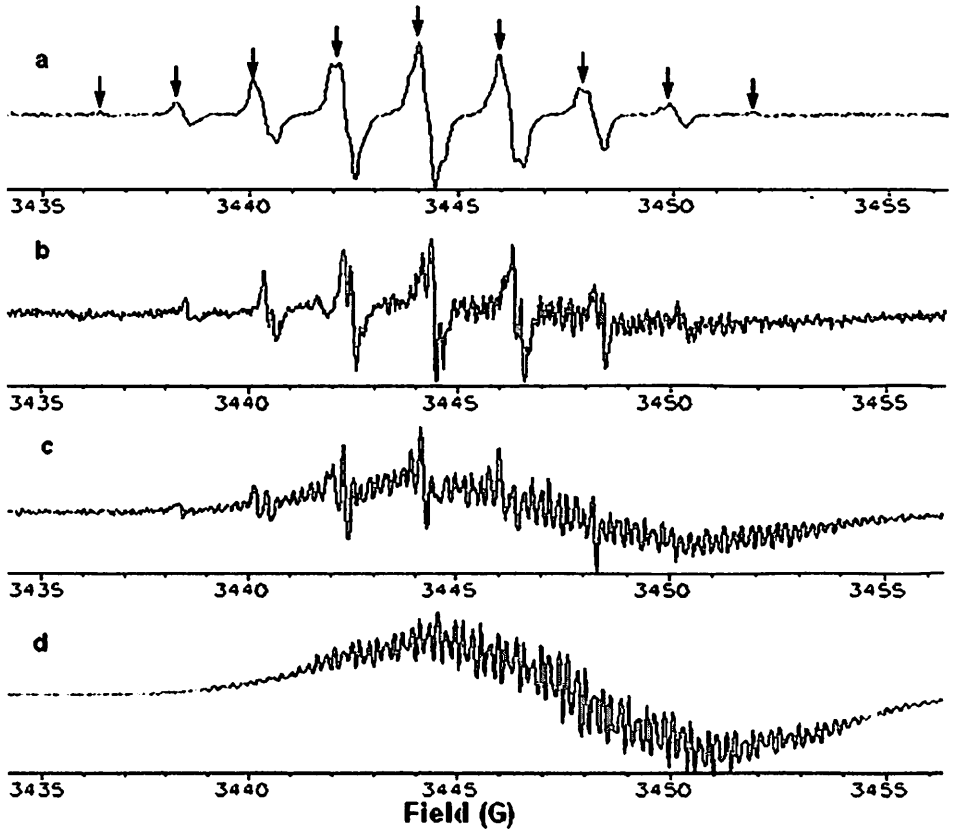

Fig.84 Evolution of the ESR spectra of **5.1d** with time (**a-d** each recorded at 5 minutes intervals) in dry acetonitrile (E = -1000mV vs Ag/AgCl; TBAP as supporting electrolyte; 294.5K); X-band frequency 9.66590GHz and center field 3445G; g 2.0041; Experimental hyperfine splitting constants are a^{H} 1.864G(6H) and 0.195G(2H); Line broadening 0.05G.

The ESR spectrum of **5.1d** (Fig.84) recorded at a potential of E -1000mV initially shows nine distinct signals corresponding to coupling of the electron to eight hydrogen atoms. This is expected, as there are eight hydrogen atoms attached to the three aromatic rings of radical **A** generated from **5.1d**. Spectral analysis shows that the signals are uniformly spaced with the hyperfine coupling constants (a^H) being 1.864G for six hydrogens and 0.195G for two hydrogens. This was simulated using these parameters and overlaid with the experimental spectra. The exact matching of the spectra with simulated spectra with the given parameters suggests that the radical formed is delocalised over the entire molecular framework. This clearly indicates that the lifetime of A in the case of **5.1d** is sufficient to get the signals in ESR spectra. This is obvious for the possible stablisation of the radical as presented in Scheme 7.

However, the ESR spectra of **5.1d** changes with time as electrolysis of the solution progresses. This may be due to decay of this radical to form the parent compound as suggested in step 2 of Scheme 6. But this is not necessarily being the only reason, as one can see the line shape changes and the hyperfine coupling are lost on prolonged standing. After 20minutes, the hyperfine are lost but it leads to a broad signal centering at 3447G. This observation is not unusual as similar observation on decay of signal leading to merger of peaks in the case of coupled systems in which coupling between anionic and radical species are observed earlier[159]. In their study they have studied the effect of 1:1 mixture of anion and anion radical. Since these systems comprises of donor quinone and acceptor phenol units their assembling is quite likely and this could result in the broadening of the ESR signal on prolonged electrolysis.

The results obtained from the electrochemical reduction **5.1e** under similar conditions are as expected, and can be explained on the basis of Schemes 6 and 7. The compound **5.1e** when electrolyzed at potential E -1050mV in acetonitrile produces the anion radical **5.1e**$^{\bullet}$ which is ESR active (Fig. 85).

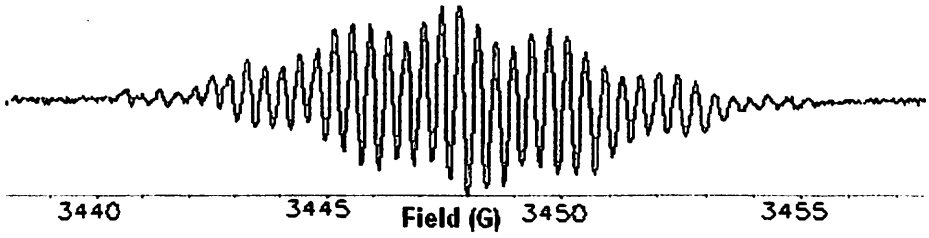

Fig.85 ESR spectra of anion radical of **5.1e** in acetonitrile (E = -1050mV vs Ag/AgCl; 0.1M TBAP; 294.5K); X-band frequency 9.66595GHz and center field 3448G; g 2.0043; a^H 2.035G (6H) and 0.204G (6H). Line broadening 0.05G

The ESR spectrum of **5.1e**$^{\bullet}$ thus obtained, consists of 49 lines as shown in Fig.85. This spectrum indicates that the electron in **5.1e**$^{\bullet}$ is extensively delocalised. When simulated using the coupling constants of 2.035G and 0.204G, it becomes evident that this spectrum of **5.1e**$^{\bullet}$ consists of seven signals corresponding to the coupling of the electron with six-meta protons. Each of the seven signals in the ESR spectrum are thus split into sets of 7 signals (septet) corresponding to a second coupling of the electron with the two methyl groups adjacent to the quinonoid C=O group, with the hyperfine coupling constant for these protons being a^{H} 0.204G. In a recent paper it is demonstrated that the second order-coupling constant of methyl group varies with the orientation of the methyl groups[158]. The six protons ortho- to the central carbon-atom is equivalent indicating that the spin density is delocalized over the entire triphenylmethyl ring system. The symmetry of the ESR spectra of **5.1e** also indicates that the phenyl groups of the quinone and the phenol rings are equivalent on the given timescale. Thus, this radical, **5.1e**$^{\bullet}$, is most stable compared to either any of the other radical anions, and there is no noticeable change in the ESR spectrum after 2hrs of standing. This is also in the expected direction, as the multiple units of methoxy groups would provide steric congestion so that the coupling with another unit would not be possible.

In conclusion we have demonstrated that the quinone-methides under consideration have wide range of properties in solution. Cation, anion, radical from these systems can be easily derived. These systems also provide means to understand isomeric cationic species having triphenylmethane unit. The special interest is the color changes of these compounds over a wide range of pH. The last property make them potential candidate as pH sensor.

Chapter 7

Experimental Section

7.1 X-Ray Crystallography

X-ray diffraction data were collected on Bruker 3-circle diffractometers with CCD area detectors ProteumM APEX or SMART 6000 or Bruker Nonius Apex 2, using graphite-monochromated Mo-$K\alpha$ radiation (λ = 0.71073 Å) from a 60W microfocus Bede Microsource® with glass polycapillary optics or a sealed tube (**5.1e**). In case of the structures that were determined at 120K, the low temperature of the crystals was maintained using Cryostream (Oxford Cryosystems) open-flow N_2 cryostats.

X-ray diffraction data for all the crystals were collected using Bruker SMART software. This software was also used for indexing and determination of the unit cell parameters. The structures were solved by direct methods and refined by full-matrix least squares against F^2 of all data, using SHELXTL software[160-162].

All non-H atom were refined by full-matrix least squares in anisotropic, all H atoms in isotropic approximation, against F^2 of all reflections. All C and O atoms including any heteroatoms were refined in anisotropic approximation. All H atoms in **2.1a**, the hydroxyl H atoms in **2.2**, **4.1** and **5.1** and all but disordered H atoms in **5.1e** were refined in isotropic approximation, the rest were treated as 'riding' in idealized positions. The isotropic parameters and the positions of the hydrogen attached to polar atoms such as O or N were refined in the final structure models. The crystallographic tables for the bis-phenols and the inclusion compounds as well as the dibenzoxanthenes and diaryl quinone methides are given at the end of this section, which includes the crystal parameters and the refinement factors.

7.2 UV-visible Spectroscopy

UV-vis absorption spectra were recorded using a U2001 Schimadzu spectrophotometer or Perkin Lambda 25 spectrophotometer equipped with double cell compartments. All the chemicals and solvents used were as obtained from the satndard suppliers such as E.Merck Germany, Sigma Aldrich USA, Ranbaxy India. The solvents for spectroscopic were of HPLC grade (Aldrich or Merck) and used as obtained. The solvatovatochromic properties of the diaryl quinone methides, **5.1** were studied in constant volumes of the solvent, within the

concentration ranging from 10^{-4} to 10^{-6}mM depending on the visible absorption of the compound.

Some of the UV-visible titration curves of **5.1** with triethylamine followed by hydrochloric acid are shown below:

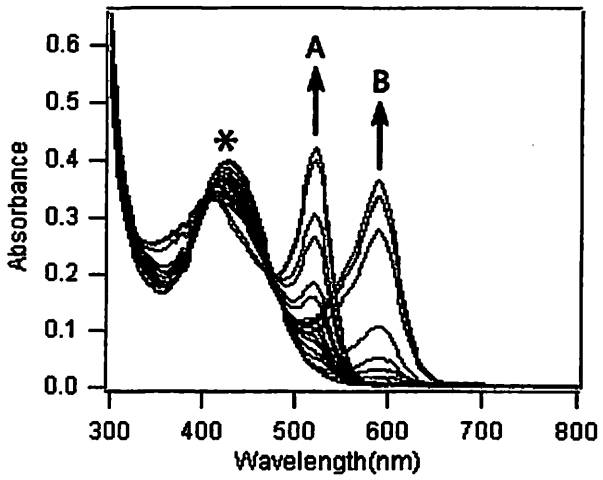

Fig.86(i) : **B)** Interaction of **5.1a** with 0.1(M) Et_3N in methanol (eight times; 20µl each; absorption at 589nm grows, **A)** followed by addition of 0.1 (M) HCl solution (100µl initially and then 20µl ten times loss of peak at 589 and appearance of original peak at 429 and followed by appearance of new peak due to acidic state at 524nm, in methanol. The absorption maximum of **5.1a** in the neutral state is indicated by the asterisk (*).

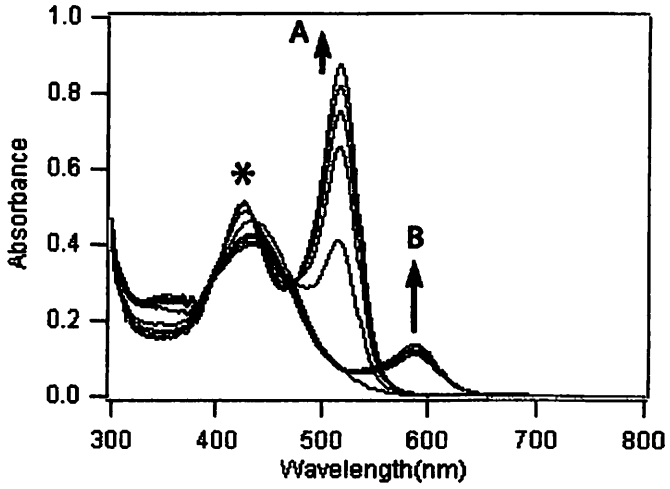

Fig.86(ii): UV-visible spectra of **5.1b** in methanol – **B)** additions of 0.1(M) Et_3N solution (20µl each five times, basic state at 598 develops, in methanol **A)** followed by 0.1(M) HCl solution in methanol (initially 100µl and then 20µl each five times acidic state at 512nm grows. * indicates the absorption maxima in the neutral state

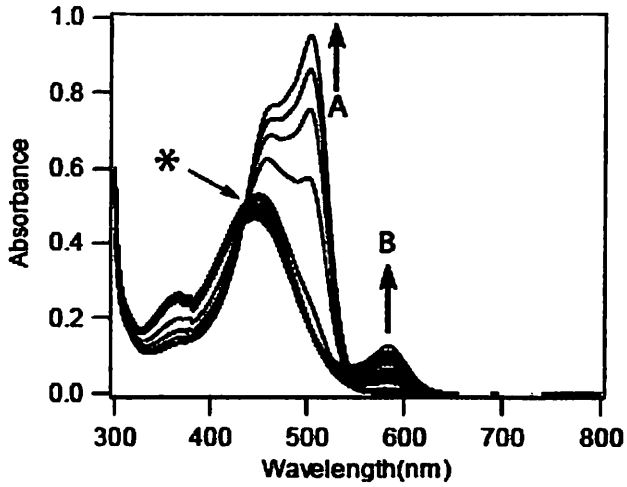

Fig.86(iii) Interaction of **5.1d** **B)** with 0.1 (M) Et_3N solution in methanol (11 additions; 20µl each a new peak at 584nm develops in addition to peak at 444nm, **A)** followed by 0.1(M) HCl in methanol (initially added 200µl then 20µl each 6 times a new peak at 504nm due to acidic state, **A**). * indicates the absorption maximum of **5.1d** in the neutral state.

A typical experiment on solvatochromism:

In a typical experiment to demonstrate solvatochromicity of the compounds, the visible spectra of 4-[(4′-hydroxy-3′,5′-dimethylphenyl)(4-N,N′-dimethylaminophenyl)methylene]-2,6-dimethylcyclohexa-2,5-dienone (4×10^{-5}mM) were recorded in methanol and dimethylformamide at compositions of [1] (2:0); [2] (1.5:0.5); [3] (1.2:0.8); [4] (1:1); [5] (0.8: 1.8); [6] (0.5 :1.5); [7] (2:0) and the changes observed in the absorption spectra are shown in Fig.86(iv).

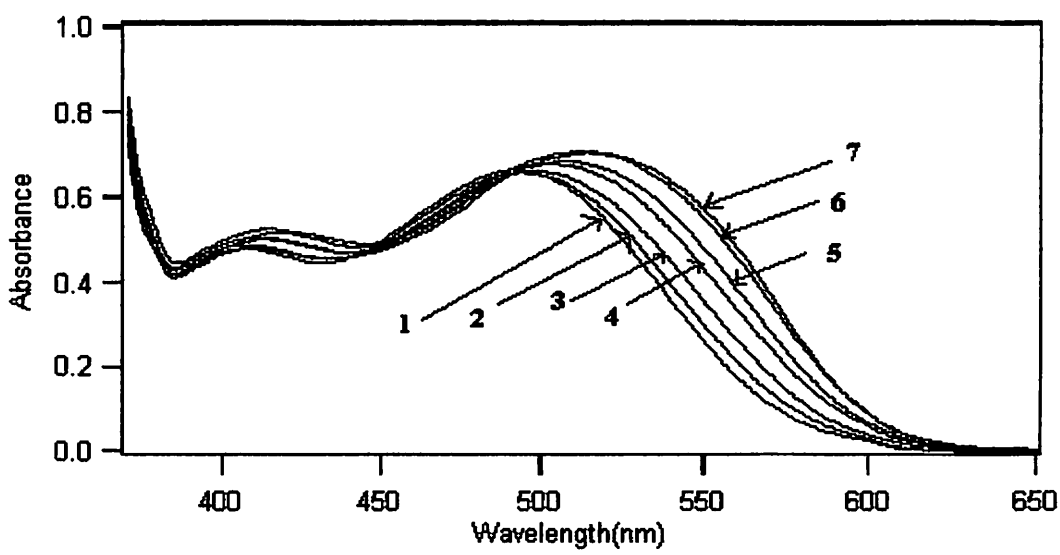

Fig.86(iv)

7.3 NMR Spectroscopy

The NMR spectra, ^{1}H, ^{13}C as well as the HOMOCOSY were recorded either in a Varian 400MHz or Bruker 400MHz or an INOVA 500MHz spectrometer. The chemical shifts in the NMR spectra are all given in ppm and tetramethylsilane as the internal standard.

The concentration dependent NMR spectra of compounds were recorded by dissolving calculated amounts of the sample in a fixed amount of appropriate solvent. The low temperatures experiments were performed using a Bruker 400MHz NMR spectrometer and the temperatures regulated by an in-built temperature control system.

7.4 Thermogravimetric Studies

The thermogravimetric studies were performed using a Mettler Toledo TGA/ STDA 851^{e} and Mettler Toledo DSC^{e} thermal analyser. Typically about 8-10mg of the samples were mounted on platinum crucibles and the TG/DSC profiles recorded at the heating rate of 10°C/min and under nitrogen atmosphere.

7.5 Mass Spectrometric Analysis

Mass spectroscopic analyses have been performed using an either a JEOL SX 102/DA-6000 Mass Spectrometer (3-nitrobenzylalcohol matrix) or an Autospec EI-Mass spectrometer. Electrospray Mass spectra were obtained using Micromass LCT Premier Spectrometer in the Electrospray mode.

7.6 Determination of Melting Points

Melting points reported here were determined using a Buchi® melting point apparatus and are uncorrected.

7.7 Cyclic Voltammetry and Electron Paramagnetic Resonance Spectroscopy

Potentiometric measurements were made with a combined glass pH electrode (having Ag/AgCl reference) obtained from BAS and calibrated with appropriate pH buffers (4.0, 7.2 and 9.0) before each measurement. Cyclic voltammograms are recorded using a Model 263 potentiostat from Princeton Applied Research (USA). All cyclic voltammetric experiments have been performed in dry degassed solvents, under nitrogen atmosphere.

Cyclic voltammograms were measured for 0.1mM solutions of the diaryl quinone methides, **5.1** in dry degassed acetonitrile at 298K. Tetrabutylammonium perchlorate (TBAP) was used as supporting electrolyte and the experimental solution was purged with dry argon before each measurement. The glassy-carbon working electrode, which was used for performing the

experiment was cleaned with electrode polishing materials available from BAS, washed witl deionised water and acetone. The non-aqueous Ag/AgCl electrode was used as reference in all the measurements while a Pt-foil ($1cm^2$) was used as counter electrode.

The in-situ ESR experiments were performed under identical conditions, as described for the cyclic voltammetric experiments. In a typical experiment, a solution of the quinone methide having concentration and containing known amount of the electrolyte, TBAP was prepared. Dry nitrogen or argon was purged through this solution for about 5minutes. This solution was then filled into the ESR cell using a syringe. The ESR cell was equipped with a Pt-mesh having dimensions of 1cm×1cm as the working electrode and a Pt-wire of diameter 0.5mm as the counter electrode. Potentials were measured against a non-aqueous Ag/AgCl electrode, which could be held in a slot at the opening of the ESR cell, such that it remains in contact with the experimental solution while electrolysis was performed. The radical species were generated upon electrolysis of the sample solution at the potentials already indicated in the text. Formation of ESR active species was monitored continuously, and the spectra recorded at definite time intervals.

The ESR experiments were performed using a Bruker X-band spectrometer calibrated with internal teslameter. Simulations of the ESR data were done using standard WinEPR software available from Bruker. The ESR spectrometer magnetic field is calibrated with respect to diphenyl picryl hydazyl radical as the standard and the spectra were recorded at room temperature.

Simulation of the ESR spectra that were obtained from **5.1d** and **5.1e** shows that the radical is delocalised over the entire ring systems. Two such simulations are given below (Fig.87, 88) which have been overlaid with the experimental spectra obtained from the measurements.

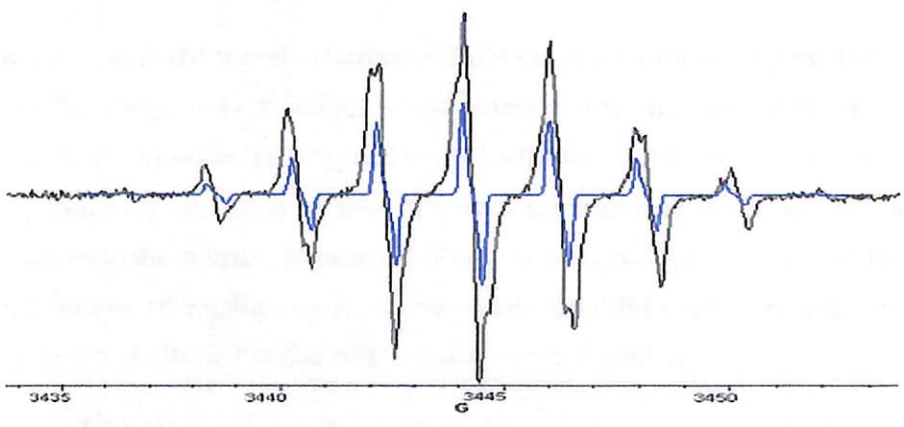

Fig.87 Experimental spectra of **5.1d** and the corresponding simulation (in blue)

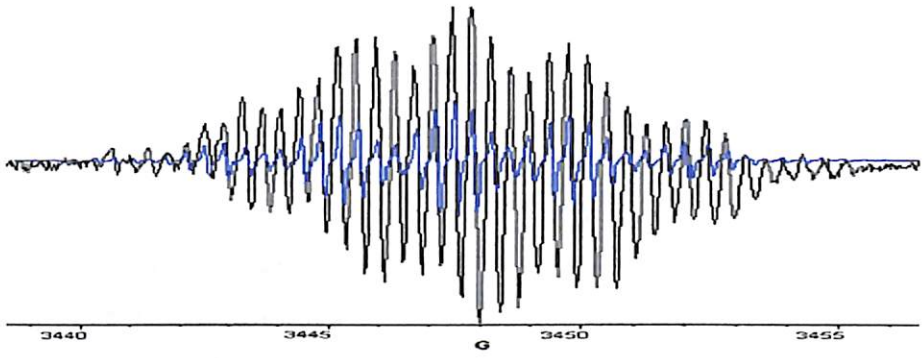

Fig.88 Experimental spectra of **5.1e** and the corresponding simulation (in blue)

7.8 Atomic Force Microscopic Studies

Atomic force microscopy experiments were performed using Digital Instruments multimode head with Nanoscope II controller. The measurements are performed in the tapping mode using a cantilever having silicon tip. The instrument was calibrated against a freshly cleaved surface of with highly ordered pyrolytic graphite (HOPG). Samples were prepared by drop casting on HOPG from 10^{-4} to 10^{-6}M solutions of **2.10** and **2.15** in toluene or chloroform.

7.9 Encapsulation studies with Cyclodextrin and CTAB

Cyclodextrins and the surfactant, cetyl trimethylammonium bromide (CTAB) was purchased from Sigma. The solvents (Sigma or Merck) used in the experiments were of spectroscopic grade, and used as such. Experiments involving aqueous solutions were performed with doubled distilled water. Stock solutions were prepared by dissolving the appropriate amount of the quinone methides in 1ml of ethanol and this solution was then diluted to 10ml. Similarly stock solutions of CTAB and cyclodextrins were prepared by dissolving appropriate amounts of the compounds in deionised water.

Stock solutions of α, β and γ-cyclodextrins of 2mM concentration were prepared in deionised water (25ml). Similarly, stock solutions of the quinone methides (10^{-5}mM) were prepared in ethanol (**5.1a-d**) and in water for **5.1e**, and the pH adjusted to 9.0 using triethylamine. During a typical experiment a calculated volume of such a solution was taken out with a graduated pipette and added to the cuvette (in case of UV-vis studies) and the volume was made up with water. To this solution the quinone methide was added from the corresponding stock solutions in aliquots (10µl) and the visible absorption spectra were recorded.

Stock solution of CTAB in deionised water (10mM) was prepared and calculated amounts of the solution (in aliquots) were taken for each experiment from this stock solution. In typical experiment, the quinone methide solution was prepared in the cuvette by adding 50µl of the

respective stock solution (2mM) in buffer solution of pH 9.0 prepared in deionised water and making up the volume to 2.5ml. The visible spectrum of this of the solution was recorded. The same solution was taken out of the spectrometer and the surfactant solution was added in small aliquots (10µl) from the CTAB stock solution (10mM). The visible absorption spectra of solution after each addition were recorded. This process continued so that sufficient number of absorptions is obtained for plotting the concentration of CTAB vs absorbance. Independent titration experiments with CTAB at different concentrations of quinone methides were carried out to study the concentration dependence of micelle formation. Volume corrections were done in each case.

7.9 Synthesis of Bis-Phenols

Three different procedures were used for the synthesis of the bis-phenols reported here. The optimized yields from different procedures are given in Table **7.3** and **7.4** corresponding to the bis-phenols **2.1** and **2.2**.

The three procedures are as follows:

Procedure I:

2,6-Dimethylphenol (0.49g, 4mmol) and benzaldehyde (0.212g, 2mmol) were dissolved in 20ml of distilled methanol and hydrochloric acid (0.1ml) added into it. The reaction mixture was put under mild reflux for 8 hours after which the solvent was removed under vacuum. Then the residue was partitioned between dichloromethane (25ml) and water (25ml), washed with $NaHCO_3$ (10% aqueous solution) and finally pure water. The organic extract was dried over anhydrous Na_2SO_4, filtered off and then the solvent removed under reduced pressure to give the crude product. Subsequent column chromatography of the crude product (Silica gel 70-120 mesh; Hexanes/Ethyl acetate 4:1) gave the corresponding bis-phenol, bis-(4-hydroxy-3,5-dimethylphenyl)(4-methoxyphenyl) methane (**2.2a**) as white solid.

Procedure II:

In a 50ml conical flask, 2,6-dimethylphenol (0.5g, 4.1mmol) and 4-nitrobenzaldehyde (0.303g, 2mmol) were dissolved in AcOH (7ml) and the solution cooled in ice (0°C). To this was added a mixture of H_2SO_4-AcOH (1:4, 10ml) dropwise over a period of 30mins. When the acid has been added the reaction mixture was kept under ice-cold condition for 3 days. Then cold water (10ml) was added to the reaction mixture and the solids are filtered, washed thoroughly with water to remove the acids and dried in air. The bis-phenol, **2.2f** was obtained as a pale yellow solid from benzene.

Procedure III:

2,6-Dimethylphenol (0.49g, 4.1mmol) and pyridine-4-carboxaldehyde (0.215g, 2mmol) were dissolved in dichloromethane (10ml) and the mixture was stirred at 0°C for 10mins. To this stirred solution trifluoroacetic acid (2ml) was added dropwise over a period of 10mins. The reaction mixture was allowed to stir for 24 hours and then quenched with sodium bicarbonate. The organic components were extracted with dichloromethane (25ml×2) and washed with water. The extracts were dried over anhydrous Na_2SO_4 and the solvent removed under vacuum. Recrystallization from chloroform gave pale yellow crystals of the bis-phenol **2.2o**.

Table 7.1 Spectroscopic data for the bis-phenols **2.1**

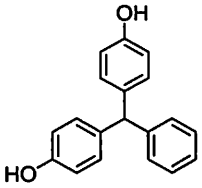 **2.1a**	Colorless solid (m.p. 148°C); FAB-MS [M^+]: 276 IR (cm^{-1}, KBr): 3206, 3023, 1600, 1508, 1242 ^{1}H NMR ($CDCl_3$, 400MHz): 7.29-7.17 (4H, m), 7.11 (2H, d, J = 7.2Hz), 6.96 (2H, d, J = 8.0Hz) , 5.42 (1H, s), 4.70 (2H, s) ^{13}C NMR ($CDCl_3$, 100MHz): 150.8, 130.5, 129.3, 128.3, 126.2, 125.0, 122.3, 117.1, 55.2
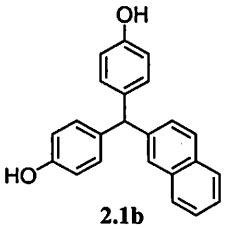 **2.1b**	Pink solid (m.p. 154°C) IR (cm^{-1}, KBr): 3242, 2921, 1592, 1475, 1203, 1168, 1037 ^{1}H NMR ($CDCl_3$, 400MHz): 7.80 (1H, t, J=4.4Hz)), 7.76 (2H, m), 7.45(3H, m), 7.32 (1H, d, J=8.0Hz), 7.14 (4H, d, J=8.0Hz), 6.84 (4H, d, J=8.0Hz), 5.40 (1H, s), 4.46(2H, bs) ^{13}C NMR ($CDCl_3$, 100MHz): 150.4, 136.2, 135.3,133.7, 132.1, 129.8, 127.8, 127.4 127.2,126.4, 125.7, 116.3, 52.6
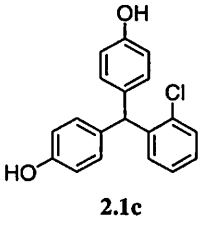 **2.1c**	Pale yellow solid (m.p. 214°C) IR (cm^{-1}, KBr): 3200, 2930, 1585, 1462, 1243, 1122 ^{1}H NMR ($CDCl_3$, 400MHz): 7.29 (1H, t, J= 2.8Hz), 7.09 (2H, m), 6.89 (1H, d, 2.8Hz), 6.83 (2H, d, J=8.0Hz), 6.68 (2H, d, J=8.0Hz), 5.73 (1H,s), 4.47 (2H, s) ^{13}C NMR ($CDCl_3$, 100MHz): 151.5, 139.3, 135.6, 133.7, 129.3, 126.2, 117.1, 54.2

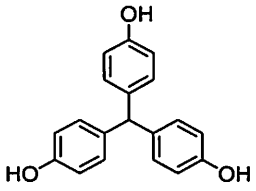 **2.1d**	Colorless solid (m.p. 239°C) IR (cm^{-1}, KBr): 3166, 2960, 1599, 1453, 1284, 1157 ^1H NMR ($CDCl_3$, 400MHz): 6.85 (6H, d, J=8.0Hz), 6.66 (6H, d, J=8.0Hz), 5.26 (1H, s), 4.83 (3H, bs). ^{13}C NMR ($CDCl_3$, 100MHz): 155.1, 135.6,129.8,116.3, 45.2
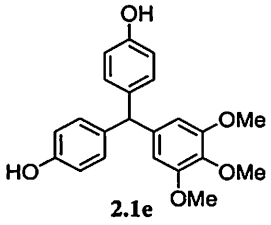 **2.1e**	Colorless solid (m.p. 182°C) IR (cm^{-1}, KBr): 3454, 2942, 1598, 1508, 1218, 1123 ^1H NMR ($CDCl_3$, 400MHz): 6.94 (4H, d, J = 8.4Hz), 6.73 (4H, d, J=8.4Hz), 6.27 (2H, s), 5.32 (1H, s), 3.81 (3H, s), 3.71 (6H, s). ^{13}C NMR ($CDCl_3$, 100MHz): 152.0, 154.2, 141.4, 135.7, 135.2, 129.2, 122.2, 117.0, 60.8, 56.2, 55.7

Table 7.2 Spectroscopic data for the bis-phenols **2.2**

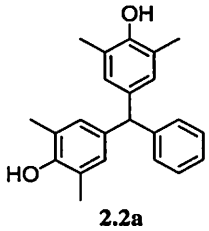 **2.2a**	Yellow solid (m.p. 136°C); FAB-MS [M^+]: 332 IR (cm^{-1}, KBr): 3589, 3467, 2918, 1606, 1505, 1445, 1220, 1009 ^1H NMR ($CDCl_3$, 400MHz): 7.30 -7. 21 (5H, m) 6.72 (4H, s), 5.3 (1H, s), 4.54 (2H, s), 2.18 (12H, s).^{13}C NMR ($CDCl_3$, 400MHz): 150.5, 147.4, 144.9, 136.1, 129.5, 129.3, 128.2, 125.9, 122.7, 55.5, 16.0. Elemental Anal. Calcd. for $C_{23}H_{24}O_2$: C 83.09%, H 7.28% Found: C 83.12%, H 7.25%
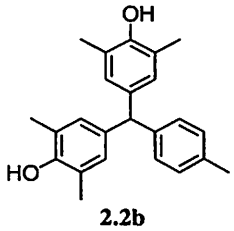 **2.2b**	Pale yellow solid (m.p. 154 °C); FAB-MS [M^+]: 346 IR (cm^{-1}, KBr): 3653, 3569, 3030, 2970, 1615, 1492, 1461, 1338, 1215, 1184, 1123, 1092 ^1H NMR ($CDCl_3$, 400MHz): 7.08 (2H, d, J=8.0Hz), 6.97(2H, d, J= 8.0Hz), 6.72 (4H,s), 5.26 (1H, s), 4.48 (2H, s), 2.32 (3H, s), 2.17 (12H, s). ^{13}C NMR ($CDCl_3$, 100MHz): 150.4, 141.9, 136.3, 135.4, 129.5, 129.2, 128.9, 122.6, 55.1, 21.0, 16.0. Elemental Anal Calcd for $C_{24}H_{26}O_2$: C 83.20%, H 7.56% Found. C 83.19%, H 7.65%

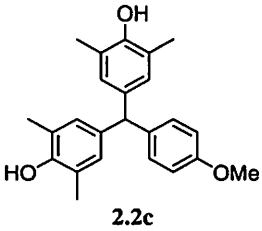

2.2c

Colorless crystals (m.p. 171°C); FAB-MS [M^+]: 362

IR (cm^{-1}, KBr): 3574, 3513, 2919, 1603, 1458, 1260, 1029

^1H NMR ($CDCl_3$, 400MHz): 7.04 (2H, d, J=8.4Hz), 6.82 (2H,d, J=8.4Hz), 6.68 (4H, s), 5.24 (1H,s) , 4.49 (2H, s) , 3.79 (3H, s), 2.18 (12H, s). ^3C NMR ($CDCl_3$, 100MHz): 157.8, 150.5, 137.2, 136.4, 130.2, 129.4, 122.7, 113.6, 55.2, 54.7, 52.6, 15.9.
Elemental Anal Calcd. for $C_{24}H_{26}O_3$: C 79.53%, H 7.23%
Found: C 79.48%, H 7.23%

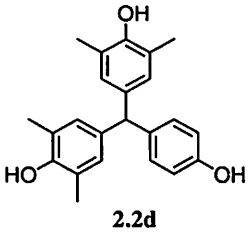

2.2d

Colorless needles (m.p. 181°C); FAB -MS [M^+]: 348

IR (cm^{-1}, KBr): 3493, 2878, 1575, 1449, 1291, 1157

^1H NMR ($CDCl_3$, 400MHz): 7.00 (2H, d, J=8.4Hz), 6.72 (2H, d, J=8.4Hz), 6.70 (4H, s), 5.24 (1H,s), 4.49 (2H, s), 3.79 (3H, s), 2.18 (12H, s).^{13}C NMR ($CDCl_3$, 100MHz): 157.7, 150.4, 137.1, 136.4, 130.2, 129.4, 122.7, 113.6, 55.2, 54.7, 15.9. Elemental Anal Calcd. for $C_{23}H_{24}O_3$: C 79.28%, H 6.94% Found: C 79.40%, H 7.02%

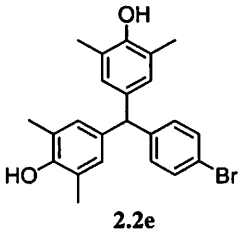

2.2e

Yellow solid (m.p. 138°C)

IR (cm^{-1}, KBr): 3580, 3519, 2930, 1609, 1491, 1194, 1250, 1040

^1H NMR ($CDCl_3$, 400MHz): 7.82 (2H, d, J= 8.4Hz), 7.28(2H, d, J= 8.4Hz), 5.25 (1H, s), 4.49 (2H,s), 3.79 (3H,s), 2.19 (12H,s).^{13}C NMR ($CDCl_3$, 100MHz): 156.2, 142.0, 135.2, 132.3, 130.6, 129.6, 125.4, 122.6, 49.3, 15.9

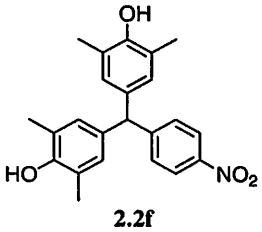

2.2f

Yellow solid (m.p. 166°C); FAB -MS [M^+]: 377

IR (cm^{-1}, KBr): 3452, 2924, 1624, 1521, 1490, 1347, 1198, 1106

^1H NMR ($CDCl_3$, 400MHz): 8.13 (2H,d, J=8.0Hz), 7.28 (2H, d, J=8.0Hz), 6.84 (4H, d, J=2.8Hz), 5.38 (1H, s), 4.57 (2H, bs), 2.20 (12H, s).

^{13}C NMR ($CDCl_3$, 100MHz): 152.7, 150.9, 146.3, 134.4, 130.1, 129.3, 123.4, 123.1, 55.3, 15.9

Pink solid (m.p. 158°C); FAB -MS [M^+]: 375

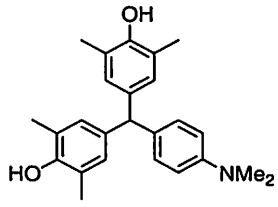

2.2g

IR (cm^{-1}, KBr): 3464, 2988, 1596, 1483, 1293, 1138, 1095

^1H NMR ($CDCl_3$, 400MHz): 6.98 (2H, d, J=8.4Hz), 6.74 (4H, s), 6.69 (2H, d, J=8.4Hz), 5.23 (1H, s), 4.64 (2H, s), 2.93 (6H, s), 2.19 (12H, s)

^{13}C NMR ($CDCl_3$, 100MHz): 150.4, 149.0, 136.8, 133.3, 129.9, 129.4, 122.6, 112.7, 54.6, 40.8, 16.0

Pale yellow solid (m.p. 184°C); FAB -MS [M^+]: 360

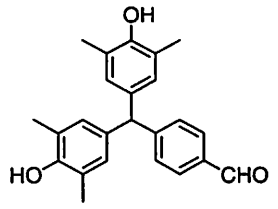

2.2h

IR (cm^{-1}, KBr): 3343, 2928, 1690, 1636, 1569, 1452, 1327, 1193

^1H NMR ($CDCl_3$, 400MHz): 9.92 (1H, s), 7.72 (2H, d, J=7.6Hz), 7.23 (2H, d, J=7.6Hz), 6.89 (4H, s), 5.12 (1H, s), 4.54 (2H, bs), 2.19 (12H, s)

^{13}C NMR ($CDCl_3$, 100MHz): 196.2, 151.5, 149.5, 147.3, 136.3, 129.3, 124.7, 124.1, 122.0, 55.3, 16.4

Yellow solid (m.p. 163°C); FAB -MS [M^+]: 360

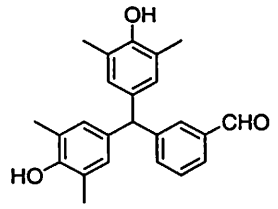

2.2i

IR (cm^{-1}, KBr): 3280, 2984, 1678, 1598, 1455, 1244, 1163

^1H NMR (MeOD-d^4, 400MHz): 9.89 (1H, s), 7.68 (1H, d, J=8.0Hz), 7.57 (2H, bs), 7.38 (2H, m), 6.95 (1H, s), 6.63 (4H, s), 5.30 (1H, s), 2.17 (12H, s). ^{13}C NMR (MeOD-d^4, 100MHz): 191.5, 156.3, 149.1, 143.3, 136.3, 129.0, 114.2, 111.7, 55.3, 16.4

Pink solid (m.p. 148°C); FAB -MS [M^+]: 378

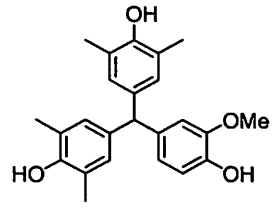

2.2j

IR (cm^{-1}, KBr): 3442, 2924, 1634, 1598, 1485, 1352, 1270, 1174

^1H NMR ($CDCl_3$, 400MHz): 6.82 (1H, d, J=8.0Hz), 6.69(4H, s), 6.63 (1H, d, J=1.63Hz), 6.53 (1H, d, J= 8.0 Hz), 5.51(1H, s), 5.22 (1H, s), 4.56(2H, s), 3.77(3H, s), 2.17(12H, s). ^{13}C NMR ($CDCl_3$, 100MHz): 150.5, 143.8, 136.9, 136.3, 129.4, 122.7, 122.1, 113.9, 112.1, 60.4, 55.1, 29.7,16.0. Elemental Anal. Calcd. For $C_{24}H_{26}O_4$: C 76.17%, H 6.92%, Found C 76.24%, H 7.01%

Colorless crystals (m.p. 197°C); FAB-MS [M^+]: 392

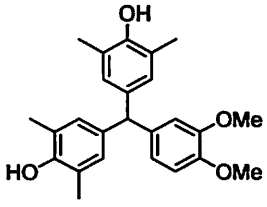

2.2k

IR (cm^{-1}, KBr): 3494, 3441, 2934, 2837, 1593, 1485, 1229, 1198

^1H NMR ($CDCl_3$, 400MHz): 6.75-6.66 (7H, m), 5.23 (1H, s), 4,57 (2H, s), 3.85 (3H, s), 3.77 (3H, s), 2.17 (12H, s). ^{13}C NMR ($CDCl_3$, 100MHz): 150.5, 148.7, 147.3, 137.6, 136.3, 129.4, 122.7, 121.4, 112.9, 110.9, 55.9, 55.0, 16.0,10.3. Elemental Anal. Calcd. for $C_{25}H_{28}O_4$: C 79.50%, H 7.19% Found: C 79.36%, H 7.20%

Pink solid (m.p. 104°C); FAB-MS [M^+]: 422

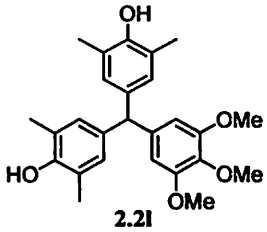

2.2l

IR (cm^{-1}, KBr): 3467, 2939, 1588, 1490, 1326, 1193, 1132, 1009

^1H NMR ($CDCl_3$, 400MHz): 6.70 (4H, s), 6.31(2H, s), 5.20 (1H, s), 4.51(2H, s), 3.83 (3H, s), 3.73 (6H, s), 2.19 (12H, s). ^{13}C NMR ($CDCl_3$, 100MHz): 152.9, 150.6, 140.5, 136.5, 135.9, 129.4, 122.7, 107.0, 60.8, 56.2, 55.7, 15.9. Elemental Anal. Calcd. for $C_{26}H_{30}O_5$: C 73.91%, H 7.16% Found: C 73.84%, H 7.20%.

Red solid (m.p. 142°C); FAB-MS [M^+]: 382

IR (cm^{-1}, KBr): 3436, 2980, 2914, 1495, 1540, 1203, 1142

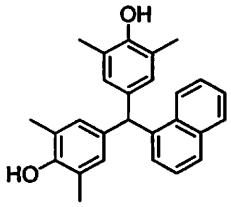

2.2m

^1H NMR ($CDCl_3$, 400MHz): 8.00 (1H, d, J= 8.0Hz), 7.83 (1H, d, J=8.0Hz), 7.72 (1H, d, J=8.0Hz), 7.42 (3H, m), 6.97 (1H, d, J=8.0Hz), 6.70 (4H, s), 6.01 (1H, s), 4.48 (2H, s), 2.16 (12H, s). ^{13}C NMR ($CDCl_3$, 100MHz): 150.4, 143. 8, 136.9, 136.3, 132.6, 129.4, 127.1, 126. 8, 123.9, 122.7, 122.2, 55.0, 16.0. Elemental Anal. Calcd. for $C_{27}H_{26}O_2$: C 84.78%, H 6.85% Found: C 84.86%, H 6.92%

Pale yellow hygroscopic solid (m.p.89°C); ES-MS [M^+]: 382

IR (cm^{-1}, KBr): 3559, 3413, 2919, 1598, 1486, 1198, 1147, 1024. ^1H NMR ($CDCl_3$, 400MHz): 7.82(1H, m), 7.74(2H, s), 7.45(3H, m), 6.76(4H, s), 5.46(1H, s), 4.53(2H, s), 2.20 (12H, s). ^{13}C NMR ($CDCl_3$, 100MHz): 150.6, 142.6, 135.9, 133.5, 132.2, 129.6, 128.3, 127.7, 127.5, 125.5, 125.8, 122.8, 55.7, 15.9

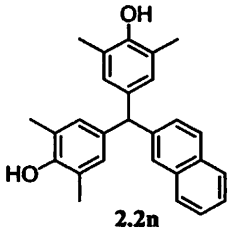

2.2n

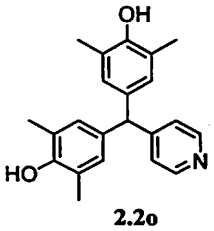

2.2o

Pale yellow solid (m.p. 205°C); FAB-MS [M^+]: 333

IR (cm^{-1}, KBr): 3385, 3083, 2914, 2079, 1634, 1485, 1147, 1004

^{1}H NMR (DMSO-d^6, 400MHz): 7.6 (2H,d, J=6.4Hz), 6.7 (2H,d, J= 6.4Hz), 6.60 (4H, s), 5.43 (1H, s), 3.70(2H, s), 2.18 (12H, s)

^{13}C NMR (DMSO-d^6, 100MHz): 156.5, 152.8, 141.6, 131.4, 129.2, 127.7, 125.1, 55.6, 17.4

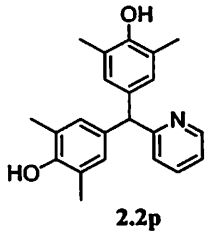

2.2p

Colorless crystals (m.p. 191°C); FAB-MS [M^+]: 333

IR (cm^{-1}, KBr): 3325, 2928, 2860, 1618, 1477, 1209

^{1}H NMR ($CDCl_3$, 400MHz): 8.64 (1H, d, J=7.2Hz), 7.68 (1H, t, J=7.2Hz), 7.57 (1H, d, J=7.2Hz), 7.12 (1H, t, J=7.2Hz), 6.64 (4H, s), 5.24 (1H, s), 2.17 (12H, s)

^{13}C NMR ($CDCl_3$, 100MHz): 152.6, 150.5, 149.6, 138.1, 137.0, 130.8, 122.3, 56.4, 17.3

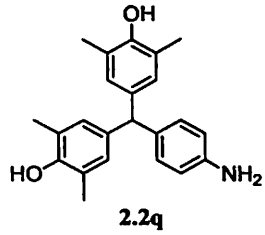

2.2q

Pink solid (m.p. 152°C); FAB-MS [M^+]: 347

IR (cm^{-1}, KBr): 3360, 3112, 2984, 1605, 1473, 1238, 1160

^{1}H NMR ($CDCl_3$, 400MHz): 6.92 (2H, d, J=8.4Hz), 6.74 (4H, s), 6.52 (2H, d, J=8.4Hz), 5.23 (1H, s), 4.05 (2H, bs), 3.48 (2H, s), 2.20 (12H, s)

^{13}C NMR ($CDCl_3$, 100MHz): 150.6, 144.2, 136.5, 135.4, 130.1, 129.6, 129.3, 123.2,118.0, 115.5, 115.2, 114.9, 54.6, 50.4, 16.5

Synthesis of 4-[bis(4-hydroxy-3,5-dimethylphenyl)-methyl]pyridinium chloride, **2.2r**:

Slow evaporation of a solution of bis-phenol **2.2o** (0.333g, 1mmol) and hydrochloric acid (0.3ml, 11.5M) in methanol (10ml) in the presence of $CuCl_2.2H_2O$ (0.01g, 6mol%) gave pale yellow crystals of **2.2r**.HCl (Yield 67%; m.p. 214°C); IR (cm^{-1}, KBr): 3385, 3083, 2914, 2079, 1634, 1485, 1147, 1006

Synthesis of 4-[bis(4-hydroxy-3,5-dimethylphenyl)-methyl]pyridinium bromide, **2.2s**:

The bis-phenol **2.2o** (0.333g, 1mmol) was dissolved in methanol. To this HBr (0.5ml, 60%) and cupric bromide (5mol%) were added. Stirring this mixture at room temperature resulted

in a homogeneous solution, which on slow evaporation gave the desired crystals of **2.2s**.HBr (Yield 54%; m.p. 219°C); IR (cm^{-1}, KBr) 3374, 2786, 2034, 1629, 1481, 1317, 1194, 1024

7.10 Synthesis of Ether-Bridged Bis-Phenols (2.5, 2.6):

Preparation of the dialdehyde, **2.4a**:

4-Hydroxybenzaldehyde (0.25g, 2.05mmol) and finely ground anhydrous K_2CO_3 (0.3g, 2.2mmol) were added into a round bottom flask (100ml) equipped with a condenser and a dropping funnel, followed by dry DMF (20ml). Ethylene glycol ditosylate (0.374g, 1mmol) was dissolved in dry DMF (10ml) inside the dropping funnel and added drop-wise into the round bottom flask under dry nitrogen atmosphere. The reaction mixture was heated at 90°C with constant stirring for 48hrs and then the solvent removed under vacuum. The residue was dissolved in dichloromethane (2×25ml) and filtered. This filtrate was collected and partitioned with Na_2CO_3 solution (10%), washed with water and the organic extract put over anhydrous Na_2SO_4. Subsequently the dichloromethane extract was filtered and the solvent removed under reduced pressure which gave **2.4a** as white solid (Yield 88%). FAB-MS [M^+]: 270; IR (cm^{-1}, KBr): 3162, 2988, 1672, 1624, 1485, 1312, 1192. ^{1}H NMR ($CDCl_3$, 400MHz): 9.92 (2H, s), 7.82 (4H, d, J= 6.8Hz), 7.08 (4H,d, J= 6.8Hz), 4.47 (4H,s). ^{13}C NMR ($CDCl_3$, 100MHz): 189.0, 161.3, 132.6, 130.5, 115.5, 56.8

Preparation of the dialdehyde, **2.4b**: Same as **2.4a** except that the starting material is 4-hydroxy-3-methoxybenzaldehyde. White solid (Yield 91%). FAB-MS [M^+]: 330; IR (cm^{-1}, KBr): 3156, 2992, 1679, 1570, 1498, 1357, 1296, 1168. ^{1}H NMR ($CDCl_3$, 400MHz): 9.89 (2H, s), 7.84 (4H, d, J=6.8Hz), 7.03 (4H, d, J=6.8Hz), 4.56 (4H, s), 3.73 (6H, s). ^{13}C NMR ($CDCl_3$, 100MHz): δ (ppm) 190.7, 163.7, 131.9, 130.2, 114.9, 69.7, 56.8.

Synthesis of **2.5b**: Procedure **II** was used. Red solid (Yield 67%); ES-MS [M^+]: 722.9; IR (cm^{-1}, KBr): 3440, 3119, 1605, 1496, 1294, 1179, 1046. ^{1}H NMR ($CDCl_3$, 400MHz): 8.01 (4H, s), 6.89 (2H, d, J=8.4Hz), 6.70 (2H,s), 6.60 (8H, s), 6.51 (2H, d, J=8.4Hz), 5.15 (2H, s), 4.21(4H, s), 3.62 (6H, s), 2.08 (24H, s). ^{13}C NMR ($CDCl_3$, 100MHz): 151.1, 148.4, 145.9, 137.9, 135.1, 128.6, 123.7, 120.9, 113.4, 112.8, 67.0, 55.5, 16.7, 16.0

Synthesis of **2.6a**: Procedure **II** was used. Red solid (Yield 32%); ES-MS [M^+]: 782.96; IR (cm^{-1}, KBr): 3380, 3046, 2885, 1595, 1412, 1290, 1091. ^{1}H NMR ($CDCl_3$, 400MHz): 9.82 (1H,s), 7.78 (2H, d, J=9.2Hz), 6.98 (2H, d, J=9.2Hz), 6.62 (4H,s), 5.18 (1H, s), 4.36 (4H,s), 2.10 (12H,s) ^{13}C NMR ($CDCl_3$, 100MHz): 190.9, 163.7, 156.8, 150.5, 137.9, 136.3, 133.3, 132.1, 130.4, 129.6, 122.7, 114.9, 66.5, 54.8, 16.4.

7.11 Synthesis of Amide-Bridged Bis-Phenols, 2.9 and 2.10:

Preparation of **2.7a-d**: In a typical procedure, the dibromo amide 2-Bromo-N-[2-(2-bromo acetylamino)-ethyl]-acetamide is prepared as follows:

Bromoacetyl bromide (2.04g, 10.0mmol) was dissolved in dry dichloromethane (5ml) and the solution is cooled to 0°C in melting ice. 1,2-Diaminoethane (0.30g, 5mmol) was dissolved in dichloromethane (10ml) and added dropwise to the acid bromide with constant stirring. Subsequently $NaHCO_3$ (1.0g, 10.2mmol) was added to the reaction mixture and then stirred for 12hr after which diethylether (20ml) is added. The precipitate was filtered at water pump and washed with cold ether (2×10ml). This residue was stirred in ethanol-chloroform (1:9) and filtrate is collected. Removal of the solvent from the filtrate under vacuum gave the bis-amide as almost white solid that may be sticky due to the presence of moisture. The yields are generally moderate.

Analytical and Spectroscopic data for the bis-phenols **2.7**

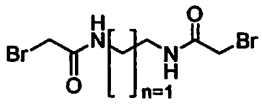

2.7a

White solid (Yield 56%); FAB-MS [M^+]: 301.8

IR (cm^{-1}, KBr): 3026, 2918, 2860, 1674, 1411, 1273, 1057

^1H NMR ($CDCl_3$, 400MHz): 6.97 (2H, bs), 3.93 (4H, s), 3.086 (4H, q, J= 6.4Hz)

^{13}C NMR ($CDCl_3$, 100MHz): 166.9, 40.3, 28.8

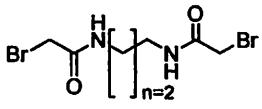

2.7b

White solid (Yield 52%); ES-MS [M+ Na^+]: 338.9

IR (cm^{-1}, KBr): 2953, 1673, 1404, 1259, 1043

^1H NMR (DMSO-d^6, 400MHz): 8.27 (2H, bs), 3.83 (4H, s), 3.08 (4H, q, J=6.4Hz), 1.56 (2H, m)

^{13}C NMR (DMSO-d^6, 100MHz): 165.9, 36.8, 29.5, 28.6

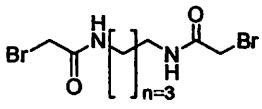

2.7c

White solid (Yield 40%); ES-MS [M+ Na^+]: 352.9

IR (cm^{-1}, KBr): 2933, 1672, 1427, 1222, 1051

^1H NMR (DMSO-d^6, 400MHz): 8.28 (2H, bs), 3.82 (4H, s), 3.06 (4H, m, J=5.2Hz), 1.40 (4H, m)

^{13}C NMR (DMSO-d^6, 100MHz): 165.8, 45.7, 29.5, 26.2

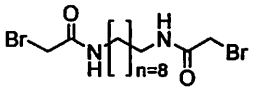

2.7d

Pale yellow solid (Yield 68%); ES-MS [M^+]: 401.8

IR (cm^{-1}, KBr): 2964, 1682, 1671, 1414, 1210, 1142

^1H NMR ($CDCl_3$, 400MHz): 8.12 (2H, bs), 3.69 (4H, s), 2.92 (4H, q, J= 6.8Hz), 1.27 (4H, m), 1.21 (10H, m)

^{13}C NMR ($CDCl_3$, 100MHz): 190.5, 167.8, 161.8, 132.0, 131.1, 115.0, 67.1, 53.4, 32.1, 24.5

Preparation of **2.8a-d**:

In a a typical experiment, 4-hydroxybenzaldehyde (0.56g, 4.6mmol), anhydrous K_2CO_3 (0.34g, 2.5mmol) and **2.7a** (0.70g, 2.3mmol) were added into a round bottom flask containing dry acetonitrile (20ml). This reaction mixture was stirred at 80°C for 30hrs under nitrogen and then the solvent removed under vacuum. The residue was extracted with dichloromethane (2×20ml), washed with aqueous Na_2CO_3 (10% solution), and then water. The organic extracts were dried over anhydrous Na_2SO_4. Removed of the solvent gave the bis-aldehyde **2.8a** as a white compound which was purified by column chromatography over silica gel with chloroform-methanol (100:0 to 95:5).

The other bis-phenols **2.8b-d** were prepared in analogous procedure.

Analytical and Spectroscopic data for the bis-phenols **2.8**
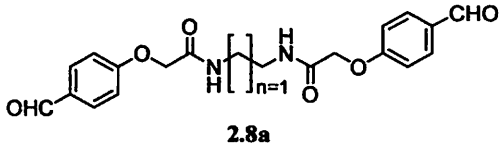 **2.8a**
White solid (Yield 56%); ES-MS [M^+]: 384.1 IR (cm^{-1}, KBr): 3103, 2923, 1696, 1657, 1558, 1460, 1216 ^1H NMR ($CDCl_3$, 400MHz): 9.97 (2H, s), 7.82 (4H, d, J= 8.0Hz), 7.19 (2H, bs), 7.00 (4H, d, J=8.0Hz), 4.54 (4H, s), 3.55 (4H, m) ^{13}C NMR ($CDCl_3$, 100MHz): 190.8, 168.6, 162.1, 132.2, 131.1, 115.2, 67.3

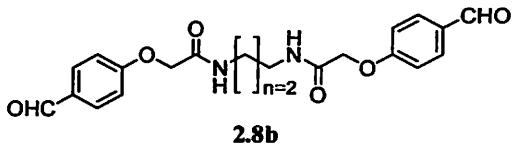

2.8b

White solid (Yield 75%); ES-MS [M+Na$^+$]: 421.1

IR (cm^{-1}, KBr): 3013, 2989, 1668, 1527, 1404, 1130.

^{1}H NMR (DMSO-d^6, 400MHz): 9.91 (2H, s), 8.27 (2H, bs), 7.81 (4H, d, J=7.2Hz), 6.99 (4H, d, J=7.2Hz), 4.42 (4H, s), 3.34 (4H, m), 1.60 (2H, m)

^{13}C NMR (DMSO-d^6, 100MHz): 190.2, 168.9, 163.4, 133.0, 131.5, 114.4, 67.6, 36.6, 29.5

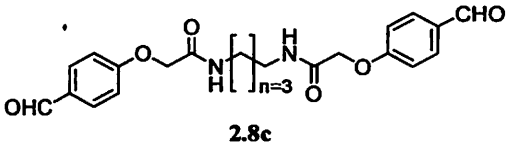

2.8c

White solid (Yield 48%); ES-MS [M+Na$^+$]: 435.2

IR (cm^{-1}, KBr): 3027, 2985, 1694, 1602, 1523,

^{1}H NMR (DMSO-d^6, 400MHz): 9.88 (2H, s), 7.81 (4H, s, J=7.6Hz), 6.99 (4H, d, J=7.6Hz), 6.56 (2H, bs), 4.53 (4H, s), 3.32 (4H, m), 1.48 (4H,m)

^{13}C NMR (DMSO-d^6, 100MHz):190.6, 166.1, 132.2, 131.4, 116.0, 61.8, 39.1, 29.7

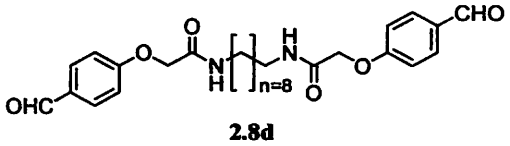

2.8d

White solid (Yield 70%); ES-MS (M+): 483

IR (cm^{-1}, KBr): 3041, 2946, 1691, 1669, 1537, 1487, 1190, 1042

^{1}H NMR ($CDCl_3$, 400MHz): 9.84 (2H, s), 7.80 (4H, d, J=7.2Hz), 6.98 (4H, d, J=7.2Hz), 6.46 (2H, b), 4.50 (4H, s), 3.27 (4H, m, J=6.4Hz), 1.45 (4H, m), 1.19 (10H, m), 1.28 (4H, m)

^{13}C NMR ($CDCl_3$, 100MHz): 190.5, 167, 161.8, 132.0, 131.1, 115.0, 67.4, 39.1, 29.4, 29.3, 29.0, 24.5

Preparation of **2.9** and **2.10**:

In a typical experiment, the bis-aldehyde, **6a** (0.49g, 1.2mmol) and 2,6-dimethylphenol (0.60g, 4.9mmol) were dissolved in acetic acid (6ml). The solution was cooled in ice (0-5°C). To this cold solution a mixture of acetic acid and sulphuric acid (10ml, 7:3) was added dropwise over a period of 20mins. After the acid had been added the solution was kept at 0°C for 72hrs and then dissolved in distilled water (20ml). The reaction mixture was allowed to reach room temperature. Washing the product with water gave a pink solid. This solid was dried and subsequently purified by column chromatography over silica gel (ethyl acetate: chloroform 1:1).

Analytical and Spectroscopic data for the bis-phenols **2.9** and **2.10**

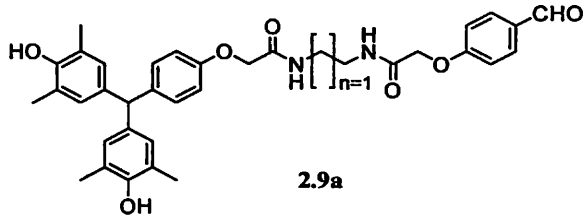

2.9a

Red solid (Yield 11.5%); ES-MS [M+Na$^+$]: 633.3

IR (cm^{-1}, KBr): 3312, 3103, 2911, 1694, 1657, 1558, 1460, 1367, 1216

^{1}H NMR ($CDCl_3$, 400MHz): 9.88 (1H, s), 7.85 (2H, d, J=8.8Hz), 7.38 (1H, bs), 7.18 (1H, bs), 7.04 (4H, d, J=8.8Hz), 6.83 (2H, d, J=8.8Hz), 6.69 (4H, s), 5.24 (1H, s), 4.80 (2H, bs), 4.53 (2H, s), 4.44 (2H, s), 3.56 (4H, bs), 2.19 (12H, s)

^{13}C NMR ($CDCl_3$, 100MHz): 190.9, 170.1, 168.4, 162.0, 155.5, 150.8, 139.1, 136.1, 132.8, 132.1, 130.7, 129.5, 123.1, 115.2, 114.6, 66.4, 54.8, 40.2, 39.1, 16.3

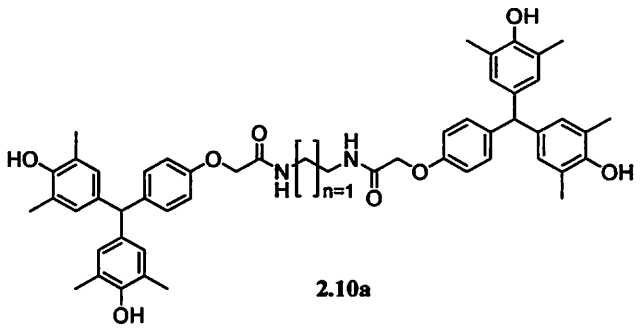

2.10a

Red solid (Yield 25.0%); ES-MS [M+Na$^+$]: 859.4

IR (cm^{-1}, KBr): 3428, 3127, 2894, 1663, 1545, 1323, 1147

^{1}H NMR ($CDCl_3$, 400MHz): 7.08 (2H,bs), 6.92 (4H, d, J=8.0Hz), 6.78 (4H, d, J=8.0Hz), 6.56 (8H, s), 5.15 (2H,s), 4.64 (4H, bs), 3.42 (4H, m), 2.12 (24H, s)

^{13}C NMR ($CDCl_3$, 100MHz): 169.5, 155.4, 150.5, 141.7, 138.8, 135.9, 130.6, 130.5, 129.7, 129.4, 122.9, 122.8, 114.4, 114.3, 67.2, 60.4, 55.7, 55.4, 39.2, 16.4, 16.0

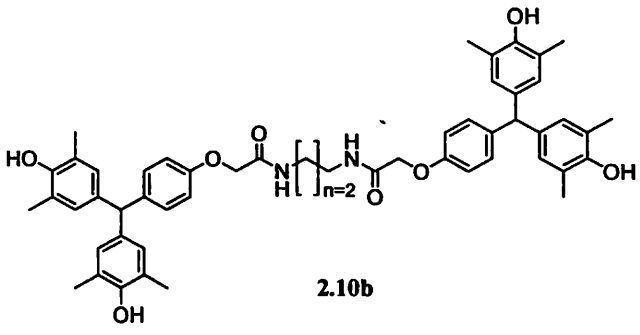

2.10b

Red solid (Yield 48.0%); ES-MS [M+Na$^+$]: 873.4

IR (cm^{-1}, KBr): 3452, 3105, 2899, 1654, 1624, 1541, 1468, 1134.

^{1}H NMR ($CDCl_3$, 400MHz): 7.14 (2H, bs), 7.07 (4H, d, J= 8.0Hz), 6.84 (4H, d, J=8.0Hz), 5.24 (2H,s), 4.63 (4H, bs), 4.42 (4H,s), 3.38 (4H, m, J=6.4Hz), 2.19 (24H, s), 1.73 (2H, m)

^{13}C NMR ($CDCl_3$, 100MHz): 168.9, 155.4, 150.7, 138.7, 136.0, 130.5, 130.1, 129.4, 129.3, 122.8, 122.7, 114.4, 114.3, 67.3, 60.3, 54.6, 35.6, 21.0, 16.4, 14.2

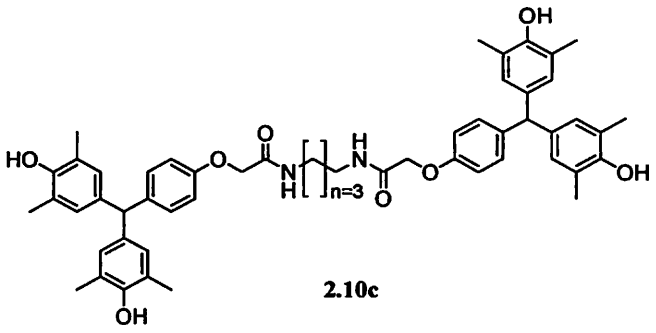

2.10c

Red solid (Yield 31.0%); ES-MS [M+Na$^+$]: 887.4

IR (cm^{-1}, KBr): 3400, 3122, 2902, 1651, 1633, 1529, 1482, 1134

^{1}H NMR ($CDCl_3$, 400MHz): 8.02 (2H,bs), 7.07 (4H, d, J=8.0Hz), 6.82 (4H, d, J=8.0Hz), 6.51 (8H, s), 5.11 (2H,s), 4.81 (4H, bs), 3.82 (4H, s), 3.11 (4H, m), 2.09 (24H, s), 1.42 (4H, m)

^{13}C NMR ($CDCl_3$, 100MHz): 168.3, 161.5, 150.8, 139.7, 136.4, 131.3, 131.0, 130.5, 130.1, 129.4, 123.1, 115.3, 114.6, 114.3, 60.3, 54.6, 35.6, 21.0, 16.3, 16.0

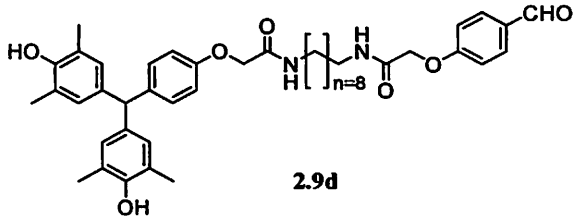

2.9d

Red solid (Yield 8.0%); ES-MS [M$^+$]: 708.4

IR (cm^{-1}, KBr): 3341, 2940, 1683, 1666, 1507, 1481, 1210,1142

^{1}H NMR ($CDCl_3$, 400MHz): 9.96 (1H, s), 7.84 (2H, d, J=8.0Hz), 7.04 (4H, d, J=8.0Hz), 6.81 (2H, d, J=8.0Hz), 6.75 (1H, bs), 6.57 (1H, bs), 5.24 (1H, s), 4.58 (2H, s), 4.53 (2H, s), 3.35 (4H, qn, J=8.4Hz), 2.20 (12H, s), 1.51 (4H, m), 1.26 (10H, bm)

^{13}C NMR ($CDCl_3$, 100MHz): 190.9, 168.5, 162.0, 155.6, 150.8, 139.0, 136.4, 132.4, 131.3, 130.8, 130.7, 129.9, 129.5, 123.1, 115.2, 114.6, 114.5, 67.7, 67.5, 54.8, 39.9, 39.2, 27.7, 29.5, 29.3, 26.9, 16.3

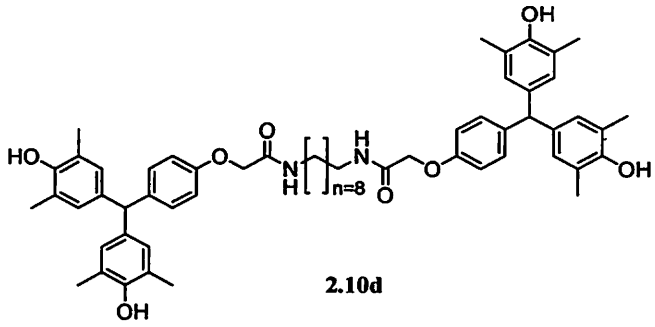

2.10d

Pale yellow solid (Yield 56%), ES-MS [M^+]: 935.2

IR (cm^{-1}, KBr): 3421, 2918, 1670, 1504, 1486, 1210, 1149

^1H NMR ($CDCl_3$, 400MHz): 7.28 (4H, s), 7.05 (4H, d, J=8.8Hz), 6.84 (4H, d, J=8.8Hz), 6.77 (1H, s), 6.69 (8H,s), 5.26 (2H, s), 4.63 (4H, bs), 3.33 (4H, q, J=6.8 Hz), 4.48 (4H, s), 2.19 (24H, s), 1.52 (4H, m), 1.30 (10H, m)

^{13}C NMR ($CDCl_3$, 100MHz): 164.6, 150.5, 135.9,129.3, 122.8, 114.3, 67.5, 54.6, 39, 29.5, 29.3,29.1, 26.7, 16.4, 16.0

Preparation of 2-bromo-N-[2-(2-bromoacetylamino) cyclohexyl] acetamide (**2.11**)

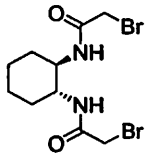

2.11

1,2-Trans-cyclohexane diamine (1.14g, 10mmol) was dissolved in dichloromethane (10ml) and added dropwise under ice-cold conditions to a stirred solution of bromoacetyl bromide (4.05g, 20.1mmol) in dichloromethane (10ml) over a period of 30mins followed by triethylamine (2.08g, 20.6mmol). The reaction mixture in dichloromethane was washed $NaHCO_3$ (5% aq. solution), and water, and extracted. The organic layer was then dried over anhydrous $MgSO_4$; removal of the solvent gave the product **2.11** as white solid (Yield 48%). FAB-MS [M^+]: 357

IR (cm^{-1}, KBr): 2943, 1661, 1504, 1216, 1007

^1H NMR ($CDCl_3$, 400MHz): 6.89 (2H, bs), 3.82 (4H, s), 3.73 (2H, m), 2.11 (2H, m), 1.80 (2H, bm), 1.36 (4H, m)

^{13}C NMR ($CDCl_3$, 100MHz): 169.4, 166.7, 54.0, 31.9, 28.9, 26.0, 24.6

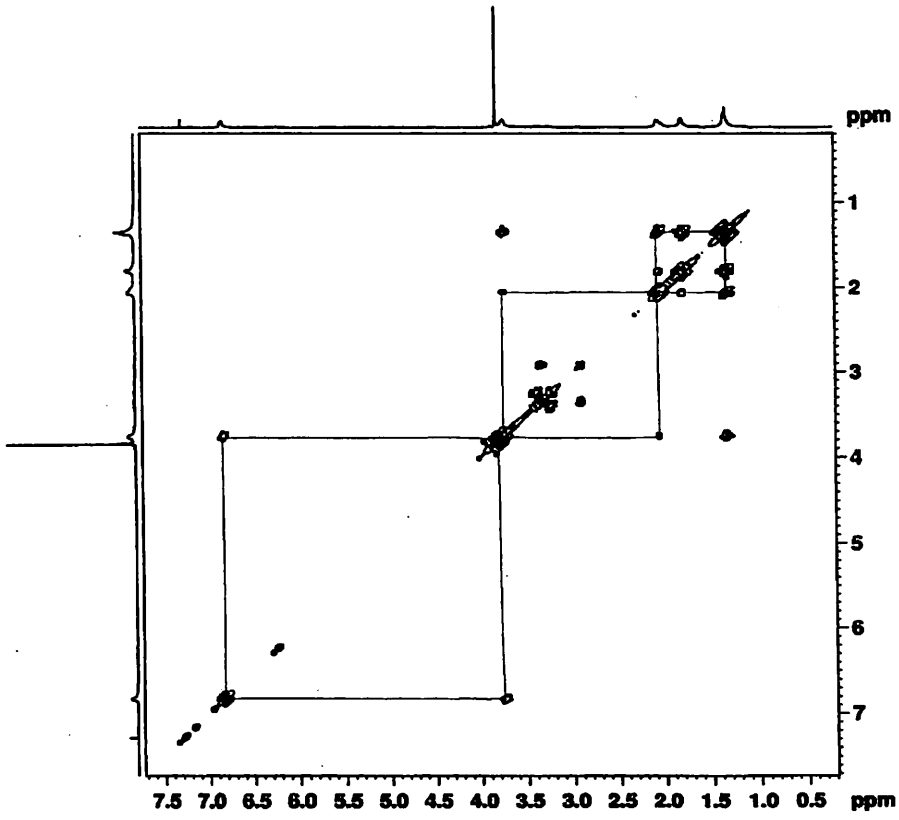

Fig.89 Proton HOMOCOSY of **2.11** in $CDCl_3$

Preparation of: 2-(4-formylphenoxy)-N-{2-[2-(4-formylphenoxy)acetylamino] cyclohexyl} acetamide (**2.12**):

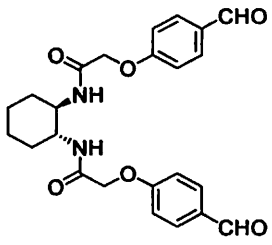

2.12

4-Hydroxybenzaldehyde (0.25g, 2.05mmol), anhydrous K_2CO_3 (0.29g, 2.1mmol) and **2.11** (0.355g, 1mmol) were added into a round bottom flask containing dry acetonitrile (20ml) under a stream of dry nitrogen. This reaction mixture was stirred at 80-82°C for 30hrs and then the solvent removed in vacuo. The residue was dissolved in dichloromethane (2×20ml), and the soluble organic fraction washed with aqueous Na_2CO_3 (5% solution), and with water. The organic extracts were dried over anhydrous Na_2SO_4 and removal of the solvent gave the

bis-aldehyde as a pale yellow compound. The yellow crude product was purified by column chromatography (over silica gel) with ethyl acetate as the eluent to obtain a white compound (Yield 64%). FAB-MS [M^+]: 438

IR (cm^{-1}, KBr): 3114, 2916, 2858,1685, 1650, 1522, 1232

^1H NMR ($CDCl_3$, 400MHz): 9.80 (2H, s), 7.74 (4H, d, J= 8.8Hz), 6.95 (4H, d, J= 8.8Hz), 6.81 (2H, bs), 4.43 (2H, d, J= 14.8Hz), 4.21 (2H, d, J= 14.8Hz), 3.75 (2H, m), 2.12 (2H, m), 1.73 (2H, m), 1.28 (4H, m)

^{13}C NMR ($CDCl_3$, 100MHz): 190.5, 167.8, 161.8, 132.0, 131.1, 115.0, 67.1, 53.4, 32.1, 24.5

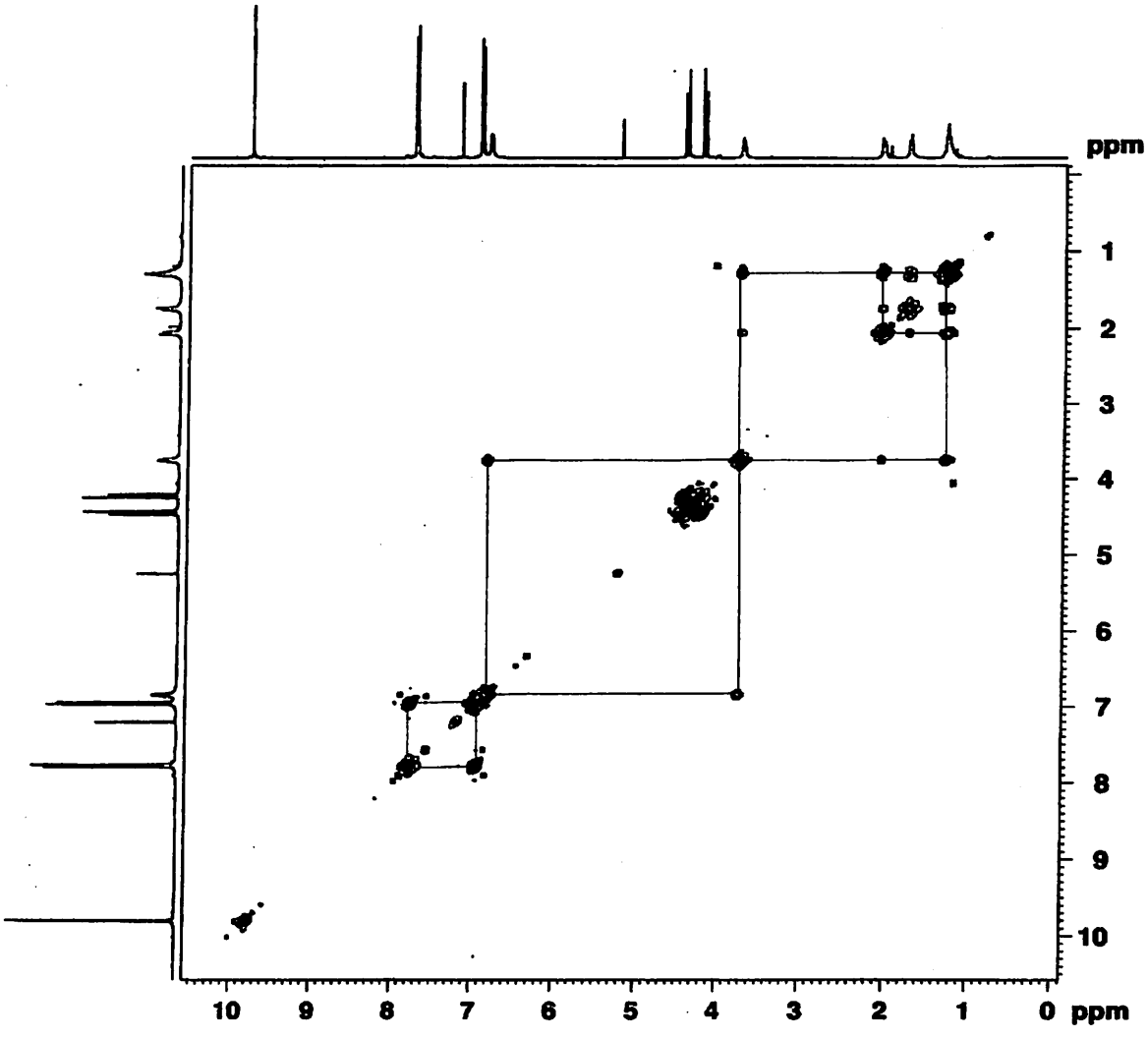

Fig.90 ^1H HOMOCOSY spectrum of **2.12** in $CDCl_3$

Synthesis of dimeric bis-phenol, **2.13**:

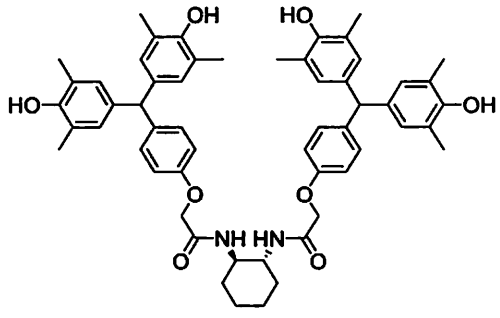

2.13

Bis-aldehyde, **2.12** (0.27g, 0.62mmol) and 2,6-dimethylphenol (0.31g, 2.5mmol) were dissolved in acetic acid (5ml) and the solution was cooled in melting ice (0-5°C). To this cold solution a mixture of acetic acid and sulphuric acid (10ml, 7:3) was added dropwise over a period of 20mins. After the acids were added, the solution was kept at 0°C for 72hrs and then diluted with distilled water (20ml). The pink solid obtained was filtered and washed free from acid and dried. Purification by column chromatography over silica gel using ethyl acetate: chloroform 1:1 as eluent gave **2.13** as a red solid (Yield 48%). ES-MS [$M+Na^+$]: 913.1

IR (cm^{-1}, KBr): 3406, 2930, 1660, 1516, 1474, 1219, 1023

^1H NMR ($CDCl_3$, 400MHz): 6.96 (4H, d, J=8.4Hz), 6.90 (2H, bs), 6.74 (4H, d, J=8.4Hz), 6.65 (8H, s), 5.25 (2H,s), 4.36 (2H, d, J=14.8Hz), 4.24 (2H, d, J=14.8Hz), 3.80 (4H, bs), 2.17 (24H, s), 1.81 (4H, m), 1.38 (4H, m)

^{13}C NMR ($CDCl_3$, 100MHz): 167.6, 163.0, 161.2, 141.2, 137.5, 133.1, 132.0, 131.0, 115.6, 67.2, 53.5, 31.1, 24.5, 16.4

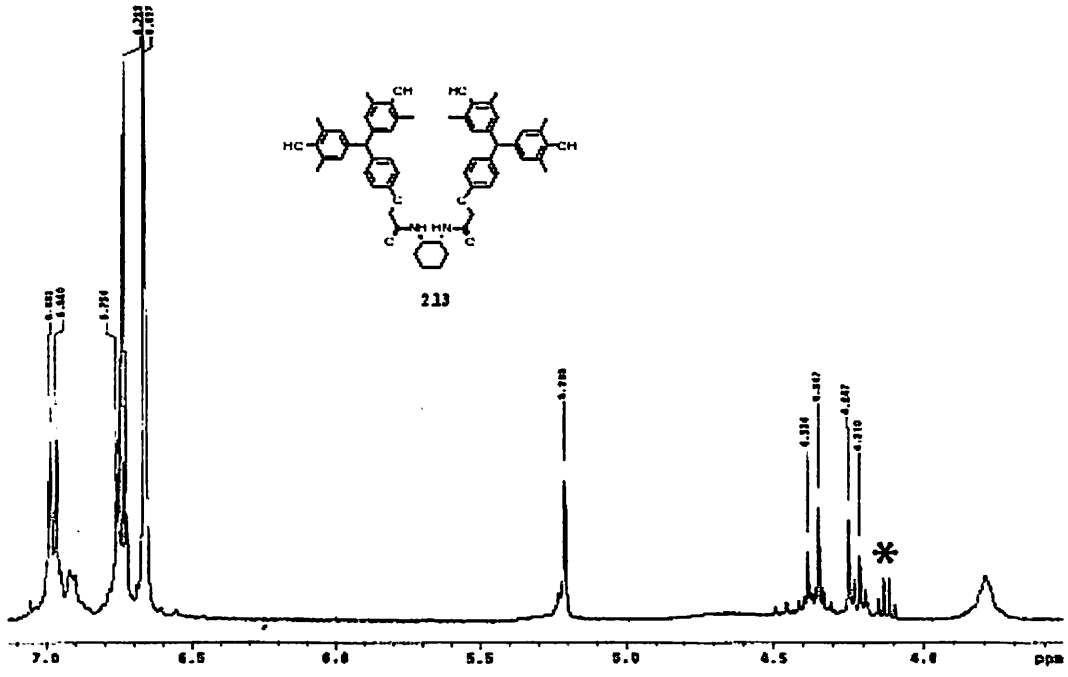

Fig.91 ^{1}H NMR spectrum of **2.13** in $CDCl_3$. (* signals due to residual ethyl acetate)

Synthesis of **2.14a** and **2.14b** from **2.2q**:

In a yypical procedure the amino bis-phenol (0.345g, 1.0mmol) was dissolved in dry dichloromethane (5ml) and stirred in ice-cold condition (0°C). Benzoyl chloride (0.142g, 1.0mmol) was added in small portions to the amine with constant stirring. Subsequently pyridine in dry ether was added dropwise to the cooled solution under a stream of dry nitrogen gas. This solution was stirred for 24hrs under nitrogen atmosphere. The amide precipitates out of the solution, which was filtered and the residue washed with ether (2×10ml). This residue was then stirred with dichloromethane and filtered (2×10ml). The product was obtained as a pale yellow solid after re-crystallization from warm methanol.

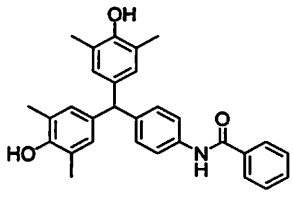

2.14a

Yellow solid (Yield 76%). ES-MS [M^+]: 451.4

IR (cm^{-1}, KBr): 3441, 2943, 2862, 1673, 1645, 1457, 1211, 1126

^{1}H NMR (DMSO-d^6, 400MHz): 9.76 (1H, s), 7.66 (2H, d, J=6.0Hz), 7.41 (2H, d, J=6.4Hz), 7.27 (1H, m), 7.18 (2H, t, J= 6.0Hz), 6.80(2H, d, J=6.4Hz), 6.39 (4H, s), 5.00 (1H, s), 3.45 (2H, bs), 1.9 (12H, s).

^{13}C NMR (DMSO-d^6, 100MHz): 166.8, 151.4, 140.6, 136.8, 135.5, 135.2, 131.7, 129.7, 128.5, 127.9, 123.9, 120.2, 54.6, 17.3.

The **2.14b** was prepared in a procedure similar to **2.14a**.

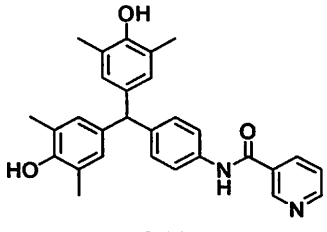

2.14b

Yellow solid (Yield 61%). ES-MS [M^+]: 451.4

IR (cm^{-1}, KBr): 3422, 2930, 2862, 1682, 1646, 1457, 1204, 1139

^{1}H NMR (DMSO-d^6, 400MHz): 9.76 (1H, s), 7.66 (2H, d, J=6.0Hz), 7.41 (2H, d, J=6.4Hz), 7.27 (1H, m), 7.18 (2H, t, J= 6.0Hz), 6.80 (2H, d, J=6.4Hz), 6.39 (4H,s), 5.00 (1H, s), 3.45 (2H, bs), 1.9 (12H, s).

^{13}C NMR (DMSO-d^6, 100MHz): 152.4, 151.9, 148.8, 138.1, 137.2, 137.0, 130.8, 130.3, 125.4, 125.2, 122.0, 56.3, 16.8

Preparation of **2.15a and 2.15b** from **2.2q**:

Bis-(3,5-dimethyl-4-hydroxyphenyl)(4-aminophenyl)methane, **2.2q** (0.346g, 1mmol) was dissolved in dry diethyl ether (15ml) and the solution cooled in ice. Isophthaloyl chloride (0.100g, 0.5mmol) was added to this solution in small portions over 1hr with continuous stirring. To this solution dry pyridine (0.160g, 2mmol) was added dropwise as a solution in ether and stirred overnight. Ther ether was removed and the residue washed with cold water and dried in vacuum. Subsequently the compound is re-dissolved in cold dichloromethane and the residue collected after filtration to obtain the desired compound **2.15a**. No further purification was required as the other compounds could be washed with dichloromethane.

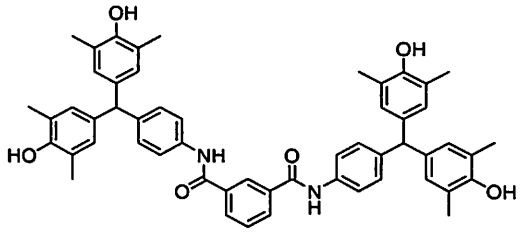

2.15a

(Yield 38%).Red solid (m.p. 142°C, decomp.); ES-MS [M^+]: 825

IR (cm^{-1}, KBr): 3370, 2922, 1648, 1713, 1517, 1404, 1319,1118

^1H NMR ($CDCl_3$, 400MHz): 10.15 (1H, s, amide NH), 8.50 (1H, s, Ar-H), 8.05 (2H, d, Ar-H, J=7.6Hz), 7.96 (1H, s, amide NH) 7.80-7.71 (4H, b, Ar-OH), 7.62 (4H, d, Ar-H, J=8.0Hz), 7.53 (1H, t, Ar-H, 7.6Hz), 6.98 (4H, d, Ar-H, J=8.0Hz), 6.57 (8H, s, Ar-H), 5.16 (2H, s, C-H), 2.07 (24H, s, Ar-CH_3).

^{13}C NMR ($CDCl_3$, 100MHz): 173.2, 169.9, 154.2, 141.5, 138.6, 137.0, 134.7,129.1, 128.8, 128.5, 123.6, 119.9, 59.5, 16.5.

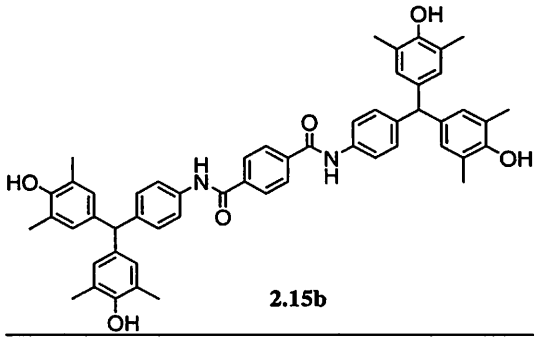

2.15b

Bis-(3,5-dimethyl-4-hydroxyphenyl)(4-aminophenyl)methane, **2.2q** (0.346g, 1mmol) was dissolved in dry diethyl ether (15ml) and the solution was cooled in ice (0°C). The

terephthaloyl chloride (0.100g, 0.5mmol) was added to the amine solution in small portions over a period of 1hr with continuous stirring. To this solution dry pyridine (0.160g, 2mmol) was added dropwise as a solution in ether and stirred overnight. Ther ether was removed and the residue washed with cold water and dried in vacuum. Subsequently the crude compound was re-dissolved in cold dichloromethane and the residue collected after filtration. Since the compound is only partially soluble in dichloromethane, the unreacted materials could easily be removed by washing with dichloromethane which gave the pure product, **2.15b**.

(Yield 54%);Yellow solid (m.p. 170°C, decomp.); ES-MS [M^+]: 825

IR (cm^{-1}, KBr): 3348, 2936, 2867, 1735, 1656, 1596, 1530, 1487, 1298, 1149

^{1}H NMR (DMSO-d^6, 400MHz): 10.34 (2H, s), 8.06 (4H, s), 8.04 (4H, s), 7.67 (4H, d, J=6.8Hz), 7.52 (4H, d, J=6.8Hz), 6.62 (8H, s), 5.20 (2H, s), 2.08 (24H, s).

^{13}C NMR (DMSO-d^6, 100MHz): 170.3, 164.6, 151.2, 140.7, 137.4, 136.6, 134.9, 129.0, 128.6, 127.6, 123.7, 120.3, 54.2.

Table 7.3

Bis-phenols (**2.1**)	Yield of **2.1** (%)*		
	Procedure **I**	Procedure **II**	Procedure **III**
2.1a	b	66	b
2.1b	b	62	b
2.1c	b	71	b
2.1d	b	50	b
2.1e	b	56	a

*Isolated yields; [a] reactions not performed; [b] reactions failed

Table 7.4			
Bis-phenols (2.2)	Yields of 2.2 (%)*		
	Procedure I	Procedure II	Procedure III
2.2a	72	72	a
2.2b	78	81	a
2.2c	63	70	a
2.2d	77	64	a
2.2e	65	80	a
2.2f	b	82	42
2.2g	b	76	66
2.2h	b	32	55
2.2i	b	46	68
2.2j	59	40	b
2.2k	78	64	b
2.2l	88	80	b
2.2m	65	71	b
2.2n	76	74	b
2.2o	b	b	82
2.2p	b	b	75

*Isolated yields; [a] reactions not performed; [b] reactions failed

7.11 Synthesis of Dibenzo[a,j] xanthenes

The dibenzoxanthenes **4.1** were prepared by condensing 2-naphthol with a few aromatic aldehydes in a simple one-pot strategy according to the following procedure:

In a typical reaction, 2-Naphthol (2.9g, 0.02mol) and benzaldehyde (1.1g, 0.01mol) were dissolved in glacial acetic acid (10 ml). The solution was stirred to dissolve the compounds and then cooled in ice. To this stirred solution, acetic acid and sulphuric acid (4:1 mixture, 15 ml) was added dropwise over 30 min. The reaction mixture was kept in an ice bath for 72h and then warmed on a water bath to about 60°C for about 1 h. After dilution of the reaction mixture with 1:1 acetic acid/water (10ml), the solid precipitate was filtered. This solid was washed free of the acid with warm water. Recrystallization from warm toluene gave the compound as colourless solid.

Analytical and spectroscopic data of **4.1**

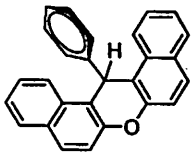

4.1a

Colorless solid (Yield 72%); FAB-MS [M^+]: 358

IR (cm^{-1}, KBr): 3073, 1593, 1460, 1255, 1081, 968

^1H NMR ($CDCl_3$, 400MHz): 8.41 (2H, d, J= 8.4Hz), 7.84-7.78 (4H, m), 7.60-7.48 (6H, m), 7.43-7.39 (2H, t, J=7.5Hz), 7.17-7.13 (2H, t, J=7.5Hz), 7.01-6.97 (1H, t, J=7.5Hz), 6.49 (1H, s)

^{13}C NMR ($CDCl_3$, 100MHz): 148.8, 145.0, 131.5, 131.1, 128.5, 126.5, 126.8, 126.4, 124.2, 122.7, 118.0, 117.4, 38.1

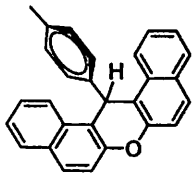

4.1b

Colorless solid (Yield 77%); FAB -MS [M^+]: 372

IR (cm^{-1}, KBr): 3421, 3077, 2918, 1594, 1506, 1459, 1239

^1H NMR ($CDCl_3$, 400MHz): 8.45 (2H, d, J=8.46 Hz), 7.85-7.75 (4H, m), 7.6 (2H, t, J=8.5Hz), 7.55 (2H,d, J=8.5Hz), 7.4 (4H, m), 7.0 (2H, d, J=8.5Hz), 6.5 (1H, s), 2.15 (3H, s)

^{13}C NMR ($CDCl_3$, 100MHz):148.0, 145.2, 139.7, 136.1, 131.3, 129.9, 128.5, 124.8, 122.6, 121.7, 117.8, 117.0, 33.7, 21.3

Pale yellow solid (Yield 70%); FAB -MS [M^+]: 403

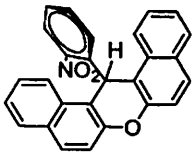

4.1c

IR (cm^{-1}, KBr): 3436, 2926, 1596, 1521, 1456, 1348, 1251

^1H NMR ($CDCl_3$, 400MHz): 8.44 (2H, d, J=8.4Hz), 8.11 (8H, m), 7.70 (4H, m), 7.48 (2H, t, J=7.6Hz), 6.90 (1H, s)

^{13}C NMR ($CDCl_3$, 100MHz): 152.8, 147.8, 145.0,130.4, 129.8, 129.5, 129.2, 127.8, 124.1, 123.7, 118.0, 116.9, 36.9

Purple crystals (Yield 90%); FAB -MS [M^+]: 437

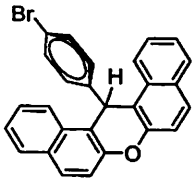

4.1d

IR (cm^{-1}, KBr): 2924, 1594, 1462, 1402, 1240, 1075, 1010

^1H NMR ($CDCl_3$, 400MHz): 8.32 (2H, d, J=8.45), 7.79 (4H, m), 7.6-7.56 (2H, dd J=7.6, 1.2Hz), 7.49-7.38 (6H, m), 7.26 (2H, m), 6.45 (1H, s)

^{13}C NMR ($CDCl_3$, 100MHz): 144.8, 144.0, 131.6, 131.1, 129.9, 129.1, 128.9, 126.9, 124.4, 122.4, 120.3, 118.0, 116.7, 37.5

Pale yellow solid (Yield 60%); FAB -MS [M^+]: 403

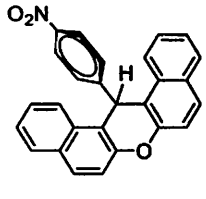

4.1e

IR (cm^{-1}, KBr): 2930, 1594, 1517, 1343, 1241

^1H NMR (DMSO-d^6, 400MHz): 8.71 (2H, d, J=8.46 Hz), 8.03-7.91 (8H, m), 7.67-7.59 (4H, m), 7.50-7.46 (2H, m), 6.93 (1H, s)

^{13}C NMR (DMSO-d^6, 100MHz): 152.6, 148.1, 145.9, 130.8, 130.7, 129.6, 128.7, 127.2, 124.7, 123.6, 123.1, 117.7, 116.2, 36.4

White solid (Yield 56%); FAB -MS [M^+]: 392

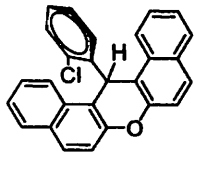

4.1f

IR (cm^{-1}, KBr): 3073, 1691, 1591, 1397, 1240, 1160

^1H NMR ($CDCl_3$, 400MHz): 8.48 (2H, d, J=8.48 Hz), 7.98-7.80 (6H, m); 7.71-7.46, (8H, m), 6.86 (1H, s)

^{13}C NMR ($CDCl_3$, 100MHz): 179.4, 157.0, 153.3, 139.5, 136.2, 135.4, 134.9, 130.1, 128.4, 122.3, 121.1, 30.5

7.12 Preparation of Diaryl Quinone Methides, 5.1

Procedure for synthesis of 5.1a

In a typical experiment, the bis-phenol **2.2a** (1.65g, 5mmol) is dissolved in acetonitrile (10ml) and a solution of ammonium persulphate (1.17g, 5.2mmol) in 5ml of water was added. The mixture was kept at 60°C for 6hrs. The crude mixture on cooling gave 4-[(4'-hydroxy-3',5'-dimethylphenyl)(phenyl)methylene]-2,6-dimethyl-cyclohexa-2,5-dien-1-one (**5.1a**) as red crystals.

The other diaryl quinone methides **5.1b -5.1e** were prepared by similar procedure to that of **5.1a** .

Analytical and spectroscopic data of **5.1**

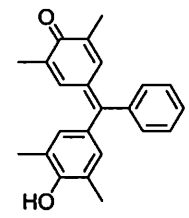

5.1a

Purple solid (Yield 43%; m.p.247-248 °C, decomp); ES-MS [M^+]: 330.3

IR (cm^{-1}, KBr): 3440, 2919, 1567, 1475, 1332, 1198, 1050

^{1}H NMR ($CDCl_3$, 400MHz): 7.43 (3H, m), 7.22 (4H, m), 7.07 (1H, s), 6.80 (1H, s), 4.94 (1H, s), 2.28 (6H, s), 2.03 (3H, s), 2.00 (3H, s)

^{13}C NMR ($CDCl_3$, 100MHz): 183.7, 153.9, 141.0, 136.1, 135.9, 135.1, 132.9, 132.2, 129.3, 127.9, 122.8, 16.8, 15.8

Elemental Anal. Calcd. for $C_{22}H_{22}O_2$: C 83.60 %, H 7.61% Found: C 83.58 %, H 7.60%

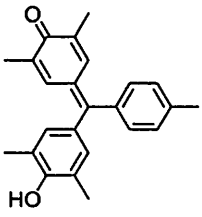

5.1b

Purple solid (Yield 37%; m.p. 261°C decomp); ES-MS [M^+]: 344.4

IR (cm^{-1}, KBr): 3218, 2912, 1603, 1562, 1476, 1296, 1240, 1189

^{1}H NMR (DMSO-d^6, 400MHz): 8.92 (1H, bs), 7.29 (2H, d, J=8.0Hz), 7.09 (2H, d, J=8.0Hz), 6.93 (4H, bs), 2.39 (3H, s), 2.06 (12H, bs)

^{13}C NMR (DMSO-d^6, 100MHz): 158.6, 139.6, 137.6, 136-133 (b), 131.9, 128.8, 20.9, 16.5

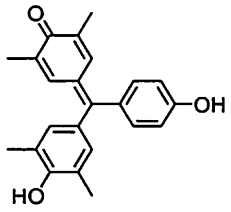 **5.1c**	Purple crystals (Yield 40%; m.p. 202°C); ES-MS [M^+]: 346.2 IR (cm^{-1}, KBr): 3450, 2922, 1624, 1595, 1542, 1478, 1328, 1141, 1045 ^{1}H NMR (DMSO-d^6, 400MHz): 10.02 (1H, bs), 7.01 (2H, d, J= 8.8Hz), 6.92 (4H, s), 6.83 (2H, d, J= 8.8Hz), 2.03 (12H, bs) ^{13}C NMR (DMSO-d^6, 100MHz): 159.6, 134.3, 131.7, 129.5, 128.4, 123.1, 115.1,114.4, 16.5 Elemental analysis calcd. for $C_{24}H_{24}O_3$ C, 80.0; H, 6.67 found C, 79.97; H, 6.62.
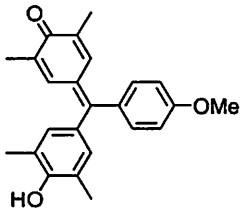 **5.1d**	Red crystals (Yield 53%; m.p. 230-233°C decomp.); ES-MS [M^+]: 360.1 IR (cm^{-1}, KBr): 3300, 2914, 1600, 1592, 1460, 1265, 1182, 1140 ^{1}H NMR (DMSO-d^6, 400MHz): 7.07 (4H, d, J=8.8Hz), 6.91 (2H, d, J=8.8Hz), 6.60 (2H, s), 3.85 (3H, s), 2.08 (12H, s) ^{13}C NMR (DMSO-d^6, 100MHz): 160.7, 158.7, 133.9, 132.6, 128.6, 113.8, 55.3, 16.6, 16.5
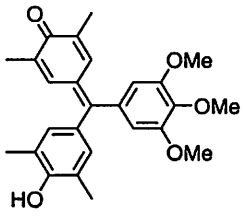 **5.1e**	Red needles (Yield 70%; m.p. 256°C decomp.); ES-MS [M^+]: 420.2 IR (cm^{-1}, KBr): 3428, 2944, 1618, 1562, 1468, 1330, 1127, 1028 ^{1}H NMR ($CDCl_3$, 400MHz): 6.94 (4H, s), 6.35 (2H, s), 3.89 (3H, s), 3.73 (6H, s), 2.09 (12H, s) ^{13}C NMR ($CDCl_3$, 100MHz): 152.6, 13.3, 134.6, 110.1, 61.0, 56.3, 16.3

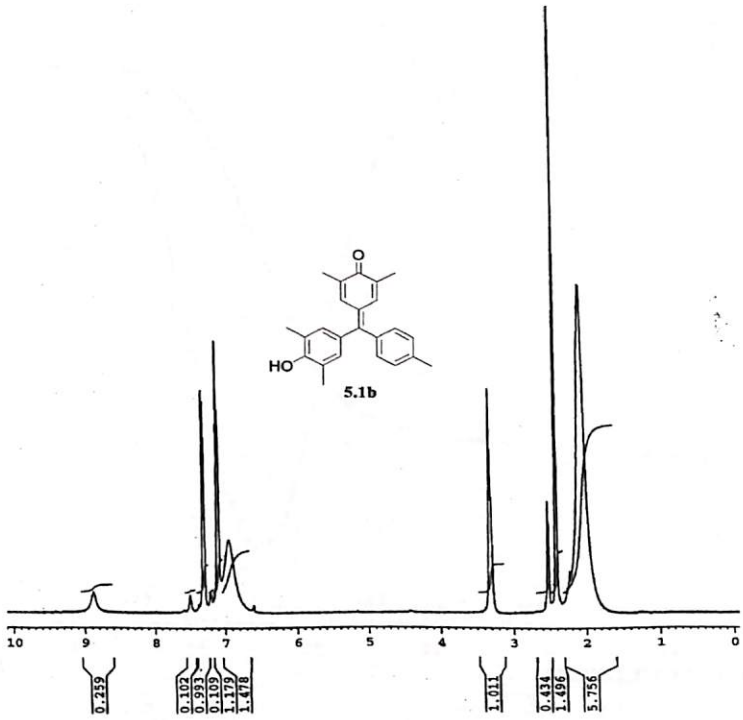

Fig.92 ^{1}H NMR spectrum of **5.1b** in dimethylsulfoxide-d^{6}

Thermogravimetry of the inclusion compounds

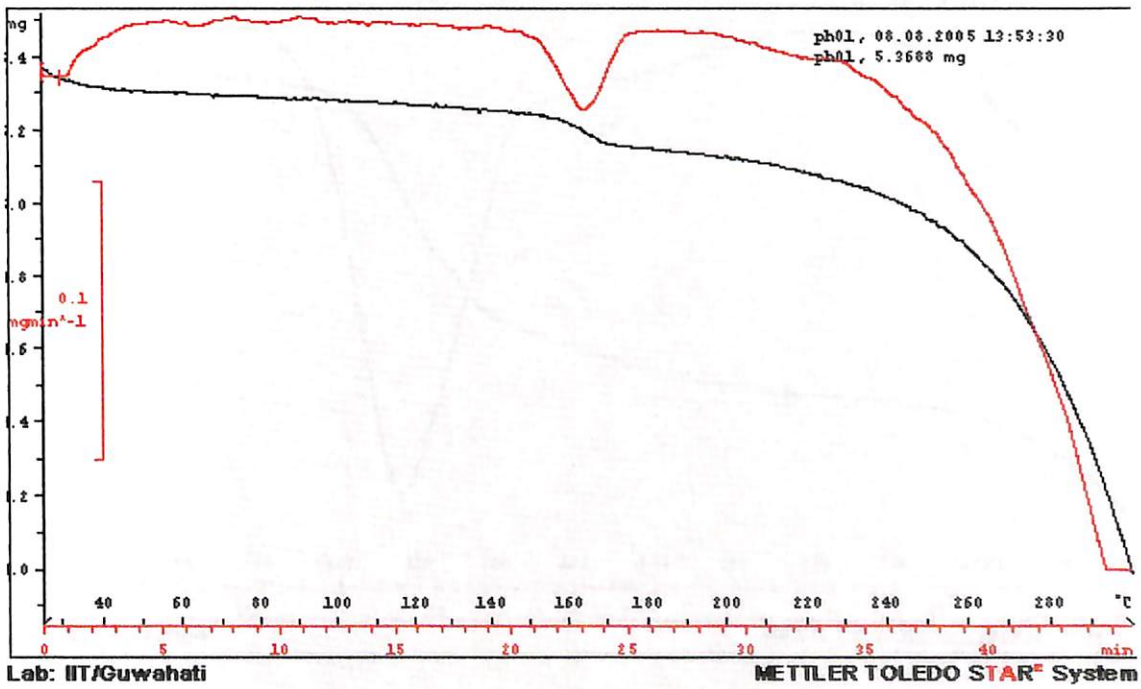

Fig.93 Thermograms and differential thermogram obtained from of the crystals of **2.2a**–water which shows loss of water occurs between 160-165°C

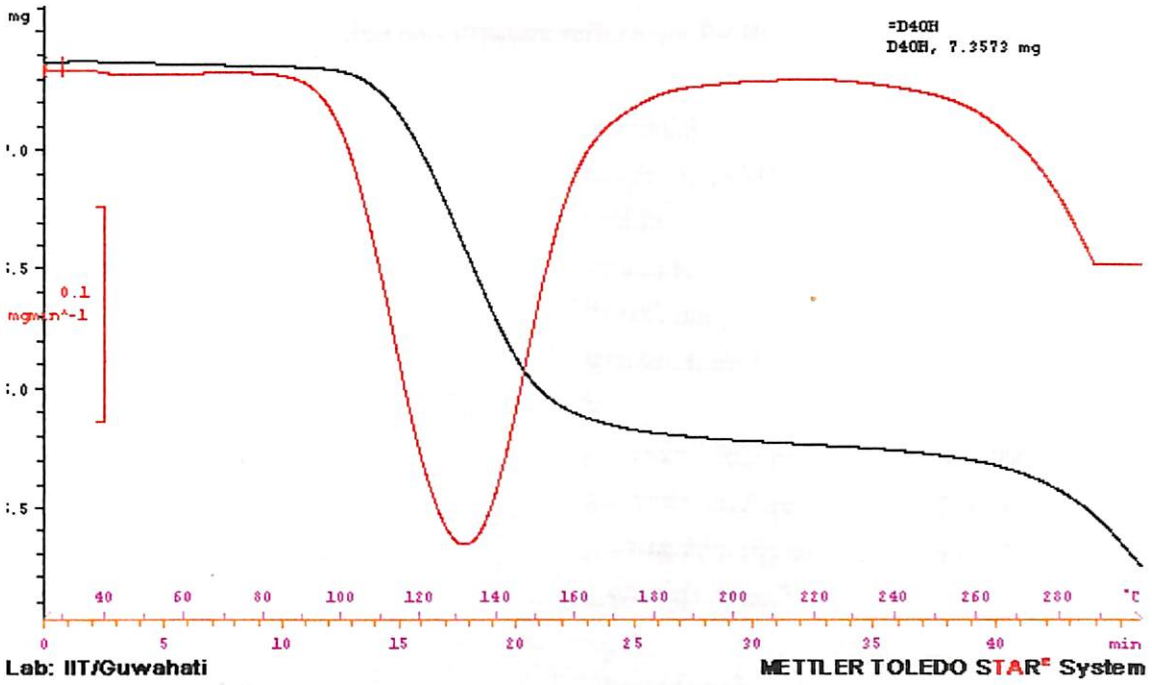

Fig.94 Thermogram of crystals of **2.2d**–toluene which shows loss of the solvent occurs between 130-133°C

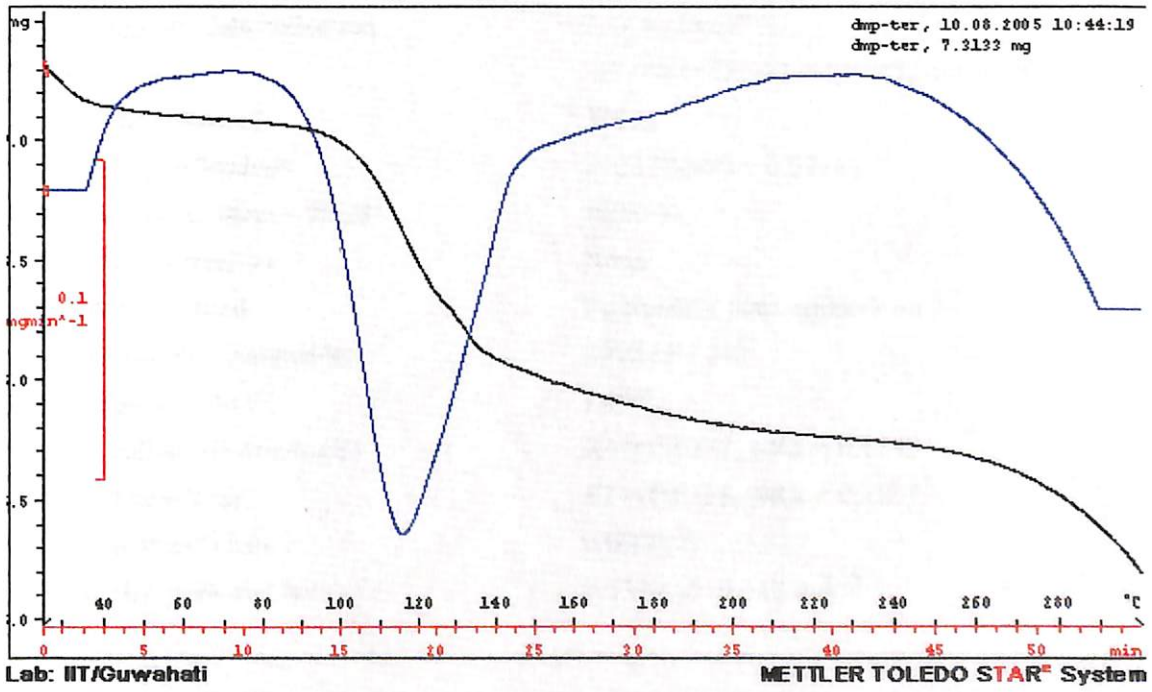

Fig.95 Thermograms and differential thermogram of the crystals of **2.2h**–benzene compound which shows loss of benzene molecules occurs between 115-120°C

Table 7.5 Crystallographic data and structure refinement for Bis(4-hydroxyphenyl)(phenyl) methane (**2.1a**) –water

Identification code	jbb05029	
Empirical formula	$C_{19}\ H_{15}\ O_2.\ H_2O$	
Formula weight	275.31	
Temperature	296(2) K	
Wavelength	71.073 pm	
Crystal system	Rhombohedral	
Space group	R-3	
Unit cell dimensions	a = 3587.33(2) pm	α = 90°.
	b = 3587.33(2) pm	β = 90°.
	c = 610.870(10) pm	γ = 120°.
Volume	6.80804(12) nm^3	
Z	18	
Density (calculated)	1.209 Mg/m^3	
Absorption coefficient	0.077 mm^{-1}	
F(000)	2610	
Crystal size	0.53 x 0.36 x 0.31 mm^3	
Theta range for data collection	1.14 to 28.28°	
Index ranges	-47<=h<=47, -47<=k<=47, -8<=l<=7	
Reflections collected	39812	
Independent reflections	3762 [R(int) = 0.0218]	
Completeness to theta = 28.28°	100.0 %	
Absorption correction	None	
Refinement method	Full-matrix least-squares on F^2	
Data / restraints / parameters	3762 / 0 / 213	
Goodness-of-fit on F^2	1.037	
Final R indices [I>2sigma(I)]	R1 = 0.0572, wR2 = 0.1643	
R indices (all data)	R1 = 0.0751, wR2 = 0.1841	
Extinction coefficient	0.0000(2)	
Largest diff. peak and hole	0.333 and -0.342 $e.Å^{-3}$	

Table 7.6 Crystallographic data and structure refinement for Bis(4-hydroxy-3,5-dimethyl phenyl) (phenyl) methane **(2.2a)**

Identification code	03srv019	
Empirical formula	C_{23} H_{24} O_2	
Formula weight	332.42	
Temperature	120(2) K	
Wavelength	0.71073 Å	
Crystal system	Monoclinic	
Space group	P 21/c	
Unit cell dimensions	a = 19.1236(11) Å	α = 90°.
	b = 5.3707(3) Å	β = 116.185(2)°.
	c = 19.2054(12) Å	γ = 90°.
Volume	1770.10(18) $Å^3$	
Z	4	
Density (calculated)	1.247 Mg/m^3	
Absorption coefficient	0.078 mm^{-1}	
F(000)	712	
Crystal size	0.42 x 0.18 x 0.08 mm^3	
Theta range for data collection	1.19 to 30.49°	
Index ranges	-26<=h<=25, -7<=k<=7, -27<=l<=26	
Reflections collected	20395	
Independent reflections	5023 [R(int) = 0.0413]	
Completeness to theta = 30.49°	93.0 %	
Absorption correction	None	
Refinement method	Full-matrix least-squares on F^2	
Data / restraints / parameters	5023 / 0 / 322	
Goodness-of-fit on F^2	1.042	
Final R indices [I>2sigma(I)]	R1 = 0.0453, wR2 = 0.1074	
R indices (all data)	R1 = 0.0727, wR2 = 0.1175	
Largest diff. peak and hole	0.314 and -0.182 $e.Å^{-3}$	

Table 7.7 Crystallographic data and structure refinement for Bis(4-hydroxy-3,5-dimethylphenyl)(4-methoxyphenyl)methane (**2.2c**)

Identification code	03srv019	
Empirical formula	$C_{24}H_{26}O_3$	
Formula weight	362.45	
Temperature	296(2) K	
Wavelength	0.71073 Å	
Crystal system	Triclinic	
Space group	P-1	
Unit cell dimensions	a = 9.771(3) Å	α = 99.62(3)°.
	b = 10.467(6) Å	β = 101.62(4) °.
	c = 11.703(7) Å	γ = 117.14(3)°.
Volume	996.2(9) $Å^3$	
Z	2	
Density (calculated)	1.208 Mg/m^3	
Absorption coefficient	0.078 mm^{-1}	
F(000)	388	
Crystal size	0.40 x 0.51 x 0.28 mm^3	
Theta range for data collection	1.86 to 25.00°	
Index ranges	-11<=h<=11, -12<=k<=12, 0<=l<=13	
Reflections collected	3515	
Independent reflections	2676 [R(int) = 0.0252]	
Completeness to theta = 30.49°	89.0 %	
Absorption correction	None	
Refinement method	Full-matrix least-squares on F^2	
Data / restraints / parameters	3515 / 0 / 349	
Goodness-of-fit on F^2	0.932	
Final R indices [I>2sigma(I)]	R1 = 0.0485, wR2 = 0.0718	
R indices (all data)	R1 = 0.1172, wR2 = 0.1406	
Largest diff. peak and hole	0.254 and -0.162 $e.Å^{-3}$	

Table 7.8 Crystallographic data and structure refinement for [Bis(4-hydroxy-3,5-dimethyl phenyl)(4-hydroxyphenyl)]methane (**2.2d**)-Toluene.

Identification code	jbb00105_0m	
Empirical formula	$C_{23}\ H_{24}\ O_3.\ C_7\ H_8$	
Formula weight	440.57	
Temperature	296(2) K	
Wavelength	71.073 pm	
Crystal system	Triclinic	
Space group	P-1	
Unit cell dimensions	a = 969.2 pm	α = 112.155(3)°.
	b = 1173.9 pm	β = 101.102(4)°.
	c = 1210.4 pm	γ = 91.062(4)°.
Volume	1.2453 nm^3	
Z	3	
Density (calculated)	1.394 Mg/m^3	
Absorption coefficient	0.091 mm^{-1}	
F(000)	558	
Crystal size	0.29 x 0.25 x 0.24 mm^3	
Theta range for data collection	4.09 to 26.75°	
Index ranges	-9<=h<=11, -14<=k<=14, -15<=l<=15	
Reflections collected	7748	
Independent reflections	4364 [R(int) = 0.0128]	
Completeness to theta = 26.75°	82.2 %	
Absorption correction	None	
Refinement method	Full-matrix least-squares on F^2	
Data / restraints / parameters	4364 / 0 / 328	
Goodness-of-fit on F^2	1.041	
Final R indices [I>2sigma(I)]	R1 = 0.0646, wR2 = 0.1873	
R indices (all data)	R1 = 0.0788, wR2 = 0.2042	
Extinction coefficient	0.004(6)	
Largest diff. peak and hole	0.426 and -0.315 $e.Å^{-3}$	

Table 7.9 Crystallographic data and structure refinement for Bis(4-hydroxy-3,5-dimethyl phenyl)(4-nitrophenyl)methane **(2.2f)** -benzene adduct

Identification code	d4no2_0m	
Empirical formula	$C_{23}\ H_{23}\ N\ O_4.\ C_6\ H_6$	
Formula weight	456.52	
Temperature	296(2) K	
Wavelength	71.073 pm	
Crystal system	Monoclinic	
Space group	P2(1)/n	
Unit cell dimensions	a = 1211.01(4) pm	$\alpha = 90°$
	b = 981.51(3) pm	$\beta = 97.277\ (2)°$
	c = 2126.07(6) pm	$\gamma = 90°$
Volume	2.50673(13) nm^3	
Z	4	
Density (calculated)	1.210 Mg/m^3	
Absorption coefficient	0.081 mm-1	
F(000)	968	
Crystal size	0.09 x 0.32 x 0.51 mm^3	
Theta range for data collection	1.84 to 30.58°	
Index ranges	-12<=h<=17, -13<=k<=13, -29<=l<=28	
Reflections collected	30424	
Independent reflections	7470 [R(int) = 0.0353]	
Completeness to theta = 30.58°	96.9 %	
Absorption correction	None	
Refinement method	Full-matrix least-squares on F^2	
Data / restraints / parameters	7470 / 0 / 400	
Goodness-of-fit on F2	1.017	
Final R indices [I>2sigma(I)]	R1 = 0.0627, wR2 = 0.1565	
R indices (all data)	R1 = 0.1361, wR2 = 0.1925	
Extinction coefficient	0.0001(9)	
Largest diff. peak and hole	0.176 and -0.201 e.Å-3	

Table 7.10 Crystallographic data and structure refinement for Bis(4-hydroxy-2,6-dimethyl phenyl)(4-aminophenyl)methane (**2.2q**) -Toluene

Identification code	bisphenol_0m	
Empirical formula	$C_{30}\ H_{33}\ N\ O_2$	
Formula weight	439.59	
Temperature	296(2) K	
Wavelength	71.073 pm	
Crystal system	Triclinic	
Space group	P-1	
Unit cell dimensions	a = 1148.26(12) pm	α= 62.491(6)°
	b = 1173.98(11) pm	β= 63.027(6)°
	c = 1246.59(13) pm	γ = 62.880(6)°
Volume	1.2622(2) nm^3	
Z	3	
Density (calculated)	1.371 Mg/m^3	
Absorption coefficient	0.087 mm^{-1}	
F(000)	558	
Crystal size	0.09 x 0.38 x 0.47 mm^3	
Theta range for data collection	1.94 to 30.72°	
Index ranges	-15<=h<=16, -15<=k<=16, -17<=l<=17	
Reflections collected	17639	
Independent reflections	6884 [R(int) = 0.0780]	
Completeness to theta = 30.72°	87.7 %	
Absorption correction	None	
Refinement method	Full-matrix least-squares on F^2	
Data / restraints / parameters	6884 / 0 / 344	
Goodness-of-fit on F^2	1.151	
Final R indices [I>2sigma(I)]	R1 = 0.0794, wR2 = 0.2325	
R indices (all data)	R1 = 0.1293, wR2 = 0.2620	
Extinction coefficient	0.001(3)	
Largest diff. peak and hole	0.546 and -0.286 e.Å-3	

Table 7.11 Crystallographic data and structure refinement for [Bis(4-hydroxy-3,5-dimethyl phenyl) methyl]-4-pyridine (**2.2o**).

Identification code	jbb00205_0m	
Empirical formula	C_{22} H_{22} N O_2	
Formula weight	332.41	
Temperature	296(2) K	
Wavelength	71.073 pm	
Crystal system	Monoclinic	
Space group	P2(1)/n	
Unit cell dimensions	a = 1185.5 pm	α= 90°.
	b = 977.6 pm	β= 101.569(2)°.
	c = 1890.8 pm	γ = 90°.
Volume	2.1469 nm^3	
Z	5	
Density (calculated)	1.285 Mg/m^3	
Absorption coefficient	0.082 mm^{-1}	
F(000)	885	
Crystal size	0.36 x 0.21 x 0.14 mm^3	
Theta range for data collection	1.87 to 26.77°	
Index ranges	-14<=h<=13, -12<=k<=12, -23<=l<=17	
Reflections collected	16529	
Independent reflections	4498 [R(int) = 0.0614]	
Completeness to theta = 26.77°	98.1 %	
Absorption correction	None	
Refinement method	Full-matrix least-squares on F^2	
Data / restraints / parameters	4498 / 2 / 248	
Goodness-of-fit on F^2	1.011	
Final R indices [I>2sigma(I)]	R1 = 0.0619, wR2 = 0.1656	
R indices (all data)	R1 = 0.1302, wR2 = 0.2041	
Extinction coefficient	0.0035(18)	
Largest diff. peak and hole	0.316 and -0.276 $e.Å^{-3}$	

Table 7.12 Crystallographic data and structure refinement for [Bis(4-hydroxy-3,5-dimethyl phenyl) methyl]-2-pyridine (**2.2p**)

Identification code	bisphenol_0m	
Empirical formula	C_{22} H_{23} N O_2	
Formula weight	333.41	
Temperature	296(2) K	
Wavelength	71.073 pm	
Crystal system	Triclinic	
Space group	P-1	
Unit cell dimensions	a = 891.05(4) pm	α= 113.398(3)°.
	b = 999.39(6) pm	β= 101.408(3)°.
	c = 1185.70(6) pm	γ = 103.448(3)°.
Volume	0.89129(8) nm^3	
Z	2	
Density (calculated)	1.242 Mg/m^3	
Absorption coefficient	0.079 mm^{-1}	
F(000)	356	
Crystal size	0.38 x 0.32 x 0.21 mm^3	
Theta range for data collection	2.78 to 30.52°	
Index ranges	-12<=h<=11, -14<=k<=13, -16<=l<=14	
Reflections collected	9754	
Independent reflections	5060 [R (int) = 0.0325]	
Completeness to theta = 30.52°	92.9 %	
Absorption correction	None	
Refinement method	Full-matrix least-squares on F^2	
Data / restraints / parameters	5060 / 0 / 319	
Goodness-of-fit on F^2	1.025	
Final R indices [I>2sigma(I)]	R1 = 0.0482, wR2 = 0.1238	
R indices (all data)	R1 = 0.0754, wR2 = 0.1452	
Extinction coefficient	0.001(6)	
Largest diff. peak and hole	0.283 and -0.201 e.$Å^{-3}$	

Table 7.13 Crystallographic data and structure refinement for [Bis(4-hydroxy-3,5-dimethyl phenyl)methyl]-4-pyridinium chloride

Identification code	04srv228	
Empirical formula	C_{22} H_{24} Cl N O_2	
Formula weight	369.87	
Temperature	120(2) K	
Wavelength	0.71073 Å	
Crystal system	Monoclinic	
Space group	P2(1)/n	
Unit cell dimensions	a = 8.6590(2) Å	α= 90°.
	b = 14.3920(17) Å	β= 102.52(14)°
	c = 15.7057(12) Å	γ = 90°.
Volume	1910.7(3) $Å^3$	
Z	4	
Density (calculated)	1.286 Mg/m^3	
Absorption coefficient	0.216 mm^{-1}	
F(000)	784	
Crystal size	0.26 x 0.15 x 0.09 mm^3	
Theta range for data collection	1.94 to 27.50°	
Index ranges	-11<=h<=11, -18<=k<=18, -20<=l<=20	
Reflections collected	21226	
Independent reflections	4383 [R(int) = 0.0577]	
Completeness to theta = 27.50°	99.6 %	
Absorption correction	Semi-empirical from equivalents	
Max. and min. transmission	0.984 and 0.953	
Refinement method	Full-matrix least-squares on F^2	
Data / restraints / parameters	4383 / 0 / 331	
Goodness-of-fit on F^2	1.076	
Final R indices [I>2sigma(I)]	R1 = 0.0267, wR2 = 0.0708	
R indices (all data)	R1 = 0.0319, wR2 = 0.0781	
Largest diff. peak and hole	0.65 and -0.24 $e.Å^{-3}$	

Table 7.14 Crystal data and structure refinement for [Bis(4-hydroxy-3,5-dimethyl phenyl)methyl]-4-pyridinium bromide

Identification code	04srv280	
Empirical formula	C22 H24 Br N O2	
Formula weight	414.33	
Temperature	120(2) K	
Wavelength	0.71073 Å	
Crystal system	Monoclinic	
Space group	P 2(1)/n	
Unit cell dimensions	a = 8.7217(4) Å	α= 90°.
	b = 14.7461(6) Å	β= 101.5940(10)°.
	c = 15.4836(6) Å	γ = 90°.
Volume	1950.73(14) $Å^3$	
Z	4	
Density (calculated)	1.411 Mg/m^3	
Absorption coefficient	2.123 mm^{-1}	
F(000)	856	
Crystal size	0.32 x 0.22 x 0.12 mm^3	
Theta range for data collection	1.93 to 30.51°	
Index ranges	-12<=h<=12, -20<=k<=21, -21<=l<=22	
Reflections collected	21226	
Independent reflections	5943 [R(int) = 0.0174]	
Completeness to theta = 30.51°	99.6 %	
Absorption correction	Semi-empirical from equivalents	
Max. and min. transmission	1.000 and 0.803	
Refinement method	Full-matrix least-squares on F^2	
Data / restraints / parameters	5943 / 0 / 331	
Goodness-of-fit on F^2	1.076	
Final R indices [I>2sigma(I)]	R1 = 0.0477, wR2 = 0.0635	
R indices (all data)	R1 = 0.1274, wR2 = 0.1398	
Largest diff. peak and hole	0.921 and -0.275 $e.Å^{-3}$	

Table 7.15 Crystallographic data and structure refinement for Bis(3,5-dimethyl-4-hydroxy phenyl)(4-aminophenyl)methane-H_2F_2

Identification code	jbb00105_0m	
Empirical formula	C_{23} H_{24} F N O_2	
Formula weight	365.43	
Temperature	296(2) K	
Wavelength	71.073 pm	
Crystal system	Triclinic	
Space group	P-1	
Unit cell dimensions	a = 540.90(3) pm	α= 67.573(4)°.
	b = 1364.51(9) pm	β= 89.159(4)°.
	c = 1522.59(10) pm	γ = 85.682(4)°.
Volume	1.03570(11) nm^3	
Z	2	
Density (calculated)	1.172 Mg/m^3	
Absorption coefficient	0.080 mm^{-1}	
F(000)	388	
Crystal size	0.80 x 0.31 x 0.09 mm^3	
Theta range for data collection	1.45 to 26.40°	
Index ranges	-6<=h<=6, -16<=k<=16, -19<=l<=18	
Reflections collected	9597	
Independent reflections	3931 [R (int) = 0.0274]	
Completeness to theta = 26.40°	92.7 %	
Absorption correction	None	
Refinement method	Full-matrix least-squares on F^2	
Data / restraints / parameters	3931 / 0 / 314	
Goodness-of-fit on F^2	1.064	
Final R indices [I>2sigma(I)]	R1 = 0.0680, wR2 = 0.1966	
R indices (all data)	R1 = 0.0796, wR2 = 0.2104	
Extinction coefficient	0.010(6)	
Largest diff. peak and hole	1.584 and -0.289 e.$Å^{-3}$	

Table 7.16 Crystallographic data and structure refinement for 14-H-14-(4-methylphenyl)-dibenzo[*a,j*]xanthene (**4.1b**).

Identification code	n2me	
Empirical formula	$C_{28}H_{20}O$	
Formula weight	372.44	
Temperature	273(2) K	
Wavelength	71.073 pm	
Crystal system	Orthorhombic	
Space group	Pna2(1)	
Unit cell dimensions	a = 1405.30(10) pm	α = 90°
	b = 1741.02(13) pm	β = 90°
	c = 792.76(6) pm	γ = 90°
Volume	1.9396(2) nm^3	
Z	4	
Density (calculated)	1.275 Mg/m^3	
Absorption coefficient	0.076 mm^{-1}	
F(000)	784	
Crystal size	0.28 x 0.39 x 0.69 mm^3	
Theta range for data collection	1.86 to 30.10°	
Index ranges	-18<=h<=19, -24<=k<=24, -11<=l<=11	
Reflections collected	23161	
Independent reflections	5288 [R (int) = 0.0241]	
Completeness to theta = 30.10°	98.8 %	
Absorption correction	None	
Refinement method	Full-matrix least-squares on F^2	
Data / restraints / parameters	5288 / 1 / 328	
Goodness-of-fit on F^2	1.008	
Final R indices [I>2sigma(I)]	R1 = 0.0373, wR2 = 0.1014	
R indices (all data)	R1 = 0.0488, wR2 = 0.1101	
Absolute structure parameter	0.4(14)	
Extinction coefficient	0.0088(13)	
Largest diff. peak and hole	0.125 and -0.135 e.Å-3	

Table 7.17 Crystallographic data and structure refinement for 14-H-14-(2-nitrophenyl)-dibenzo[*a,j*]xanthene (**4.1c**)

Identification code	jbb00205_0m	
Empirical formula	$C_{27}H_{17}NO_3$	
Formula weight	403.42	
Temperature	296(2) K	
Wavelength	71.073 pm	
Crystal system	Orthorhombic	
Space group	Cmc2(1)	
Unit cell dimensions	a = 1748.14(2) pm	α= 90°.
	b = 1454.13(2) pm	β= 90°.
	c = 794.640(10) pm	γ = 90°.
Volume	2.01999(4) nm^3	
Z	4	
Density (calculated)	1.327 Mg/m^3	
Absorption coefficient	0.087 mm^{-1}	
F(000)	840	
Crystal size	0.62 x 0.31 x 0.31 mm^3	
Theta range for data collection	1.82 to 24.73°	
Index ranges	-20<=h<=20, -17<=k<=17, -9<=l<=9	
Reflections collected	12465	
Independent reflections	1796 [R(int) = 0.0240]	
Completeness to theta = 24.73°	100.0 %	
Absorption correction	None	
Refinement method	Full-matrix least-squares on F^2	
Data / restraints / parameters	1796 / 1 / 167	
Goodness-of-fit on F^2	1.037	
Final R indices [I>2sigma(I)]	R1 = 0.0267, wR2 = 0.0715	
R indices (all data)	R1 = 0.0279, wR2 = 0.0728	
Absolute structure parameter	1.3(14)	
Extinction coefficient	0.0094(7)	
Largest diff. peak and hole	0.113 and -0.092 e.$Å^{-3}$	

Table 7.18 Crystallographic data and structure refinement for Rosolic acid - ethyl acetate

Identification code	ra_01	
Empirical formula	$C_{19} H_{14} O_2 . C_4 H_8 O_2$	
Formula weight	274.30	
Temperature	296(2) K	
Wavelength	71.073 pm	
Crystal system	Monoclinic	
Space group	P2(1)/n	
Unit cell dimensions	a = 1152.73(2) pm	α = 90°
	b = 855.54(2) pm	β = 96.337(10)°
	c = 2009.80(4) pm	γ = 90°
Volume	1.96997(7) nm3	
Z	5	
Density (calculated)	1.156 Mg/m3	
Absorption coefficient	0.074 mm-1	
F(000)	720	
Crystal size	0.57 x 0.34 x 0.17 mm^3	
Theta range for data collection	1.95 to 30.57°	
Index ranges	-16<=h<=16, -12<=k<=12, -28<=l<=28	
Reflections collected	18017	
Independent reflections	5955 [R(int) = 0.0212]	
Completeness to theta = 30.57°	98.2 %	
Absorption correction	None	
Refinement method	Full-matrix least-squares on F2	
Data / restraints / parameters	5955 / 0 / 291	
Goodness-of-fit on F2	1.072	
Final R indices [I>2sigma(I)]	R1 = 0.0749, wR2 = 0.2084	
R indices (all data)	R1 = 0.1039, wR2 = 0.2306	
Largest diff. peak and hole	0.897 and -0.554 e.Å-3	

Table 7.19 Crystallographic data and structure refinement for 4-[(4'-hydroxy-3',5'-dimethylphenyl)(phenyl)methylene]-2,6-dimethyl-cyclohexa-2,5-dien-1-one (**5.1a**)

Identification code	03srv005	
Empirical formula	$C_{23}H_{22}O_2$	
Formula weight	330.41	
Temperature	120(2) K	
Wavelength	0.71073 Å	
Crystal system	Triclinic	
Space group	P-1	
Unit cell dimensions	a = 10.7663(8) Å	α= 82.261(3)°.
	b = 12.3118(10) Å	β= 81.154(3)°.
	c = 14.6261(10) Å	γ = 71.654(3)°.
Volume	1810.6(2) $Å^3$	
Z	4	
Density (calculated)	1.212 Mg/m^3	
Absorption coefficient	0.076 mm^{-1}	
F(000)	704	
Crystal size	0.28 x 0.22 x 0.06 mm^3	
Theta range for data collection	1.41 to 30.44°	
Index ranges	-14<=h<=14, -16<=k<=16, -20<=l<=17	
Reflections collected	13949	
Independent reflections	9645 [R(int) = 0.0562]	
Completeness to theta = 30.44°	87.7 %	
Absorption correction	None	
Refinement method	Full-matrix least-squares on F^2	
Data / restraints / parameters	9645 / 0 / 467	
Goodness-of-fit on F^2	0.986	
Final R indices [I>2sigma(I)]	R1 = 0.0722, wR2 = 0.1286	
R indices (all data)	R1 = 0.1809, wR2 = 0.1602	
Largest diff. peak and hole	0.271 and -0.262 $e.Å^{-3}$	

Table 7.20 Crystallographic data and structure refinement for4-[(4'-hydroxy-3',5'-dimethylphenyl)(4-hydroxyphenyl)methylene]-2,6-dimethyl-cyclohexa-2,5-dien-1-one (**5.1c**)

Identification code	RJ-DQ-OH	
Empirical formula	$C_{23}H_{22}O_3$	
Formula weight	346.41	
Temperature	120(2) K	
Wavelength	0.71073 Å	
Crystal system	Monoclinic	
Space group	*C*2/*c* (No. 15)	
Unit cell dimensions	*a* = 13.3611(13) Å	α= 90°
	b = 16.0207(16) Å	β= 95.69(1)°
	c = 16.6309(17) Å	γ = 90°
Volume	3542.4(6) $Å^3$	
Z	8	
Density (calculated)	1.299 g/cm^3	
Absorption coefficient	0.085 mm^{-1}	
F(000)	1472	
Crystal size	0.24 × 0.13 × 0.07 mm^3	
θ range for data collection	2.26 to 27.48°	
Index ranges	$-17 \leq h \leq 17, -20 \leq k \leq 20, -21 \leq l \leq 21$	
Reflections collected	17182	
Independent reflections	4070 [R(int) = 0.0659]	
Reflections with I>2σ(I)	2577	
Completeness to θ = 27.48°	99.9 %	
Absorption correction	None	
Refinement method	Full-matrix least-squares on F^2	
Data / restraints / parameters	4070 / 0 / 323	
Largest final shift/e.s.d. ratio	0.004	
Goodness-of-fit on F^2	0.915	
Final R indices [I>2σ(I)]	R1 = 0.0483, wR2 = 0.1053	
R indices (all data)	R1 = 0.0817, wR2 = 0.1153	
Largest diff. peak and hole	0.338 and -0.217 $e.Å^{-3}$	

Table 7.21 Crystallographic data and structure refinement for 4-[4'-hydroxy-3',5'-dimethyl-phenyl)(4-methoxyphenyl)]-cyclohexa-2,5-dieone (**5.1d**)

Identification code	rj42	
Empirical formula	$C_{24}H_{24}O_3$	
Formula weight	360.43	
Temperature	120(2) K	
Wavelength	71.073 pm	
Crystal system	Monoclinic	
Space group	P2(1)/c	
Unit cell dimensions	a = 1004.7(1) pm	α= 90°.
	b = 1390.4(2) pm	β= 105.10(1)°.
	c = 1457.1(2) pm	γ = 90°.
Volume	1.9652(4) nm^3	
Z	4	
Density (calculated)	1.218 Mg/m^3	
Absorption coefficient	0.079 mm^{-1}	
F(000)	768	
Crystal size	0.30 x 0.24 x 0.20 mm^3	
Theta range for data collection	2.56 to 30.00°	
Index ranges	-14<=h<=13, -19<=k<=19, -20<=l<=20	
Reflections collected	23571	
Independent reflections	5736 [R(int) = 0.0371]	
Completeness to theta = 30.00°	95.2 %	
Absorption correction	None	
Refinement method	Full-matrix least-squares on F^2	
Data / restraints / parameters	5736 / 0 / 263	
Goodness-of-fit on F^2	1.037	
Final R indices [I>2sigma(I)]	R1 = 0.0447, wR2 = 0.0571	
R indices (all data)	R1 = 0.1240, wR2 = 0.1308	
Extinction coefficient	0.0006(16)	
Largest diff. peak and hole	0.411 and -0.302 $e.Å^{-3}$	

References

1. Delaviz, Y.; Gibson, H.W. *Macromolecules* **1992**, *25*, 18
2. Saiz, E.; Fabre, M.J.; Gargallo, L.; Radic, D.; Hernandez-Fuentes, I. *Macromolecules* **1989**, *22*, 3660
3. Kricheldorf, H. R.; Bohme, S.; Schwarz, G.; Schultz, C.-L. *Macromolecules* **2004**, *37*, 1742
4. Alizadeh, A.; Sohn, S.; Quinn, J.; Marand, H.; Shank, L. C.; Iler, H. D. *Macromolecules* **2001**, *34*, 4066
5. Brunelle, D.J.; Shannon, T.G. *Macromolecules* **1991**, *24*, 3035-3044
6. Robyr, P.; Gan, Z.; Suter, U. W. *Macromolecules* **1998**, *31*, 6199
7. Koch, T.; Ritter, H. *Macromolecules* 1995, *28*, 4806-4809
8. Nishide, H.; Yoshioka, N.; Inagaki, K.; Tsuchida, E. *Macromolecules* **1988**, *21*, 3119
9. Kricheldorf, H. R.; Schwarz, G. *Macromol. Rapid Commun.* **2003**, *24*, 359
10. Kricheldorf, H. R.; Vakhtangishvili, L.; Fritsch, D. *J. Polym. Sci., Part A: Polym. Chem.* **2002**, *40*, 2967
11. Kricheldorf, H. R.; Hobzova, R.; Schwarz, G.; Vakhtangishvili, L. *Macromolecules* **2005**, *38*, 1736
12. Delaviz, Y.; Gibson, H.W. *Macromolecules* **1992**, *25*, 18
13. Ünsal, Ö.; Godt, A. *Chem. Eur. J.* **1999**, *5*, 1728
14. Duda, S.; Godt, A. *Eur. J. Org. Chem.* **2003**, 3412
15. Godt, A.; Duda, S.; Ünsal, O.; Thiel, J.; Härter, A.; Roos, M.; Tschierske, C.; Diele, S. *Chem. Eur. J.* **2002**, *8*, 5094
16. Kanekiyo, Y.; Naganawa, R.; Tao, H. *Chem. Comm.* **2002**, 2698
17. Kanekiyo, Y.; Naganawa, R.; Tao, H. *Angew. Chem. Int. Ed.* **2003**, *42*, 3014
18. Noyori, R. in *Asymmetric Catalysis in Organic Synthesis*; John Wiley & Sons: New York, 1994
19. Lu, G.; Li, X.; Chen, G.; Chan, W.L.; Chan, A.S.C. *Tetrahedron Asymmetry*, **2003**,*14*, 449
20. Hopp, L.; Megee, S. O.; Lloyd, J. B. *J. Med. Chem.* **1998**, *41*, 4421
21. Lubczyk, V.; Bachmann, H.; Gust, R. *J. Med. Chem.* **2002**, *45*, 5358
22. Suzuki, T.; Nakagawa, Y.; Takano, I.; Yaguchi, K.; Yasuda, K. *Environ. Sci. Technol.* **2004**, *38*, 2389
23. Shadyro, O.I.; Edimecheva, I.P.; Glushonok, G.K.; Ostrovskaya, N.I.; Polozov, G.I.; Murase, H.; Kagiya, T. *Free Radical Res.* **2003**, *37*, 1087
24. Amorati, R.; Lucarini, M.; Mugnaini, V.; Pedulli, G. F. *J. Org. Chem.* **2003**, *68*, 5198
25. Faith, H.E. *J. Am. Chem. Soc.* **1950**, *72*, 837
26. Baeyer, A. *Ber*, **1872**, *5*, 1096
27. Ledderer L. *J. Prakt. Chem.* **1894**, *50*, 223
28. Beaver, D.J.; Stoffel, P.J. *J. Am. Chem. Soc.* **1953**, *74*, 3410
29. Harden, W.C.; Reid, E.E. *J. Am. Chem. Soc.* **1932**, *54*, 4325
30. Westeppe, U.; Fengler, G.; Casser, C.; Hajek, M.; Freitag, D.; Waldmann, H. *German Patent*. **1991**, DE 4003437 A1 19910808
31. Schnell, H.; Krimm, H. *Angew. Chem.* **1963**, *75*, 662
32. Inagaki, T.; Tanioka, R.; Zushi, K. *Japanese Patent* JP 06087775 A2 19940329
33. Patrascu, E.; Frey, J.W.; Sendner, H. *Eur. Pat. Appl.* **1996**, EP 94-810711 19941209
34. Schönberg, A.; Fateen, A.K.; Sammour, E.A. *J. Org. Chem.* **1958**, *23*, 2025
35. Wolff, W. *Chem. Ber.* **1893**, *26*, 83
36. Pechmann, H.V.; Duisberg, C. *Dtsch. Chem. Ber.* **1883**, *16*, 22119
37. Nowakowska, E.; Daszliewicz, Z.; Kyziol, J.B. *Tetrahedron Lett.* **1998**, *39*, 451

38. Rudzevich, Y.; Rudzevich, V.; Schollmeyer, D.; Thondorf, I.; Böhmer, V. *Org. Lett.* **2005**, *7*, 613
39. Driver, J.E.; Lai, T.F. *J. Chem. Soc.* **1958**, 3219
40. Dinger, M.B.; Scott, M.J. *J. Chem. Soc. Perkin 1* **2000**, 1741
41. Jung, M.E.; Jachiet, D.; Khan, S.I.; Kim, C. *Tetrahedron Lett.* **1995**, *36*, 361
42. Gump, W. S.; Vitucci, J. C. *J. Am. Chem. Soc.***1945**, *67*, 238
43. Vessieres, A.; Top, S.; Pigeon, P.; Hillard, E.; Boubeker, L.; Spera, D.; Jaouen, G. J. *Med. Chem.* **2005**, *48*, 3937
44. Sprung, M.M. *J. Am. Chem. Soc.* **1941**, *63*, 334
45. Steelink, C.; Fitzpatrick, J.D.; Kispert, L.D., Hyde, J.S. *J. Am. Chem. Soc.* **1968**, *90*, 4354
46. Campbell, T.W.; Coppinger, G.M. *J. Am. Chem. Soc.* **1952**, *74*, 1469
47. Becker, H. D. *J. Org. Chem.* **1967**, *32*, 2115
48. Desiraju, G.R. in *The Crystal as a Supramolecular Entity*, ed. Lehn, J.-M., John Wiley and Sons, Chichester, 1996
49. Brammer, L. in *Crystal Design: Structure and Function, Perspectives in Supramolecular Chemistry*, Vol. 7, Ed Desiraju, G.R., John Wiley & Sons: Sussex, 2003
50. Aitipamula, S.; Desiraju, G.R.; Jaskólski, M.; Nangia, A.; Thaimattam, R. *CrystEngComm* **2003**, *5*, 447
51. Aitipamula, S.; Thallapally, P.K.; Thaimattam, R.; Jaskolski, M.; Desiraju, G.R. *Org. Lett.* **2002**, *4*, 921
52. Thallapally, P.K.; Katz, A.K.; Carrell, H.L.; Desiraju, G.R. *Chem. Comm.* **2002**, 344
53. Kim, H.S.; Jeffrey, G.A.; Rosenstein, R.D. *Acta. Cryst. Sect B.* **1971**, *27*, 307
54. Aitipamula, S.; Nangia, A.; Thaimattam, R.; Jaskólski, M. *Acta Cryst. C* **2003**, *39*, o481
55. Venkataramanan, B.; Guan James, W.L.; Vittal, J.J.; Suresh, V. *Cryst. Growth Des.* **2004**, *4*, 553
56. Zakaria, C.M.; Ferguson, G.; Lough, A.J.; Glidewel, C. *Acta Cryst. C* **2002**, *38*, o1
57. Fournier, J.-H.; Maris, T.; Simard, M.; Wuest, J. D. *Cryst. Growth Des.* **2003**, *3*, 535
58. Sawaki, T.; Endo, K.; Kobayashi, K.; Hayashida, O.; Aoyama, Y. *Bull. Chem. Soc. Jpn.* **1997**, *70*, 3075
59. Suzuki, H. *Tetrahedron. Lett.* **1992**, *33*, 6319
60. Suzuki, H.; Takagi, H. *Tetrahedron Lett.* **1993**, *34*, 4805
61. Suzuki, H.; Takagi, H.; Sato, R. *Tetrahedron Lett.* **1997**, *38*, 4563
62. Wright, R.S.; Vinod, T.K. *Tetrahedron Lett.* **2003**, *44*, 7129
63. Kobayashi, K.; Shirasaka, T.; Horn, E.; Furukawa, N. *Tetrahedron Lett.* **2000**, *41*, 89
64. Kobayashi, K.; Kobayashi, N.; Ikuta, M.; Therrien, B.; Sakamoto, S.; Yamaguchi, K. *J. Org. Chem.* **2005**, *70*, 749
65. Kobayashi, K.; Shirasaka, T.; Sato, A.; Horn, E.; Furukawa, N. *Angew. Chem. Int. Ed.* **1999**, *38*, 3483
66. Palin, D.E.; Powell, H.M. *J. Chem. Soc.* **1947**, 208
67. Powell, H.M. *J. Chem. Soc.* **1948**, 61
68. Powell, H.M. J. Chem. Soc. **1948**, 815
69. Ermer, O. *Helv. Chim. Acta.* **1991**, *74*, 1339
70. Ermet, O.; Robke, C. *J. Am. Chem. Soc.* **1993**, *115*, 10077
71. Aitipamula, S.; Nangia, A. *Chem. Comm.* **2005**, 3159
72. Tanaka, K.; Okada, T; Toda, F. *Angew. Chem. Int. Ed.* **1993**, *32*, 1147
73. Urbanczyk-Lipkowska, Z.; Yoshizawa, K.; Toyota, S.; Toda, F. *CrystEngComm.* **2003**, *5*, 114
74. Nassimbeni, L.R.; Su, H. *Acta Cryst B.* **2001**, *57*, 394
75. Loehlin, J.H.; Etter, M.C.; Gendreau, C.; Cervasio, E. *Chem. Mater.* **1994**, *6*, 1218
76. Goldberg, I.; Stein, Z.; Kai, A.; Toda, F. *Chem. Lett.* **1987**, 1617
77. Toda, F.; Tanaka, K.; Hyoda, T.; Mak, T.C.W. *Chem. Lett.* **1988**, 107

78. Glidewell, C.; Ferguson, G.; Gregson, R.M.; Campana, C.F. *Acta Cryst. B* **2000**, *56*, 68
79. Ferguson, G.; Glidewell, C.; Gregson, R.M.; Meehan, P.R. *Acta Cryst. B* **1998**, *54*, 330
80. Ferguson, G.; Glidewell, C.; Gregson, R.M.; Meehan, P.R.; Patterson, I.L.J. *Acta Cryst. B* **1998**, *54*, 151
81. Whitesides, G.M.; B. Grzybowski, B. *Science* **2002**, *295*, 2418
82. Muthukumar, M.; Ober, C.K.; Thomas, E.L. *Science* **1997**, *277*, 1225
83. Martin, T.; Obst, U.; Rebek Jr. J. *Science* **1998**, *281*, 1842
84. Bowden, N.; Terfort, A.; Carbeck, J.; Whitesides, G.M. *Science* **1997**, *276*, 233
85. Smela, E.; Inganas, O.; Lundstrom, I. *Science* **1995**, *268*, 1735
86. Zubarev, E. R.; Pralle, M. U.; Sone, E. D.; Stupp, S. I. *J. Am. Chem. Soc.* **2001**, *123*, 4105
87. Radzilowski, L. H.; Carragher, B. O.; Stupp, S. I. *Macromolecules* **1997**, *30*, 2110
88. Sastri, S.B.; Stupp, S.I. *Macromolecules* **1993**, *26*, 5657
89. Messmore, B. W.; Sukerkar, P. A.; Stupp, S. I. *J. Am. Chem. Soc.* **2005**, *127*, 7992
90. Gunther, J.; Stupp, S.I. *Langmuir* **2001**, *17*, 6530
91. Zubarev, E.R.; Pralle, M.U.; Li, L.; Stupp, S.I. *Science* **1999**, *283*, 523
92. McArdle, C.P.; Jennings, M.C.; Vittal, J.J. Puddephatt, R.J. *Chem. Eur. J.* **2001**, *7*, 3572
93. McArdle, C. P.; Van, S.; Jennings, M. C.; Puddephatt, R. J. *J. Am. Chem. Soc.* **2002**, *124*, 3959
94. Desiraju, G.R. *Acc. Chem. Res.* **1991**, *24*, 290
95. Muthuraman, M.; Masse, R.; Nicoud, J.-F.; Desiraju, G. R. *Chem. Mater.* **2001**, *13*, 1473
96. Driver, J.E.; Mok, S.F. *J. Chem. Soc.* **1955**, 3914
97. Shultz, D.A.; Zhao, Q. *Tetrahedron Lett.* **1996**, *37*, 8837
98. Davies, J.E.D.; Finocchiaro, P.; Herbstein, F.H. in *Inclusion Compounds: Structural Aspects of Host Lattices Formed by Organic Compounds*, Vol. 2, Academic Press, London 1984
99. Saied, O.; Marris, T.; Wang, X.; Simard, M.; Wuest, J.D. *J. Am. Chem. Soc.* **2005**, *127*, 10008
100. Endo, K.; Sawaki, T.; Koyanagi, M.; Kobayashi, K.; Masuda, H.; Aoyama, Y. *J. Am. Chem. Soc.* **1995**, *117*, 8341
101. Sarma, R.J.; Baruah, J.B. *Dyes and Pigments* **2004**, *61*, 39
102. Powell, H.M.; Wetters, B.D.P. *Chem. Ind. London* **1955**, 256
103. Tedesco, C.; Immediata, I; Gregoli, L.; Vitaliano, L.; Immirzi, A.; Neri, P. *CrystEngComm.* **2005**, *7*, 449
104. Desiraju, G.R.; Steiner, T. *The Weak Hydrogen Bond*, IUCr Monographs on Crystallography 9, Oxford University Press, Oxford 1999
105. Ilioudis, C.A.; Hancock, K.S.B.; Georganopoulou D.G.; Steed, J.W. *New J. Chem.* **2004**, *24*, 787
106. Shannon, R.D.; Prewitt, C.T. *Acta Cryst.* B **1969**, *25*, 925
107. Rowland, R.S.; Taylor, R. *J. Phys. Chem.* **1996**, *100*, 73
108. Sarma, R.J.; Baruah, J.B. *Dyes and Pigments* **2005**, *64*, 91
109. Sirkencioglu, O.; Talinli, N.; Akar, A. *J Chem. Res. (S)* **1995**, *12*, 502
110. Van Allan, J.A.; Giannini, D.D.; Whitesides, T.H. *J. Org. Chem.* **1982**, *47*, 820
111. Georghiou, P.E.; Ashram, M.; Li, Z.; Chaulk, S.G. *J. Org. Chem.* **1995**, *60*, 7284
112. Biali, S.E. *Synlett* **2003**,1
113. Poupelin, J.P.; Saint-Ruf, G.; Lacroix, R.; Narcisse, G.; Foussard-Blanpin, O.; Uchida-Ernouf, G. *Eur. J. Med. Chem.* **1978**, *13*, 381
114. Amouri, H.; Le Bras, J. *Acc. Chem. Res.* **2002**, *35*, 501
115. Alam, I.; Sharma, S.K.; Gutsche, C.D. *J. Org. Chem.* **1994**, *59*, 3716
116. Arduini, A.; Bosi, A.; Pochini, A.; Ungaro, R. *Tetrahedron* **1985**, *41*, 3095
117. Rosenau, T.; Potthast, A.; Elder, T.; Kosma, P. *Org. Lett.* **2002**, *4*, 4285

118. Gorner, H. *Photochem. Photobiol. Sci.* **2003**, *2*, 524
119. Swartz, A. M.; Barra, M.; Kuntz, D. *J. Org. Chem.* **2004**, *69*, 3198 and references within
120. Cabaret, D.; Adediran, S.A.; Garcia Gonzales, M.J.; Pratt, R.F.; Wakselman, M. *J. Org. Chem.* **1999**, *64*, 713
121. Myers, J. K.; Cohen, J. D.; Widlanski, T. S. *J. Am. Chem. Soc.***1995**, *117*, 11049
122. Stowell, J. K.; Widlanski, T. S., Kutateladze, T. G.; Raines, R. T. *J. Org. Chem.* **1995**, *60*, 6930
123. Dyall, L.K.; Winstein, S. *J Am. Chem. Soc.* **1972**, *94*, 2196
124. Bolon, D.A. *J. Org. Chem.* **1970**, *35*, 3666
125. Harrer, W.; Kurreck, H.; Reusch, J.; Gierke, W. *Tetrahedron* **1975**, *31*, 625
126. Shultz, D.A.; Zhao, Q. *Tetrahedron Lett.* **1996**, *37*, 8837
127. Oh, M.; Carpenter, G.B.; Sweigart, D.A. *Angew. Chem. Int. Ed.* **2002**, *41*, 3650
128. Lewis, T.W.; Paul, I.C.; Curtin, D.Y. *Acta Cryst. B* **1980**, *36*, 70
129. Senthil Kumar, V.S.; Addlagatta, A.; Nangia, A.; Robinson, W.T.; Broder, C.K.; Mondal, R.; Evans, I.R.; Howard, J.A.K.; Allen, F.H. *Angew. Chem. Int. Ed.* 2002, 41, 3848
130. Senthil Kumar, V.S.; Nangia, A. *Chem. Comm.* 2001, 2392
131. Laurence, C.; Berthelot, M.; Graton, J.; in *The Chemistry of Phenols* eds. Rappoport, Z. Vol. 1 Hydrogen-bonded complexes of phenols, Wiley, 2003, West Sussex, p586
132. Reichardt, C. *Chem. Rev.* **1994**, *94*, 2319
133. F. Strohbusch, *Tetrahedron* **1972**, *28*, 1915
134. Olah, G. A. *J. Org. Chem.* **2001**, *66*, 5943
135. Irie, M. *J. Am. Chem. Soc.* **1983**, *105*, 2078
136. Naya, S.; Yoda, K.; Nitta, M. *Tetrahedron*, **2004**, *60*, 4953
137. Naya S.; Nitta, M. *J.C.S. Perkin Trans 2* **2000**, 2427
138. Wang, H.; Gabbai, F. *Angew. Chem. Int. Ed.* **2004**, *43*, 184 and references within
139. Anderson, L.C. *J. Am. Chem. Soc.* **1930**, *52*, 4567
140. Duxbury, D.F. *Chem. Rev.* **1993**, *93*, 381
141. Shchepinov, M.S.; Korshun, V.A. *Chem. Soc. Rev.* **2003**, *32*, 170
142. Minnock, A.; Lin, L.S.; Morg, M.J.; Crow, S.D.G.; Waring, M.J.; Sheh, L. *Bioconjugate Chem.* **2001**, *12*, 870
143. Chu, S.S.; Reich, S.H. *Biorg. Med. Chem. Lett.* **1995**, *5*, 1053
144. Zhang, X.; Gramlich, G.; Wang, X.; Nau, W.M. *J. Am. Chem. Soc.* **2002**, *124*, 254
145. Moscatelli, A.; Galarneau, A.; Di Renzo, F.; Ottaviani, M.F. *J. Phys. Chem. B* **2004**, *108*, 18580
146. Sabate, R.; Gallardo, M.; de la Maza, A.; Estelrich, J. *Langmuir* **2001**, *17*, 6433
147. Bales, B.L.; Tiguida, T.I.; Zana, R. *J. Phys. Chem. B* **2004**, *108*,14948
148. Reekmans, S.; De Schryver, F.C. in *Frontiers in Supramolecular Organic Chemistry and Photochemistry* Eds. Schneider, H.-J.; Durr, H. VCH, New York, 1991, p 302
149. Rajca, A. *Chem. Rev.* **1994**, *94*, 871
150. Dougherty, D.A. *Acc. Chem. Res.* **1991**, *24*, 88
151. Rajca, A.; Utapamanya, S.; Xu, J. *J. Am. Chem. Soc.* **1991**, *113*, 9235
152. Nishide, H.; Doi, R.; Oyaizu, K.; Tsuchida, E. *J. Org. Chem.* **2001**, *66*, 1680
153. Nishide, H.; Kaneko, T.; Nii, T.; Katoh, K.; Tsuchida, E.; Lahti, P. M. *J. Am. Chem. Soc.* **1996**, *118*, 9695
154. Nishide, H.; Takahashi, M.; Takashima, J.; Pu, Y.-J.; Tsuchida, E. *J. Org. Chem.* **1999**, *64*, 7375
155. Anderson, K.K.; Dougherty, D.A. *Advanced Materials*, **1998**, *10*, 688
156. Rebmann, A.; Zhou, J.; Rieker, A.; Stegmann, H.B. *J. Chem. Soc. Perkin 2* **1997**, 1615
157. Harrer, W.; Kurreck, H.; Reusch, J.; Gierke, W. *Tetrahedron* **1975**, *31*, 625
158. Richter, S.N.; Maggi, S.; Mels, S.C.; Palumbo, M.; Freccero, M. *J. Am. Chem. Soc.* **2004**, *126*, 13973
159. Ballester, M.; Pascual, I.; Torres, J. *J. Org. Chem.* **1990**, *55*, 3044

160. Sheldrick, G.M.. SHELXS97, *Program for the Solution of Crystal Structures*, Univ. of Gottingen, Germany (1997)
161. Sheldrick, G.M. SHELXL97, *Program for the Refinement of Crystal Structures*. Univ. of Gottingen, Germany (1997)
162. SHELXTL Release 5.10; *The Complete Software Package for Single Crystal Structure Determination*. Bruker AXS Inc., Madison, WI 53719-1173 (1997)

List of Publications

Articles/Papers based on this study have appeared in:

R.J. Sarma, A.S. Batsanov, R. Kataky, J.B. Baruah; Structural Investigations on Quinone Methides for Understanding their Properties in Confined Medium, *Journal of Inclusion Phenomenon and Macrocyclic Chemistry* (in press)

C. Tamuly, R.J. Sarma, A.S. Batsanov, A.E. Goeta, J.B. Baruah; 4-[Bis(4-hydroxy-3,5-dimethyl phenyl)methyl]pyridinium Chloride and Bromide, *Acta Crystallographica C* **2005**, *C61*, 324-327

R.J. Sarma, J.B. Baruah; One-Step Synthesis of Dibenzoxanthenes, *Dyes and Pigments*, **2005**, *64*, 91-92

R.J. Sarma, J.B. Baruah; Synthesis and Characterization of Bis(4-hydroxy 3,5-dimethyl phenyl)(aryl)methanes as Precursors for Three-State Indicators, *Dyes and Pigments*, **2004**, *61*, 39-47

Articles that are expected to appear soon:

R.J. Sarma, J.B. Baruah; Spectroscopic and Electrochemical Properties of 4-[(4'-Hydroxy-3', 5'-dimethylphenyl)(aryl)methylene]-2,6-dimethylcyclohexa-2,5-dienones (*Communicated*)

R.J. Sarma, J.B. Baruah; Aromatic Guest Binding in *Bis*-phenol Assemblies (*Communicated*)